



**HAL**  
open science

# UNC93B1, an endosomal TLR chaperone, regulates the activation of the endoplasmic reticulum proteins IRE1 $\alpha$ and STING in dendritic cells

Lucie Maisonneuve

► **To cite this version:**

Lucie Maisonneuve. UNC93B1, an endosomal TLR chaperone, regulates the activation of the endoplasmic reticulum proteins IRE1 $\alpha$  and STING in dendritic cells. Immunology. Université Paris Cité, 2023. English. NNT : 2023UNIP5021 . tel-04746289

**HAL Id: tel-04746289**

**<https://theses.hal.science/tel-04746289v1>**

Submitted on 21 Oct 2024

**HAL** is a multi-disciplinary open access archive for the deposit and dissemination of scientific research documents, whether they are published or not. The documents may come from teaching and research institutions in France or abroad, or from public or private research centers.

L'archive ouverte pluridisciplinaire **HAL**, est destinée au dépôt et à la diffusion de documents scientifiques de niveau recherche, publiés ou non, émanant des établissements d'enseignement et de recherche français ou étrangers, des laboratoires publics ou privés.

**Université Paris Cité**  
**Ecole doctorale Bio Sorbonne Paris Cité n°562**  
***Institut Necker Enfants Malades (INEM) – INSERM U1151***

**UNC93B1, an endosomal TLR chaperone, regulates the activation of the  
endoplasmic reticulum proteins IRE1 $\alpha$  and STING in dendritic cells**

Par Lucie MAISONNEUVE

**Thèse de doctorat en Immunologie**

Dirigée par Bénédicte MANOURY

Présentée et soutenue publiquement le 20 avril 2023

Devant un jury composé de :

Dr Lena ALEXOPOULOU  
DR2 CNRS, Aix-Marseille Université

Rapportrice

Dr Jean-Charles GUERY  
DR1 INSERM, Université Toulouse III

Rapporteur, Président du Jury

Dr Paula NUNES-HASLER  
Assistant Professor, PhD, Université de Genève

Examinatrice

Dr Tony AVRIL  
Ingénieur de recherche, PhD, Université de Rennes

Examineur

Dr Bénédicte MANOURY  
DR1 CNRS, Université Paris Cité

Directrice de thèse



**Université Paris Cité**  
Ecole doctorale Bio Sorbonne Paris Cité n°562  
*Institut Necker Enfants Malades (INEM) – INSERM U1151*

**UNC93B1, an endosomal TLR chaperone, regulates the activation of the  
endoplasmic reticulum proteins IRE1 $\alpha$  and STING in dendritic cells**

Par Lucie MAISONNEUVE

**Thèse de doctorat en Immunologie**

Dirigée par Bénédicte MANOURY

Présentée et soutenue publiquement le 20 avril 2023

Devant un jury composé de :

Dr Lena ALEXOPOULOU  
DR2 CNRS, Aix-Marseille Université

Rapportrice

Dr Jean-Charles GUERY  
DR1 INSERM, Université Toulouse III

Rapporteur, Président du Jury

Dr Paula NUNES-HASLER  
Assistant Professor, PhD, Université de Genève

Examinatrice

Dr Tony AVRIL  
Ingénieur de recherche, PhD, Université de Rennes

Examinateur

Dr Bénédicte MANOURY  
DR1 CNRS, Université Paris Cité

Directrice de thèse



## RESUME

### UNC93B1, une protéine chaperone des TLRs endosomaux, régule l'activation des protéines du réticulum endoplasmique IRE1 $\alpha$ et STING dans les cellules dendritiques.

Les cellules dendritiques (CDs) sont des effecteurs clés reliant l'immunité innée et adaptative. Elles reconnaissent directement les agents pathogènes infectants par le biais de récepteurs de l'immunité innée (Pattern recognition receptors ou PRR), comme les récepteurs Toll-like (TLR), et initient des réponses immunitaires efficaces contre eux. Elles produisent en effet un large panel de cytokines et chimiokines pro-inflammatoires et augmentent l'expression de leurs molécules de co-stimulation suite à une infection. Les cellules dendritiques sont des cellules présentatrices d'antigènes (CPA) cruciales, capables de présenter des peptides pathogéniques ou associés à une tumeur via les molécules du CMH pour activer les lymphocytes T et initier une réponse adaptative.

Fortement exprimée dans les CDs, UNC93B1, une molécule hautement conservée, composée de 12 passages transmembranaires et résidant dans le réticulum endoplasmique (RE), a été identifiée comme un régulateur clé dans le repliement et le trafic vers les endosomes des TLRs intracellulaires qui détectent les acides nucléiques des microbes. En effet, une mutation du gène *Unc93b1* (mutation 3d) entraîne une inhibition de l'interaction entre UNC93B1 et les TLRs intracellulaires et bloque leur signalisation. Chez la souris, la mutation 3d d'UNC93B1 entraîne également un défaut de présentation croisée antigénique et une subséquente croissance tumorale accrue et rapide, probablement en raison d'un défaut de présentation croisée des antigènes associés aux tumeurs par les CDs. N'interagissant pas seulement avec les TLRs, UNC93B1 a pour rôle de médier l'activation d'autres protéines dans le RE, comme STIM1 et STING.

Dans le RE, IRE1 $\alpha$  est l'un des 3 acteurs majeurs de l'UPR, une réponse adaptative déclenchée lors de la perturbation de l'homéostasie des protéines du RE et dont la fonction est de restaurer les fonctions altérées de l'organelle. Si l'homéostasie du RE ne peut pas être restaurée, l'UPR induit alors des signaux pro-apoptotiques. La régulation de l'activation d'IRE1 $\alpha$  reste peu claire, en particulier dans les CDs où il joue

un rôle majeur dans la survie des CD8 et la présentation croisée antigénique du CMH de classe I. Nous apportons la preuve qu'UNC93B1 lie le domaine transmembranaire d'IRE1 $\alpha$  et régule sa fonction. Nous avons montré que dans les CD8 portant la mutation 3d, IRE1 $\alpha$  n'est plus associé à BiP, ce qui entraîne son activation. De plus, l'inhibition de l'activité d'IRE1 $\alpha$  dans les CD8 3d restaure la présentation croisée antigénique *in vitro* et limite la croissance tumorale *in vivo*. Dans l'ensemble, nos données mettent en évidence le rôle essentiel d'UNC93B1 dans la régulation de la présentation antigénique du CMH de classe I dans les CD8 en contrôlant l'activité d'IRE1 $\alpha$ .

En plus d'IRE $\alpha$ , nous avons également examiné la régulation de STING par UNC93B1, car il a été démontré que les deux protéines interagissent, UNC93B1 favorisant potentiellement la régulation négative de STING. Nous avons constaté que, dans les CD8, UNC93B1 contrôle STING différemment et semble essentiel pour sa signalisation. De plus, dans les CD8 3d, l'interaction entre UNC93B1 et STING est conservée mais la mutation induit une diminution significative du trafic et de la signalisation STING. Ces données préliminaires indiquent, qu'en plus de favoriser l'activation d'IRE1 $\alpha$ , UNC93B1 semble jouer un rôle important dans la voie interféron médiée par STING.

Mots clés : Cellule dendritique, UNC93B1, présentation croisée, réticulum endoplasmique, IRE1 $\alpha$ , STING.

## ABSTRACT

### UNC93B1, an endosomal TLR chaperone, regulates the activation of the endoplasmic reticulum proteins IRE1 $\alpha$ and STING in dendritic cells.

Dendritic cells (DCs) are key immune cells linking innate and adaptive immunity. They express a wide range of pattern recognition receptors (PRRs), such as Toll-like receptors (TLRs), which recognize specific molecular patterns expressed by pathogens. Following pathogen infection, DCs produce a large panel of pro-inflammatory cytokines and chemokines and increase the expression of their co-stimulatory molecules to present pathogenic-associated peptides on MHC molecules to prime T cells and initiate adaptive immunity.

Strongly expressed in DCs, UNC93B1, a highly conserved 12-membrane spanning molecule residing in the endoplasmic reticulum (ER), has been identified as a key regulator in the folding and trafficking to endosomes of intracellular TLRs that detect microbial nucleic acids. A single mutation in the *Unc93b1* gene (3d mutation) results in the absence of UNC93B1 interaction with intracellular TLRs and inhibition of their signalling, indicating that the association of UNC93B1 to intracellular TLRs is mandatory for their function. UNC93B1 also associates with the ER calcium sensor, STIM1 and this interaction is mandatory for MHC class I antigen cross presentation in DCs. UNC93B1 is also shown to control the production of type I interferon (IFN $\alpha$ ) mediated by STING, an innate immune receptor involved in antiviral response.

In the ER, IRE1 $\alpha$  is one of the 3 sensor proteins of the Unfolded Protein Response (UPR) which is an adaptive response triggered upon disruption of ER protein homeostasis and whose function is to restore the altered functions of the ER. If ER homeostasis cannot be restored, the UPR then induces pro-apoptotic signals. Regulation of IRE1 $\alpha$  activation is not well understood, particularly in DCs where it plays a major role in survival and MHC class I antigen cross presentation. We provide evidence that UNC93B1 binds the transmembrane domain of IRE1 $\alpha$  and regulates its function. We find that in DCs bearing the 3d mutation, IRE1 $\alpha$  is no longer associated to BiP which leads to increased IRE1 $\alpha$  activity. Furthermore, inhibition of IRE1 $\alpha$  activity in 3d DCs restores MHC class I antigen cross presentation in vitro and limits tumour



growth in vivo. Our data highlight the essential role of UNC93B1 in regulating MHC class I antigen presentation in DCs by controlling IRE1 $\alpha$  activity.

We also find that UNC93B1 associates with STING and positively regulates IFN- $\gamma$  STING dependent signalling. In DCs silenced for UNC93B1 or expressing the 3d mutant, trafficking of STING from ER to Golgi is delayed which leads to reduced IFN- $\gamma$  secretion.

Altogether, our data suggest an important role for UNC93B1 in regulating IRE1 $\alpha$  and STING activities in DCs.

Key words: Dendritic cell, UNC93B1, cross presentation, endoplasmic reticulum, IRE1 $\alpha$ , STING.

## REMERCIEMENTS

C'est après 3 ans et 5 mois de thèse et d'expériences, scientifiques et humaines, que je prends le temps de remercier les nombreuses personnes qui m'ont accompagnées au cours de cette période.

Je tiens tout d'abord à remercier ma directrice de thèse, Bénédicte Manoury, qui a su me guider au cours de ces années. Bénédicte, je te remercie pour ta supervision, tes conseils et le partage de ton savoir-faire depuis que je suis arrivée en stage de Master. Merci d'avoir été présente à toutes les étapes des différents projets sur lesquels nous avons travaillé. Je souhaite le meilleur pour ton laboratoire, qui accueille et accueillera de plus de plus de membres, qui j'espère, feront avancer les nombreuses histoires que tu as commencé.

Je voudrais également remercier les rapporteurs de cette thèse, qui ont très gentiment accepté de relire et évaluer mon travail. Merci à Léna Alexopoulou et Jean-Charles Guery de prendre du temps (pourtant précieux) afin de m'aider dans la finalisation de mon doctorat.

Faisant aussi parti de mon jury de thèse, je tiens à remercier les examinateurs de ma soutenance, Paula Nunes-Hasler et Tony Avril. Dear Paula, I would like to thank you for accepting to be a part of my jury since long ago, even after the changes we've had to go through. It's a pleasure to have you listen to my project. Cher Tony, merci encore d'avoir accepté, depuis longtemps également. Je suis ravie que votre expertise se joigne aux diverses discussions qui auront lieu lors de ma soutenance.

I also want to thank, with all my heart, the post-doctoral fellow working in our laboratory, Katrina Podsypanina. Katrina, thank you for everything you've done for the project, not only for the great results you've brought, but also for your numerous advices and your kindness.

Merci au reste de l'équipe Manoury. Moïse, je tiens à te remercier pour ton aide précieuse dans le projet et au quotidien. J'ai toute confiance en tes capacités et je sais que tu pourras aller au bout de tes ambitions.

Je tiens également à remercier les anciens membres de l'équipe Manoury, Clarissa, Micaela, Elisa et Thibault. Clarissa, tu es celle qui m'a le plus appris, lorsque je

débutais en stage de Master. J'applique tes conseils encore aujourd'hui et je n'oublierai pas la gentillesse et la patience dont tu as fait preuve lorsque nous travaillions ensemble. Je te souhaite tout le meilleur dans ta carrière et vie actuelle. Micaela, you were my number one support for two years. Thanks to your advices, your jokes and your support, I've managed to go through difficult times. I hope you are doing great, wherever you are at the moment, and that you are thriving in the path you chose. Elisa, thank you so much for your spreading happiness throughout the year you've stayed. You were of great help too and I wish you all the best. Thibault, je garde encore ta tasse aujourd'hui, et je me réjouis en repensant aux très bons moments que nous avons passé ensemble. Bien que tu ne sois pas resté longtemps, tu resteras un de mes coups de cœur. Je ne te souhaite que du bonheur et beaucoup de réussite.

Merci aux collègues et amis qui m'ont soutenu au cours de ces trois années, et qui ont su diminuer le stress des manipulations et résultats. Un merci tout particulier à Laure, qui a généreusement accepté de relire mon introduction de thèse et qui m'a donné de précieux conseils tout au long de ce doctorat. Marjolène, je te suis également très reconnaissante, pour ta bonne humeur, tes histoires de vélo, les nombreuses sorties organisées et ton incroyable sens de l'organisation.

Un très grand merci à mes doctorantes du tonnerre, Maeva, Ayse et Perrine. Nous avons toutes les quatre commencé notre thèse en même temps, et alors que je clôture mon doctorat, je repense à nos bons moments et à votre soutien au quotidien. Je vous souhaite le meilleur, pour le présent et le futur. Une fois la thèse obtenue pour nous toutes, il faudra changer le nom du groupe pour Docteurs du tonnerre.

Claire, tes paroles de soutien, tes petits plats et nos discussions de fin de soirée m'auront donné beaucoup de force au cours de l'année passée. C'est pour cela que je tiens à te remercier. Tu m'as apporté l'aide émotionnelle dont j'avais besoin, jour après jour. Je sais que tu seras l'une des seules à lire ces mots et je suis sûre que ce petit paragraphe sera ta partie préférée du manuscrit. Je voudrais aussi remercier Latifa, Coline et Maëva, qui ont aussi été présentes à mes côtés et m'ont souhaité, à de nombreuses reprises, tout le meilleur pour ma thèse.

Merci à Catherine et Stéphane, pour m'avoir accueilli, de nombreuses fois, avec un bon verre de vin et un plat chaud à l'appartement. Merci pour ces grandes discussions

sur les Schtroumpfs et autres sujets passionnants. Catherine, je reviendrai te rendre visite après mon départ, tu n'oublieras pas ma tête de sitôt.

Enfin, je tiens à remercier mes parents. Merci pour votre patience, pour le champagne, pour les questions, certes un peu idiotes mais drôles, concernant mon travail en laboratoire. Merci à Pierre, qui a su être patient et me conduire aux quatre coins de l'île de France. Merci à tous les trois d'avoir été et de rester mon principal pilier.



## TABLE DES MATIERES

Résumé .....	2
Abstract .....	4
Remerciements .....	6
Table des matières .....	10
Abbreviation list .....	12
Introduction.....	16
I.    Dendritic cells: roles and subsets .....	16
A. Dendritic cells: an overview.....	16
B. Conventional dendritic cells.....	17
C. Plasmacytoid dendritic cells .....	18
D. Other types of dendritic cells .....	18
E. In vitro generation of dendritic cells.....	20
II.   Innate immune recognition and responses mediated by DCs .....	21
A. Toll-like receptors.....	21
1. Surface Toll-like receptors .....	23
2. Intracellular Toll-like receptors.....	24
B. Other pattern recognition receptors: C-type lectin receptors, Nod-like receptors and RIG-1-like receptors .....	27
C. cGAS-mediated innate recognition and STING activation.....	27
D. Innate immune responses .....	29
III.  Antigen presentation: a link to adaptive immunity.....	31
A. MHC I antigen presentation.....	31
1. Classical antigen presentation .....	32
2. Antigen cross-presentation .....	33
a. Antigen entry in endosomes/phagosomes.....	33
b. Vacuolar antigen cross-presentation .....	34
c. Cytosolic antigen cross-presentation: antigen export from phagosomes to the cytosol.....	34
d. Cytosolic antigen cross-presentation: peptide loading on MHC class I .....	36
B. MHC II antigen presentation.....	38
IV.  Adaptive immune effectors: T and B lymphocytes.....	41
A. T lymphocytes activation .....	41
1. CD8 <sup>+</sup> T lymphocytes .....	41
2. CD4 <sup>+</sup> T lymphocytes .....	42
B. B lymphocytes activation.....	43
V.   UNC93B1 and its crucial role in innate recognition and antigen presentation .....	44
A. UNC93B1 and its role in endosomal TLR signalling.....	44
1. UNC93B1 interaction with endosomal TLRs is required for their signalling.....	44

2.	UNC93B1 interaction with endosomal TLRs is required for their trafficking .....	45
3.	UNC93B1 interaction with endosomal TLRs is required for their folding .....	47
B.	UNC93B1 3d mutation .....	48
C.	Human UNC93B1 mutants in disease.....	49
D.	UNC93B1 interactome .....	50
1.	STIM1/UNC93B1 complex in MHC I antigen cross-presentation....	50
2.	STING/UNC93B1 complex in type I INF response .....	51
VI.	Endoplasmic reticulum stress and the unfolded protein response.....	52
A.	The UPR: IRE1 pathway .....	52
B.	The UPR: PERK and ATF6 pathways.....	53
VII.	The UPR role in immune cell homeostasis and responses .....	56
A.	UPR-mediated factors and IRE1 $\alpha$ role in TLR signalling.....	56
B.	IRE1 $\alpha$ /XBP1 role in B cell development .....	58
C.	Regulation of the IRE1 $\alpha$ pathway in antigen presentation.....	59
D.	The role of IRE1 $\alpha$ and PERK in cell migration .....	61
E.	UPR activation in cancer: beneficial or detrimental for the immune tumoral microenvironment?.....	62
VIII.	Thesis project .....	64
A.	Problematics on IRE1 regulation.....	64
B.	Problematics on STING regulation.....	65
C.	Thesis project.....	66
	Results.....	68
I.	UNC93B1 regulates the unfolded protein response sensor IRE1 $\alpha$ in DCs	68
II.	UNC93B1 regulates STING signalling in DCs .....	110
	Discussion and conclusion .....	120
I.	UNC93B1 association with its interactants .....	120
II.	UNC93B1 and the UPR regulate STIM1 activity.....	123
III.	IRE1 $\alpha$ activation in DCs and its impact on immune functions.....	124
A.	IRE1 $\alpha$ and antigen presentation.....	126
B.	IRE1 $\alpha$ and the tumoral immune microenvironment .....	127
C.	IRE1 $\alpha$ and TLR signalling .....	128
IV.	UNC93B1 and STING .....	129
V.	Conclusion.....	131
VI.	Materials and methods .....	132
	References .....	134
	Table des figures .....	162
	Liste des tables.....	163
	Annexes.....	164
	Résumé substantiel .....	166

## ABBREVIATION LIST

AEP: Asparagine endopeptidase	CIITA: MHC class II transactivator
AP: Adaptor protein	CITA: MHC class I transactivator
APC: Antigen presenting cell	CLEC-9A: C-type lectin domain family 9 member A
ATF6/4: Activating transcription factor 6/4	CLIP: Class II-associated li peptide
ATP: Adenosine triphosphate	CLR: C-type lectin receptor
BAK: BCL-2 antagonist/killer	COP-I/II: Coat protein I/II
BAX: BCL-2 associated X	CXCL: C-X-X motif chemokine ligand
BCL11A: B-cell lymphoma/leukemia 11A	DAMPS: Damage associated molecular patterns
BCL-2: B cell lymphoma 2	DC: Dendritic cell
BCR: B cell receptor	DNA: Desoxyribonucleic acid
BDCA: Blood dendritic cell antigen	ECD: Extracellular domain
BiP: Immunoglobulin heavy chain binding protein	eIF2 $\alpha$ : Eucaryotic translation initiation factor 2 $\alpha$
BLIMP1: B-lymphocyte-induced maturation protein 1	ER: Endoplasmic reticulum
BM: Bone marrow	ERAD: ER-associated degradation
BMDC: Bone marrow derived dendritic cell	ERAP: ER aminopeptidase
CCL: C-C motif chemokine ligand	ERGIC: ER-Golgi intermediate compartment
CCR: C-C motif chemokine receptor	ESCRT: Endosomal sorting complex required for transport
CD: Cluster of differentiation	FIt3-l: Fms-like tyrosine kinase ligand
cDC: Conventional dendritic cell	GM-CSF: Granulocyte macrophage colony stimulating factor
CDP: Common DC progenitor	Grp94: Glucose regulated protein 94
CFSE: Carboxyfluorescein succinimidyl ester	HIV: Human immunodeficiency virus
cGAMP: Cyclic GMP-AMP	HSE: Herpes simplex encephalitis
cGAS: Cyclic GMP-AMP synthase	Hsp: Heat-shock protein
CHOP: CCAAT/enhancer-binding protein homolog	HSV: Herpes simplex virus
	IgM: Immunoglobulin M



IL: Interleukin

INF: Interferon

IRAK: IL-1 receptor associated kinases

IRAP: Insulin-regulated endopeptidase

IRE1: Inositol-requiring enzyme 1

IRF: Interferon regulatory factor

LPS: Lipopolysaccharide

LRR: Leucine-rich repeats

MDSC: Myeloid derived suppressor cell

MHC: Major histocompatibility complex

MIIC: MHC-II containing compartment

Mo-DC: Monocyte-derived dendritic cell

MyD88: Myeloid differentiation primary response gene 88

NF- $\kappa$ B: Nuclear factor  $\kappa$  light chain enhancer of activated B cells

NK: Natural killer

NLR: Nod-like receptor

NLRC5: NLR Family CARD Domain Containing 5

NOX2: NADPH Oxidase 2

ORAI1: ORAI Calcium Release-Activated Calcium Modulator 1

OT-I/II: Anti-OVA T cell receptor I/II

OVA: Ovalbumin

PAMPS: Pathogen associated molecular patterns

pDC: Plasmacytoid dendritic cell

PERK: PKR-like ER protein kinase

PLC: Peptide loading complex

PRR: Pattern recognition receptor

RIDD: Regulated IRE1-dependent decay

RIG: Retinoic acid-inducible gene

RNA: Ribonucleic acid

ROS: Reactive oxygen species

SAVI: STING-associated vasculopathy with onset in infancy

SLE: Systemic lupus erythematosus

SOCE: Store operated calcium entry

STIM1: Stromal interaction molecule 1

STING: Stimulator of interferon genes

SYK: Spleen associated tyrosine kinase

TAP: Transporter association with antigen processing

TAPBP: TAP-binding protein

TBK1: Tank binding kinase 1

TCR: T cell receptor

TERS: Transmissible ER stress

TFEB: Transcription factor EB

TG: Thapsigargin

TGF $\beta$ : Transforming growth factor  $\beta$

Th: T helper cell

TIR: Toll/IL-1 receptor

TLR: Toll-like receptor

TM: Tunicamycin

TNF $\alpha$ : Tumour necrosis factor  $\alpha$

TOLLIP: Toll-interacting protein

TRAIL: TNF-related apoptosis-inducing ligand

TRIF: TIR domain containing adaptor protein inducing INF $\beta$

UNC93B1: UNC 93 homolog B1

UPR: Unfolded protein response

WT: Wild-type

XBP1: X-box binding protein 1

XCR1: X-C motif chemokine receptor 1



## INTRODUCTION

### **CHAPTER I: Dendritic cells: roles and subsets.**

The concept of immunology arose at the end of the XIX<sup>th</sup> century, when the predominant paradigm upon the occurrence of infectious diseases was the germ theory, suggested by Louis Pasteur and Robert Koch. This theory brought the notion that pathogens were the only actors and causality of infectious diseases, while it disregarded possible host defences. However, several scientists had different opinions and various works highlighted the existence of host protection against pathogens. E. Metchnikoff was the first to describe macrophages and neutrophils as potent phagocytes, able to uptake and kill microbes. While E. Metchnikoff introduced innate immunity, two other immunologists, E. Behring and P. Ehrlich described antibodies, their role in pathogen elimination and their specificity against the infectious agent. As the mechanisms and immune cells involved in adaptive immunity became a work of interest for many scientists, describing the role of T and B lymphocytes, the link between innate and adaptive immunity remained obscure. In the process of studying T cells, P. Doherty and R. Zinkernagel reported that antigen recognition by T lymphocytes was mediated by major histocompatibility complex (MHC) molecules (Zinkernagel and Doherty, 1979). This process was described to happen through antigen presenting cells (APCs), though their characteristics remained unclear. C. Janeway Jr. later described key innate immune receptors known as pattern recognition receptors (PRRs) which, upon encounter of pathogens, initiate activation and maturation of APCs (Janeway and Medzhitov, 2002). These discoveries along with description of dendritic cells (DCs) by R. Steinman, provided a strong link between innate and adaptive responses. Indeed, DCs express a wide range of PRRs allowing them to recognise infectious microbes and mediate potent T cell activation.

#### A. Dendritic cells: an overview

Dendritic cells were first described in 1973 (Steinman and Cohn, 1973) while the link between innate and adaptive immunity was still unclear. Steinman et al. observed a novel cell type in mouse peripheral lymphoid organs, distinct from monocytes or macrophages, by phase contrast microscopy followed by electronic microscopy. They

were then called dendritic cells because of their morphology, as they form tree-like extensions or dendrites. The same group later described the role of DCs in the activation of T lymphocytes (Steinman and Cohn, 1974), linking them to adaptive immunity. During inflammation, DCs were also shown to recognise a variety of microbial antigens through PRRs, enabling them to mature, to secrete pro-inflammatory cytokines and to express co-stimulatory molecules for efficient T cell activation.

Dendritic cells are localised in secondary lymphoid organs, such as the spleen and lymph nodes, as well as in peripheral tissues, and in various non-lymphoid organs or in blood. In peripheral tissues, they are referred to as sentinel cells as they are one of the first immune cells to actively recognise pathogens and initiate immune defences. DCs were described to originate from myeloid precursors that give rise to a common DC progenitor (CDP) in the bone marrow, and can then differentiate into different pre-DC subsets in blood and in tissues (Geissmann et al., 2010).

DCs can be divided in two main categories: resident DCs and migratory DCs. Resident DCs are located in secondary lymphoid organs and keep an immature state at steady state, with low expression of co-stimulatory molecules. Migratory DCs can be found in peripheral tissues and non-lymphoid organs. They can migrate to lymph nodes through the lymph and acquire a mature state characterised by high levels of co-stimulatory molecules (Segura, 2016).

#### B. Conventional dendritic cells

Whether they are resident or migratory, DCs can be divided in a variety of subpopulations. Conventional DCs (cDCs) are short-lived and constantly renewed from bone marrow precursors. They can be separated into two subsets: cDC1 and cDC2. cDC1s were described to be especially efficient to activate cytotoxic T lymphocytes in response to viral infections and tumour cells. In mice, they're characterised by their dependence on the transcription factors Batf3 and IRF8 for their development and express specific DC markers such as XCR1 and Clec9A, as well as CD8a for resident cDC1s (Croizat et al., 2010; Bachem et al., 2012). In human, cDC1s express other specific markers such as CD141 and BDCA3 (Dzionek et al., 2000; Robbins et al., 2008). They were shown to be a rare population and represent around 10% of DCs in the blood (Segura, 2016). In both mouse and human, cDC1s were

described to be the main cell type performing MHC class I antigen cross-presentation, a crucial process in anti-viral and anti-tumoral immunity, described later in chapter 3 of the introduction. This role of cDC1s was highlighted in mice deficient for Batf3 (Hildner et al., 2008), showing no cDC1 development and failure to cross-present antigens.

cDC2s were shown to be efficient in helper T cell activation, inducing mostly Th2 and Th17 responses, mainly involved in extracellular pathogens elimination. In mice, they express specific markers such as CD11b and CD172a while their development is dependent on the transcription factors IRF4 and RelB. In human, they also express specific markers such as CD1c and BDCA1. They represent a high percentage of DCs in the blood, between 40 and 45% (Geissmann et al., 2010; Segura, 2016; Anderson et al., 2021).

### C. Plasmacytoid dendritic cells





Plasmacytoid DCs (pDCs) are long lived cells, mostly reported as resident DCs, but can also be recruited to peripheral tissues and migrate during inflammation. They were first described in human and called Interferon-producing cells (IPC), as they specialise in type I interferon responses which is an essential feature of anti-viral immunity (Siegal et al., 1999; Cella et al., 1999). In mice, their development is dependent on the transcription factors BCL11A and E2-2 and they specifically express Siglech and CD317. Mouse pDCs have been portrayed to be poorly efficient at antigen presentation and T cell activation in comparison to cDCs, though human pDCs can present antigens and activate Th1 responses. In human, they specifically express BDCA2 and BDCA4 (Dzionek et al., 2000), differentiating them from other peripheral blood mononuclear cells (PBMCs) in the blood, where they represent around 40% of DCs.

### D. Other types of dendritic cells

Apart from the three main DC subtypes mentioned above, other DC populations have been described, such as Langerhans cells or monocyte derived DCs. Murine Langerhans cells can be found in skin and mucosa, that they colonised before birth as they are derived from embryonic monocytes (Hoeffel et al., 2012). In both human and mouse, they can migrate to lymph nodes and are potent T helper cells activators (Romani et al., 1989). Human Langerhans cells come from a different lineage than conventional DCs and monocytes. They differentiate from hematopoietic precursors

present in the skin and in mucosal tissues before birth. In contrast to mouse Langerhans cells, this human DC subset can cross-present antigens to activated CD8 T cells.

DCs can also be generated from blood monocytes and are then referred to as monocyte-derived DCs (mo-DCs) or inflammatory DCs (Geissmann et al., 2003; Auffray et al., 2007). In both human and mouse, monocyte differentiation into DCs mostly happen in context of infection or sterile inflammation, leading to monocyte recruitment to the site of inflammation and expression of DC markers such as MHC class II, CD11b in mouse or CD1c in human. Mo-DCs also display effective DC functions as migration to secondary lymphoid organs or antigen presentation (Segura, 2016).

	 cDC1	 cDC2	 pDC	 moDC
<b>Main role and localisation</b>	<ul style="list-style-type: none"> <li>• Antigen cross-presentation</li> <li>• TCD8 priming</li> <li>• TLR3 signalling</li> </ul> Spleen, lymph nodes, peripheral tissues	<ul style="list-style-type: none"> <li>• TCD4 priming</li> <li>• Th2/Th17 induction</li> </ul> Spleen, lymph nodes, peripheral tissues	<ul style="list-style-type: none"> <li>• Type I IFNs production</li> <li>• Efficient anti-viral responses</li> </ul> Spleen, lymph nodes, blood	<ul style="list-style-type: none"> <li>• Humoral immunity - T follicular helper cells activation</li> </ul> Peripheral tissues, blood, lymph nodes
<b>Markers</b>				
<b>Mouse</b>	XCR1, Clec9A, CD8 (resident), CD103	CD11b, CD172a, CD206 (migratory)	Siglec H, CD317, B220	CD14, CD64, CD11b, CD172a
<b>Human</b>	XCR1, Clec9A, CD141	CD1c, CD11b, CD172a	CD303, CD304, CD123	CD14, CD64, CD1a, CD1c
<b>Transcription factors</b>	IRF8, Batf3, ZBTB46	IRF4, ZBTB46	IRF4, IRF7, IRF8	IRF4, ZBTB46

**Figure 1: Dendritic cell (DC) subsets characteristics in human and mouse.** The main DC subtypes found in the organism are conventional DCs (cDCs), plasmacytoid DCs (pDCs) or monocyte derived DCs (moDCs). They each have their own characteristics and markers in human and mouse.

### E. In vitro generation of dendritic cells

Human mo-DCs can be generated *in vitro*, by culturing PBMCs with GM-CSF together with IL-4, inducing mainly CD1c and CD1a-expressing DCs that efficiently present soluble antigens to naïve T cells (Sallusto and Lanzavecchia, 1994). Other cytokine combinations can be used along with GM-CSF such as IL-7, leading to expression of MHC II, CD1c, co-stimulatory molecules and CD21 by mo-DCs. These cells mediate efficient CD4<sup>+</sup> T cell activation and strong CD8<sup>+</sup> T cell cytotoxic activities (Takahashi et al., 1997). INF $\alpha$  together with GM-CSF generates tumor necrosis factor (TNF)-related apoptosis-inducing ligand (TRAIL)-expressing DCs, showing strong helper T cell activation and efficient responses against HIV infection (Santini et al., 2000). Lastly, a combination of IL-4 and IL-2 with GM-CSF induces mo-DCs secreting high levels of IL-12, IL-1 $\beta$  and TNF $\alpha$  that help the priming of helper T cells (Sanarico et al., 2006).

In mice, while important, the DC population is quite rare in the whole organism and in secondary lymphoid organs, where other cell types represent much larger populations. It is then difficult to purify primary DCs directly from tissues as the spleen. To cope with this difficulty, DCs can be generated *in vitro* or DC cell lines can be used. In mice, DCs can be differentiated *in vitro* from bone marrow (BM) precursors with specific cytokines. The cell type induced is then called bone marrow derived dendritic cell or BMDC. For instance, bone marrow cells can be cultured with the cytokine GM-CSF, generating CD11c positive BMDCs able to present antigens. Another way is to culture BM precursors with Flt3-ligand, cytokine promoting DC survival and differentiating the precursors into cDC1-like and mostly cDC2-like BMDCs. While with this technique, DCs are able to efficiently present antigens and acquire some of the markers expressed by cDC1s and cDC2s *in vivo*, such as CD11c, CD8a or CD11b, they do not express all the markers and the percentage of cDC1-like generated cells is quite low. To cope with this, a technique to generate BMDCs using NOTCH-signalling and Flt3-ligand was proposed (Kirkling et al., 2018). In this method, OP9 stromal cells expressing the NOTCH receptor DL-1 are co-cultured with bone marrow precursors along with Flt3-ligand. This technique gives rise to a high percentage of cDC1-like BMDCs, which were reported to be the closest to splenic cDC1s, phenotypically speaking.



## **CHAPTER II: Innate immune recognition and responses mediated by DCs.**

Innate immunity is characterised by the immediate recognition of non-self or danger signals, such as pathogens or tumoral cells, by myeloid cells. This recognition leads to secretion of pro-inflammatory cytokines and chemokines by myeloid cells, activating and attracting surrounding immune cells. A pro-inflammatory environment then arises to eliminate the detected danger.

As mentioned previously, DCs are important innate immune actors as they display a large variety of PRRs and are able to recognise and respond to many pathogen-associated molecular patterns (PAMPs) or damage-associated molecular patterns (DAMPs). PAMPs are rather conserved motifs expressed by most microbes and pathogens an organism can encounter, as lipopolysaccharide (LPS) on gram negative bacteria or unmethylated CpG motifs in microbial DNA. DAMPs are products generated through cellular damage, such as extracellular nucleotides or extracellular heat-shock proteins.

### **A. Toll-like receptors**

PRRs are present in various cell types, from DCs and macrophages to endothelial and epithelial cells. Within PRRs, one family of receptors has been widely described: Toll-like Receptors (TLRs). 10 different TLRs can be found in human and 12 in mouse, each recognising and responding to various microbial patterns. The Toll gene was discovered in 1985 in *Drosophila melanogaster* (Anderson et al., 1985), where it was described to code for a transmembrane Toll protein (Hashimoto et al., 1988). It was then observed that its cytoplasmic domain showed homology with the human IL-1 receptor (Gay and Keith, 1991) and that *Drosophila* Toll displayed anti-fungal actions (Lemaitre et al., 1996).

It was later, in 1997, that the team led by Charles Janeway described the first human homologue of the *Drosophila* Toll, called human Toll, in macrophages (Medzhitov and Janeway, 1997). The same group then described the role of human Toll in controlling NF- $\kappa$ B activation to induce pro-inflammatory cytokines secretion and co-stimulatory molecules expression by Jurkat T cells (Medzhitov et al., 1997). Not long after, the group of Bruce Beutler studied mice resistant to LPS and highly susceptible to gram-

negative bacteria infections. They discovered mutations located in the *Tlr4* locus, and human Toll was then associated to TLR4 while its involvement in LPS recognition was highlighted (Poltorak et al., 1998).

TLRs engage ligands present in the extracellular milieu or in endosomes by their highly conserved extracellular domain (ECD) composed of Leucine-rich repeats (LRR). Their cytoplasmic Toll/IL-1 receptor (TIR) domain relays an intracellular signal via the TIR-containing adaptor molecules MyD88 or TRIF (Beutler, 2004; Lin et al., 2010). The TLR-TIR domain contains highly conserved regions divided in three boxes: box 1 (F/Y)DA, box 2 RDXXPG and box 3 FW (Figure 2). In box 1 (F/Y)DA, tyrosine residues in position 647, 680 and 870 are conserved in all TLRs except 1,6 and 12 and are phosphorylated upon ligand binding to mediate MyD88 recruitment to TLR4 (Medvedev et al., 2007) and, in the case of Y870, to stabilise mature TLR9 (Biswas et al., 2018). TLR-MyD88-dependent signalling involves the recruitment and activation of IL-1 receptor-associated kinases (IRAKs). Depending on the cell type, this leads to the activation of NF- $\kappa$ B, mitogen-activated kinases and/or interferon regulatory factor (IRF) transcription factors which in turn initiate different transcriptional profiles shaping subsequent immune responses (Figure 3).

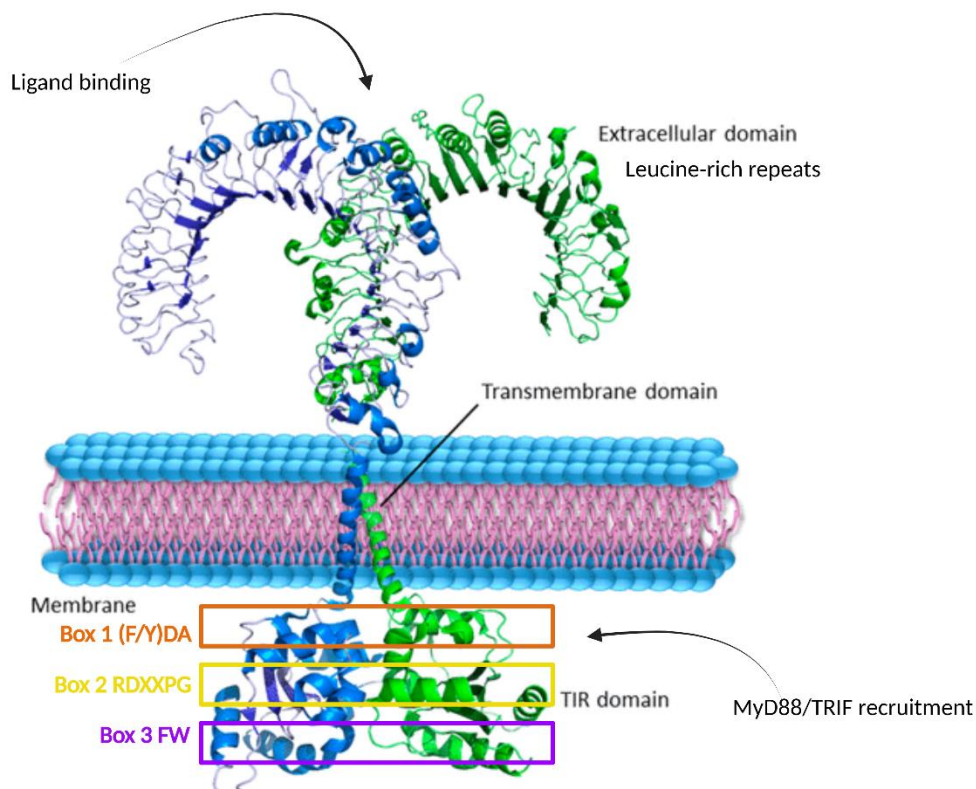


**Figure 2: A toll-like receptor dimer structure.** TLRs assemble in dimers to bind their ligand and activate their signalling. Their cytosolic domain contains a TIR domain, necessary for the recruitment of the adaptors MyD88 or TRIF. Image from: Federico et al., 2020. Modulation of the innate immune response by targeting Toll-like receptors: A perspective on their agonists and antagonists. *J. Med. Chem*, 63, 22, 13466–13513. <https://doi.org/10.1021/acs.jmedchem.0c01049>.

TLRs are all synthesised in the endoplasmic reticulum (ER), where their glycosylation, folding and quality control occur. Once correctly formed, they traffic through the Golgi apparatus to their final destination, where they can encounter their ligands. The majority of TLRs form homodimers upon simultaneous ligand recognition; heterodimers are only formed by TLR2, with either TLR1 or TLR6 and TLR11 with TLR12. After ligand binding, their activation triggers the production and secretion of various pro-inflammatory cytokines and the increased expression of co-stimulatory molecules on APCs, making them prone to induce adaptive immunity. TLRs have been divided in two main categories: surface TLRs and endosomal/intracellular TLRs.

#### 1. Surface Toll-like receptors

Surface TLRs include TLR1, 2, 4, 5, 6 in both human and mouse and TLR10 in human. TLR4 recognises lipopolysaccharide (LPS), and is therefore able to respond to a large variety of Gram-negative bacteria. TLR5 binds to the bacterial protein flagellin, present on multiple Gram-positive and negative bacteria. TLR2 associates with TLR1 or TLR6 to signal and recognises lipopeptides from Gram-positive bacteria. Most surface TLRs signal through the adaptor protein MyD88 which is recruited by their TIR domain upon ligand binding and forms with IRAK-4 “the Myddosome”, starting a signalling cascade to activate NF- $\kappa$ B which in turns triggers the production of pro-inflammatory cytokines such as IL-6, IL-8 or TNF $\alpha$ . MyD88 also initiates the production of type I interferons (INF) by phosphorylating interferon regulatory factors (IRF) 5 or 7. TLR4 also recruits TRIF, another adaptor protein, activating NF- $\kappa$ B and phosphorylating IRF3 for type I INFs production (Yamamoto et al., 2002; Barton and Medzhitov, 2003; Moresco et al., 2011). To activate TRIF signalling, TLR4 is internalised in a dynamin-dependent pathway to endosomes (Kagan et al., 2008). Dynamin GTPases have been shown to mediate plasma membrane invaginations to form early endosomes. Upon ligand binding, TLR4 primarily signals through MyD88 at the plasma membrane and is further able to activate TRIF signalling in early endosomes (Figure 3).

## 2. Intracellular Toll-like receptors

Intracellular TLRs traffic from the ER to the endosomes, where their signalling pathway can be activated. Among them, we find TLR3, 7, 8, 9 in both human and mouse and 11, 12 and 13 in mouse. Most of them are specialised in nucleic acid recognition and were reported to be particularly efficient against viral infections. TLR9 is specific for double-stranded DNA detection, especially unmethylated CpG motifs (Hemmi et al., 2000) which are largely present in microbial DNA in comparison to mammalian DNA. TLR9 signalling is efficient in response to DNA viruses such as mouse cytomegalovirus (Krug et al., 2004a) and herpes simplex virus (Krug et al., 2004b) infections. TLR7 and TLR8 recognise single-stranded RNA (Diebold et al., 2004; Heil et al., 2004), and particularly guanosine and uridine-rich RNA, present in viruses as human immunodeficiency (HIV) or Influenza viruses. TLR7 and 9 are widely expressed by murine DCs, while TLR9 is barely expressed in human DCs. However, both TLR7 and 9 were reported to be exclusively present in human and murine pDCs, where they efficiently signal for type I interferon responses (Lund et al., 2003; Coccia et al., 2004). TLR7 and 9 recruit MyD88 to trigger their activation cascade. TLR3, on the other hand, is specific to cDC1s (Lauterbach et al., 2010), where TLR3 expression is higher than in other DCs. This receptor is specialised in double-stranded RNA recognition (Alexopoulou et al., 2001) and recruits the adaptor protein TRIF for its signalling (Blasius and Beutler, 2010; Moresco et al., 2011) (Figure 3).

Less described, TLR11 and 12 induce potent innate responses against parasites, as *Toxoplasma Gondii*. Indeed, they recognise the protein profilin and initiate IL-12 production, required for efficient parasite elimination (Yarovinsky et al., 2005; Koblansky et al., 2013). TLR13, as TLR11 and TLR12, has been shown to be only expressed in mice and is mostly found in splenic macrophages and DCs. TLR13 specifically recognises and responds to vesicular stomatitis virus (Shi et al., 2011). TLR11, 12 and 13 signal through MyD88, triggering NF- $\kappa$ B-dependent pro-inflammatory cytokine secretion and potent interferon responses.

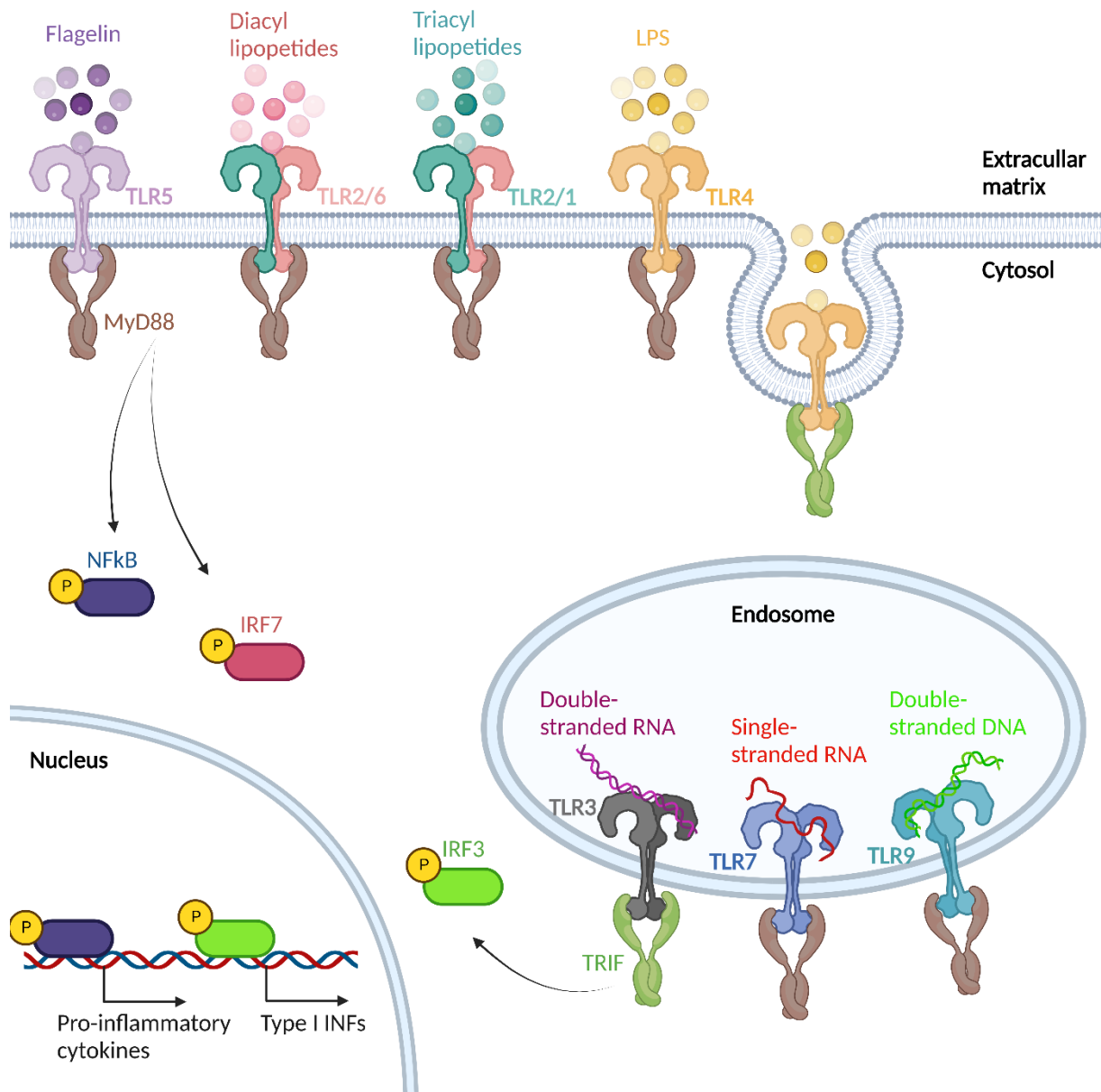


**Figure 3: Surface and endosomal Toll-like receptors (TLRs) signalling.** Once TLRs bind their ligand, they recruit MyD88 or TRIF and activate the transcription factors NF-κB or IRF to induce the production of pro-inflammatory cytokines and type I interferons.

An important part of ligand binding on endosomal TLRs is the internalisation of pathogens by the cell, and various pathways have been highlighted. Among them, direct viral infection can lead to engulfment of viral nucleic acids inside the endosomes. Cells can also perform phagocytosis or macropinocytosis, in which DCs can uptake big extracellular particles or large amounts of extracellular fluid (Blasius and Beutler, 2010).

Intracellular TLR trafficking from the ER to endosomes is another crucial step for their activation. They rely in Adaptor proteins (APs), which mediate the uptake of various cargoes into endosomes or lysosomes in a clathrin-dependent way, and chaperones for their trafficking. Indeed, AP-2 seems to be necessary for TLR9 to traffic to endosomes and AP-3 for TLR9 to translocate to late lysosome related organelles. Lack of AP-3 in DCs and macrophages leads to the restriction of TLR9 in VAMP3<sup>+</sup> early endosomes and inhibits its translocation to LAMP1<sup>+</sup> lysosomes. AP-3 is localised in the trans-golgi network and in VAMP3<sup>+</sup> endosomes where it interacts with TLR9 upon stimulation. This complex translocates further to late LAMP1<sup>+</sup> lysosomes. Furthermore, inhibition of TLR9 translocation to LAMP1<sup>+</sup> compartments suppresses recruitment of TRAF3 and IRF7 to MyD88, and leads to a lack of type I INF signalling after TLR9 stimulation. These data indicate a need for TLR9 to traffic to LAMP1<sup>+</sup> lysosomes to promote type I INFs, through its interaction with AP-3 (Sasai et al., 2010a). However, AP-3 deficiency does not impact NF- $\kappa$ B signalling, and IL-12 production and secretion remain unchanged compared to wild type cells. This data led to the conclusion that NF- $\kappa$ B signalling must occur in early VAMP3<sup>+</sup> compartments. Furthermore, AP-3 deficiency also decreases TLR7-mediated type I INF production, though its trafficking to endosomes was not assessed. Intracellular TLR trafficking was also described to be dependent on chaperone proteins such as Grp94 which is necessary for TLR1, 2, 4, 5, 7 and 9 signalling (Wu et al., 2012), PRATA4 which mediates the traffic of TLR1, 2, 4, 7 and 9 (Takahashi et al., 2007), and UNC93B1 which was shown to interact with the endosomal TLRs 3, 7, 8, 9, 11, 12 and 13 to allow their trafficking to endosomes and their correct folding in the ER (Tabeta et al., 2006; Kim et al., 2008) (chapter 5).

Once they reach the endosomes, the ECD of intracellular TLRs are cleaved to induce their signalling cascade. It has indeed been reported for TLR3, 7 and 9, mainly in DCs and macrophages (Ewald et al., 2008; Garcia-Cattaneo et al., 2012; Hipp et al., 2013). Nucleic acid sensing TLRs processing is carried throughout two distinct steps. The first step is mediated either by asparagine endopeptidase (AEP) (Sepulveda et al., 2009a) or cathepsins (Park et al., 2008) which cleave LRR15 and remove the majority of the TLR ECD. The second step consists in final trimming of this ectodomain and is regulated by cathepsins (Ewald et al., 2011).

While endosomal TLRs recognise efficiently microbial nucleic acids, they can also be stimulated by host DNA or RNA. Nucleic acid sensing TLRs presence in endosomes

was defined to be a mechanism preventing possible autoimmune reactions as, in normal conditions, host nucleic acids do not reach these compartments and are degraded in the cytoplasm by active nucleases. Despite this, some intracellular TLRs have been associated with autoimmune diseases. TLR7 has been linked to systemic lupus erythematosus (SLE), characterised by recognition of self-RNA and production of self-antibodies by B cells (Christensen et al., 2006; Fairhurst et al., 2008). Recently, TLR7 was directly associated to lupus in human and mouse as a gain-of-function of a TLR7 variant led to SLE development (Brown et al., 2022). Although TLR7 was reported to promote the disease, TLR9 was said to be rather protective.

#### B. Other pattern recognition receptors: C-type lectin receptors, Nod-like receptors and RIG-1-like receptors

While TLRs have been the most studied innate immune receptors, other PRRs are expressed in cells and allow various microbial recognition. C-type lectin receptors (CLRs) are transmembrane PRRs specialised in fungi recognition, although they are also able to respond to bacterial and viral infections. The family of Nod-like receptors (NLRs) counts numerous members, all localised in the cytoplasm. Two of them, NOD1 and NOD2 can directly recognise specific PAMPS, and are specialised in bacteria peptidoglycans detection. Once activated, they trigger NF- $\kappa$ B and IRF3/7 pathways. Other NLR members, such as NLRP3, require two signals for their activation: the first one being most often microbial detection through TLRs and the second one being any cellular stress released by damaged cells. Their activation leads to their oligomerisation and inflammasome formation, which can then trigger secretion of IL-1 $\beta$  and IL-18 (Wen et al., 2013). Retinoic acid-inducible gene (RIG-1)-like receptors are also localised in the cytoplasm and are activated by viral double-stranded RNA, eliciting INF production (Takeuchi and Akira, 2010).

#### C. cGAS-mediated innate recognition and STING activation

Cyclic GMP-AMP synthase (cGAS) is an important innate receptor involved in high type I INF responses following microbial infections (Sun et al., 2013). cGAS is localised in the cytosol and can bind to double stranded DNA released by viruses or cellular damage. DNA binding to cGAS leads to the production of cyclic GMP-AMP (cGAMP) which can be then detected by the stimulator of interferon genes (STING), a transmembrane ER protein (Ablasser et al., 2013). Following cGAMP binding, STING

translocates to the Golgi apparatus where it activates TBK1, or Tank binding kinase 1, which phosphorylates itself (Shang et al., 2012; Zhang et al., 2019). pTBK1 then phosphorylates STING and IRF3 (Liu et al., 2015; Zhao et al., 2016). Phosphorylation of IRF3 leads to its dimerization and translocation to the nucleus, inducing type I INF production. Moreover, pTBK1 also leads to NF- $\kappa$ B activation which induces the production of pro-inflammatory cytokines (de Oliveira Mann et al., 2019) (Figure 4). Finally, STING is ubiquitinated and targeted for degradation by the proteasome or by lysosomal proteases after a COP-I-mediated transport from ER-Golgi intermediate compartment (ERGIC) to lysosomes (Hopfner and Hornung, 2020).

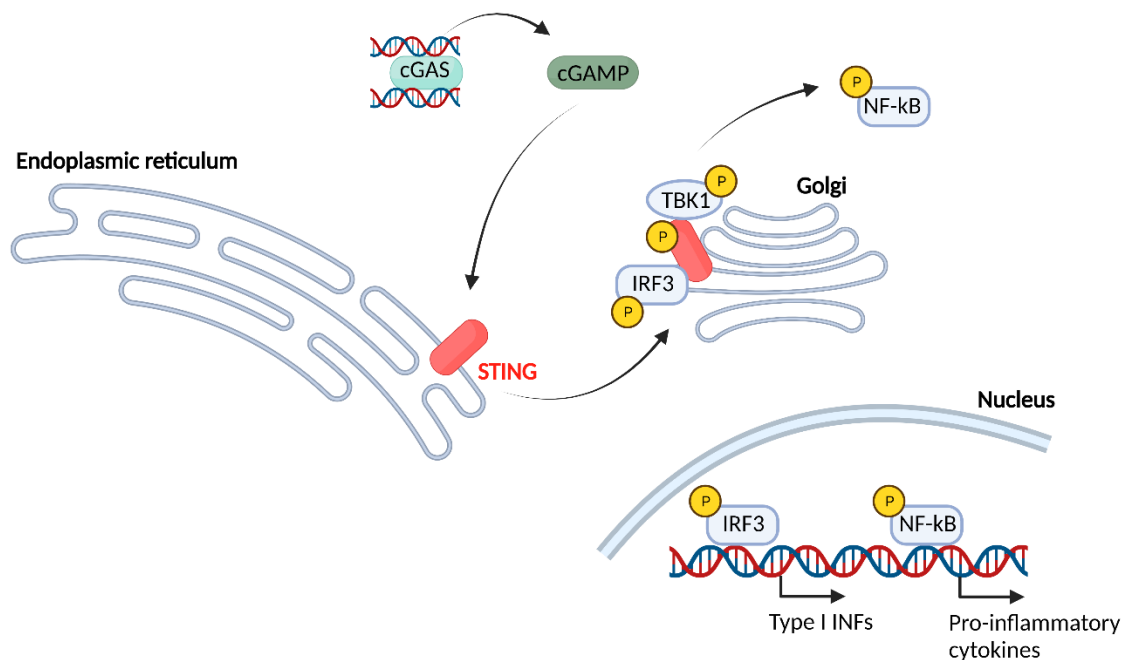


**Figure 4: STING signalling pathway.** cGAS binds dsDNA and generates cGAMP that in turns activate STING. STING translocates to the Golgi and induces activation of TBK1, IRF3 and NF- $\kappa$ B for production of type I INFs and pro-inflammatory cytokines.

Factors regulating STING signalling pathway in cells are then important to induce efficient immune responses to pathogenic DNA, but also to stop this reaction from getting overly or chronically activated. Indeed, gain-of-function mutants of STING have been involved in autoimmune disorders and interferonopathies. Several of these mutations were described in children suffering from systemic inflammation and were referred to as SAVI (STING-associated vasculopathy with onset in infancy) (Liu et al.,



2014). Another STING-mediated interferonopathy, the COPA syndrome, is generated by a mutation in the COPA gene, coding for a COP-I complex protein, COP- $\alpha$ . This mutation leads to impaired COP-I vesicles-mediated transport and blocks STING degradation. STING then remains in the Golgi apparatus after its activation and continuously induces type I INF production (Deng et al., 2020).

Despite abundant literature, the regulation of STING remains unclear, especially in myeloid cells. In this regard, STING has been described to associate with STIM1 in the ER, keeping STING in an inactive state. STIM1 is an ER calcium sensor, controlling calcium influx in this organelle. Mechanistically, STIM1 retains STING in the ER, and the absence of STIM1 in macrophages leads to STING translocation to the Golgi and its activation at the steady state (Srikanth et al., 2019). Thus, STIM1 deficiency leads to autoimmune-like disorders with high type I INF responses. In addition, STING also associates with TOLLIP, a cytosolic adaptor protein modulating IL-1 receptor and TLR-NF- $\kappa$ B signalling. TOLLIP stabilises STING at steady state by preventing its degradation in lysosomes (Pokatayev et al., 2020).

Although the main steps of STING signalling pathway have been identified, still unanswered questions remain on the trafficking and degradation of activated STING. Indeed, whether STING needs to translocate to the Golgi in order to activate TBK1 is unclear, although we know that this step is necessary for type I INF production. In addition, while STING migration from the Golgi to the lysosomes is required for its degradation after activation, the turnover kinetics of the protein remain unclear. It is then of interest to study STING interacting partners, in order to better understand the tight regulation of this innate immune receptor.

#### D. Innate immune responses

Following PRRs activation, DC orchestrate a maturation program leading to the increased expression of co-stimulatory molecules, MHC molecules, chemokine receptors and secretion of cytokines and chemokines which result in priming of T lymphocytes. Pro-inflammatory cytokines such as IL-6, TNF $\alpha$  and IL-1 $\beta$  play a crucial role in T and B cell priming and proliferation, while type I INFs are mainly involved in anti-viral responses. Also secreted by DCs, IL-12 and IL-23 are involved in T lymphocyte differentiation into Th1 and Th17 respectively. In contrast, IL-10 leads to the development of regulatory T cells. DCs also migrate to secondary and tertiary

lymphoid organs after maturation thanks to the chemokine receptor CCR7. Moreover, DCs secrete various chemokines as CCL3, CCL4 or CXCL10 (Sallusto et al., 1999), not only inducing their migration but also recruiting B and T cells, neutrophils, monocytes, or other types of DCs in secondary lymph nodes.

DCs can either positively regulate T cell responses, inducing effector T cells, through the expression of CD80, CD86 or CD40 or negatively regulate T lymphocyte responses and lead to tolerance, by the upregulation of PDL-1 or PDL-2. DC maturation also decreases their antigen uptake capacities but increases their ability to process antigens. Except for cDC1s, they upregulate the factor TFEB after maturation. TFEB overexpression leads to an enhanced lysosomal proteases activity, decreasing the lysosomal pH and increasing antigen degradation. Even though DC maturation and activation are often linked, both terms remain separated. Indeed, DCs can sense pro-inflammatory signals, such as TNF $\alpha$ , from surrounding cells and upregulate several co-stimulatory molecules without fully maturing. Following that, they secrete IL-10 and induce tolerogenic T cell responses (Menges et al., 2002).

DCs also have cytotoxic activities. Indeed, they are able to secrete TNF $\alpha$  which, when bound to its receptor TNFR1, induces the cleavage of procaspases and cellular apoptosis (Wong et al., 1992; Ding et al., 2011). While DC cytotoxic activity is not as strong as NK or CD8<sup>+</sup> T cells capacities, this process was shown to be efficient against tumoral and viral infected cells. Stimulated DCs can also upregulate TRAIL to induce tumoral cell death. TRAIL binds to its receptors TRAILR1 or TRAILR2 to promote apoptosis in tumoral cells (Falschlehner et al., 2009; Kalb et al., 2012).

### **CHAPTER III: Antigen presentation: a link to adaptive immunity.**

Altogether, DCs activation and maturation through microbial or cell damage recognition leads to secretion of pro-inflammatory cytokines and high expression of co-stimulatory molecules, such as CD80, CD86 or CD40. Co-stimulatory molecules have specific receptors or ligands expressed on T cells and constitute a part of the signalling necessary for T cell priming and activation. Another signal is required for T cell activation to specific antigens: antigen presentation on major histocompatibility complex (MHC) molecules. While antigen presentation through MHC molecules is referred to as the primary signal or signal 1 for T cell activation, co-stimulatory interactions constitute what is called the signal 2. In the organism, two different types of MHC molecules are expressed: MHC class I which stimulates CD8<sup>+</sup> or cytotoxic T cells and MHC class II activating CD4<sup>+</sup> or helper T cells.

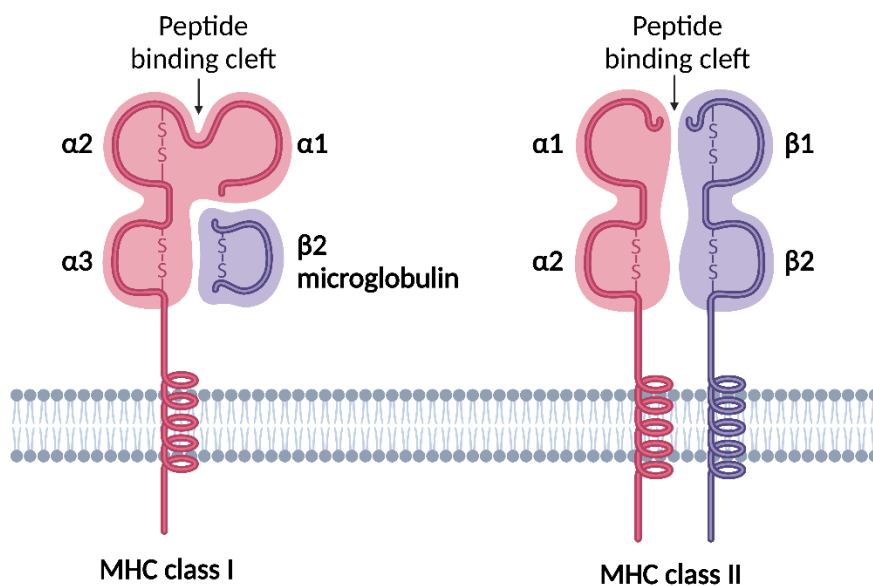


**Figure 5: Major histocompatibility complex (MHC) molecules class I and II structures.** Both MHC molecules are transmembrane proteins composed of two chains,  $\alpha$  and  $\beta$ .

#### **A. MHC class I antigen presentation**

MHC I antigen presentation allows priming and activation of cytotoxic T cells, leading to killing of infected or tumoral cells. MHC I is expressed in all nucleated cells, though T cell priming needs further activation signals through co-stimulatory molecules

expressed by professional antigen-presenting cells (APCs) such as DCs, macrophages or B cells. Once primed, cytotoxic T cells can then recognise infected or tumour-modified cells to induce their apoptosis.

### 1. Classical antigen presentation

More than abnormal or pathogenic peptide recognition by CD8<sup>+</sup> T cells, MHC I also presents normal peptides, displaying the healthy status of the cell. Classically, MHC I is therefore an indicator of the cell's state, whether it's infected, tumoral or healthy, by presenting endogenous antigens and triggering or not cytotoxic T cell responses. MHC I molecules are transmembrane heterodimers composed of a heavy chain  $\alpha$  and a light chain,  $\beta$ 2-microglobulin (Townsend et al., 1989) (Figure 5). They are folded in the endoplasmic reticulum where the heavy chain is first bound to calnexin, promoting its stability before its association with the  $\beta$ 2-microglobulin. In addition, before peptide loading in the ER, the MHC I heterodimers tightly associate with two ER chaperones, ERp57 and calreticulin, to preserve them from degradation.

Before peptide binding, endogenous proteins need to be ubiquitinated and processed by the proteasome in the cytoplasm. Generated peptides can then enter the ER through a transporter called TAP, an heterodimer composed of TAP1 and TAP2, that shifts conformation when linking a peptide with high affinity, allowing its entry into the ER lumen. Once in the ER, some peptides need to be trimmed as MHC I molecules allow binding of 8 to 10 amino acid peptides and longer peptides are generated by the proteasome. ER aminopeptidases (ERAP in human or ERAAP in mouse) are required for this step while peptides that fail to bind MHC I molecules are eliminated through ER-associated degradation (ERAD) (Joffre et al., 2012; Mantel et al., 2022).

For correct peptide loading on MHC I, several proteins and chaperones are required, allowing MHC I molecules stability and peptide binding. This group of proteins is called the peptide loading complex (PLC), comprising of factors as ERp57, calreticulin, TAP or TAPBP (tapasin or TAP-binding protein) (Neefjes et al., 2011; Blees et al., 2017). TAPBP mediates peptide loading by linking MHC I to TAP and selecting peptides with high affinity for antigen presentation. TAP or TAPBP deficient cells fail to present antigens to CD8<sup>+</sup> T cells. Indeed, in these cells, peptides fail to enter the ER, MHC I molecules folding is impaired or low affinity peptides are presented to T cells, leading to a weaker immune response. The PLC is also needed for exit of loaded MHC

I molecules from the ER and further trafficking to the plasma membrane. Indeed, TAPBP and calreticulin were shown to prevent incorrectly loaded MHC I molecules to leave the ER.

Once MHC I-peptide complexes leave the ER, they reach the ERGIC where they go through further quality control before reaching the cis-Golgi, and finally the plasma membrane (Figure 6).

The expression of MHC I and the TAP subunit TAP1 have been reported to be under the control of the transcription factor CITA (MHC class I transactivator) or NLRC5 (Meissner et al., 2010). NLRC5 expression is mostly controlled by interferon  $\gamma$  production but can also be induced after viral infection or TLR activation. However, NLRC5-dependent MHC I expression is not clear, as some authors reported normal MHC I expression in NLRC5<sup>-/-</sup> splenocytes and macrophages stimulated with INF $\gamma$ , indicating the involvement of another pathway (Robbins et al., 2012).

## 2. Antigen cross-presentation

Although MHC I was classically described to be specialised in endogenous antigen presentation, another pathway showed great importance in anti-viral and anti-tumoral responses. Called MHC class I antigen cross-presentation, this pathway relies on the loading of exogenous peptides on MHC I molecules (Carbone and Bevan, 1990). While all nucleated cells do express MHC I molecules, not all cells have the ability to cross-present. Indeed, DCs are very potent cross-presenting cells (Shen et al., 1997), especially cDC1s, in human and mouse. Antigen cross-presentation allows DCs to present microbial or tumoral antigens, without being themselves infected or tumoral, to prime and activate cytotoxic T cells against infected or tumoral cells.

### a. Antigen entry in endosomes/phagosomes

Antigen entry in DCs is mediated by different pathways: endocytosis, phagocytosis and macropinocytosis, the latest being especially used by DCs. Macropinocytosis consists in plasma membrane invaginations leading to a large engulfment of extracellular fluid, containing secreted proteins as well as microbial antigens in case of infections (Sallusto et al., 1995). While this uptake mechanism is major in immature DCs, mature DCs perform it less. Phagocytosis can be either non-specific, with the uptake of all types of particles, or receptor mediated. Antigen entry through receptor recognition

involves various surface proteins, such as mannose receptors, which recognise mannose and fucose expressed in microorganisms (Segura et al., 2009); Fc $\gamma$  receptors (Machy et al., 2000), detecting immunocomplexes; or Clec9A, specifically expressed by cDC1 and recognising cell debris after apoptosis. Receptor mediated uptake can be either clathrin-dependent endocytosis or clathrin-independent for larger particles. Once in endosomes or phagosomes, antigens are first processed and turned into protein fragments. DCs ability to cross present antigens relies on their endosome/phagosome capacity not to completely degrade the internalised antigens as their pH is higher than in macrophages, rendering their proteases less active (Delamarre et al., 2005). Therefore, peptides can be generated and loaded on MHC I molecules.

b. Vacuolar antigen cross-presentation

Two antigen cross-presentation pathways have been previously described: the vacuolar and the cytosolic pathways (Joffre et al., 2012). Vacuolar cross-presentation relies on antigen processing in endolysosomes/phagolysosomes into peptides that can directly be loaded on MHC I molecules present in these compartments (Pfeifer et al., 1993). This processing relies on lysosomal protease activities, such as cathepsin S, necessary for efficient vacuolar antigen cross-presentation (Shen et al., 2004). Once loaded, MHC I-peptide complexes can directly travel to the plasma membrane and be recognised by CD8<sup>+</sup> T cells (Figure 6).

c. Cytosolic antigen cross-presentation: antigen export from phagosomes to the cytosol

The cytosolic pathway relies on antigen processing by the proteasome in the cytosol. For this, antigens internalised in endosomes/phagosomes have to reach the cytosol (Kovacsovics-Bankowski et al., 1993; Kovacsovics-Bankowski and Rock, 1995). While the mechanisms behind this step remain unclear, several possibilities have been raised and studied.

Among them, endosomal membrane rupture was reported. It can be caused by reactive oxygen species (ROS) production through cell debris recognition by Clec9A or NADPH Oxidase 2 (NOX2) recruitment to endosomes. The latest disrupts the lipid membrane integrity and leads to endosomal content release (Dingjan et al., 2016). Clec9A recognition causes both the receptor and its ligand internalisation in

phagosomes and triggers SYK signalling. Recruited SYK binds to Clec9A cytosolic domain causing a localised oxidative burst and ROS activity, leading to endosomal membrane rupture (Canton et al., 2021). DCs were described to display sustained and higher ROS production than macrophages, especially cDC1s, consistent with their high capacity to cross-present antigens. While phagosome damage allows antigens to be processed through the proteasome in the cytosol and to be cross-presented, it is also toxic for the cell to release endosomal content such as cathepsins and hydrolases. Therefore, phagosomal damage needs to be controlled and it was reported to be regulated by the ESCRT (endosomal sorting complex required for transport) machinery. Among the ESCRT complexes, ESCRT III is involved in membrane repair as it forms helical filaments along the damaged parts of the endosomal membrane and controls endosomal content leakage. Showing its role in antigen cross-presentation, ESCRT III silencing leads to increased export of antigens to the cytosol and enhanced antigen cross-presentation, due to a lack of endosomal membrane repair (Gros et al., 2022).

Endosome to cytosol export of antigens has been also suggested to be regulated by several members of the endoplasmic reticulum-associated degradation (ERAD) members such as p97, Hrd1 or Sec61. The ERAD machinery was originally described to be involved in misfolded proteins retro-translocation from the ER to the cytosol.

The AAA ATPase p97 provides energy for ERAD retro-translocation channels and has been shown to be required for cross-presentation in DCs. To this day, p97 is the strongest candidate for its involvement in endosome to cytosol export, as content release from phagosomes has been observed upon recombinant p97 addition in isolated phagosomal compartments (Ackerman et al., 2006). Moreover, silencing of p97 in DCs results in decreased peptide release from phagosomes (Ménager et al., 2014). It can also be noted that, after ovalbumin (OVA)-mediated mannose receptor activation and poly-ubiquitination, p97 is recruited to endosomes and may then stimulate antigen release (Zehner et al., 2011).

Another ERAD protein, the ubiquitin ligase Hrd1, has been proposed as a channel candidate for antigen endosome to cytosol translocation. Hrd1 knockdown impairs antigen export to the cytosol and cross-presentation as well as MHC II antigen presentation (Zehner et al., 2015). However, this effect might be related to other disruptions in the cells, since Hrd1 knockdown induces ER stress and therefore

activates ER factors that were shown to be involved in antigen presentation (further discussed in chapter 7). Furthermore, Hrd1 role in antigen cross-presentation remains controversial as its knockdown did not seem to have a strong impact on OVA cross-presentation in another study (Grotzke and Cresswell, 2015).

Lastly, the ERAD protein Sec61 is also involved in MHC I antigen cross-presentation. Sec61 is the main actor of the Sec61 translocon localised at the ER membrane which mediates the translocation of many newly synthesised proteins into the ER (Rapoport, 2007). The translocon is a complex of three proteins: Sec61, composed of three subunits constituting a pore through the ER membrane, Sec62 and Sec63 (Voorhees and Hegde, 2016). This Sec61 channel remains closed until it is primed through binding of the Sec62-Sec63 complex, opening the channel lateral gate and allowing polypeptide translocation into the ER. Also recruited to endosomes, it was suggested that Sec61 could mediate endosome to cytosol export of antigens as other ERAD proteins may do. Indeed, Sec61 knockdown or Sec61 exclusion of endosomes rendered DCs unable to efficiently cross-present antigens (Zehner et al., 2015). However, Sec61 deficiency disrupts phagosomes and ER homeostasis along with ER-phagosomes contact sites, important for MHC I antigen presentation.

In a more recent study, Sec61 activity was specifically blocked with mycolactone, a drug targeting the alpha subunit of Sec61 and keeping the channel in a closed conformation. This Sec61 blockade led to decreased MHC I classical and cross presentations, though didn't affect protein or peptide translocation from the ER or the endosomes to the cytosol (Grotzke et al., 2017). Unlike previously thought, the Sec61 translocon appears to not directly transport antigens from endosomes to the cytosol, though it probably regulates another channel or another step of the process.

#### d. Cytosolic antigen cross-presentation: peptide loading on MHC class I

Once antigens reach the cytoplasm, they can be processed through the proteasome. After processing, peptides can either enter the ER or phagosomes, both pathways through TAP (Figure 6). Indeed, members of the PLC are expressed in both compartments, along with MHC I molecules (Guermónprez et al., 2003a). Trimming of peptides in phagosomes happen through insulin-regulated endopeptidases (IRAP) before loading on MHC I (Saveanu et al., 2009). A deletion of IRAP in mice has been



previously associated with a decrease in MHC I antigen cross presentation, highlighting its key role in the process (Weimershaus et al., 2012).

While the cytosolic pathway has been reported to be fully TAP-dependent, since peptides need to enter TAP-containing compartments to be loaded on MHC I molecules, the vacuolar pathway has been often described as TAP-independent. However, it was assessed that TAP is not only a transporter for peptides but is also involved in MHC I stability and loading of high affinity peptides (Chefalo et al., 2003). Indeed, TAP deficient cells show an accumulation of MHC I molecules at ERGIC sites as they are not stable enough to get through late quality control steps in this compartment (Raposo et al., 1995). However, TAP deficient DCs can still cross-present by allowing loaded MHC I molecules stuck in ERGIC compartments to traffic to phagosomes and to the plasma membrane (Barbet et al., 2021). While this has been reported as a backup for TAP deficiency, this pathway may also lead to autoimmune reactions as low affinity self-peptides may be presented to cytotoxic T cells.

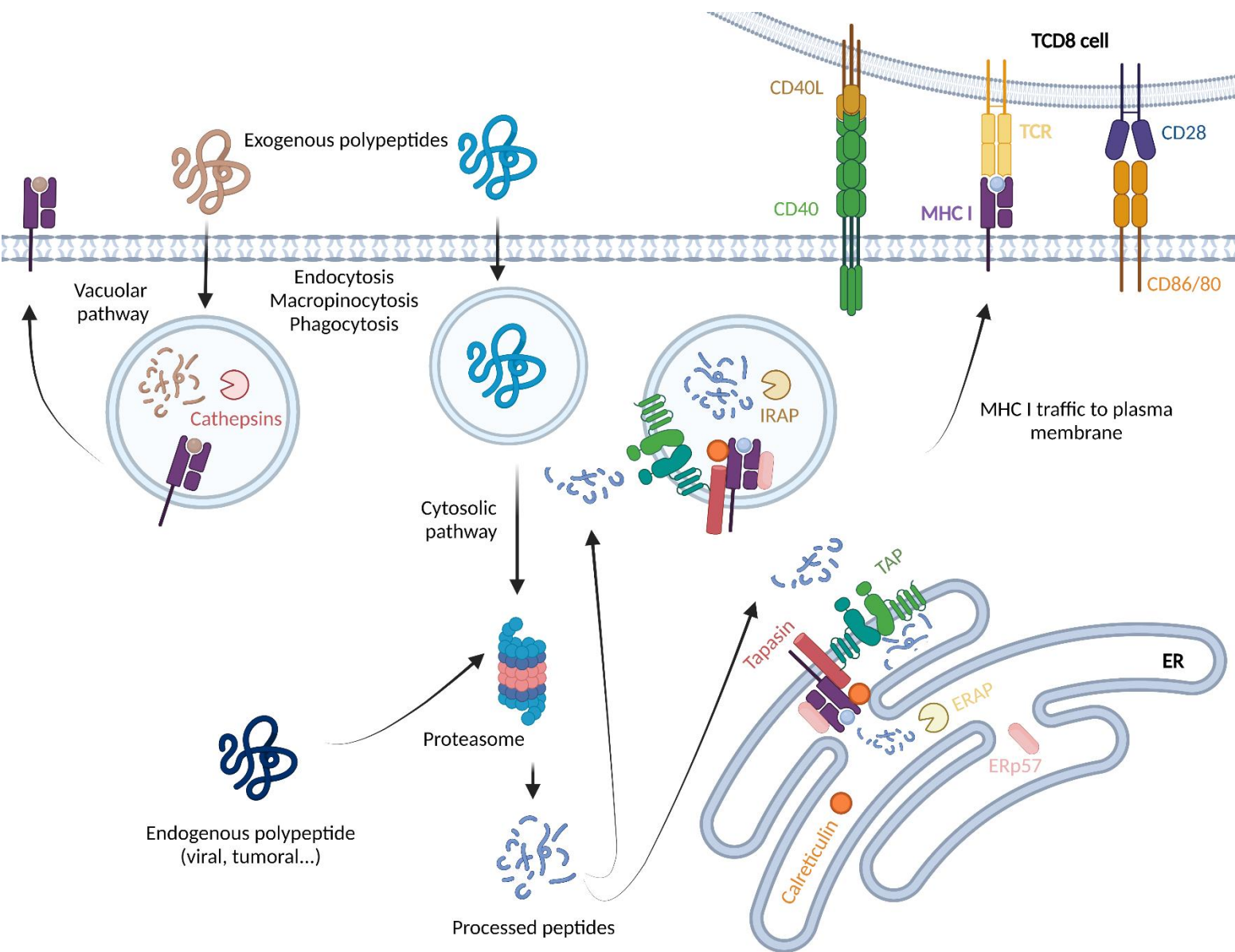


**Figure 6: Major histocompatibility complex (MHC) class I antigen presentation pathways.** Classical antigen presentation consists of processing of endogenous antigens by the proteasome before their loading on MHC I. Antigen cross-presentation of exogenous antigens can occur through two pathways: vacuolar with direct processing and loading of peptides in endosomes, and cytosolic with processing of peptides by the proteasome in the cytosol before loading on MHC I molecules in endosomes or in the ER.

## B. MHC class II antigen presentation

MHC class I is not the only molecule presenting peptides to T lymphocytes as MHC class II also present antigens, and specifically regulates CD4<sup>+</sup> T cells activation.

MHC class II presents peptides to helper T cells, leading to their proliferation and activation, so they can also induce production of specific antibodies and secretion of pro-inflammatory cytokines by B cells. MHC II molecules were originally described to be expressed only by professional APCs: B cells, macrophages and DCs. However, MHC II expression can also be induced by INF $\gamma$  in non-APCs such as fibroblasts, endothelial cells or epithelial cells. Induction of MHC II expression is controlled by the major transactivator CIITA, recruited at the MHC II gene locus (Steimle et al., 1994; Reith et al., 2005). In immature DCs, CIITA promoter is bound by a complex enhancing its expression, composed of PU.1, NF- $\kappa$ B, SP1 and IRF8, leading to high transcription of CIITA and MHC II molecules. DC maturation drives out this complex, which is replaced by BLIMP1, inhibiting CIITA transcription. Even though MHC II synthesis is important in immature DCs, its half-life is limited, and MHC II turnover kinetics are quite rapid. In mature DCs, MHC II half-life is increased, and its expression is stabilised at the plasma membrane.

MHC II  $\alpha$  and  $\beta$  chains are first assembled in the ER (Figure 5) and associate with the invariant chain Ii. MHC class II-Ii complexes traffic to the plasma membrane before being endocytosed in late endosomes and delivered to late MHC II-containing compartments (MIIC). MHC II endocytosis is mediated by targeting motifs present in Ii, recruiting the adaptor protein AP-2, regulating clathrin-dependent endosomal delivery (Dugast et al., 2005). MIIC, characterised by high proteases activity, are where antigen processing and peptide loading occur. Proteases such as asparaginyl endopeptidase and cathepsins can, in MIIC, catalyse Ii degradation and antigen processing into peptides (Riese et al., 1996; Nakagawa et al., 1998; Manoury et al., 1998; Hsieh et al., 2002). Ii degradation first concerns its N-terminal domain, leaving a residual class II-associated Ii peptide (CLIP) in MHC II peptide binding groove. This process prevents low affinity peptides to be loaded on MHC II and eventually presented to CD4<sup>+</sup> T cells. High affinity peptides generated in the MIIC can replace CLIP and be loaded on MHC II molecules (Denzin and Cresswell, 1995), which can then traffic to the plasma membrane (Neefjes et al., 2011; Roche and Furuta, 2015) (Figure 7).

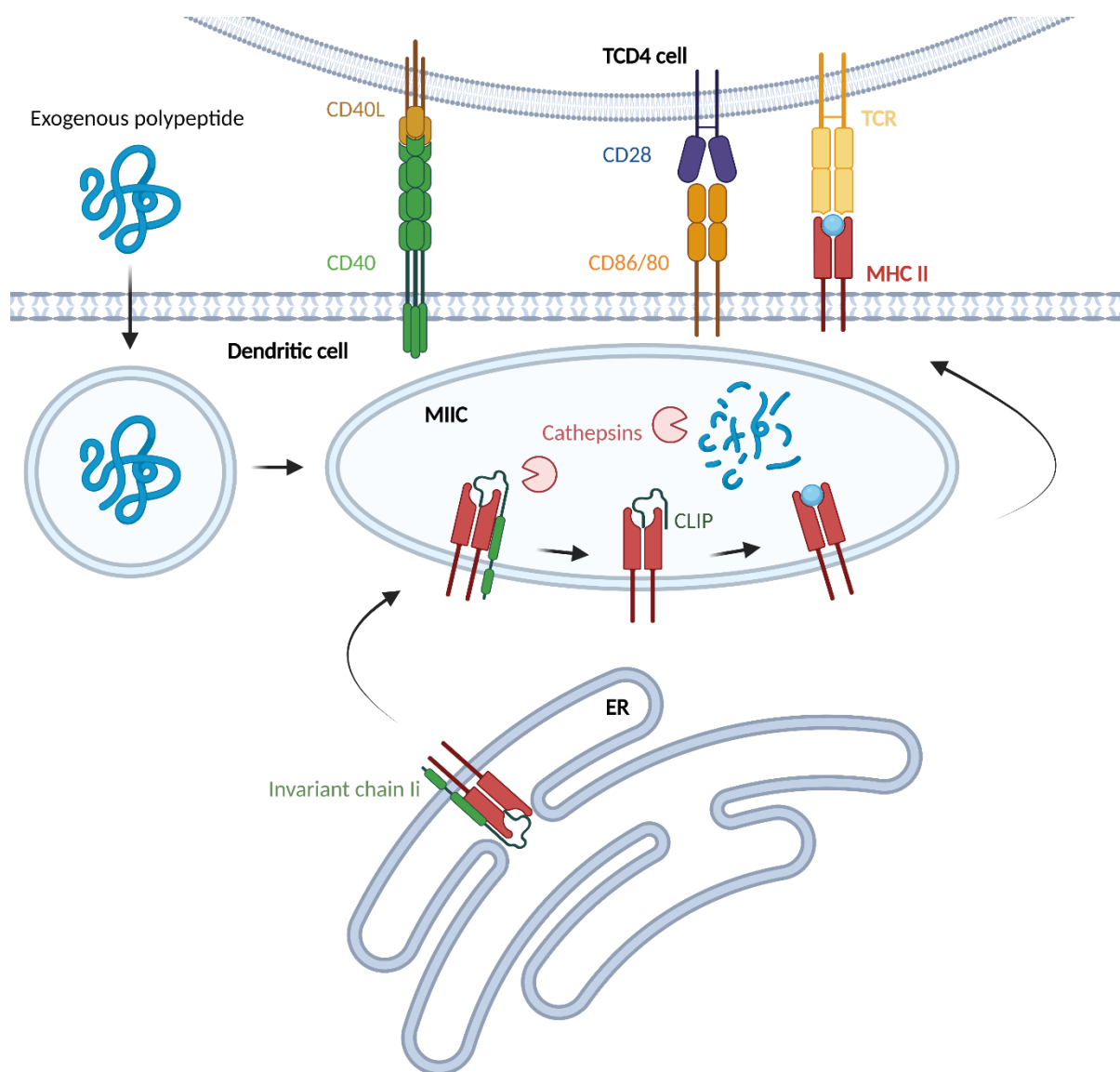


**Figure 7: Major histocompatibility complex (MHC) class II exogenous antigen presentation pathway.** MHC II-Ii complexes translocate to MIIC compartments, where antigens can be processed into peptides and loaded onto MHC II.

## **CHAPTER IV: Adaptive immune effectors: T and B lymphocytes.**

### **A. T lymphocytes activation**

As previously mentioned, for DCs to prime naive T lymphocytes into effector T lymphocytes, several signalling steps are required. The first signal is antigen presentation through MHC molecules, as described just before. The second signal is the expression of co-stimulatory molecules by mature DCs. Their binding to their ligand or receptor on T cells is necessary for naive T cells to become effectors and activate their immune functions. However, co-stimulatory molecules can either regulate effector functions, as binding of CD80/CD86 on DCs to CD28 on T cells, or can be tolerogenic, as the expression of PDL-1 on DCs results in the expansion of regulatory T cells. Finally, a third signal is also required and is mediated by cytokines produced by DCs. Cytokine production can be induced through co-stimulatory DC-T cell interaction as the binding of CD40 on DCs to CD40-ligand on T cells leads to the secretion of IL-12 by DCs. Various cytokines are secreted by DCs and some of them can induce specific T cell responses. Indeed, it has been described that IL-4 promotes Th2 differentiation while IL-12 and type I INF induce Th1 differentiation. In contrast, memory T cells, which have already encountered specific antigens, only need signal 1 (antigen presentation by MHC molecules) to become effector T cells.

#### **1. CD8<sup>+</sup> T lymphocytes**

Once CD8<sup>+</sup> T cells are primed against a specific antigen into effector cytotoxic T cells, their main role becomes to induce death signals in target cells bearing the antigen on their MHC I molecule. TCR binding on the MHC I-antigen complex results in activation of two main cytotoxic pathways to induce target cell apoptosis (Henkart and Catalfamo, 2004). The first pathway described is mediated by perforin and granzymes, contained in granules secreted by cytotoxic T cells recognising a target cell. Perforin is a water-soluble protein that has the ability to create pores in membranes once agglomerated. Once secreted from T cells, perforin creates pores in the target cell plasma membrane and allow the entry of enzymes also secreted in granules, granzymes A and B. Granzymes are serine proteases able to induce target cell apoptosis. Granzyme B is able to directly process procaspases, leading to their activation and further apoptosis. Granzyme A is able to cleave an ER complex called SET, which carries an inactive

DNase. This cleavage induces activation of the DNase, that then translocates to the nucleus and leads to DNA single strand breaks, resulting in cell death. The other pathway involved in cytotoxic T lymphocyte-mediated cell death is Fas-ligand/Fas signalling. Once the TCR recognises its specific MHC I-peptide complex, Fas-ligand expression is induced at the surface of T cells. Fas-ligand then binds its receptor, Fas, on target cells and this interaction leads to processing and activation of caspase 8 and caspase 3, mediating apoptosis. For this cytotoxic pathway, the target cell needs to express Fas on its surface and to bear the appropriate internal death pathway.

## 2. CD4<sup>+</sup> T lymphocytes

CD4<sup>+</sup> T cells are, on another hand, primed through MHC II antigen presentation by professional APCs. CD4<sup>+</sup> T lymphocytes then differentiate into different T helper cells: T helper 1 (Th1), T helper 2 (Th2) or T helper 17 (Th17). A tight balance between the differentiation of the three subsets must be kept as a high activation of either of them can lead to immune diseases. T helper lymphocytes differentiation into one subset relies on APC production of specific and diverse cytokines following PRR signalling. Th1 differentiation is driven by the secretion of IL-12 and INF $\alpha$  by DCs as well as interaction between the co-stimulatory molecule CD40 with its ligand. It was shown that among cDCs, cDC1s mostly induced Th1 immunity. Th1 lymphocytes were described to mediate immune responses mostly against intracellular pathogens and to promote macrophage activation. Th2 cells, however, are mediated by IL-4 or IL-10 secretion and induce immune defences against extracellular parasites and allergens through mast cells and eosinophils activation (Romagnani, 1995). Th2 lymphocytes direct immune responses towards macrophage inhibition, and an increase in their differentiation has been reported to dampen phagocyte activity during chronic inflammation (Onoé et al., 2007). This indicates a need to keep a balanced development of the different subtypes. Lastly, T helper cells can also differentiate into Th17, induced by IL-6 or TGF $\beta$  and named after their main function, IL-17 production. IL-17 has been reported to be involved in high pro-inflammatory responses as it leads to strong pro-inflammatory cytokines and chemokines secretion, mediating tissue infiltration and efficient responses against extracellular pathogens (Bettelli et al., 2007). T helper cells have also been linked to humoral immunity and potent activation of B cells.

## B. B lymphocytes activation

In secondary lymphoid organs, B cells may encounter pathogenic antigens coming from the periphery through follicular DCs. B cells are able to recognise antigens with their BCR. Once internalised, antigens are processed into peptides and loaded on MHC class II molecules to interact with CD4<sup>+</sup> T cells. B cells then migrate to interfaces between B and T zones of secondary lymphoid organs to interact with CD4<sup>+</sup> T lymphocytes. Previously primed T helper cells can then induce B cell proliferation and formation of the germinal center, as well as short-lived plasma cells staying in secondary lymphoid organs and memory B cells. In the germinal center, B cells undergo somatic hypermutation to enhance the specificity of the antibodies produced against the encountered antigen. They then differentiate into long-lived plasma cells that migrate to the bone marrow or gut-associated lymphoid tissues and memory B cells (Ise and Kurosaki, 2021). While undifferentiated B cells keep antibodies at their surface, plasma cells have the ability to secrete specific immunoglobulins, a key immune response for complete elimination of extracellular pathogens.

## **CHAPTER V: UNC93B1 and its crucial role in innate recognition and antigen presentation.**

UNC93B1 is an endoplasmic reticulum protein composed of 598 amino acids and 12 transmembrane domains. It was first described in 1980, when an orthologue of the human UNC93B1 was discovered in *Caenorhabditis elegans* and was found to potentially be a potassium channel regulator. Human UNC93B1 is a conserved protein, and orthologues with similar sequences can be found in distantly related species such as *Caenorhabditis elegans*, *Arabidopsis thaliana*, *Drosophila melanogaster*, mouse, and human (Kashuba et al., 2002). It can be noted that human and mouse UNC93B1 share 85% of homology.

### **A. UNC93B1 and its role in endosomal TLR signalling**

The role of UNC93B1 in the TLR pathway was discovered using a forward genetic screen in mice with N-ethyl-N-nitrosourea. Germline homozygous mutations were generated in several mice and one of them led to the inability of cells and mice to produce TNF $\alpha$  following TLR3, TLR7 and TLR9 stimulation. This mutation was characterised to be recessive and specific to nucleic acid sensing, as immune responses to LPS, Pam3 or PGN-LTA remained unchanged compared to control mice. Following this finding, the mutated phenotype was named “triple d” or “3d”, regarding the triple TLR defect described. After genetically mapping the 3d locus, they found a single mutation in chromosome 19, exon 9 of the gene *Unc93b1*, encoding a protein of the same name. Expression of WT UNC93B1 in 3d cells restored TLR 3, 7 and 9 signalling, indicating a major role of UNC93B1 in intracellular TLR response (Tabeta et al., 2006).

#### **1. UNC93B1 interaction with endosomal TLRs is required for their signalling**

It was later described that UNC93B1 interacts with intracellular TLRs 3, 7, 8, 9 and 13 in the endoplasmic reticulum and in endosomes (Brinkmann et al., 2007; Shi et al., 2011). Moreover, in mice, UNC93B1 was also reported to interact with endosomal TLRs 11 and 12 (Pifer et al., 2011; Andrade et al., 2013). This interaction was shown to be essential for endosomal TLR signalling. Indeed, in 3d cells where a defect in intracellular TLR responses is observed, UNC93B1/TLR interaction was lost



(Brinkmann et al., 2007) (Figure 8). Although UNC93B1 role is often labelled as restricted to endosomal TLRs, it has been reported once that it interacts with TLR5, a surface TLR, to regulate its activation in a similar way than intracellular TLRs. This was not observed for other surface TLRs (1, 2, 4, 6), which do not depend on UNC93B1 for their function (Huh et al., 2014). Even though UNC93B1 is necessary for all intracellular TLRs signalling, it was observed to mediate their activity differently. Indeed, UNC93B1 keeps a tight balance between TLR9 and TLR7 activation, being biased towards TLR9 signalling and repressing TLR7 responses (Fukui et al., 2009). This function allows UNC93B1 to control TLR7 activity and TLR7-dependent autoimmune responses. As described previously, upregulated TLR7 signalling can lead to systemic lupus erythematosus and mutations in TLR7 locus were directly correlated to this disease in children (Brown et al., 2022). The amino acid aspartic acid in position 34 (D34) of UNC93B1 has been reported to be important in TLR7 repression. Indeed, D34A mutation in UNC93B1 results in increased TLR7 signalling and the development of a lupus-like phenotype in mice expressing the mutant (Fukui et al., 2009, 2011). An UNC93B1 glycosylation site, an asparagine in position 272, was reported to be important for TLR9 and MyD88 activation after CpG stimulation. However, this requirement was not observed for TLR7 signalling (Song et al., 2022).

## 2. UNC93B1 interaction with endosomal TLRs is required for their trafficking

UNC93B1 interaction with nucleic acid sensing TLRs has been reported to be necessary for their traffic from the ER to endosomes (Kim et al., 2008; Lee et al., 2013). Indeed, UNC93B1 is required for the egress of intracellular TLRs into COP-II vesicles from the ER membrane. UNC93B1 brings these TLRs to their signalling compartment, and the complexes TLR-UNC93B1 are detected in endosomes (Kim et al., 2008). In 3d cells, where UNC93B1/TLR interaction and intracellular TLR signalling are abrogated, a defect in endosomal TLR trafficking was also observed. This indicated a clear role of UNC93B1 in TLRs translocation to endosomes, preceding their activation and signalling (Figure 8).

Models of TLRs trafficking from ER to endosomes have been proposed and describe a role of the adaptor protein complexes; AP-2 being necessary for TLR9 to traffic from the ER to endosomes and AP-3 from endosomes to lysosomes. It was first described that the AP-2 complex is recruited by an UNC93B1 tyrosine-based motif to bring TLR9 to endosomes. Indeed, a mutation in this UNC93B1 motif leads to TLR9/UNC93B1

mis-trafficking and defect in signalling (Lee et al., 2013). Although AP-3 recruitment by UNC93B1 has not been reported, it was shown that a knock-out of AP-3 leads to a decreased trafficking of UNC93B1 to lysosome related organelles (Sasai et al., 2010). UNC93B1-mediated trafficking of TLRs to endosomes has also been described to be dependent on another ER transmembrane protein, LRRC59 (Leucine-rich repeat containing protein 59). It was shown that upon ligand internalisation, UNC93B1 associates with LRRC59 to regulate TLRs translocation to endosomes. A knockdown of LRRC59 indeed resulted in a decreased signalling of TLR3, 8 and 9 but not of TLR4 and a slower TLR3 trafficking to the endosomes (Tatematsu et al., 2015).

For endosomal TLRs to signal, it was shown that their ectodomains had to be cleaved. For TLR3 and TLR9 activation, UNC93B1 must detach from them in endosomes so they can be cleaved and activate their signalling pathways. This was not observed for TLR7 as it appears that its association with UNC93B1 remains after activation, again showing how differently UNC93B1 regulates each endosomal TLR (Majer et al., 2019b). The termination of TLR7 signalling in endosomes is regulated by UNC93B1 phosphorylation and binding to Syntenin-1, which brings the complex to exosomes for degradation (Majer et al., 2019a).

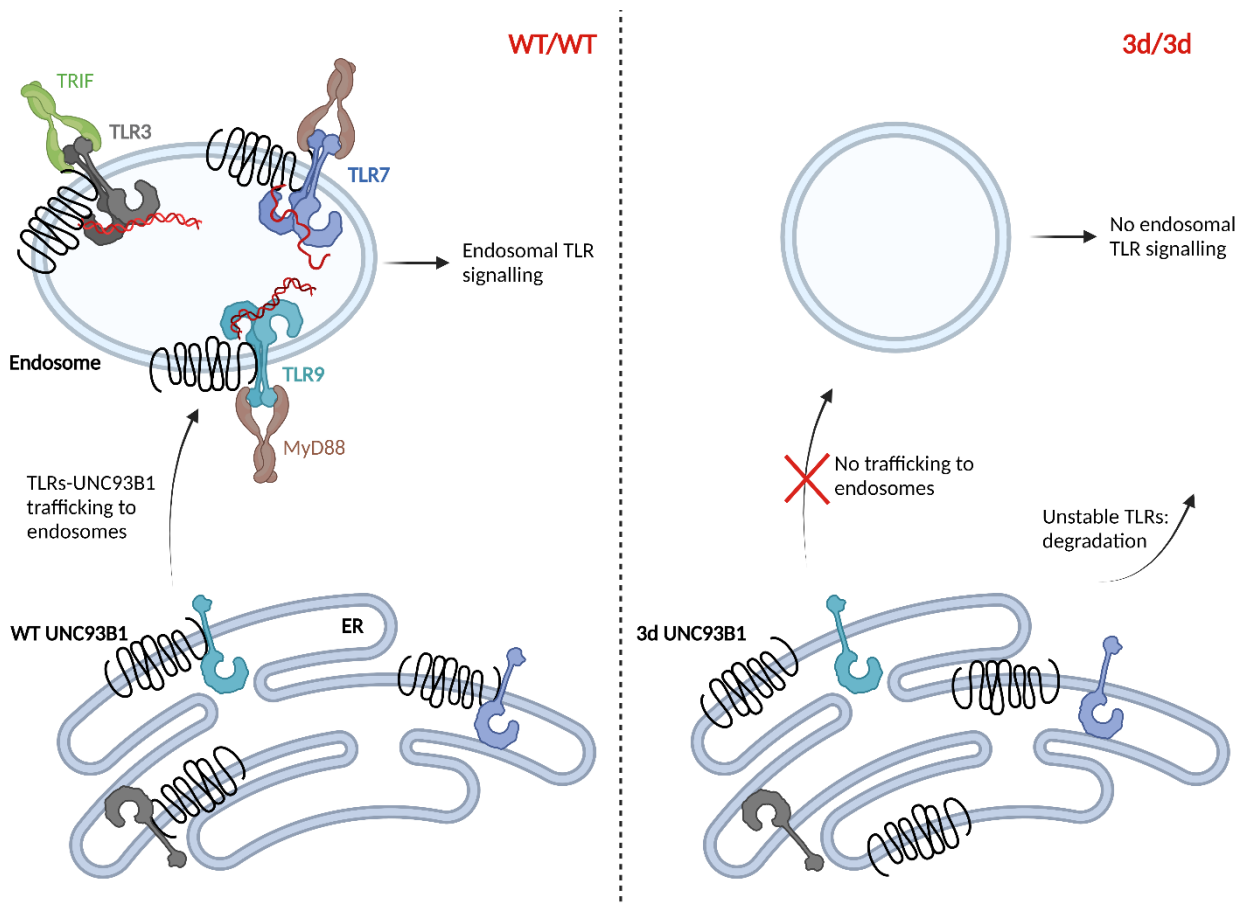


**Figure 8: UNC93B1 is necessary for Toll-like receptors (TLRs) trafficking.** UNC93B1 interacts with intracellular TLRs and regulates their trafficking from ER to endosomes. In 3d cells, UNC93B1 doesn't interact with TLRs, inhibiting their translocation to endosomes and further activation.

### 3. UNC93B1 interaction with endosomal TLR is required for their folding

In addition of regulating TLRs localisation to endosomes, UNC93B1 was reported to control their folding. Indeed, in 3d DCs, where intracellular TLR-UNC93B1 association is abrogated, intracellular TLRs expression is highly decreased compared to WT DCs. Expression of an UNC93B1 ER-retained mutant allows stabilisation of intracellular TLRs and their trafficking to endosomes, though to a lesser extent than in WT cells. It was then possible for UNC93B1 to partially rescue endosomal TLR signalling by restoring their proper folding without mediating their trafficking (Pelka et al., 2018).

All of these studies have highlighted the chaperone function of UNC93B1, regulating the folding and trafficking of endosomal TLRs to enable their signalling.

## B. UNC93B1 3d mutation

UNC93B1 3d mutation is a substitution in position 412 of the protein, replacing a histidine by an arginine (Tabeta et al., 2006) (Figure 9). This residue is conserved among other orthologues of UNC93B1 in vertebrates such as chicken, rat, mouse, and human. Developed in mice, this mutant allows us to study immune defects related to UNC93B1. It is important to note that 3d mice have no developmental defects and normal fertility when bred. They also have a normal development of lymphoid organs and regular numbers of peripheral T cells, B cells, natural killer cells and natural killer T cells. However, as mentioned previously, 3d cells are unable to respond to endosomal TLR ligands and 3d mice are therefore more susceptible to various viral or bacterial infections. Indeed, 3d mice weakly respond to pathogens such as mouse cytomegalovirus, *Listeria monocytogenes* or *Staphylococcus aureus* (Koehn et al., 2007).

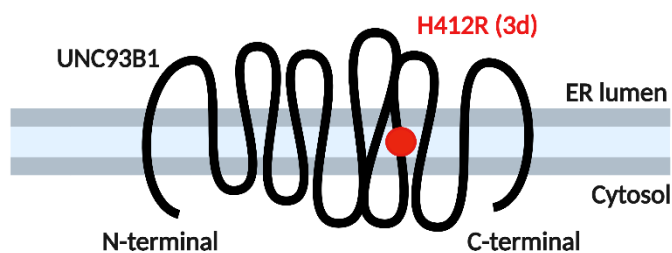


**Figure 9: UNC93B1 H412R (3d) mutation.** UNC93B1 is localised in the ER and contains 12 transmembrane domains. The 3d mutation is characterised by a substitution in position 412 of a histidine (H) into an arginine (R).

While the 3d mutation was primarily described as a defect in intracellular TLR responses, it was reported to also cause impaired MHC I antigen cross-presentation and decreased MHC II antigen presentation (Tabeta et al., 2006). Indeed, 3d DCs show a high decrease of cytotoxic T cell proliferation upon exogenous antigen presentation on MHC I, though no change in MHC I expression has been clearly observed. In 3d mice, MHC II antigen presentation is impacted to a lesser extent, and was reported to remain unchanged in UNC93B1 knocked-down human DCs (Koehn et al., 2007). UNC93B1 involvement in MHC II antigen presentation therefore is still questionable. While there are evidences showing that UNC93B1 mediates MHC I

antigen cross-presentation, all the pathways and mechanisms involved remain unclear to this day. Along with this, 3d mice show inefficient tumour rejection, leading to rapid tumour growth compared to WT mice (Maschalidi et al., 2017). This is probably due to the lack of MHC I antigen cross-presentation by 3d DCs, crucial for anti-tumoral responses.

### C. Human UNC93B1 mutants in disease

In human, UNC93B1 expression has been shown to be the highest in brain and heart tissues. Following its crucial role in immunity, UNC93B1 mutants in human have been associated with immune defects such as hypersensitivity to herpes virus, leading to herpes simplex encephalitis (HSE), also highlighting its crucial role in the brain. Two HSE patients described were from consanguineous families and presented a homozygous UNC93B1 mutation leading to the complete loss of expression of the protein (Casrouge et al., 2006; Sancho-Shimizu et al., 2011). HSE is one of most common encephalitis in children, and is characterised by migration and reactivation of herpes simplex viruses HSV-1 or HSV-2 in the brain, causing a localised inflammation. UNC93B1 mediated TLR-deficiency leads to susceptibility to various viruses in patients, especially HSVs, caused by a lack of viral recognition and low interferon responses. The absence of UNC93B1 in brain, where it is normally highly expressed, appears to impair the immune response to viruses from neurons, astrocytes and immune cells, at the origin of diseases as HSE (Lafaille et al., 2012).

As previously cited, a mutation of UNC93B1 was at the origin of a lupus-like phenotype in mice (Fukui et al., 2009). Furthermore, high levels of UNC93B1 were found in SLE patients B cells along with antibodies against self-dsDNA. However, no human UNC93B1 mutant has been described to directly correlate with SLE in patients (Kiener et al., 2021).

## D. UNC93B1 interactome

### 1. STIM1/UNC93B1 complex in MHC I antigen cross-presentation

To assess how UNC93B1 regulates antigen cross-presentation in DCs, Bénédicte Manoury's group has analysed the expression of genes involved in antigen cross-presentation from published microarrays from WT and 3d spleens. *Stim1* gene was the most significantly downregulated in 3d spleen in comparison to WT. (Maschalidi et al., 2017). STIM1 is an ER calcium sensor which is activated following depletion of  $Ca^{2+}$  in the ER (S. L. Zhang et al., 2005). Activation of STIM1 leads to the apposition of the ER membranes close to the plasma membrane, where STIM1 associates with ORAI1 to allow the replenishment of  $Ca^{2+}$  into the cytosol and in the ER. STIM1 function is therefore important for calcium influx inside the ER, and can control the activity of several ER chaperones. Furthermore, upon ER calcium depletion, STIM1 brings the ER membrane close to the phagosomes, creating calcium hotspots, process shown to upregulate phagocytosis in macrophages (Nunes et al., 2012). In DCs, STIM1 deficiency leads to loss of phagosomal  $Ca^{2+}$  hotspots, reduced lysosomal proteolytic activity characterised by low IRAP activity and inhibition of phagosomal maturation which result in altered antigen cross-presentation (Nunes-Hasler et al., 2017). IRAP was previously shown to be necessary for the final trimming of peptides, an important step for antigen processing (Saveanu et al., 2009). The role of STIM1 in immune responses has been widely described, particularly in T cells, where STIM1 deficiency leads to impaired T cell proliferation, activation and cytokine secretion and subsequent patients immunodeficiency (Feske et al., 2010; Samakai et al., 2013).

UNC93B1 and STIM1 interaction has been reported to be essential for STIM1 activation when calcium depletion occurs, and was shown to be inhibited in 3d DCs (Maschalidi et al., 2017). UNC93B1 3d mutation in DCs indeed leads to impaired calcium influx and reduced STIM1 oligomerisation, showing a role of UNC93B1 in STIM1 conformation. Furthermore, expression of a constitutive active form of STIM1, which no longer requires association with UNC93B1 for its function, restored antigen cross-presentation in 3d DCs (Maschalidi et al., 2017). In addition, 3d DCs showed an increased endosomal pH, resulting in decreased lysosomal proteases activity and therefore weak antigen processing, involved in cross-presentation. The change in endosomal pH is believed to be caused by impaired STIM1 activity since lysosomal

calcium hotspots are important for proteases activity and pH stabilisation. Overall, these data gave us an insight on one of the mechanisms involved in the regulation of antigen cross-presentation by the ER chaperone UNC93B1.

## 2. STING/UNC93B1 complex in type I INF response

In addition to endosomal TLRs and STIM1, UNC93B1 was described to interact with STING in the ER, an interferon signalling molecule described previously (chapter 2). The role of UNC93B1 in mediating STING activity is still unclear, but it was reported that UNC93B1 brings STING to lysosome for degradation to dampen its activation. Indeed, higher STING protein levels along with increased type I INF signature were observed in UNC93B1 knocked-down or knocked-out cells. According to these studies, in UNC93B1 3d mutated cells, STING fails to be downregulated by the ER chaperone as well (He et al., 2021; Zhu et al., 2022).

However, all these experiments were mostly conducted in transfected fibroblasts or HEK293T cell lines, hardly comparable to myeloid cells. Therefore, it remains of interest to investigate UNC93B1-mediated regulation of STING in these cells, especially in dendritic cells.

## **CHAPTER VI: Endoplasmic reticulum stress and the unfolded protein response.**

ER has a fundamental function in regulating secretory and transmembrane protein biogenesis, folding, assembly, trafficking and degradation, an important part of protein homeostasis. Quality control steps are necessary to assess the correct folding of proteins and their egress from the ER. If the requirements are not met, misfolded proteins can be eliminated through the ER-associated degradation (ERAD) pathway or autophagy. The ERAD pathway mediates ubiquitination of proteins, allowing their exit from the ER and their degradation by the proteasome in the cytosol.

While the folding and degradation machineries act together to deal with the newly translated proteins entering the ER, a fine balance between these two machineries must be in place. Disruption of this balance can cause the accumulation of misfolded proteins in the ER, associated to a stressed phenotype, and is therefore referred to as ER stress. ER stress can be induced by perturbation in calcium stocks and transport, lipid membrane changes, glycosylation inhibition or reactive oxygen species (ROS) production. To restore ER homeostasis, the unfolded protein response (UPR) is initiated through activation of three major proteins: Inositol-requiring enzyme 1 (IRE1), PKR-like ER protein kinase (PERK) and Activating transcription factor 6 (ATF6). When ER stress is induced, IRE1, PERK and ATF6 get activated via the release of BiP, an ER lumen chaperone, and elicit the transcription of ER chaperones to increase protein folding and ERAD members to decrease protein load. Unresolved ER stress leads to induction of pro-apoptotic signals in the cell, through the UPR.

### **A. The UPR: IRE1 pathway**

IRE1 is to this day the most described UPR factor, and is the most conserved throughout evolution (Tirasophon et al., 1998). IRE1 exists in two isoforms: IRE1 $\alpha$ , which is expressed ubiquitously in all cell types and is essential for cell viability, and IRE1 $\beta$ , only expressed in the lung and intestine. IRE1 $\alpha$  has been widely studied in various models while the exact role and regulation of IRE1 $\beta$  are still unclear. IRE1 is an ER transmembrane protein, composed of a N-terminal region localised in the ER lumen, which is bound to BiP at the steady state and a cytosolic C-terminal region which contains a kinase and an endonuclease domain. Upon activation, BiP is released from IRE1 and IRE1 auto-phosphorylates through its kinase domain and gets



oligomerised. IRE1 oligomerisation induces the activation of its endonuclease domain, resulting in unconventional splicing of *Xbp1* mRNA, giving rise to translation of a transcription factor called XBP1s for XBP1 spliced (Yoshida et al., 2001; Calfon et al., 2002). XBP1s translocates to the nucleus and drives the expression of several chaperones, ERAD members and genes involved in lipid biogenesis to restore protein folding. IRE1 has also been reported to directly cleave several specific mRNAs, through a process called Regulated IRE1-dependent decay (RIDD), allowing IRE1 to attenuate the protein load (Iwawaki et al., 2001; Hollien and Weissman, 2006; Hollien et al., 2009) (Figure 10). Most of the reported RIDD targets contain a consensus sequence in a stem loop conformation, which is similar to the cleavage site of *Xbp1* mRNA by IRE1. This consensus sequence remains however controversial as it is not kept in all described RIDD targets. Furthermore, some of the mRNAs directly cleaved by IRE1 seem to be cell-type specific.

The activation of IRE1 has been described following two distinct models. The first reports that activation of IRE1 is dependent on the release of BiP from IRE1, BiP being free to bind misfolded proteins in the ER lumen while IRE1 gets oligomerised (Pincus et al., 2010). The second model states that IRE1 directly recognises misfolded proteins through its N-terminal domain, which harbours a peptide-binding groove, allowing a change in IRE1 conformation and its oligomerisation (Gardner and Walter, 2011). In the second model, BiP is still released from IRE1 upon activation but is not the main signal triggering the UPR actor.

#### B. The UPR: PERK and ATF6 pathways

Among the three main UPR actors, while IRE1 has been the most studied, the other two are also crucial in stress-mediated cell responses. Upon ER stress, PERK is detached from BiP and is phosphorylated, leading to its activation. This response leads to eIF2 $\alpha$  phosphorylation by PERK cytoplasmic kinase domain (Harding et al., 1999). Once phosphorylated and activated, eIF2 $\alpha$  decreases protein translation in order to reduce protein load during ER stress. A few mRNAs escape this translation inhibition, leading to an increased PERK-dependent production of some proteins. One of them, ATF4, is a transcription factor regulating genes involved in amino acid metabolism, oxidative stress resistance or apoptosis (Harding et al., 2000) (Figure 10).

The third UPR actor, ATF6, is transported from the ER to the Golgi apparatus by COP-II vesicles upon ER stress (Yoshida et al., 1998; Haze et al., 1999). In the Golgi, ATF6 is cleaved and its N-terminal domain, which was reported to be a bZIP transcription factor called pATF6-N, is released. pATF6-N is translocated to the nucleus and regulates genes involved in ER membrane expansion, ERAD and protein folding (Figure 10).

The UPR has been described to be involved in many cellular pathways and responses, including immune functions. Indeed, the three major actors of the UPR are activated following immune stimulation, and thus can play a role in immune responses against pathogens or tumoral cells. Furthermore, the UPR being involved in the main functions of the ER, it is therefore an important feature for several cell type's development, differentiation, or maturation.

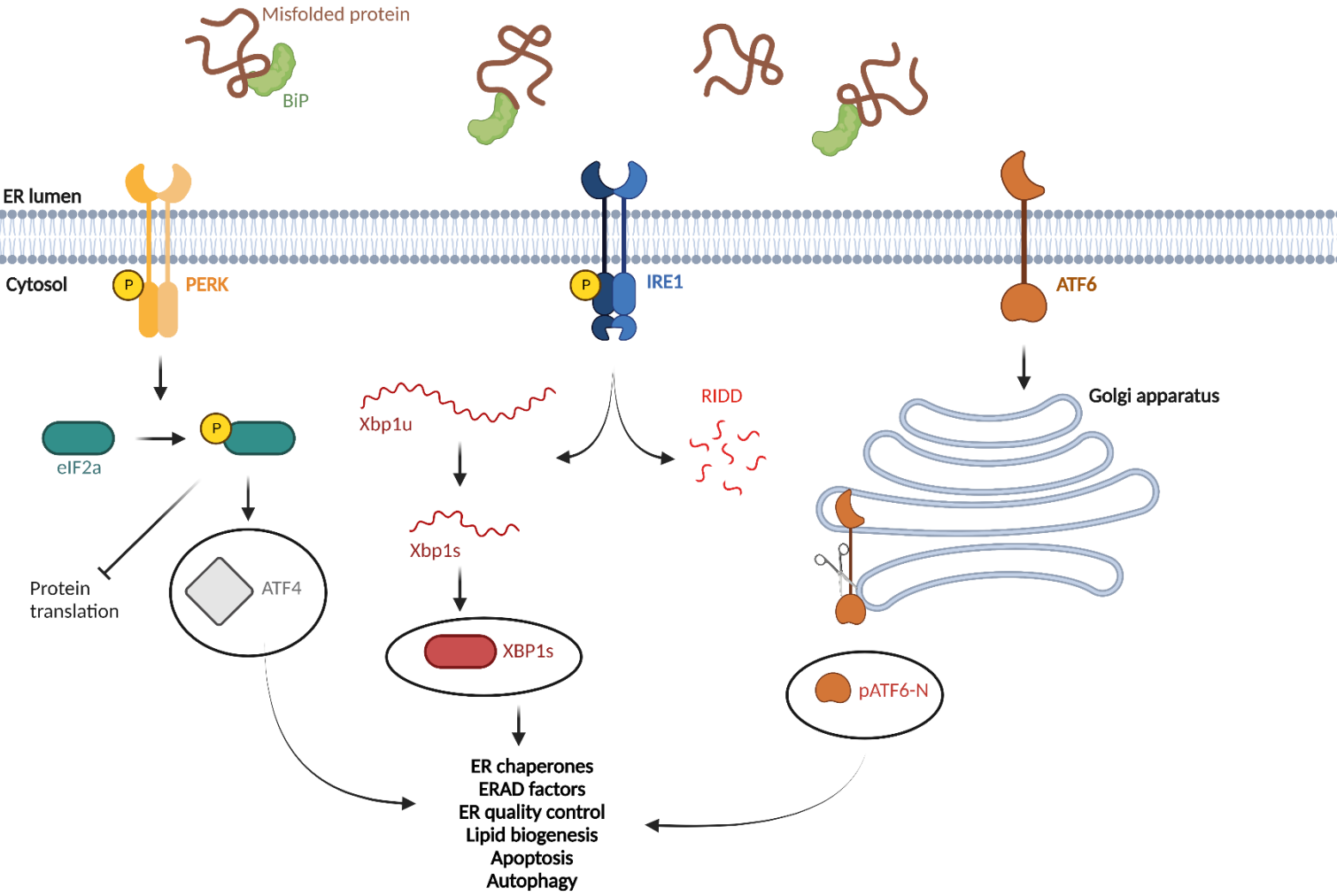


**Figure 10: The three arms of the unfolded protein response (UPR): PERK, IRE1 and ATF6.** Following endoplasmic reticulum (ER) stress, IRE1, PERK and ATF6 get activated to give rise to the production of the transcription factors ATF4, XBP1s and pATF6-N, inducing the expression of ER chaperones, quality control proteins or ER-associated degradation (ERAD) factors. The three UPR branches also lead to a decreased protein translation or protein load in the ER, following ER stress.

## **CHAPTER VII: The UPR role in immune cell homeostasis and responses.**

### **A. UPR-mediated factors and IRE1 $\alpha$ role in TLR signalling**

As previously stated, TLR signalling is important to initiate innate immune responses, leading to pro-inflammatory phenotypic and transcriptomic changes in cells, particularly in macrophages and in dendritic cells. Along with the recruitment and activation of the transcription factors NF- $\kappa$ B or IRF3/5/7, TLR signalling selectively triggers the UPR. In most cases, TLR ligands only activate one branch out of three of the UPR. In macrophages, TLR2 and 4 stimulation was shown to induce IRE1 $\alpha$ /XBP1 axis while inhibiting both PERK and ATF6 branches (Martinon et al., 2010). Of note, the UPR branches are not necessarily activated through ER stress and misfolded proteins, as TLRs don't always involve an imbalance in ER homeostasis. In pDCs, the upregulation and splicing of XBP1 was also reported after TLR7 stimulation (Beisel et al., 2017). In the context of TLR stimulation, knockdown of XBP1 or inhibition of XBP1 activity in cells results in a decrease in pro-inflammatory cytokine signature, indicating a role of IRE1 $\alpha$  in inflammation. Mechanistically, the transcription factor XBP1s was found to interact with Il6 and Tnf promoters, potentially increasing their expression (Martinon et al., 2010). Of note, XBP1s was not able to trigger the production of these pro-inflammatory cytokines by itself, as a TLR trigger appeared to be needed as well. Furthermore, XBP1 deficient mice infected with the pathogen *Francisella tularentis*, which binds TLR2, showed decreased pro-inflammatory signature and increased bacterial burden compared to control mice. Altogether, this indicates that TLR and XBP1 act in synergy to trigger pro-inflammatory responses in macrophages and in DCs, in order to eliminate the pathogenic burden (Figure 8).

Indeed, XBP1 overexpression or pharmacological ER stress compounds together with TLR ligands stimulation in macrophages and DCs show an increase in the production of IL-6, TNF $\alpha$ , IFN $\beta$ , or IL-23 (Smith et al., 2008; Janssens et al., 2014; Martins et al., 2016). In DCs, high IL-23 secretion due to both TLR and ER stress triggers was linked to autoimmune diseases as psoriasis (Papp et al., 2017). In mice developing psoriasis, inhibiting *Xbp1* splicing in DCs allowed a decreased IL-23 signature and reduced psoriasis burden (Wang et al., 2013). In this context, *Xbp1* was used as a therapeutic target against inflammatory diseases. While the mechanism of UPR-mediated pro-

inflammatory signature remains to be fully elucidated, we can speculate a few of them. First, the binding of XBP1s or XBP1-related proteins to cytokine promoters may play a role by enhancing their translation. Moreover, ER stress along with LPS stimulation in macrophages induces greater IRF3 recruitment to *Irfn1* promoter than stimulation with LPS alone (Zeng et al., 2010). Finally, it was shown that one of the XBP1s targets, upregulated upon activation of IRE1 $\alpha$ , is Grp94 and is required for TLR 1, 2, 4, 5, 7 and 9 to traffic from the ER to their final destination where they can signal (Park et al., 2021).

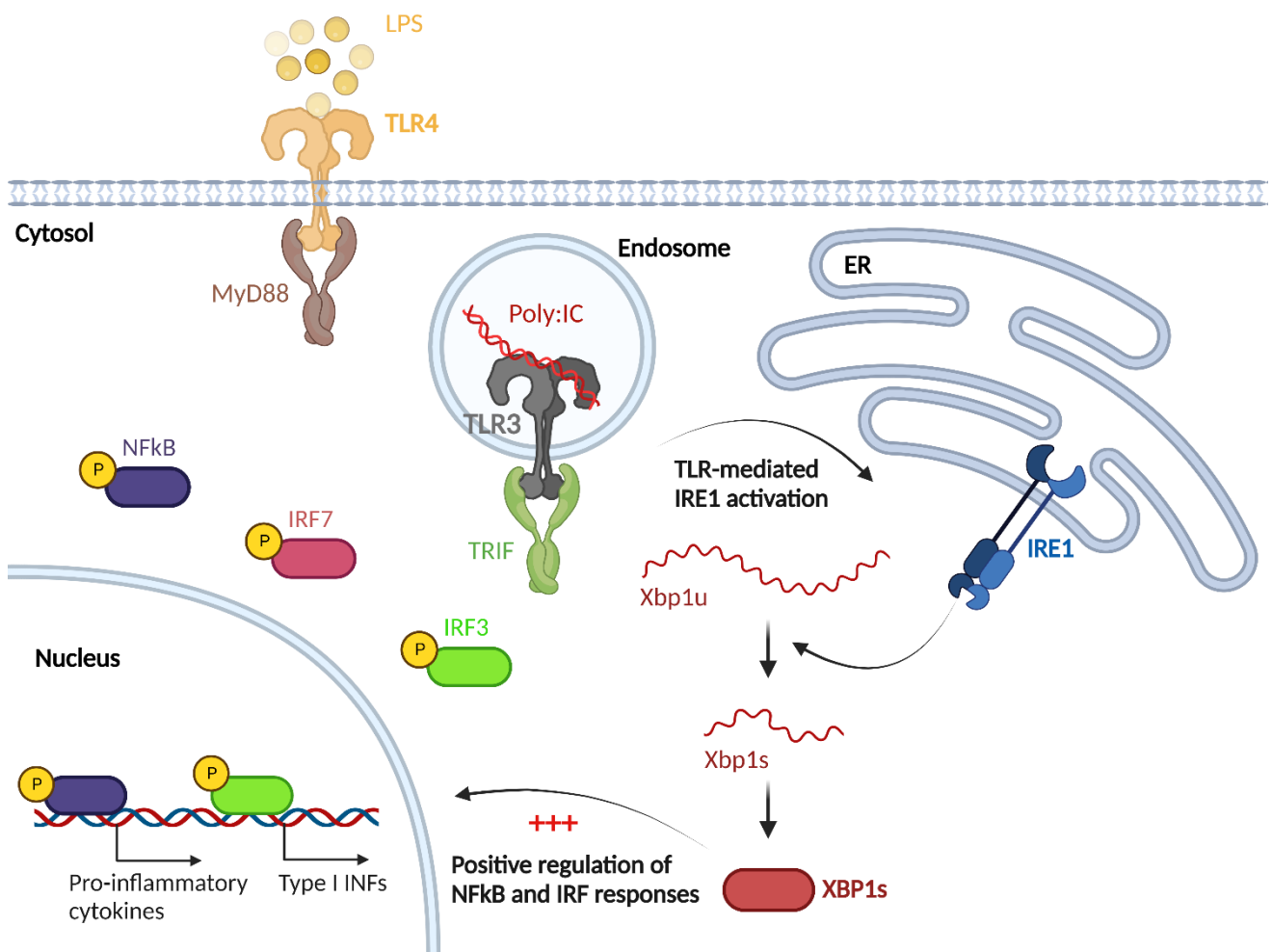


**Figure 11: Synergism between Toll-like receptors (TLRs) signalling and IRE1 $\alpha$  activation for pro-inflammatory cytokine and type I interferons production.** In dendritic cells and macrophages, activation of TLRs lead to triggering of IRE1 and splicing of Xbp1. The transcription factor XBP1s then participates to TLR-mediated responses, enhancing the expression of pro-inflammatory cytokines and type I interferons.

As previously indicated, ER stress does not induce pro-inflammatory cytokine production by itself. Though unable to initiate type I INF production alone, ER stress was described to trigger IRF3 phosphorylation and its translocation to the nucleus in macrophages, a step necessary but not sufficient for interferon response (Liu et al., 2012). Several theories arose to explain this result and highlighted the possible need to recruit other proteins than IRF3 or NF- $\kappa$ B on cytokine promoters to trigger their production, which may only occur through PRR signalling. It was also pointed out that only a portion of IRF3 is phosphorylated following ER stress, suggesting perhaps a threshold for IRF3 phosphorylation to induce cytokine translation. Moreover, when using thapsigargin, which depletes Ca<sup>2+</sup> in the ER, IRF3 phosphorylation was shown to be dependent on STING signalling. STING-related IRF3 phosphorylation in this context suggest that ER stressors can possibly hijack some immune pathways to increase immune responses, such as INF production.

These findings have highlighted the role of ER stress in innate immunity and have shown that the UPR promotes pro-inflammatory responses and is important in macrophages and DCs immune defense in response to pathogens infection.

#### B. IRE1 $\alpha$ /XBP1 role in B cell development

Not only playing a role in innate immunity, XBP1 also mediates adaptive immune responses, and it has been shown for B cell maturation into antibody-secreting plasma cell (Iwakoshi et al., 2003; K. Zhang et al., 2005). B cells mature in the spleen after antigen encounter and interaction with primed helper T cells, where they become immunoglobulin-secreting cells or plasma cells. For this transformation, B cells largely expand their ER so they can take in and correctly fold the large load of immunoglobulins that are to be secreted (Wiest et al., 1990). Along with that, an increased expression of several ER chaperones as BiP, Grp94 or pERp1 was observed during B cell maturation. Two master regulators of plasma cell differentiation, IRF4 and BLIMP1, have been reported to both mediate B cell maturation and anticipate the high protein load by priming the UPR (Shapiro-Shelef et al., 2003). Indeed, they were shown to induce high XBP1 expression in maturing B cells, which appears to be necessary for terminal differentiation into plasma cells and antibody secretion. XBP1 deficiency in mice results in normal B cell numbers but renders them unable to secrete immunoglobulins, which can be lethal upon pathogen infection depending on antibody production for their clearance. Looking further into the role of XBP1 in B cell

differentiation, it was described that XBP1 deletion in B cells leads to an increased expression and activation of IRE1 $\alpha$ , triggering high RIDD-mediated mRNA cleavage. In B cells, among RIDD targets, the  $\mu$  chain of immunoglobulin M (IgM) can be found. The BCR is a surface IgM, and RIDD activation can then impair B cell activation and antibody secretion (Benhamron et al., 2014). While IRE1 $\alpha$ /RIDD axis activation is involved in reduction of immunoglobulin translation, IRE1 $\alpha$  knock-out mice also show reduced antibody production capacities. IRE1 $\alpha$  has indeed been reported to be required for B cell lymphopoiesis at early stages.

While XBP1 activity seems to be in favour of both innate and adaptive immune responses, RIDD activation disfavours adaptive immunity through low antibody production. Thus, altogether, it highlights the importance of IRE1 $\alpha$  in both pro-inflammatory and tolerogenic reactions.

### C. Regulation of the IRE1 $\alpha$ pathway in antigen presentation

Initiating efficient adaptive immunity or tolerance through innate immune signals, antigen presentation in DCs is tightly regulated. Important steps in antigen presentation such as MHC molecules folding or MHC I peptide loading take place in the ER, and involve ER chaperones and transporters. One of the first observations made in mouse splenic cDCs was the high expression and constitutive activation of IRE1 $\alpha$  in cDC1s at steady state, which was not found in cDC2s (Osorio et al., 2014). This activation of IRE1 $\alpha$  showed splicing of XBP1 but no constitutive RIDD activity. As cDC1s are important cells for antigen cross-presentation, the role of IRE1 $\alpha$  and XBP1 in this process was further studied.

Mice with conditional XBP1 knockdown in DCs were used and, as in B cells, XBP1 deficiency leads to high IRE1 $\alpha$  activation and induction of the RIDD pathway. It was reported that MHC class I antigen cross-presentation was highly impaired in XBP1 $^{-/-}$  cDC1s, as they were unable to efficiently activate CD8 $^{+}$  T cells following antigen uptake. In XBP1 $^{-/-}$  cDC1s, several RIDD mRNA targets related to MHC I antigen presentation and specific to DCs were cleaved. Among the RIDD targets cleaved in XBP1 $^{-/-}$  cDC1s, mRNAs involved in peptide loading, vesicular trafficking and antigen endocytosis were described (Osorio et al., 2014). Indeed, *Tapbp* (Tapasin), necessary for TAP-mediated MHC I peptide loading in the ER and endosomes, was part of the degraded mRNAs. Along with *Tapbp*, *Ergic3*, mediating MHC I molecules trafficking

from the ER to the plasma membrane through the ERGIC compartment, was downregulated as well. The mRNA *Itgb2*, encoding the integrin receptor CD18 involved in antigen phagocytosis and T cell activation, was also degraded through RIDD. Lastly, another mRNA found to be decreased in XBP1<sup>-/-</sup> cDC1s was *ERp44*, an ER protein that cycles between the ER and Golgi to control several proteins localisation in the ER. ERp44 is responsible for the retention of ERAP1 in the ER, enzyme involved in peptide trimming for loading on MHC I molecules (Hattori et al., 2012). However, *ERp44* mRNA was also decreased in IRE1<sup>-/-</sup> DCs, although to a lesser extent than in XBP1<sup>-/-</sup> cells, suggesting that it is not a specific RIDD target.

It was then hypothesised that the MHC I antigen cross-presentation defect observed in XBP1<sup>-/-</sup> cDC1s is a result of RIDD abnormal activation. Furthermore, XBP1 deficiency in DCs leads to a decreased expression of CD11c in splenic DCs, altering their phenotype, and resulting in an impaired ER homeostasis shown by an abnormal morphology of the ER detected with high-resolution microscopy (Osorio et al., 2014).

While impaired MHC class I antigen cross-presentation was RIDD-mediated in XBP1<sup>-/-</sup> cDC1s, altered DC phenotype and ER homeostasis were dependent on XBP1 deficiency, as they were also observed in IRE1<sup>-/-</sup> DCs. Once again, RIDD activation was highlighted as detrimental for immune functions while XBP1 seemed to promote DC homeostasis.

Questions were then raised on whether IRE1 $\alpha$  inhibition or activation in DCs were detrimental or beneficial for MHC I antigen cross-presentation. To study this, the role of IRE1 $\alpha$  in cross-presenting capacities of Flt3-ligand derived BMDCs challenged with melanoma-associated antigens was assessed (Medel et al., 2019). First of all, it must be noted that in contrast to cDC1s, in vitro generated BMDCs do not exhibit steady state IRE1 $\alpha$  activation. However, it was observed that challenging BMDCs with melanoma lysates led to IRE1 $\alpha$  activation, along with XBP1 splicing but no RIDD induction. In addition, antigen-mediated IRE1 $\alpha$  activation is important for MHC I cross-presentation as inhibition of IRE1 $\alpha$  RNase activity leads to a defect in this function. A similar question was raised when DCs were infected with the parasite *Toxoplasma Gondii* (Poncet et al., 2021). As observed with melanoma lysates, the parasite also led to an activation of IRE1 $\alpha$  and XBP1 splicing while the RIDD pathway was not triggered. In this context, MHC I cross-presentation of secreted parasite antigens was also dependent on IRE1 $\alpha$  activity as its inhibition or deletion strongly decreased the DCs



ability to activate T cells. Both these studies highlighted a role of IRE1 $\alpha$  activation and XBP1 splicing in positively regulating MHC I antigen cross-presentation. The activation of IRE1 $\alpha$  is probably linked to PRR-mediated recognition of antigens and was shown to mediate pro-inflammatory cytokine responses as well as MHC I antigen presentation. Thus, it appears that the IRE1 $\alpha$ /XBP1 axis is required for efficient MHC I cross-presentation of tumoral and pathogen-associated antigens in DCs. We may speculate that XBP1s positively regulates MHC I cross-presentation through the upregulation of ERAD members such as Hrd1 or of the Sec61 translocon. Indeed, as previously described, both factors might be required for efficient antigen cross-presentation by DCs.

Nevertheless, the same requirements were not observed for OVA-mediated antigen presentation in cDC1s and BMDCs. In cDC1s, which express activated IRE1 $\alpha$  at steady state, a deletion of IRE1 did not lead to defect in cross-presentation of OVA (Osorio et al., 2014; Medel et al., 2019). Furthermore, in Flt3-ligand derived BMDCs challenged with OVA, no activation of IRE1 $\alpha$  or splicing of XBP1 were seen, and their inhibition had therefore no effect on MHC I cross-presentation of OVA antigens. Though, it must be noted that OVA-mediated cross-presentation is artificial, and DCs are experimentally pushed to present and activate T cells, so IRE1 $\alpha$  activity may not be required in this context. While the exact mechanisms of IRE1 $\alpha$  role in MHC I antigen cross-presentation remain unclear, IRE1 $\alpha$  activation in the context of infections or tumours is required for efficient antigen cross-presentation to activate CD8<sup>+</sup> T cells.

However, partially refuting this theory, a study recently showed that inhibition of IRE1 $\alpha$  RNase activity led to increased cross-presentation capacities by BMDCs. In this report, OVA did activate IRE1 $\alpha$ , triggering XBP1 splicing and RIDD mRNAs targets cleavage. In their study, they showed that MHC class I mRNA was one of RIDD targets, which explains the benefits of inhibiting IRE1 $\alpha$  activity for cross-presentation in DCs. Moreover, in mice bearing a tumour, inhibition of IRE1 $\alpha$  led to an increased expression of MHC I in DCs present in the tumoral environment, correlating with tumour regression (Guttman et al., 2022). Even though these data are in contradiction with previous works, it can be again noted that IRE1 $\alpha$  RIDD activity is what seems to be deleterious for antigen cross-presentation, as reported by Osorio *et al.*, though MHC I had not been described to be a RIDD target in this report.

#### D. The role of IRE1 $\alpha$ and PERK in cell migration

Independently of its function as a UPR actor, IRE1 $\alpha$  was shown to be involved in cell migration. It associates with filamin A, a protein linking actin filaments involved in cytoskeleton dynamics, and was reported to regulate its phosphorylation and downstream activity in controlling cellular migration and cellular development. Indeed, a deficiency in IRE1 $\alpha$  caused impaired cell migration and altered filamin A activity, which was shown to be at the origin of defective brain development (Urrea et al., 2018). IRE1 $\alpha$  therefore is also important in cytoskeleton dynamics and cell migration, key feature of mature or activated immune cells for inducing potent and rapid responses.

Not only interacting with IRE1 $\alpha$ , filamin A was also shown to associate with PERK, and PERK deficiency was reported to disrupt cell migration. Furthermore, this interaction is required for ER-plasma membrane contacts and STIM1-mediated calcium influx (van Vliet and Agostinis, 2017). PERK then has a role in intracellular calcium flux and, together with IRE1 $\alpha$ , in cell migration, both processes being critical for efficient immune responses.

#### E. UPR activation in cancer: beneficial or detrimental for the immune tumoral microenvironment?

Although IRE1 $\alpha$ -dependent XBP1 activation described previously in melanoma associated DCs responses was shown to have a positive outcome, XBP1 activation in cancer models was reported to mostly have deleterious effects on tumoral rejection, rather promoting tumour growth (Cubillos-Ruiz et al., 2015). It has to be noted that in tumour cells and tumour microenvironment, ER stress is constitutively activated through various mechanisms (Chen and Cubillos-Ruiz, 2021). Within them, we can find hypoxia, a lack of oxygen dysregulating protein folding in the ER; limited glucose, impacting glycosylation processes and calcium flux; ROS accumulation and an acidic pH. Genetic alterations and some oncogenes upregulation also cause a sustained ER stress in cancer cells and cancer environment. Indeed, several oncogenes promote a high protein synthesis and cancer cells require rapid ER expansion for efficient division and proliferation. Oncogenic transformation has been reported to constitutively activate the IRE1 $\alpha$  and PERK axis, both appearing to facilitate tumour growth. Indeed, XBP1 maintains ER homeostasis and cell growth, playing its protective role in cancer cells and promoting survival. Furthermore, in a glioblastoma cell line, it was described that XBP1 positively regulates angiogenesis, increasing cancer cell migration and myeloid cell infiltration (Lhomond et al., 2018). However, RIDD activation had rather opposing

effects, attenuating angiogenesis and cancer expansion. RIDD has also been associated to cell death in excessive ER stress conditions. A balanced IRE1 $\alpha$  activation between XBP1 and RIDD may then determine cancer cell fate and mediate the clinical outcome.

While rapid IRE1 $\alpha$  activation in DCs by tumoral cells may induce CD8<sup>+</sup> T cell activation and proliferation to eliminate abnormal cells, long-termed UPR trigger in cancer seems to have a deleterious effect on DCs functions and tumour progression. As described just before, ER stress is constitutively activated in cancer cells. It is known that myeloid immune cells such as DCs or macrophages are recruited to the tumoral environment and remain close to cancer cells. Tumour infiltrating myeloid cells are then exposed to factors secreted by ER stressed tumour cells, leading to potent UPR activation in immune cells. This process is referred to as transmissible ER stress (TERS) and has been shown to have deleterious effects on DCs immune responses and capacities to prime CD8<sup>+</sup> T cells (Mahadevan et al., 2011, 2012).

Indeed, TERS in DCs leads to an upregulation of pro-inflammatory and tumorigenic cytokines secretion, both promoting immunosuppression in the tumoral environment and chronic inflammation. Long-term inflammation has been associated with tumour progression through increased ROS production, angiogenesis or excessive myelopoiesis. Abnormal myelopoiesis is a common feature described in multiple cancers and results in a lack of mature and competent DCs at the tumour site as well as an accumulation of immature myeloid cells, displaying immunosuppressive functions and referred to as myeloid derived suppressor cells (MDSCs) (Ostrand-Rosenberg and Sinha, 2009).

TERs in DCs has also been associated to a decreased capacity for them to cross-present tumour-associated antigens and prime CD8<sup>+</sup> T cells. First, UPR activation in DCs results in immunosuppressive factors upregulation, as arginase 1 or prostaglandin E2 (PGE2). Arginase 1 is secreted by DCs and once internalised by neighbouring T cells, has the ability to process L-arginine, an essential actor for T cell activation (Norian et al., 2009). Moreover, chronic IRE1 $\alpha$ /XBP1 activation in DCs leads to lipid accumulation through high triglyceride biosynthesis and lipid droplet formation, this process efficiently decreasing DCs abilities to present antigens. In addition, inhibition of the IRE1 $\alpha$ /XBP1 axis in DCs associated with ovarian cancer led to an attenuated lipogenesis and restored antigen presentation.

## **CHAPTER VIII: Thesis project**

### **A. Problematics on IRE1 $\alpha$ regulation**

Being involved in essential cellular pathways, from restoring cellular homeostasis after stress to mediating adequate immune responses, IRE1 $\alpha$  activation and inactivation has to be tightly regulated. IRE1 $\alpha$  has been reported to interact with different complexes and chaperones in the ER, giving rise to the term UPRosome. IRE1 $\alpha$  interactants are key elements in determining cell fate upon ER stress, directing IRE1 $\alpha$  towards sustained activation or inhibition to promote cell survival or cell death (Woehlbier and Hetz, 2011).

The Sec61 translocon, which allows translocation of newly synthesised proteins into the ER, as previously described in chapter 3, is part of the IRE1 $\alpha$  interactome. First described to regulate IRE1 $\alpha$  RNase activity, the interaction between IRE1 $\alpha$  and the Sec61 translocon is necessary for IRE1 $\alpha$  to efficiently cleave its mRNA targets, such as *Xbp1*, upon ER stress (Plumb et al., 2015). Another member of the translocon complex, Sec63, which binds Sec61, recruits BiP to IRE1 $\alpha$  to lock IRE1 $\alpha$  in an inactive state by suppressing its high order oligomerisation and thus inhibiting its RNase activity (Li et al., 2020). Overall, it was highlighted that while the Sec61 translocon is required for IRE1 $\alpha$  to be activated during acute ER stress, it is also necessary for the protein to go back to an inactive state during prolonged ER stress. Along with this, another IRE1 $\alpha$  interactant, RNH1, a ribonuclease or RNase inhibitor, was shown to attenuate IRE1 $\alpha$  RNase activity upon sustained ER stress (Tavernier et al., 2018).

Two proapoptotic proteins, part of the BCL-2 family, BAK and BAX, form a complex with IRE1 $\alpha$  at the ER membrane and regulate IRE1 $\alpha$  activation upon ER stress (Hetz et al., 2006). IRE1 $\alpha$  activity is also dependent on several heat-shock proteins (Hsp), a group of chaperones expressed in the cell and responsible for the conformation of multiple factors, such as Hsp90, Hsp72 and Hsp47. Hsp90 binds IRE1 $\alpha$  and PERK cytoplasmic domains, and is required for both UPR actors stability at the ER membrane (Marcu et al., 2002). Hsp72, also described to bind IRE1 $\alpha$  cytoplasmic domain, was shown to enhance *Xbp1* splicing to promote cell survival upon ER stress (Gupta et al., 2010). Finally, Hsp47 was reported to associate to IRE1 $\alpha$  ER luminal domain quickly after ER stress, exchanging with BiP, to induce IRE1 $\alpha$  oligomerisation and activation (Sepulveda et al., 2018a).

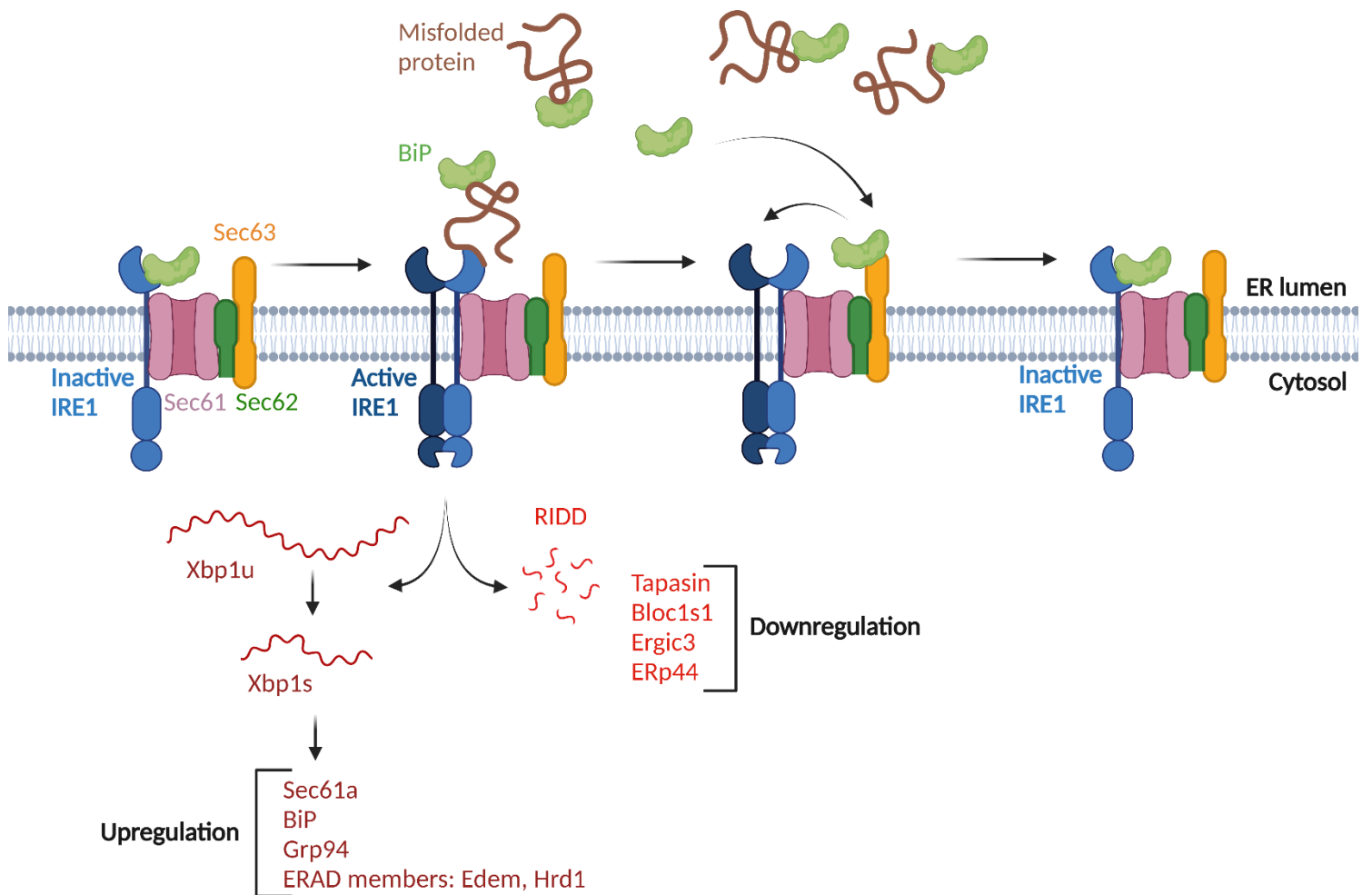


**Figure 12: Model: Regulation of IRE1 $\alpha$  activation by the Sec61 translocon and BiP.** BiP, the major chaperone keeping IRE1 $\alpha$  in an inactive state, is reportedly recruited by Sec63, part of the Sec61 translocon, to be brought back to IRE1 $\alpha$  after prolonged ER stress. After activation of IRE1 $\alpha$ , BiP and members of the Sec61 translocon are part of the upregulated proteins while RIDD targets are downregulated.

### B. Problematics on STING regulation

Involved in efficient and important interferon responses following the detection of cytoplasmic nucleic acid, the cGAS/STING pathway is crucial in various microbial and stress responses. Although, STING must be tightly regulated in cells as its constant activation was shown to lead to severe interferonopathies. In order to get activated following cytoplasmic nucleic acid recognition by cGAS, STING recruits TBK1,

necessary for phosphorylation of IRF3. While this is a known mechanism, the kinetics of TBK1, STING and IRF3 activation and phosphorylation remain unclear.

In order to better understand STING activation and degradation processes in cells, factors regulating STING were studied. Amongst them, TOLLIP was described as a STING partner, reportedly preventing its degradation and keeping stable levels of STING protein in cells (Pokayatev et al., 2020). On another hand, STIM1 also associates to STING in the ER at steady state and is required to keep STING in an inactive form. Indeed, in macrophages, it was observed that STIM1 deficiency leads to a chronic activation of STING and type I interferon production at steady state (Srikanth et al., 2019).

STING degradation is a crucial part of its regulation and is required to keep cellular homeostasis. STING degradation was shown to be mediated through its ubiquitination and to be sent to lysosomal compartments by ESCRT members, such as HGS or VPS37A (Gentili et al., 2023).

#### C. Thesis project: UNC93B1 and its role in IRE1 $\alpha$ activation and STING signalling

During my thesis, our goal was to identify new UNC93B1 clients and to assess their regulation by UNC93B1 in murine DCs. We used the homozygous UNC93B1 mutated 3d/3d mice, known to make endosomal TLRs and STIM1 unable to bind UNC93B1 and to cause a defect in their activation. While 3d DCs are resistant to microbial nucleic acid stimulation, as their endosomal TLRs don't get triggered, they also show an impaired MHC class I antigen cross-presentation, partially due to a compromised STIM1 function and a lack of calcium hotspots in phagosomes.

Looking for new UNC93B1 clients, we analysed microarrays data comparing WT and 3d spleens from mice. Amongst the downregulated mRNAs in 3d spleens compared to WT, STIM1 was identified, which led to its identification as an UNC93B1 partner. Another downregulated mRNA in 3d spleens was found to be *Ern1*, coding for the ER stress sensor IRE1 $\alpha$ . As previously explained, IRE1 $\alpha$  has a major role in MHC class I antigen cross-presentation, though whether its activation is beneficial or detrimental to this immune function is still to be discussed. In this context, the ER chaperone UNC93B1 appears to be a good candidate as an IRE1 $\alpha$  regulator in DCs, and will further deepen our knowledge on IRE1 $\alpha$  role in the immune system. In this regard, we

assessed IRE1 $\alpha$  activation in UNC93B1 mutated 3d DCs and its involvement in the impaired antigen cross-presentation observed in these cells.

In the second part of the thesis, we took an interest in a known partner of UNC93B1 in transfected cell lineages, STING. As STING is linked to various autoimmune syndromes and interferonopathies, the factors promoting STING activation or inactivation in myeloid cells are still to be investigated. In transfected HeLa cells and fibroblasts, UNC93B1 was shown to send STING to degradation upon its triggering. Although, their interaction and this function of UNC93B1 has never been assessed in myeloid cells, known to produce high amounts of pro-inflammatory cytokines and type I interferons, and where UNC93B1 is highly expressed. To decipher the role of UNC93B1 in STING activation, our goal was to assess STING regulation in UNC93B1 deficient cells or UNC93B1 mutated 3d DCs.

## **RESULTS \_ PART I: UNC93B1 regulates the unfolded protein response sensor IRE1 $\alpha$ in dendritic cells.**

While IRE1 $\alpha$  regulation has been studied for years, and various IRE1 $\alpha$  interactants have been identified, many aspects of IRE1 $\alpha$  activation and inactivation remain unclear, especially in myeloid cells. During my thesis project, our team focused on understanding how IRE1 $\alpha$  activation is controlled in DCs. Our interest in IRE1 $\alpha$  arose because we found a tight association between IRE1 $\alpha$  and UNC93B1, which has been previously studied in our group and is mandatory for intracellular TLRs signalling. Indeed, in 3d mice spleen, IRE1 $\alpha$  mRNA expression is significantly downregulated when compared to WT mice. This result led us to wonder if IRE1 $\alpha$  activity was possibly disrupted in 3d DCs, and participating in the various immune defects previously described in 3d cells. More generally, we investigated the role of UNC93B1 in IRE1 $\alpha$  activity.

In DCs, we showed that IRE1 $\alpha$  and UNC93B1 associate in the ER, through IRE1 $\alpha$  transmembrane domain. This interaction was increased in 3d DCs which harbour IRE1 $\alpha$  activation at the steady state, leading to the splicing of XBP1 and the cleavage of several RIDD targets. Several RIDD mRNA targets code for genes of the PLC and are thus required for antigen presentation. We then wondered if IRE1 $\alpha$  activation was responsible for the antigen cross-presentation defect and rapid tumour growth observed in 3d DCs. Indeed, IRE1 $\alpha$  RNase inhibition led to a restored antigen cross-presentation and limited tumoral progression in 3d DCs. Moreover, mechanistically, IRE1 $\alpha$  activation in 3d DCs can be explained by the loss of BiP binding to IRE1 $\alpha$ .





**The endoplasmic reticulum chaperone UNC93B1 regulates the unfolded protein response sensor IRE1 $\alpha$  in dendritic cells for control of cross-presentation**

Lucie Maisonneuve<sup>1</sup>, Moïse de Lavergne<sup>1</sup>, Micaela Lopez-Alarcon<sup>1</sup>, Malaiyalam Mariappan<sup>2</sup>, Mélanie Brinkmann<sup>3</sup>, Guillaume Darrasse-Jèze<sup>4</sup>, Eric Chevet<sup>5</sup>, Katrina Podsypanina<sup>1</sup> and Bénédicte Manoury<sup>1\*</sup>

1 Institut Necker Enfants Malades, INSERM U1151-CNRS UMR 8253, Université Paris Cité, Faculté de Médecine Necker, France

2 Department of Cell Biology, Nanobiology Institute, Yale School of Medicine, United States

3 Helmholtz Centre for Infection Research, Braunschweig, Germany

4 INSERM UMR\_S 959, hôpital la Pitié salpêtrière, Paris, France

5 UMR INSERM U1242, Centre de lutte contre le cancer Eugène Marquis, Rennes, Université de Rennes 1, France

\* corresponding author: Bénédicte Manoury, INEM, INSERM U1151-CNRS UMR 8253, Université Paris Cité, Faculté de Médecine Necker, 160 rue de vaugirard 75015 Paris, France, benedicte.manoury@inserm.fr

## Highlight

- The chaperone UNC93B1 interacts with the ER stress sensor IRE1 $\alpha$
- In DCs expressing a non-functional UNC93B1 protein, IRE1 $\alpha$  is constitutively activated
- Inhibition of IRE1 $\alpha$  restores MHCI antigen cross presentation and delays tumour growth in cells and mice expressing a non-functional UNC93B1 protein
- Lack of BiP association with IRE1 $\alpha$  in DCs expressing a non-functional UNC93B1 protein renders IRE1 $\alpha$  constitutively active

## Summary

Inositol requiring enzyme (IRE1 $\alpha$ ) is the most evolutionary conserved sensor of endoplasmic reticulum (ER) stress and contributes to several pathologies when dysregulated. Regulation of IRE1 $\alpha$  activation is not well understood particularly in dendritic cells (DCs) where it plays a major role in DCs survival and MHC class I antigen cross presentation. Herein, we provide evidence that UNC93B1, which chaperones intracellular TLRs, binds the transmembrane domain of IRE1 $\alpha$  in the ER. We find that in DCs expressing *Unc93b1* gene with a single nucleotide substitution (H412R or 3d), IRE1 $\alpha$  RNase activity is increased. Mechanistically, mutated UNC93B1 compromises the interaction between BiP and IRE1 $\alpha$ , leading to IRE1 $\alpha$  constitutive activation. Furthermore, inhibition of IRE1 $\alpha$  in 3d expressing DCs and mice restores MHC class I antigen cross presentation and delays tumour growth. Our data highlight the essential role of UNC93B1 in controlling IRE1 $\alpha$  activity in DCs and thus regulating MHC class I antigen cross-presentation.

## Keywords

IRE1 $\alpha$ , UNC93B1, dendritic cells, MHC class I antigen cross-presentation

## Introduction

UNC93B1, a highly conserved 12-membrane spanning molecule residing in the endoplasmic reticulum (ER), is a key regulator in the trafficking<sup>1</sup> to endosomes and folding<sup>2</sup> of intracellular Toll-like receptors (TLRs) that detect microbial nucleic acids. A mutation in the *Unc93b1* gene (H in position 412 to R also named 3d mutation) results in the inhibition of intracellular TLRs signalling in dendritic cells (DCs) and confers resistance to HSV infection in humans<sup>3,4</sup>. Recently, UNC93B1 was shown to differentially regulate intracellular TLRs signalling, in particular TLR7 and TLR9. While, in endosomes, the release of TLR9 from UNC93B1 is required for TLR9 activation<sup>5</sup>, activated TLR7 remains associated with UNC93B1<sup>6</sup>. Moreover, TLR7 stimulation leads to UNC93B1 phosphorylation, ubiquitinylation and binding to syntenin-1, targeting the complex UNC93B1-TLR7 for degradation. In mice, UNC93B1 mutation at the syntenin-1 binding site leads to excess of TLR7 signalling and to autoimmunity. Thus, UNC93B1 regulates individual TLRs by distinct mechanisms. UNC93B1 is also essential for antigen cross-presentation: a process in DCs where exogenous antigens are presented by the major histocompatibility complex class I (MHC I) pathway to prime CD8<sup>+</sup> effector T cells against pathogens and tumours. This function requires the interaction of UNC93B1 with the ER calcium sensor STIM1 or stromal interaction protein molecule 1<sup>7,8</sup>.

In eukaryotes, the ER is the largest cellular organelle. Beyond its role in calcium homeostasis and in lipid synthesis, this compartment has a fundamental function in regulating secretory and transmembrane protein biogenesis, folding, assembly, trafficking, and degradation, an important part of protein homeostasis<sup>9</sup>. This process is essential for cell survival and function and thus is tightly regulated. Disruption of protein homeostasis in the ER triggers an adaptive Unfolded Protein Response (UPR) whose main function is to restore ER homeostasis. The UPR attenuates translation and induces expression of genes whose products are selectively involved in protein folding, quality control, and protein degradation. Inositol Requiring Enzyme 1 alpha or IRE1 $\alpha$  mediates the UPR together with Protein Kinase RNA (PKR)-like ER kinase (PERK) and the Activating transcription factor 6 alpha (ATF6 $\alpha$ ). IRE1 $\alpha$  is a type I transmembrane protein that exhibits cytosolic kinase and endoribonuclease (RNase) activities and is the most conserved ER stress sensor. Upon activation, IRE1 $\alpha$  oligomerizes and trans-autophosphorylates, which leads to a conformational change in the RNase domain. As a consequence, IRE1 $\alpha$  RNase catalyses the non-conventional splicing of the transcription factor X-Box Binding Protein (XBP1) mRNA. This yields a potent transcription factor (XPB1s) that activates the transcription of genes whose products are involved in protein folding and ER-associated degradation (ERAD)<sup>10</sup>. In addition, IRE1 $\alpha$  selectively degrades

mRNAs and microRNAs through a process called Regulated IRE1-Dependent Decay of RNA (RIDD). IRE1 $\alpha$  is expressed and active at steady state in type 1 conventional DCs (cDC1), the subset of spleen DCs important for MHC I antigen cross-presentation<sup>11</sup>. cDC1 lacking XBP1 display hyperactivation of RIDD, abnormal ER morphology, and impaired MHC I antigen cross-presentation, highlighting a role for the IRE1 $\alpha$ -XBP1 axis in cDC1 biology<sup>12</sup>. In addition, recently, loss of XBP1 in cDC1 was associated with the survival or death of DCs resident in specific organs and the ability of these DCs to switch off protein synthesis and to control RIDD activity<sup>13</sup>. In contrast, in bone marrow-derived DCs (BM-DCs), IRE1 $\alpha$  inhibition was shown to reduce MHC I antigen cross-presentation when cells are pulsed with melanoma cell lysate<sup>14</sup>. However, antigen uptake in DCs was shown to trigger the RIDD pathway to directly cleave MHC I mRNA, and the use of a specific kinase IRE1 $\alpha$  inhibitor in DCs led to an increase in MHC I antigen cross-presentation<sup>15</sup>.

Despite these findings, molecular events regulating ER stress and IRE1 $\alpha$  activation, as well as the nature of IRE1 $\alpha$  interactome, are still not completely characterized, especially in DCs, where IRE1 $\alpha$  plays a major role in cell survival and MHC class I antigen cross-presentation. In the present study, we find that UNC93B1 associates with IRE1 $\alpha$  transmembrane domain in DCs. A single amino acid substitution (H in position 412 to R) in UNC93B1 transmembrane domain 9 enhances IRE1 $\alpha$ -UNC93B1 binding, disrupts IRE1 $\alpha$ -BiP association and leads to an increase in IRE1 $\alpha$  RNase activity. Furthermore, inhibiting IRE1 $\alpha$  activity in UNC93B1 H412R DCs restores MHC class I antigen cross-presentation *in vitro* and delays tumour growth *in vivo*.

## Results

**IRE1 $\alpha$  interacts with UNC93B1 in dendritic cells.** We have previously shown that in UNC93B1 H412R or 3d DCs, UNC93B1 is no longer associated with intracellular TLRs and STIM1, leading to their loss of function. To investigate if UNC93B1 binds to other proteins in the ER, we explored our previous results on gene expression in wild-type (WT) and 3d spleen<sup>7</sup>, and found that *Ern1* mRNA is down regulated in 3d spleen (Supplementary Fig.1a). To validate this result, we measured both mRNA and protein expression of IRE1 $\alpha$  in different subsets of DCs present in the spleen and found similar expression in conventional-, type 1 conventional- and Bone-marrow (BM)- DCs from WT and 3d mice (Supplementary Fig.1b, c). Like for STIM1 which showed reduced gene expression in 3d spleen compared to WT but identical protein level, we hypothesized that IRE1 $\alpha$  function or activity might be modified in 3d DCs. Furthermore, in XBP1 deficient cDC1 which have increased IRE1 $\alpha$  activity, down regulation of

*Stim2*, a murine homolog of the *Stim1* gene, was reported<sup>12</sup>. We first assessed possible interaction between UNC93B1 and IRE1 $\alpha$ . HeLa cells were co-transfected with Ern1-HA and Unc93b1<sup>WT</sup> or Unc93b1<sup>3d</sup> both in fusion with mCherry, and overexpressed tagged proteins were co-immunoprecipitated. We found that both WT and mutated UNC93B1 did interact with IRE1 $\alpha$  (Fig. 1a). To validate this result, we used a proximity ligation assay which allows for reporting the proximity between proteins *in situ* when they are within a 40nm range<sup>16,17</sup>. Enhanced proximity between 3d and IRE1 $\alpha$  was detected in HeLa cells overexpressing IRE1 $\alpha$ -HA and 3d-FLAG when compared to cells overexpressing wild type (WT)-UNC93B1-FLAG (Fig. 1b). Then, we determined the sub-cellular distribution of IRE1 $\alpha$ -HA and UNC93B1-FLAG proteins. Colocalization of both proteins was quantified using the Mander's coefficient. 3d-UNC93B1 exhibited a higher colocalization index with IRE1 $\alpha$  than WT-UNC93B1, consistent with the PLA data. To test if this interaction could be detected on endogenous, we co-immunoprecipitated endogenous IRE1 $\alpha$  and UNC93B1 proteins from WT and 3d primary DCs using a homemade UNC93B1 antibody which is specific for UNC93B1 and only worked in non-denaturing conditions (Supplementary Fig. 1d). In this context, we noticed lower expression of UNC93B1 in 3d DCs suggesting perhaps a faster degradation of the protein or its aggregation which could result in reduced recognition of the antibody (Supplementary Fig. 1c, e). As shown in Fig.1d and 1e, both WT and 3d proteins bind IRE1 $\alpha$ . In addition, upon thapsigargin (TG) treatment, an ER stressor that acts by blocking SERCA2B thus leading to ER Calcium depletion, the IRE1 $\alpha$ /UNC93B1 interaction remained stable (Fig. 1d, e). Of note, increased IRE1 $\alpha$ -UNC93B1 association is detected in 3d DCs and cells treated with TG. (Fig. 1d). Interestingly, IRE1 $\alpha$  did not co-immunoprecipitate with STIM1, which is known to form a complex with UNC93B1 (Supplementary Fig. 2a). Using the proximity ligation assay, our results corroborated a close proximity between WT UNC93B1 and IRE1 $\alpha$  which was enhanced in the presence of the 3d protein, in contrast to what we saw with STIM1 (Fig. 1f, Supplementary Fig. 2b). Interestingly, proximity between UNC93B1 and IRE1 $\alpha$  also increased upon TG treatment but only in WT DCs, and remains at the same level in DCs expressing 3d UNC93B1 treated or not with TG (Fig. 1f). Our data indicate that UNC93B1 interacts with IRE1 $\alpha$  and that the interaction is enhanced during ER stress and in DCs expressing the 3d mutant, which no longer binds intracellular TLRs and STIM1.

**The transmembrane region of IRE1 $\alpha$  is required for the association with UNC93B1.** We previously showed that UNC93B1 binds the luminal domain of STIM1<sup>7</sup>. More recently, the amino acids residues 152-240 in the luminal domain and close to the transmembrane region of STIM1 were reported to play an essential role in STIM1 binding to UNC93B1<sup>18</sup>. Thus, to

identify the site of interaction between IRE1 $\alpha$  and UNC93B1, HeLa cells were co-transfected with Ern1-HA mutants lacking either the luminal ( $\Delta$ LD 30-408) or the cytosolic ( $\Delta$ CD 477-977) domain of IRE1 $\alpha$  (Fig. 2a) and Unc93b1<sup>WT</sup> or <sup>3d</sup> -mCherry cDNAs, and IRE1 $\alpha$ -UNC93B1 complexes were co-immunoprecipitated using an RFP antibody. Both IRE1 $\alpha$  mutants retained the association capacity with WT UNC93B1 (Fig. 2b, left panel), suggesting that deletion of either the luminal or the cytosolic domain of IRE1 $\alpha$  had no effect on the interaction with UNC93B1. To our surprise, interaction between  $\Delta$ LD-IRE1 $\alpha$  or  $\Delta$ CD-IRE1 $\alpha$  and mutated UNC93B1 was conserved in 3d-UNC93B1 expressing cells (Fig. 2b, right panel). Furthermore, deletion ( $\Delta$ 10) of an evolutionary conserved 10 amino acid sequence (434-443) in the juxtamembrane of IRE1 $\alpha$  (Supplementary Fig. 3a), essential for the binding to the Sec61 translocon channel<sup>19,20</sup>, did not alter the interaction of IRE1 $\alpha$  with WT- or 3d-UNC93B1 (Supplementary Fig. 3b), demonstrating that IRE1 $\alpha$  and STIM1 use different regions to bind UNC93B1. UNC93B1 interacts with TLR9 but not with a TLR9 chimera protein expressing the transmembrane domain (TMD) of TLR4 indicating that TLR9 binds UNC93B1 via its TMD<sup>21</sup>. We then next assessed whether the TMD of IRE1 $\alpha$  (amino acids 444-464, Fig. 2c) was also required for binding to UNC93B1 as it was suggested for TLR9. To address this, we used a mutant of IRE1 $\alpha$  bearing the TMD of calnexin (IRE1-CNX-TMD construct<sup>22</sup>). As shown in Fig. 2d, expression of the IRE1 $\alpha$  CNX TMD chimera abolished the interaction with WT and with 3d UNC93B1. Moreover, single mutations at amino acids S439, T446, S450, T451 in the juxtamembrane and the TMD of IRE1 $\alpha$  (Supplementary Fig. 3a) did not influence the association between IRE1 $\alpha$  and WT or 3d UNC93B1, thereby indicating that amino acids 446, 450 and 451 within IRE1 $\alpha$  TMD are not important for the binding to WT or 3d UNC93B1 (Supplementary Fig. 3b). Of note, the rates of transfection in HeLa cells of WT Ern1-HA,  $\Delta$ LD-Ern1-HA,  $\Delta$ CD-Ern1-HA, TMD-Ern1-HA and Unc93b1<sup>WT</sup>-mCherry or Unc93b1<sup>3d</sup>-mCherry cDNAs were similar (Supplementary Fig. 3c, 3d). These results suggest that IRE1 $\alpha$  binds to UNC93B1 proteins through its transmembrane region.

**UNC93B1 shapes IRE1 $\alpha$  activity in dendritic cells.** We hypothesized that the increase of binding between 3d-UNC93B1 and IRE1 $\alpha$  observed in DCs and in HeLa cells (see Fig. 1) might impact on IRE1 $\alpha$  RNase activity. To test this hypothesis, we first monitored the amounts of spliced and unspliced forms of *Xbp1* mRNA using conventional PCR in WT and 3d cDC1, where the expression of IRE1 $\alpha$  is high (<sup>12</sup>, Supplementary Fig. 1c). While WT cDC1 did not express *Xbp1s*, 3dcDC1 exhibited some spliced *Xbp1*, which is enhanced in both cells upon TG treatment (Fig. 3a). To assess the activity of XBP1s in WT and 3d cDC1 and BM-DCs, we measured mRNA levels of *BiP*, *Sec61*, *Sec63*, *Edem 1*, *Chop* and *Grp94*, previously reported



XBP1s target genes<sup>23</sup>. Real-time PCR indicated that *Sec63* and *Edem 1* mRNA levels were significantly reduced in 3d BM-DCs, while levels of *Sec61* and *BiP* mRNAs remained identical between WT and 3d BM-DCs (Fig. 3b). As expected, all these XBP1s target genes were significantly induced following ER stress (Fig. 3b). In addition, mRNAs levels of *Chop* or *Grp94*, target genes of the three arms of the UPR, IRE1 $\alpha$ , ATF6 and PERK, were increased in 3d BM-DCs (Fig. 3b, Supplementary Fig. 3a). We then quantified the expression levels of the RIDD targets such as *Tabpb*, *ERp44*, *Ergic53* and *Bloc1s1*. Analysis of the canonical RIDD genes, *ERp44* and *Tabpb*, showed a clear decrease in their expression level in 3d BM-DCs and cDC1, while *Bloc1s1* and *Ergic53* remain globally unaffected (Fig. 3c, 3d). Again, as expected, mRNA RIDD targets are cleaved upon ER stress (Fig. 3c, 3d). Finally, to test IRE1 $\alpha$  activity in WT and 3d DCs, we used an RNA *Xbp1* probe which bears the consensus IRE1 $\alpha$  cleavage site (CAUGUCCGCAGCGCAUG) and emits fluorescence at 670 nm (Cy5) when cleaved by IRE1 $\alpha$ . As a proof of concept, the cleavage of the RNA *Xbp1* probe upon time was detected *in vitro* with human recombinant IRE1 $\alpha$  (Supplementary Fig. 4b). In addition, MKC8866 or 4 $\mu$ 8c, known IRE1 $\alpha$  RNase inhibitors<sup>24,25</sup>, inhibit the human recombinant IRE1 $\alpha$  *in vitro* (Supplementary Fig. 4b). We then measured the RNase activity of endogenous IRE1 $\alpha$  in DCs using this probe. Lysates from WT or 3d DCs treated or not with TG to activate IRE1 $\alpha$ , were immunoprecipitated with IRE1 $\alpha$  antibody, incubated with the RNA *Xbp1* probe and Cy5 fluorescence was detected upon time. In WT cells, IRE1 $\alpha$  RNase activity raised over time, reflecting the cleavage of the probe, and was enhanced following TG treatment (Supplementary Fig. 4c). IRE1 $\alpha$  RNase activity was significantly higher in DCs expressing 3d-UNC93B1 and did not further increase upon TG treatment. IRE1 $\alpha$  RNase activity detected in WT DCs treated with TG was similar to that detected in 3d DCs whether or not they were treated with TG (Fig. 3e, right panel).

We then assessed ER morphology using immunofluorescence microscopy with an anti-KDEL antibody<sup>26</sup>. Confocal microscopy images displayed aberrant clusters of ER cisternae shown by an accumulation of the marker KDEL in 3d cDC1s and cDC2s (Fig. 3f), a result similar to that in XBP1 deficient cells with hyper activation of IRE1 $\alpha$ <sup>12</sup>. This is not surprising as we reported earlier<sup>7</sup> that 3d DCs have a defect in oligomerization of STIM1, a protein involved in Ca<sup>2+</sup> homeostasis, a process known to affect ER morphology. Thus, 3d-UNC93B1 expression enhances IRE1 $\alpha$  RNase activity and alters ER morphology in DCs, likely to linked to constitutive ER stress.

**Inhibition of IRE1 $\alpha$  in 3d dendritic cells or mice restores antigen cross-presentation and decreases tumour growth.** cDC1, which are the predominant cells which cross present antigens *in vivo*, have an essential role in priming CD8<sup>+</sup> T cells against pathogens. cDC1s from XBP1 deficient mice with increased IRE1 $\alpha$  activity and enhanced cleavage of the RIDD mRNA target *Tabpb*, showed impaired presentation of dead cell antigens<sup>12</sup>. We found lower levels of *Tabpb* mRNAs in 3d BM-DCs and cDC1 (Fig. 3c, d). The *Tabpb* gene encodes Tapasin, a protein required for the assembly of MHC I molecules with antigenic peptides. Thus, we investigated the contribution of activated IRE1 $\alpha$  to MHC I antigen cross-presentation in 3d BM-DCs by using the IRE1 $\alpha$  RNase inhibitors MKC8866 or 4 $\mu$ 8C. WT or 3d BM-DCs were treated with 4 $\mu$ 8C for 30 minutes prior to incubation with ovalbumin (OVA) coated beads for 6 hours. BM-DCs were then washed, fixed and co-cultured with CFSE labeled OT-I T cells (T cells expressing a T cell receptor specific for MHC class I- ovalbumin peptide complex, MHC I-SIINFEKL), and proliferation of T cells was assessed 72 hours later. As previously shown<sup>7</sup>, while WT BM-DCs support proliferation of OT-I T cells in response to OVA-coated beads, 3d BM-DCs have a defect in presenting ovalbumin from particulate antigens (Fig. 4a, b). Remarkably, inhibition of IRE1 $\alpha$  resulted in the restoration of antigen cross-presentation in 3d DCs, nearly to the same level as in WT DCs (Fig. 4a, b). At the same time, IRE1 $\alpha$  RNase inhibition did not impact on antigen cross-presentation in WT DCs (Fig. 4a, b). Cell of either genotype, incubated or not with 4 $\mu$ 8C, presented equally the SIINFEKL peptide, that does not require antigen processing (Fig. 4a, b). To assess antigen presentation to CD4<sup>+</sup> T cells, similar experiments were performed using OT-II T cells, which express a T cell receptor recognizing MHC class II-OVA peptide complexes (MHCII-323-339). We noticed no difference in OT-II proliferation induced by WT or 3d BM-DCs, treated or not with 4 $\mu$ 8C in the presence of soluble OVA (Supplementary Fig. 5a). We and others have previously shown that antigen cross-presentation is important for the induction of anti-tumour response. To examine the role of IRE1 $\alpha$  in antigen cross-presentation in the context of tumour progression, we first subcutaneously inoculated 2x10<sup>5</sup> B16 melanoma cells expressing ovalbumin (B16-OVA), followed by daily injections (day -1 to day 21) of 15mg/kg of MKC8866 intra-peritoneally. As previously published<sup>7</sup>, tumours grew faster in 3d mice in comparison to WT mice (Fig. 4c, Supplementary Fig. 5b). Consistent with our *in vitro* results, treatment with MKC8866 reduced tumour growth in both WT and 3d mice. We then injected 2x10<sup>5</sup> B16-OVA subcutaneously 24h before adoptively transferring or not 2x10<sup>6</sup> OT-I T cells, followed by repeated injections (day -1 to day 21) of 15mg/kg of MKC8866. OT-I T cells transfer alone induces significant delay in tumour growth in WT, but not in 3d mice, as previously described<sup>7</sup>. However, injection of MKC8866 together with OT-I T cells significantly reduced tumour growth in 3d mice. We

conclude that blocking IRE1 $\alpha$  activity in 3d DCs or mice restores antigen cross-presentation *in vitro* and delays tumour growth *in vivo*.

**3d-UNC93B1 protein suppresses BiP-IRE1 $\alpha$  association in dendritic cells.** Our data indicate that mRNA levels of *Sec63* are severely reduced in 3d BM-DCs (Fig 3b). In addition, proteomic studies confirmed that *Sec63* is down regulated in 3d DCs in comparison to WT DCs (data not shown). *Sec63* is part of the translocon channel and was shown to recruit and activate BiP via its luminal domain to bind IRE1 $\alpha$ , thus suppressing the activity of IRE1 $\alpha$ <sup>22</sup>. As such, BiP plays a central role in regulating the oligomerization and activity of IRE1 $\alpha$  (Fig. 5a). We hypothesized that BiP association with IRE1 $\alpha$  might be reduced in DCs expressing 3d-UNC93B1, which would explain the constitutive IRE1 $\alpha$  activity in these cells. First, we measured BiP protein expression and found identical expression between WT and 3d DCs at steady state or following ER stress (treatment with TG and tunicamycin) (Supplementary Fig. 6a). Second, we used PLA to monitor IRE1 $\alpha$ -BiP proximity in WT and 3d BM-DCs, a technic allowing us to visualize proximity between endogenous IRE1 $\alpha$  and BiP *in situ*. Confocal microscopy images detected no BiP protein in proximity to IRE1 $\alpha$  in 3d DCs at steady state when compared to WT cells (Fig. 5b). As a control, tunicamycin treatment, which induces ER stress, abrogates IRE1 $\alpha$ -BiP proximity in WT DCs. Furthermore, proximity and colocalization between *Sec63* and IRE1 $\alpha$  is also reduced in 3d DCs (Supplementary Fig. 6c, d). This result implies that 3d-UNC93B1 protein inhibits the binding of BiP to IRE1 $\alpha$  by altering the localization of *Sec63*.

## Discussion

Our studies shed light on the mechanistic understanding how IRE1 $\alpha$  activity is controlled in dendritic cells. Here, we report that the intracellular chaperone UNC93B1 binds to IRE1 $\alpha$  to regulate its localization and function.

Using co-immunoprecipitation and PLA experiments at steady state and under conditions of ER stress, we showed a dynamic association between UNC93B1 and IRE1 $\alpha$ , mediated by IRE1 $\alpha$  transmembrane domain. This association is increased upon ER stress, and is preserved in the presence of the 3d-UNC93B1 mutant. Confocal microscopy experiments confirmed stronger colocalization between UNC93B1 and IRE1 $\alpha$  in cells expressing 3d-UNC93B1 protein in comparison to cells expressing WT UNC93B1. This indicates 3d-UNC93B1 mutant protein recruits IRE1 $\alpha$  to a specific localization in the ER in sub-

domains, possibly as a consequence of loss of association with intracellular TLRs and/or STIM1 (Fig. 6).

In normal cells, UNC93B1 is responsible for the transport of intracellular TLRs from ER to endosome, an organelle where their cleavage and signalling takes place<sup>1,21,27</sup>. It is known that mutations in UNC93B1, including 3d, disrupt the interaction with intracellular TLRs and their level of expression, and lead to autoimmunity<sup>28,29</sup>. In addition, human patients with loss of function of UNC93B1 are more susceptible to viral infections<sup>4</sup>. Recently, the Cryo-EM structure between TLR3 or TLR7 and UNC93B1 was resolved<sup>30</sup>. These data reveal that TLR3 and TLR7 use a common structure to interact with UNC93B1. Both regions of TLRs, the TMD and the juxta-membrane region, make contacts with the helix bundle of TMD6 in UNC93B1. However, the stoichiometry of these complexes differs. While two UNC93B1 proteins interact with TLR7 dimers, only one associates with TLR3 monomer, possibly explaining why UNC93B1 needs to dissociate from TLR3 but not from TLR7 for their activation. It is tempting to speculate that in the absence of interaction with TMD of TLRs, the mutant 3d-UNC93B1 becomes available for enhanced association with IRE1 $\alpha$ .

UNC93B1 was shown to interact with the luminal domain of STIM1, a calcium sensor in the ER, that contains EF and SAM motifs, both important for STIM1 function<sup>7,8</sup>. At

steady state, STIM1 EF domain binds Ca<sup>2+</sup> and keeps STIM1 in a stable inactivated conformation. Upon Ca<sup>2+</sup> depletion, EF-SAM domains open out to allow STIM1 to rapidly oligomerize. More recently, generation of a truncated STIM1 mutant lacking a part of the SAM domain (aa between 152-214) failed to immunoprecipitate with UNC93B1, suggesting that the binding site for UNC93B1 is in the STIM1 SAM domain and that UNC93B1 might facilitate STIM1 oligomerization<sup>18</sup>. Upon Ca<sup>2+</sup> depletion, UNC93B1 helps STIM1 to reach the plasma membrane to interact with ORA1 for Ca<sup>2+</sup> replenishment. In the presence of 3d-UNC93B1, reduced amount of STIM1 reaches the PM faster, together with partial accumulation of the 3d-UNC93B1 mutant, suggesting again that the conformation/localization of both proteins might be altered. In addition, absence of UNC93B1 changes localization of STIM1 in the ER, indicating that UNC93B1 might control STIM1 trafficking within specific ER domains<sup>18</sup>. It is possible that the altered conformation of the 3d-UNC93b1 mutant favors association with IRE1 $\alpha$  at the expense of binding STIM1.

The regulation of IRE1 $\alpha$  activity depends on a protein-protein interaction network, which is probably cell specific. This network has been investigated using different methods including yeast 2-hybrid, interaction proteomics<sup>31,32</sup> or other targeted approaches. Functional annotation of the IRE1 $\alpha$ -interactome revealed the enrichment of proteins involved in protein

folding in the ER and antigen processing and presentation. Several proteins interact with IRE1 $\alpha$  and help to stabilize IRE1 $\alpha$  structure. At steady state, BiP is associated with IRE1 $\alpha$  along with SEC61, SEC63, HSP47 and Erdj4<sup>33</sup>. When cells are stressed, the level of unfolded proteins in the ER rises and promotes dissociation of BiP from the luminal domain of IRE1 $\alpha$ <sup>34</sup>. This dissociation induces dimerization and activation of IRE1 $\alpha$ . However, recent studies demonstrate that IRE1 $\alpha$  can also directly bind misfolded proteins in the ER, which promotes IRE1 $\alpha$  conformational change and oligomerization<sup>35</sup>. We also noticed that ER homeostasis is altered in 3d DCs, resulting in aberrant clustered of ER cisternae, similar to what was observed in XBP1 deficient DCs<sup>12</sup>. In addition, using two conformation-specific UNC93B1 antibodies recognizing endogenous UNC93B1 cytosolic domains, UNC93B1 expression is barely detectable in 3d DCs. Altogether, this suggest that 3d-UNC93B1 protein might be misfolded thus promoting ER stress. Furthermore, our PLA experiments show loss of association between IRE1 $\alpha$  and BiP in 3d-UNC93B1 cells. Thus, increased association between IRE1 $\alpha$  and the misfolded 3d-UNC93B1 mutant might induce changes in the conformation of IRE1 $\alpha$ , leading to its dissociation from BiP. Future work addressing mechanisms by which UNC93B1 controls IRE1 $\alpha$  activation should provide new insights in IRE1 $\alpha$  pathway. In particular, how IRE1 $\alpha$  folds, activates and responds to ER stress in the absence of UNC93B1 is currently under investigation in our laboratory.

Using conventional and real-time PCR, we show that the increased interaction between endogenous 3d mutant UNC93B1 and IRE1 $\alpha$  is associated with increased *Xbp1 mRNA* splicing and RIDD mRNA target cleavage. Recently, the role of IRE1 $\alpha$  in antigen cross-presentation was highlighted<sup>12,14</sup>. Indeed, in cDC1 lacking XBP1, IRE1 $\alpha$  protein expression and activity is exacerbated, leading to a defect in MHC I antigen cross-presentation of apoptotic cells. Both abnormal ER morphology and the increase in RIDD activity could account for the loss of exogenous antigen presentation in XBP1 deficient DCs. Actually, fusion of ER membranes to phagosomes<sup>36,37</sup> and expression of transcripts such as *Tapbp*, lost in XBP1 deficient cells, are central for the MHC I antigenic cross-presentation pathway<sup>12</sup>. Our results demonstrate that, similar to DCs lacking XBP1, RIDD target *Tapbp* mRNA is cleaved in 3d DCs. Loss of Tapasin expression might account for the decrease in antigen cross-presentation we observed in 3d DCs. To further support this, blocking IRE1 $\alpha$  activity in 3d DCs, using an IRE1 $\alpha$  specific inhibitor, is sufficient for restoring antigen cross-presentation *in vitro* and effective cross-priming of CD8<sup>+</sup> T cells in a tumour model *in vivo*.

In summary, our data identify IRE1 $\alpha$  as a binding partner for UNC93B1, and suggest a new biological role for UNC93B1 in ER stress in DCs. Furthermore, the association between UNC93B1 and IRE1 $\alpha$  might determine the oligomerization state of IRE1 $\alpha$  and thus predict the

cellular stress response. IRE1 $\alpha$  plays a major role in ER stress, which is central to multiple pathologies from inflammation to cancer. Identifying new proteins involved in ER stress, such as UNC93B1, could contribute to understanding how this process is regulated and be used as a strategy for interfering with inflammation.

## Methods

**Mice.** C57BL/6 mice were purchased from INEM animal facility (INSERM U1151). UNC93B1 3d/3d C57BL/6 mice were a gift by Dr B. Ryffel (CDTA, Orléans). Both WT and 3d colonies were bred at INEM and their genotype was routinely assessed with PCR followed by sequencing or restriction site mutation assay. Animals were housed under SOPF (Specific and Opportunist Pathogen Free) conditions, at stable temperature (around 22°C) with a 12-hour light-dark cycle. OT-I and OT-II (CD45.1+) TCR-transgenic mice were kindly given by Drs. van Ender (INEM, Paris) and Fahraeus (IRSL, Paris). UNC93B1<sup>-/-</sup> mice were kindly provided by Dr. Brinkmann (HZI, Braunschweig). Experiments were performed with 8 to 12-weeks old mice, male and female, weighing 20 to 30g, given access to food and water *ad libitum*. All experimental procedures were carried out in accordance with the guidelines of the French Veterinary Department and were approved by an ethical committee (code number: A-75–2003).

**Tumour growth.** Tumoral growth measurements were performed by first injecting the IRE1 $\alpha$  inhibitor MKC8866 (from Dr. Chevet – Biosit, Rennes) intraperitoneally at 15mg/kg at day -1 in the treated mice of the cohort. At day 0, 2x10<sup>5</sup> B16-OVA melanoma cells were injected subcutaneously in the flank. At day 1, 2x10<sup>6</sup> OT-I T cells were injected retro-orbitally. While tumors grew and until the mice were sacrificed, MKC8866 was injected every day.

**Primary dendritic cells preparation.** Conventional dendritic cells (cDCs) were purified from C57BL/6 WT and 3d/3d mice spleens after subcutaneous injection of B16 melanoma cells secreting the cytokine Flt3-L. Spleens were taken after 10 to 14 days of tumoral growth and were processed with collagenase D 1mg/mL, diluted in pure RPMI (Roswell Park Memorial Institute) 1640 medium and supplemented with 20 $\mu$ g/mL of DNase I. After digestion, cells were incubated in red blood cell lysis buffer (0.15M NH<sub>4</sub>Cl, 0.1M NaHCO<sub>3</sub>, 0.1mM EDTA) for 1

minute at room temperature. Splenic cells were stained with CD19-BV510, CD3-PE, CD11c-BV711, CD11b-APCefluor780 and 7AAD and cDCs were sorted using a BD FACS Aria III. Bone marrow derived dendritic cells (BM-DCs) were generated from C57BL/6 WT, and 3d/3d mice. Bone marrow cells were cultured in complete IMDM (Iscove's Modified Dulbecco's Medium, 10% FBS, 1% L-glutamine, 1% penicillin/streptomycin, 50 $\mu$ M  $\beta$ -mercaptoethanol) supplemented with 20ng/mL of GM-CSF (Peprotech, 315-03). Bone marrow cells were differentiated into BMDCs in 7 to 8 days as previously described<sup>7</sup>.

**Plasmid purification.** pUNO mUNC93B1-HA plasmid (Invivogen) was cloned into pmCherry-C1 or c-flag-pcDNA3.1 plasmids<sup>7</sup>. WT and mutant plasmids of IRE1 $\alpha$ -HA (IRE1 $\alpha$ - $\Delta$ LD, IRE1 $\alpha$ - $\Delta$ CD, IRE1 $\alpha$ -TMD CNX, IRE1 $\alpha$ - $\Delta$ 10, IRE1 $\alpha$ -STST) were generated as previously described<sup>19,22</sup>. MAX Efficiency DH5 $\alpha$  competent cells (Thermo Fisher) were transformed with 1 to 10ng of plasmids. Bacteria were then grown in LB medium supplemented with 100 $\mu$ g/mL of antibiotics (Ampicillin or Kanamycin) and the plasmids were purified using the Nucleobond Xtra Maxi EF kit (Macherey-Nagel). The high copy plasmid purification protocol provided by the manufacturer was followed. Purified DNA was resuspended in nuclease-free water.

**Transfection in HeLa cells.** HeLa cells were cultured in 6-well plates (0.1x10<sup>6</sup> cells per well), in complete RPMI medium (RPMI 1640 medium with 10% FBS, 1% L-glutamine, 1% penicillin/streptomycin) at 37°C with 5% CO<sub>2</sub>, overnight before transfection. Jet-Prime (Ozyme) reagents were mixed with 1 $\mu$ g of IRE1 $\alpha$ -HA and 0.5 $\mu$ g of UNC93B1-mCherry or FLAG plasmids and incubated in HeLa cells following the manufacturer's instructions. Cells were transfected for 40 to 48 hours before analysis by flow cytometry or processed for western blot or immunoprecipitation.

**Immunoprecipitation and western blot.** Cells stimulated or not with 1 $\mu$ M of thapsigargin (SIH-399, StressMarq Biosciences) for 30 minutes were lysed in NP-40 or digitonin lysis buffer (150mM NaCl, 50mM Tris pH7.5, 5mM MgCl<sub>2</sub> and 0.5% NP-40 or 1% digitonin) supplemented with protease inhibitors and phosphatase inhibitors for 30 minutes on ice. Immunoprecipitation of endogenous complexes was performed by incubating 0.8 to 1 mg of proteins from cell lysates on magnetic protein G beads (Invitrogen) coated with IRE1 $\alpha$  or UNC93B1 antibodies (Supplementary table 1). Washes were performed with PBS Tween 0.02%. The next day, proteins were eluted with LDS Sample Buffer 4X at 95°C for 5 minutes or at room temperature for 30 minutes when visualizing UNC93B1 by western blot. For immunoprecipitation of

transfected proteins in HeLa cells, RFP-beads (Chromotek) or HA-beads (Invitrogen) were incubated with 0.8 to 1 mg of proteins from cell lysates. For RFP-beads, washes were performed with 10mM Tris pH7.5, 150mM NaCl, 0.5mM EDTA, 0.05% NP-40 and cell lysates were left on the beads for 2 hours at 4°C. For HA-beads, washes were performed with TBS Tween 0.05% and cell lysates were incubated with the beads overnight at 4°C. Proteins were eluted in LDS Sample Buffer 4X at 95°C for 5 minutes. Total cell lysates were mixed with LDS sample buffer 4X with or without heat-denaturation (when visualizing UNC93B1). For western blot, proteins were separated in a 4-12% SDS Nu-PAGE Bis-Tris gel at 120V for 1 hour and 30 minutes in MOPS running buffer. They were then transferred on a PVDF membrane using the P0 dry transfer protocol from iBlot2 (Thermo Fisher). Membranes were incubated with primary antibodies (Supplementary table 1) overnight at 4°C. The next day, secondary antibodies coupled to HRP were incubated on membranes for an hour at room temperature. PICO Plus or Atto ECL (Invitrogen) were used to visualize proteins by chemiluminescence.

**Microarrays.** Microarray data were analyzed from the project GSE41496 Gene Expression Omnibus executed on Agilent-028005 SurePrint G3 Mouse GE 8x60K. The original experiments were performed to compare the whole transcriptome from spleens of Chabaudi-infected mice to control mock-infected mice, which were either wild-type or defective in various TLR-related molecules. The data set description can be found via the following link: <https://www.ncbi.nlm.nih.gov/geo/query/acc.cgi?acc = GSE41496>. From these data, we analyzed control spleens from UNC93B1 3d/3d (GSM1018264, GSM1018265, GSM1018266, GSM1018267) and WT/WT (GSM1018240, GSM1018241, GSM1018242, GSM1018243) mice. The data were processed as previously described<sup>7</sup>.

**RT-PCR and RT-quantitative PCR.** RNA was extracted from steady state or thapsigargin treated cells (1µM, 1 hour 30 minutes) using the Illustra RNA minispin kit (GE Healthcare) and the manufacturer's protocol was followed. Purified RNA was resuspended in RNase-free water. RNA concentration was measured using Nanodrop (Thermo Fisher) and 400ng of RNA were processed into cDNA, using a reverse transcription mix (Applied Biosciences). For regular PCR, RNA was amplified using Phire Green PCR Master Mix (Thermo Fisher) in a Biometra thermocycler. Amplified samples were run in a 3% agarose gel supplemented with 0.007% of GelRed and the bands were visualized using a GelDoc XR+ reader. For qPCR, cDNA was amplified with a SYBR Green Master Mix (Applied Biosciences) in a Biorad thermocycler, using the appropriate annealing temperature and concentration for each primer (Supplementary table 2). The annealing temperature of each primer was assessed using the



Tm calculator website (Thermo Fisher). Data were analyzed with the Biorad software and the threshold was set to 100 to calculate the C<sub>t</sub> values.

**Immunofluorescence.** HeLa cells were cultured on glass coverslips before transfection with IRE1 $\alpha$ -HA and UNC93B1-FLAG for 48 hours. Primary dendritic cells were left to adhere on fibronectin-treated coverslips. Cells were first incubated in PHEM buffer diluted 1:1 in warm media (PHEM 2X: 120mM PIPES, 50mM Hepes, 20mM EGTA, 4mM MgAc, pH 6.9) for 5 minutes at 37°C. They were then fixed with cold 100% methanol for 3 minutes at room temperature. Cells were permeabilized in buffer (0.01% TritonX-100, 0.05% BSA in PBS) for 30 minutes at room temperature before incubation with primary antibodies (Supplementary table 1) for 1 hour at room temperature or overnight at 4°C. Secondary antibodies were left on coverslips for 30 minutes at room temperature. Cells were fixed again with 4% paraformaldehyde for 5 minutes before incubation with NH<sub>4</sub>Cl 50mM for 5 minutes, at room temperature. Coverslips were then mounted on glass slides. Images were acquired on a confocal microscope Leica SP8 gSTED. To assess colocalization, single channel images were first segmented using Ilastik software to suppress background signal. Then, on Fiji, ROIs were drawn to outline individual cells, and colocalization was measured and expressed as Mander's coefficient using the JaCoP plugin. All this processed was automated using a program written by Nicolas Goudin (INEM, Paris).

**Proximity ligation assay.** Cells were cultured on glass coverslips and stimulated with 1 $\mu$ M thapsigargin for 30 minutes or 1 $\mu$ g/mL tunicamycin (128195, Cell Signaling Technology) for 4 hours. As described in the immunofluorescence methods, cells were fixed with methanol, incubated with permeabilization buffer and with primary antibodies (Supplementary table 1). The following steps were carried out using the Duolink PLA reagents (Sigma Aldrich) according to manufacturer's instructions. Images were acquired on a confocal microscope Leica SP8 gSTED and analysis were done on Icy bioimage analysis software. PLA index was calculated on a stack of 15 images.

**IRE1 $\alpha$  RNase activity assay.** Steady state or thapsigargin treated (1 $\mu$ M for 30 minutes) BM-DCs were lysed in NP40 lysis buffer (150mM NaCl, 50mM Tris pH7.5, 5mM MgCl<sub>2</sub> and 0.5% NP-40) and cell lysates were immunoprecipitated for IRE1 $\alpha$  coupled to beads overnight. The beads were then resuspended in buffer A (20mM hepes pH 7.5, 1mM MgOAc, 50mM KOAc) and a dark opaque 96-well plate (Greiner bio-one) was used to assess IRE1 $\alpha$  enzymatic

activity. A master mix containing 1µg of IRE1α substrate probe coupled to Cy5 (50-CAUGUCCGCAGCGCAUG-30), 20mM ATP and 2mM DTT diluted in buffer A was then added to each well. The probe emits fluorescence when cleaved by IRE1α. Fluorescence measurements were taken every minute for three to five hours at 37°C with a Clariostar plate reader (Cy5 excitation: 651nm, emission: 670nm). Recombinant IRE1α (0.5µg) activity was assessed as a positive control. Buffer incubated with the RNA probe master mix was used as a negative control. Recombinant IRE1α (0.5µg) incubated with the IRE1α RNase inhibitors MKC8866 and 4µ8c was used to assess the efficiency of the inhibitors and the specificity of the assay.

**In vitro antigen cross presentation and MHC class II antigen presentation assays.** For antigen cross-presentation, beads (Polybeads Polystyrene 3.0 Micron Microspheres) were incubated with 1mg of OVA (1mg OVA + 9mg BSA), 3mg of OVA (3mg OVA + 7mg BSA) or 10mg of BSA overnight at 4°C. The next day, coated beads were resuspended in complete IMDM (Ratio: 3mL of medium for 30µL of beads). BMDCs, preincubated or not with 25µM of the IRE1α inhibitor 4µ8C (MedChemExpress, HY-19707) for 30 minutes, were stimulated with OVA-coated beads, BSA-coated beads as a negative control or SIINFEKL at 0.05ng/mL as a positive control for six hours. For MHC II antigen presentation, BMDCs were stimulated with 3mg/mL of soluble OVA, 3mg/mL of soluble BSA as a negative control and 50µg/mL of OVA peptide 323-339 as a positive control for six hours. After washing the plate with medium, BMDCs were fixed with PBS 0.0008% glutaraldehyde for one minute, quenched with PBS glycine 200mM and washed with PBS. Lymph nodes from OT-I or OT-II mice were processed and resuspended in pure RPMI before being labelled with CFSE (2,5µg/mL) for 10 minutes at 37°C. The cells were quenched and washed with complete RPMI medium. CFSE-labelled OT-I or OT-II T cells were co-cultured with the OVA-presenting BMDCs or control BMDCs at ratio 1:1 for three days in complete RPMI medium. CD8<sup>+</sup> or CD4<sup>+</sup> T cell proliferation was monitored by flow cytometry. Cells were stained with anti-CD11c and anti-CD8a or anti-CD4 antibodies to discriminate CD8<sup>+</sup> or CD4<sup>+</sup> T cells from BMDCs by flow cytometry.

**Flow cytometry.** For intracellular staining, cells were permeabilized and fixed using a FOXP3 Fix/perm buffer set (Biolegend) for 20 minutes on ice. They were then stained with primary antibodies (Supplementary table 1) diluted in permeabilization buffer for 30 minutes on ice. Secondary antibodies were diluted at 1/1000e in permeabilization buffer and incubated with the cells for 30 minutes on ice. Stained cells were acquired with a BD LSR Fortessa flow cytometer and analyzed using FlowJo (Treestar) software.

**Statistical analyses.** Statistics were calculated with GraphPad Prism and *p* values were determined using Student's *t* test. Two way ANOVA was used for group comparison and one way ANOVA when comparing two distinct groups. Data are represented with mean ± standard error of mean (SEM).

### **Data availability**

The data are available upon request from [benedicte.manoury@inserm.fr](mailto:benedicte.manoury@inserm.fr)

### **Acknowledgements**

This study as supported by grants from INSERM, CNRS, INCA (INCAPLBIO19-075) and Université Paris Cité; the MRT fellowships to LM and MDL and an EMBO long term fellowship (ALTF 573-2018) for MML. The authors are grateful for Drs B. Ryffel (Orléans, France) and Ramanujan Hegde (LMB, Cambridge, UK) for providing the 3d mice and homemade Sec61 $\alpha$ , Sec61 $\beta$ , Sec63 antibodies respectively, and to Nicolas Goudin (INEM) for image analysis macro design.

### **Author contributions**

BM, KP and LM designed the study and LM, MML, KP and BM performed experiments. LM, MDL, KP and BM analyzed and interpreted data. MB, MB and EC provided critical research tools. BM wrote the manuscript and supervised the whole project.

### **Competing financial interests**

There are no competing financial interests

## References

1. Lee, B. L. *et al.* UNC93B1 mediates differential trafficking of endosomal TLRs. *eLife* **2**, e00291 (2013).
2. Pelka, K. *et al.* The Chaperone UNC93B1 Regulates Toll-like Receptor Stability Independently of Endosomal TLR Transport. *Immunity* **48**, 911-922.e7 (2018).
3. Tabeta, K. *et al.* The Unc93b1 mutation 3d disrupts exogenous antigen presentation and signaling via Toll-like receptors 3, 7 and 9. *Nat. Immunol.* **7**, 156–164 (2006).
4. Casrouge, A. *et al.* Herpes Simplex Virus Encephalitis in Human UNC-93B Deficiency. *Science* **314**, 308–312 (2006).
5. Majer, O. *et al.* Release from UNC93B1 reinforces the compartmentalized activation of select TLRs. *Nature* **575**, 371–374 (2019).
6. Majer, O., Liu, B., Kreuk, L. S. M., Krogan, N. & Barton, G. M. UNC93B1 recruits syntenin-1 to dampen TLR7 signalling and prevent autoimmunity. *Nature* **575**, 366–370 (2019).
7. Maschalidi, S. *et al.* UNC93B1 interacts with the calcium sensor STIM1 for efficient antigen cross-presentation in dendritic cells. *Nat. Commun.* **8**, 1640 (2017).
8. Nunes-Hasler, P. *et al.* STIM1 promotes migration, phagosomal maturation and antigen cross-presentation in dendritic cells. *Nat. Commun.* **8**, 1852 (2017).
9. Frakes, A. E. & Dillin, A. The UPR ER : Sensor and Coordinator of Organismal Homeostasis. *Mol. Cell* **66**, 761–771 (2017).
10. Hetz, C., Chevet, E. & Oakes, S. A. Erratum: Proteostasis control by the unfolded protein response. *Nat. Cell Biol.* **17**, 1088–1088 (2015).
11. Hildner, K. *et al.* *Batf3* Deficiency Reveals a Critical Role for CD8 $\alpha$  + Dendritic Cells in Cytotoxic T Cell Immunity. *Science* **322**, 1097–1100 (2008).
12. Osorio, F. *et al.* The unfolded-protein-response sensor IRE-1 $\alpha$  regulates the function of CD8 $\alpha$ + dendritic cells. *Nat. Immunol.* **15**, 248–257 (2014).
13. Tavernier, S. J. *et al.* Regulated IRE1-dependent mRNA decay sets the threshold for dendritic cell survival. *Nat. Cell Biol.* **19**, 698–710 (2017).
14. Medel, B. *et al.* IRE1 $\alpha$  Activation in Bone Marrow-Derived Dendritic Cells Modulates Innate Recognition of Melanoma Cells and Favors CD8+ T Cell Priming. *Front. Immunol.* **9**, 3050 (2019).
15. Guttman, O. *et al.* Antigen-derived peptides engage the ER stress sensor IRE1 $\alpha$  to curb dendritic cell cross-presentation. *J. Cell Biol.* **221**, e202111068 (2022).
16. Leuchowius, K., Weibrecht, I. & Söderberg, O. In Situ Proximity Ligation Assay for Microscopy and Flow Cytometry. *Curr. Protoc. Cytom.* **56**, (2011).
17. Misawa, T. *et al.* Microtubule-driven spatial arrangement of mitochondria promotes activation of the NLRP3 inflammasome. *Nat. Immunol.* **14**, 454–460 (2013).
18. Wang, W.-A. & Demarex, N. The mammalian trafficking chaperone protein UNC93B1 maintains the ER calcium sensor STIM1 in a dimeric state primed for translocation to the ER cortex. *J. Biol. Chem.* **298**, 101607 (2022).
19. Plumb, R., Zhang, Z.-R., Appathurai, S. & Mariappan, M. A functional link between the co-translational protein translocation pathway and the UPR. *eLife* **4**, e07426 (2015).

20. Sundaram, A., Plumb, R., Appathurai, S. & Mariappan, M. The Sec61 translocon limits IRE1 $\alpha$  signaling during the unfolded protein response. *eLife* **6**, e27187 (2017).
21. Brinkmann, M. M. *et al.* The interaction between the ER membrane protein UNC93B and TLR3, 7, and 9 is crucial for TLR signaling. *J. Cell Biol.* **177**, 265–275 (2007).
22. Li, X. *et al.* A Molecular Mechanism for Turning Off IRE1 $\alpha$  Signaling during Endoplasmic Reticulum Stress. *Cell Rep.* **33**, 108563 (2020).
23. Park, S.-M., Kang, T.-I. & So, J.-S. Roles of XBP1s in Transcriptional Regulation of Target Genes. *Biomedicines* **9**, 791 (2021).
24. Le Reste, P. J. *et al.* Local intracerebral inhibition of IRE1 by MKC8866 sensitizes glioblastoma to irradiation/chemotherapy in vivo. *Cancer Lett.* **494**, 73–83 (2020).
25. Cross, B. C. S. *et al.* The molecular basis for selective inhibition of unconventional mRNA splicing by an IRE1-binding small molecule. *Proc. Natl. Acad. Sci.* **109**, (2012).
26. Ho, T. T. *et al.* Autophagy maintains the metabolism and function of young and old stem cells. *Nature* **543**, 205–210 (2017).
27. Sepulveda, F. E. *et al.* Critical Role for Asparagine Endopeptidase in Endocytic Toll-like Receptor Signaling in Dendritic Cells. *Immunity* **31**, 737–748 (2009).
28. Fukui, R. *et al.* Unc93B1 biases Toll-like receptor responses to nucleic acid in dendritic cells toward DNA- but against RNA-sensing. *J. Exp. Med.* **206**, 1339–1350 (2009).
29. Fukui, R. *et al.* Unc93B1 Restricts Systemic Lethal Inflammation by Orchestrating Toll-like Receptor 7 and 9 Trafficking. *Immunity* **35**, 69–81 (2011).
30. Ishida, H. *et al.* Cryo-EM structures of Toll-like receptors in complex with UNC93B1. *Nat. Struct. Mol. Biol.* **28**, 173–180 (2021).
31. Sepulveda, D. *et al.* Interactome Screening Identifies the ER Luminal Chaperone Hsp47 as a Regulator of the Unfolded Protein Response Transducer IRE1 $\alpha$ . *Mol. Cell* **69**, 238-252.e7 (2018).
32. Urra, H. *et al.* IRE1 $\alpha$  governs cytoskeleton remodelling and cell migration through a direct interaction with filamin A. *Nat. Cell Biol.* **20**, 942–953 (2018).
33. Bertolotti, A., Zhang, Y., Hendershot, L. M., Harding, H. P. & Ron, D. Dynamic interaction of BiP and ER stress transducers in the unfolded-protein response. *Nat. Cell Biol.* **2**, 326–332 (2000).
34. Oikawa, D., Kimata, Y., Kohno, K. & Iwawaki, T. Activation of mammalian IRE1 $\alpha$  upon ER stress depends on dissociation of BiP rather than on direct interaction with unfolded proteins. *Exp. Cell Res.* **315**, 2496–2504 (2009).
35. Karagöz, G. E. *et al.* An unfolded protein-induced conformational switch activates mammalian IRE1. *eLife* **6**, e30700 (2017).
36. Guermonprez, P. *et al.* ER-phagosome fusion defines an MHC class I cross-presentation compartment in dendritic cells. *Nature* **425**, 397–402 (2003).
37. Cebrian, I. *et al.* Sec22b Regulates Phagosomal Maturation and Antigen Crosspresentation by Dendritic Cells. *Cell* **147**, 1355–1368 (2011).

## Figure Legends

**Fig. 1 | IRE1 $\alpha$  associates with UNC93B1 in DCs and the interaction is enhanced in 3d cells.** **a** Immunoprecipitation of RFP-tagged proteins in HeLa cells transfected with Ern1 $\alpha$ -HA and WT or 3d UNC93B1-mCherry cDNAs, followed by a western blot for HA and Cherry (n=3). **b** HeLa cells were transfected with Ern1 $\alpha$ -HA and WT or 3d UNC93B1-FLAG cDNAs. IRE1 $\alpha$ -HA-UNC93B1-FLAG association (yellow dots) was detected using the Duolink proximity ligation assay with anti-FLAG and anti-HA specific antibodies. Nuclei are in blue and stained with DAPI. PLA signals are quantified with Icy (n=6 experiments, n=21 cells for NT, n=25 cells for WT and n=41 cells for 3d, mean  $\pm$  SEM, unpaired two-tailed t test, \*\*p<0.01). **c** Immunofluorescence experiment and colocalization analysis between IRE1 $\alpha$ -HA (red) and WT or 3d UNC93B1-FLAG (green) in transfected HeLa cells. Quantification of colocalization was measured using a JaCoP plugin (see Methods, n=4 experiments, n=57 cells for WT and n=45 cells for 3d, mean  $\pm$  SEM, unpaired two-tailed t test, \*\*\*\*p<0.0001). **d** UNC93B1 was immunoprecipitated with UNC93B1 antibody from WT and 3d DCs and immunoblotted with anti-UNC93B1 and anti-IRE1 $\alpha$  antibodies. Cells were treated with 1 $\mu$ M of thapsigargin (TG) for 30 minutes before immunoprecipitation (n=4). **e** IRE1 $\alpha$  was immunoprecipitated with IRE1 $\alpha$  antibody from WT and 3d DCs and immunoblotted with anti-UNC93B1 and anti-IRE1 $\alpha$  antibodies. Cells were treated with 1 $\mu$ M of thapsigargin (TG) for 30 minutes before immunoprecipitation (n=5). **f** IRE1 $\alpha$ -UNC93B1 association (yellow dots) was detected using the Duolink proximity ligation assay with anti-UNC93B1 and anti-IRE1 $\alpha$  specific antibodies. BMDCs were treated with TG for 30 minutes before the staining. Nuclei are in blue. PLA signals are quantified with Icy (n=5 experiments for NS, n=3 experiments for TG-stimulated, n=56 cells for WT NS, n=39 cells for 3d NS, n=12 cells for WT+TG and n=12 cells for 3d+TG, unpaired two-tailed t test, \*\*p<0.001). NT: Non transfected. NS: Non stimulated.

**Fig. 2 | The transmembrane region of IRE1 $\alpha$  is required for its association with UNC93B1.** **a** Schematic representation of IRE1 $\alpha$  protein (SP: signal peptide, LD: luminal domain, TMD: transmembrane domain, CD: cytosolic domain). **b** Immunoprecipitation of RFP-tagged proteins in HeLa cells transfected with WT,  $\Delta$ LD or  $\Delta$ CD IRE1 $\alpha$ -HA and WT or 3d UNC93B1-mCherry, followed by a western blot for HA and mCherry proteins.  $\Delta$ LD: deletion of IRE1 $\alpha$  luminal domain.  $\Delta$ CD: deletion of IRE1 $\alpha$  cytosolic domain (n=3). **c** Schematic representation of IRE1 $\alpha$  and its transmembrane domain sequence. **d** Immunoprecipitation of RFP-tagged proteins in HeLa cells transfected with WT or TMD-CNX IRE1 $\alpha$ -HA and WT or 3d UNC93B1-mCherry, followed by a western blot for HA and mCherry proteins. TMD-CNX: mutant of IRE1 $\alpha$  bearing the transmembrane domain (TMD) of calnexin (n=3).

**Fig. 3 | UNC93B1 controls IRE1 $\alpha$  activity in DCs.** **a** RT-PCR analysis of XBP1 spliced (XBP1s) or unspliced (XBP1u) in murine splenic cDC1. XBP1 mRNA expression was assessed in comparison to GAPDH. (n=5). **b** RT-qPCR analysis of unfolded protein response (UPR) targets in BM-DCs. Cells were treated with 1 $\mu$ M of TG for 1h30. (n=5). **c** RT-qPCR analysis of regulated IRE1-dependent decay (RIDD) targets in BM-DCs. Cells were treated with 1 $\mu$ M of TG for 1h30. (n=5). **d** RT-qPCR analysis of RIDD targets in splenic cDC1. Cells were treated with 1 $\mu$ M of TG for 1h30. (n=4). **e** IRE1 $\alpha$  RNase activity assay in BM-DCs. IRE1 $\alpha$  was immunoprecipitated overnight with anti IRE1 $\alpha$  antibody and incubated with the XBP1/RIDD-Cy5 probe. Experiments were pooled at t=120 min and values were compared to unstimulated WT DCs (NS). Cells were treated with 1 $\mu$ M of TG for 30 minutes. (n=5 for WT, n=3 for 3d). (In **a**, **b**, **c**, **d** and **e**: mean  $\pm$  SEM, unpaired two-tailed t test, \*p<0.1, \*\*p<0.01 \*\*\*p<0.001). **f** Immunofluorescence showing KDEL (ER staining) in red and DAPI (nucleus) in blue, in WT and 3d splenic cDC1 and cDC2 (n=2). NS: Non stimulated.

**Fig. 4 | IRE1 $\alpha$  inhibition partially restores MHC I antigen cross-presentation and limits tumor growth in 3d DCs and mice.** **a** BM-DCs from WT or 3d mice were incubated with different concentrations of OVA beads, BSA beads or OVA peptide (SIINFEKL, 50 pg/mL) for 6h, fixed with 0.0008% glutaraldehyde, and co-cultured with CFSE labelled CD8<sup>+</sup> OT-I T cells. T cell proliferation was monitored by CFSE dilution 72h later. BM-DCs were preincubated with 25 $\mu$ M of 4 $\mu$ 8c for 30 minutes before addition of OVA/BSA beads, or OVA peptide. **b** Quantification of OT-I cells division is shown as a mean percentage of proliferating cells (n=3, mean  $\pm$  SEM, paired two-tailed t test, \*\*p<0.01, \*\*\*p<0.001). **c** WT or 3d mice were injected with 2x10<sup>5</sup> sc B16-OVA melanoma cells before adoptively transferred or not with OT-I cells (2x10<sup>6</sup> cells). MKC8866 was injected IP every day until day 24 (15mg/kg) (n=3 for NT, n=4 for OT-I, n=5 for OT-I + MKC8866, unpaired two-tailed t-test, \*p<0.01). Tumor growth was measured every 2-3 days. NS: not stimulated. NT: No treatment.

**Fig. 5 | IRE1 $\alpha$ -BiP interaction is disrupted in 3d DCs.** **a** Regulation of IRE1 $\alpha$  activity by both BiP and Sec63. **b** IRE1 $\alpha$ -BiP association (yellow dots) was detected using the Duolink proximity ligation assay with anti-BiP and anti-IRE1 $\alpha$  specific antibodies. Cells were treated with 1 $\mu$ g/mL of tunicamycin (TN) for 4 hours. (n=3 experiments, n=38 cells for WT NS, n=37 cells for 3d NS, n=41 cells for WT+TN and n=36 cells for 3d+TN, mean  $\pm$  SEM, unpaired two-tailed t test, \*\*\*p<0.001). Nuclei are in blue. NS: Non stimulated.

**Fig. 6 | UNC93B1 binds IRE1 $\alpha$ , STIM1 and intracellular TLRs in DCs.** At steady state, IRE1 $\alpha$  is in an inactive monomeric conformation which recruits BIP. In 3d DCs, UNC93B1 interactions with STIM1 and intracellular TLR are abolished while its association with IRE1 $\alpha$  is enhanced. Upon stress, BiP is released from IRE1 $\alpha$  luminal domain and IRE1 $\alpha$  oligomerized. IRE1 $\alpha$  then splices XBP1 mRNA and cleaves specific RIDD mRNAs targets such as *tapbp* (tapasin). Hypothesis: In 3d DCs, the weak antigen degradation caused by impaired STIM1 activity and the cleavage of mRNAs of the peptide loading machinery due to chronic activation of IRE1 $\alpha$  lead to an altered antigen cross-presentation.

**Supplementary fig. 1 | IRE1 $\alpha$  and UNC93B1 expression in different DC subtypes. a** Microarray analysis showing the absolute *Ern1* gene expression difference between WT and 3d, and the relative fold changes in *Ern1* gene expression in 3d vs WT splenocytes. Gene downregulation is shown in blue. **b** RT-qPCR analysis of *Ern1* in WT and 3d BM-DCs. (n=5, mean  $\pm$  SEM, unpaired two-tailed t test). **c** Western blot analysis of IRE1 $\alpha$  and UNC93B1 in WT and 3d BM-DCs, cDCs and cDC1s. **d** Western blot in WT and UNC93B1 deficient DCs using conformational UNC93B1 antibodies recognising the N-terminal or the C-terminal cytosolic regions of the protein or a commercial UNC93B1 antibody. **e** Intracellular flow cytometry analysis of UNC93B1 using the N-terminal and C-terminal conformational antibodies in WT and 3d BM-DCs.

**Supplementary fig. 2 | STIM1 associates with WT UNC93B1 but not with IRE1 $\alpha$ .** **a** WT and 3d DCs were immunoprecipitated with anti-IRE1 $\alpha$  antibody and immunoblotted with anti-UNC93B1, -STIM1 and -IRE1 $\alpha$  antibodies (n=3). **b** STIM1-UNC93B1 association (yellow dots) was detected in BM-DCs using the Duolink proximity ligation assay with anti-UNC93B1 and anti-STIM1 specific antibodies. (n=3 experiments, n=22 cells for WT and n=16 cells for 3d, unpaired two-tailed t test, \*\*p<0.001). Nuclei are in blue.

**Supplementary fig. 3 | IRE1 $\alpha$ -HA mutants are transfected equally in HeLa cells. a** Schematic representation of IRE1 $\alpha$   $\Delta$ 10 and STST mutants. **b** Immunoprecipitation of HA-tagged proteins in HeLa cells transfected with WT,  $\Delta$ 10 or STST IRE1 $\alpha$ -HA and WT or 3d UNC93B1-FLAG, followed by a western blot for HA and FLAG. **c** Transfection rates of IRE1 $\alpha$ -HA WT,  $\Delta$ LD and  $\Delta$ CD and UNC93B1-mCherry WT and 3d in HeLa cells measured by flow



cytometry. Non transfected cells were used as a negative control. Percentages represent the double transfected cell population (n=2). **d** Transfection rates of IRE1 $\alpha$ -HA WT or TMD-CNX and UNC93B1-mCherry WT or 3d in HeLa cells measured by flow cytometry. Non transfected cells were used as a negative control. Percentages represent the double transfected cell population (n=2).

**Supplementary fig. 4 | IRE1 $\alpha$  activity is upregulated in 3d cDC1s and can be measured with a fluorescence assay.** **a** RT-qPCR analysis of unfolded protein response (UPR) target CHOP in cDC1s. (n=5, mean  $\pm$  SEM, unpaired two-tailed t test, ns: not significant). **b** IRE1 $\alpha$  recombinant (IRE1r) RNase activity assay. IRE1r was incubated with the XBP1/RIDD-Cy5 probe and fluorescence was measured at excitation 651nm and emission 670nm at different times. IRE1r was incubated with 25 $\mu$ M of IRE1 inhibitors (MKC8866 and 4 $\mu$ 8c) for 30 minutes before monitoring cleavage of the probe. **c** IRE1 $\alpha$  RNase activity assay in BM-DCs. IRE1 $\alpha$  was immunoprecipitated and incubated with an XBP1/RIDD-Cy5 probe for different times. Fluorescence was measured at excitation 651nm and emission 670nm. Cells were treated with 1 $\mu$ M of TG for 30 minutes before immunoprecipitation.

**Supplementary fig. 5 | IRE1 $\alpha$  inhibition doesn't affect MHC class II antigen presentation by DCs and decreases tumoral growth in both WT and 3d mice.** **a** BM-DCs from WT or 3d mice were incubated with soluble OVA, BSA or OVA peptide 323-339 (50  $\mu$ g/mL) for 6h, fixed with 0.0008% glutaraldehyde, and co-cultured with CFSE labelled CD4<sup>+</sup> OTII T cells. T cell proliferation was monitored by CFSE dilution 72h later. BM-DCs were preincubated with 25 $\mu$ M of 4 $\mu$ 8c for 30 minutes before addition of soluble OVA or OVA peptide (n=3). **b** WT or 3d mice were injected with B16-OVA melanoma cells (2x10<sup>5</sup> sc) at day 0 with or without MKC8866 inhibitor (day -1 to day 24, 15mg/kg) and tumors were measured every 2 to 3 days (n=5 for each group).

**Supplementary fig. 6 | IRE1 $\alpha$  association to Sec63 is reduced in 3d DCs.** **a** Western blot analysis of BiP in WT and 3d BM-DCs. Cells were treated with 1 $\mu$ M of thapsigargin (TG) for 1h30 and with 1  $\mu$ g/mL of tunicamycin (TN) for 4h. **b** IRE1 $\alpha$ -Sec63 association (yellow dots) was detected in BM-DCs using the Duolink proximity ligation assay with anti-IRE1 $\alpha$  and anti-Sec63 specific antibodies. (n=1 experiment, n=9 cells for WT and n=7 cells for 3d, mean  $\pm$  SEM, unpaired two-tailed t test, ns: non significant). Nuclei are in blue. **c** Immunofluorescence experiment and colocalization analysis between IRE1 $\alpha$  (green) and Sec63 (red) in WT and 3d

BM-DCs. Quantification of colocalization was measured using JaCoP plugin (see Methods) (n=1 experiment, n=23 cells for WT and n=14 cells for 3d, mean  $\pm$  SEM, unpaired two-tailed t test, ns: non significant).

**Supplementary table 1 | List of antibodies used.** WB: Western Blot, IF: Immunofluorescence, IP: Immunoprecipitation, PLA: Proximity ligation assay, FC: Flow cytometry.

**Supplementary table 2 | List of primers used for PCR.**



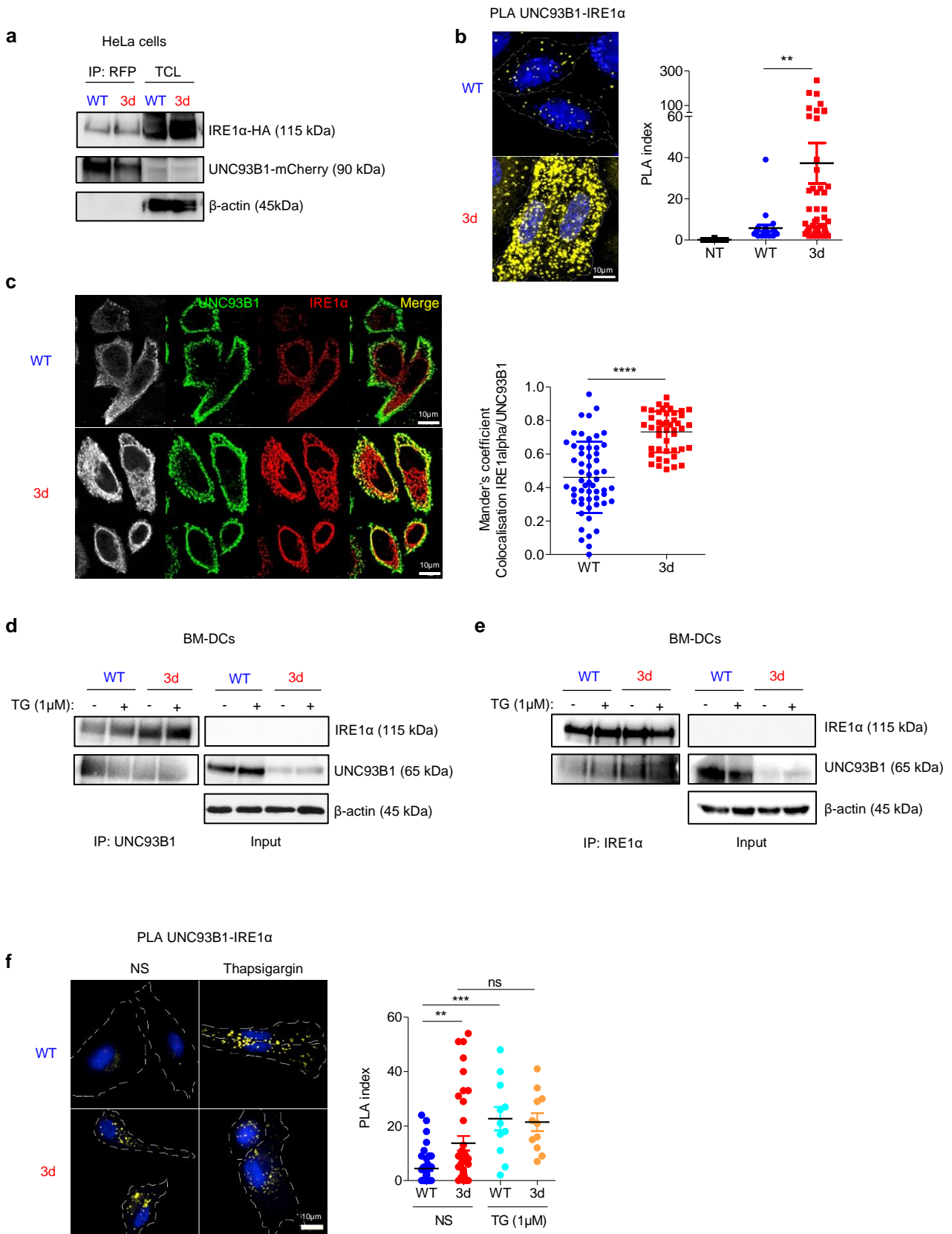


**Figure 1**

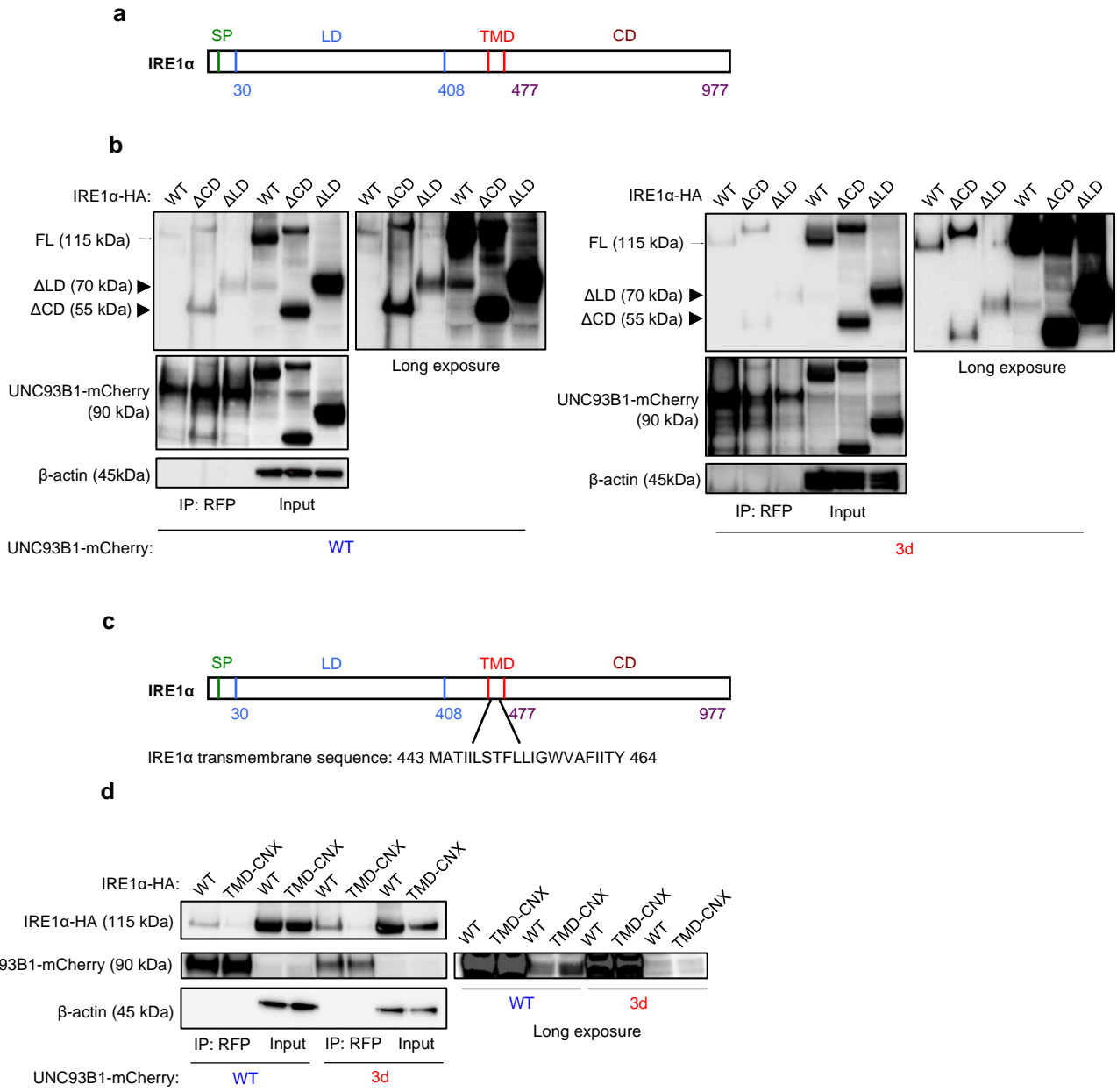


**Figure 2**

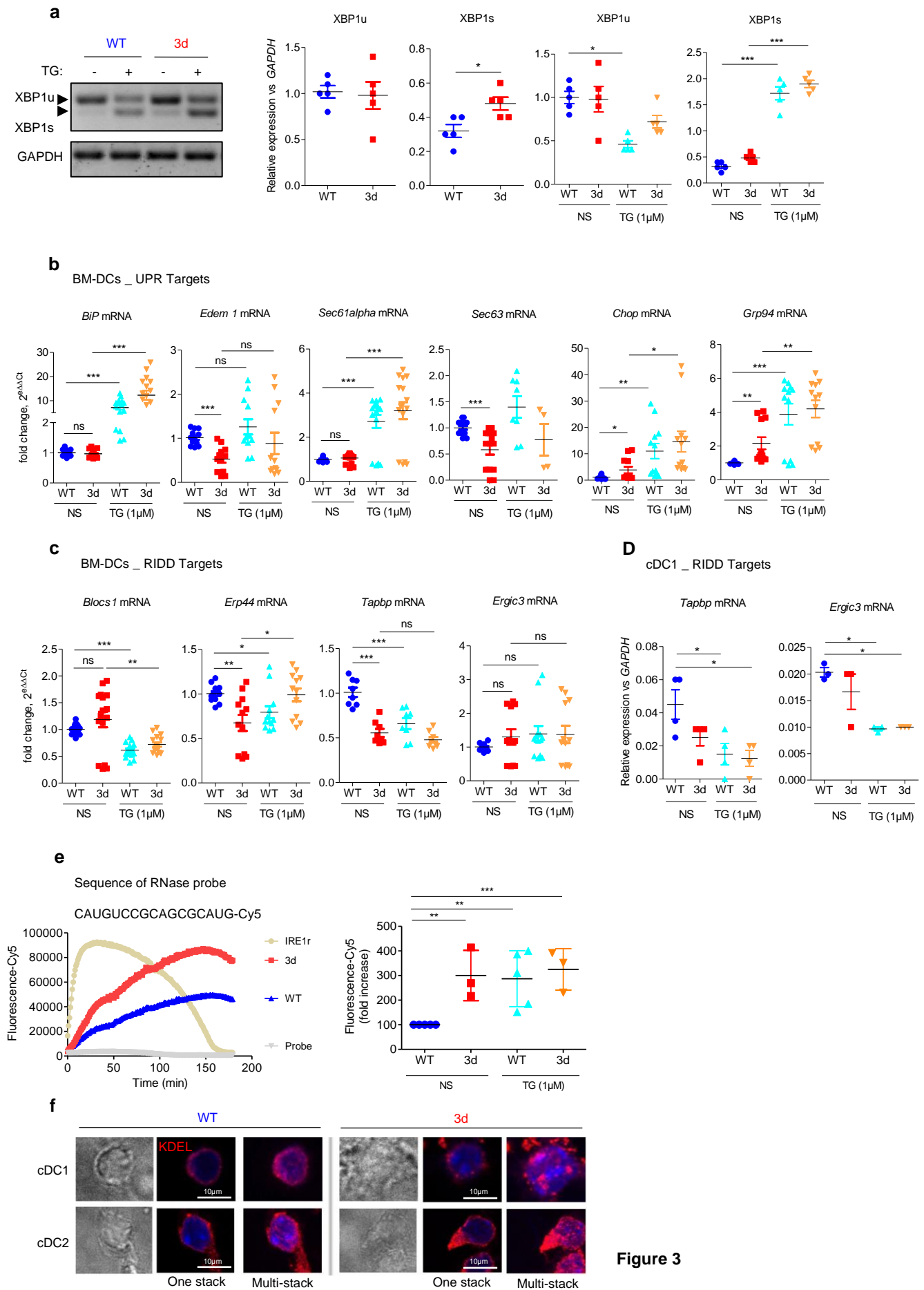


**Figure 3**

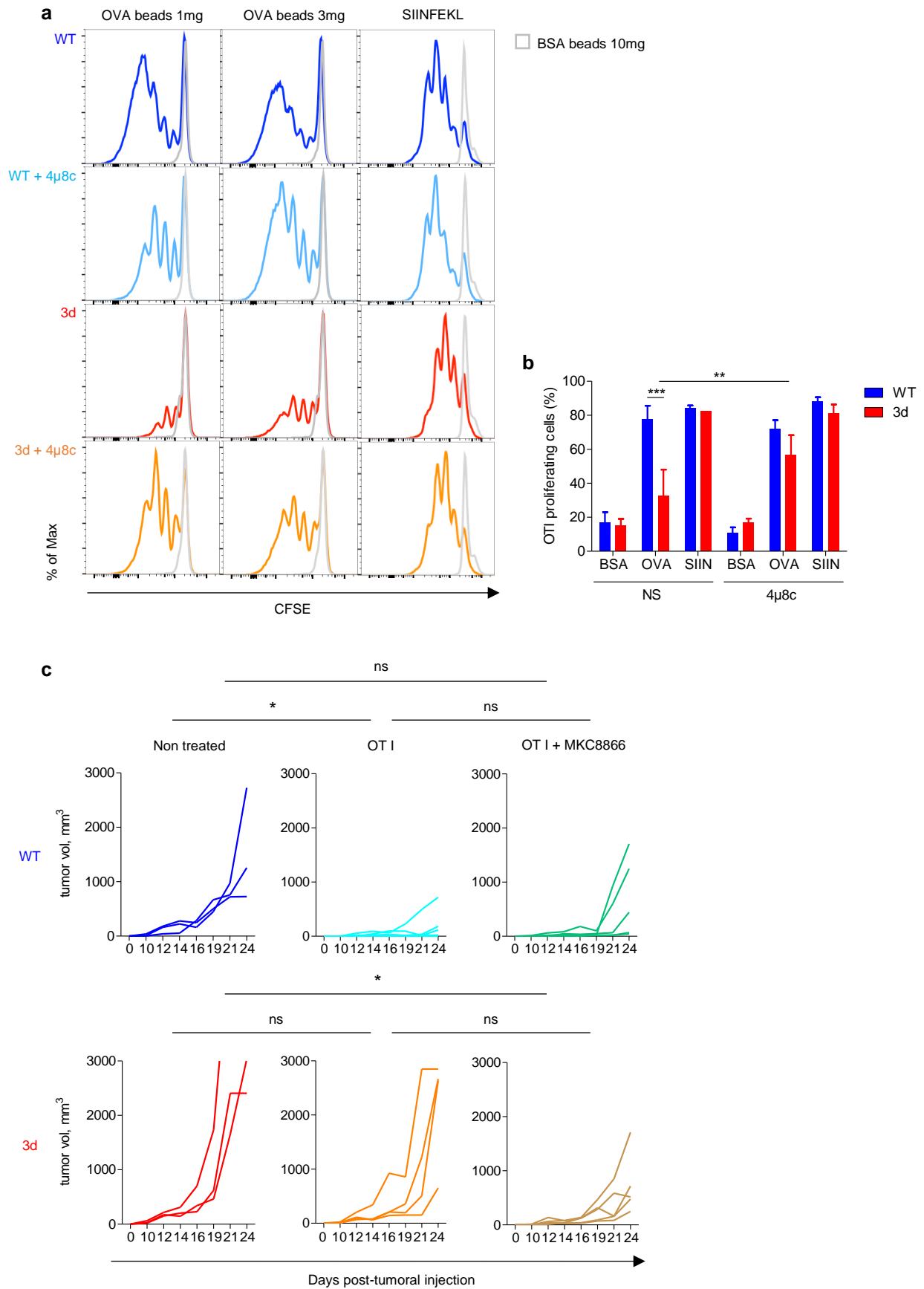


**Figure 4**

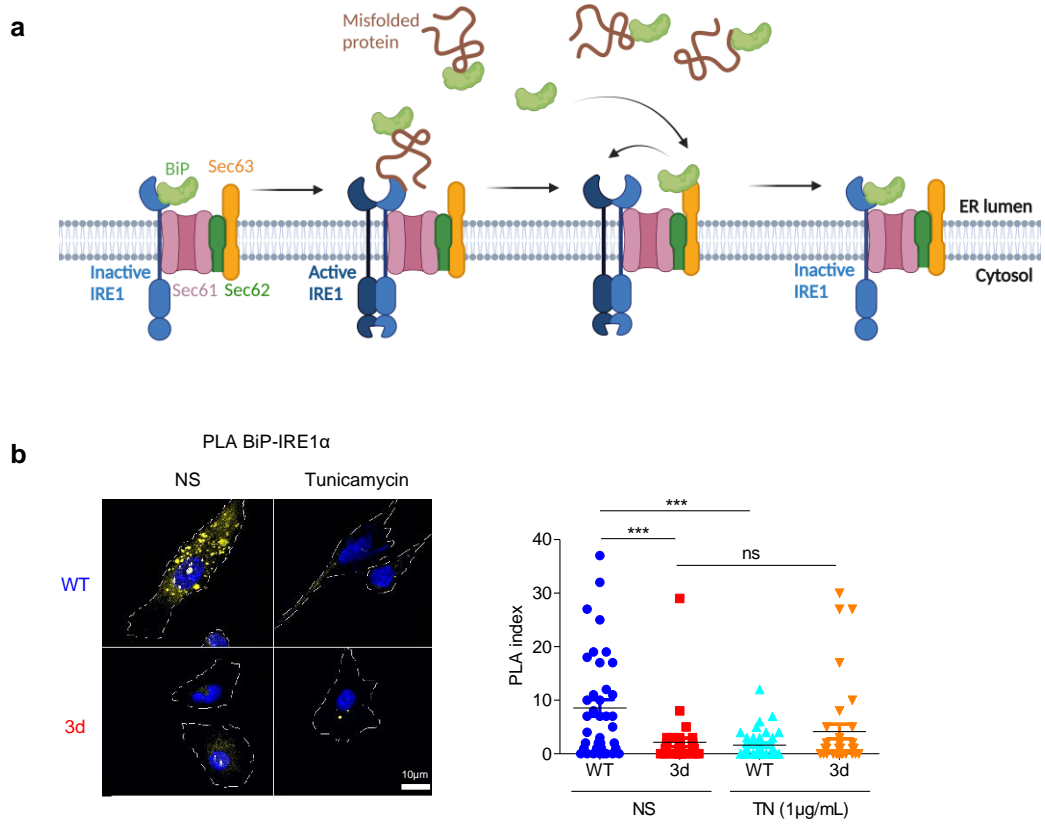


**Figure 5**



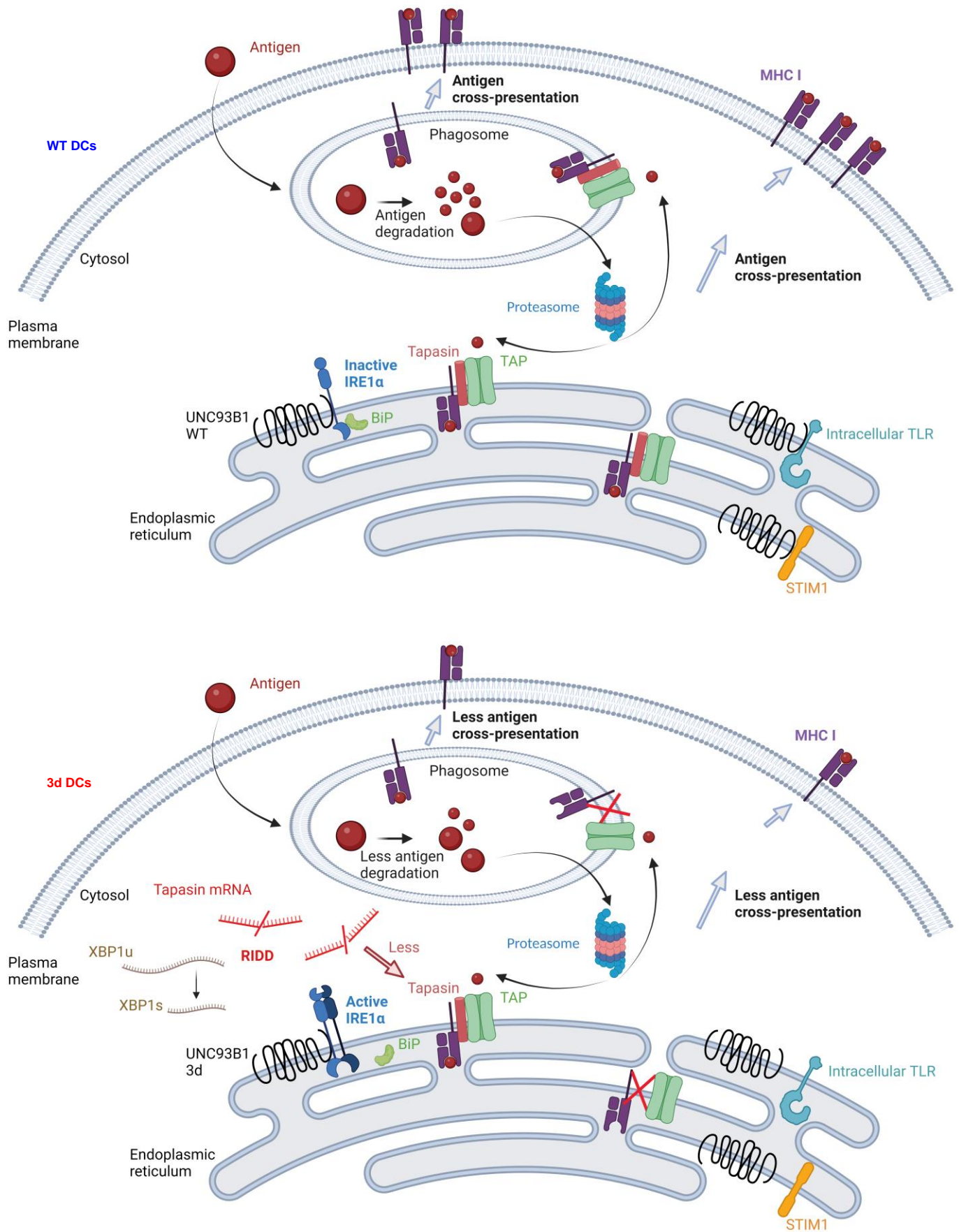
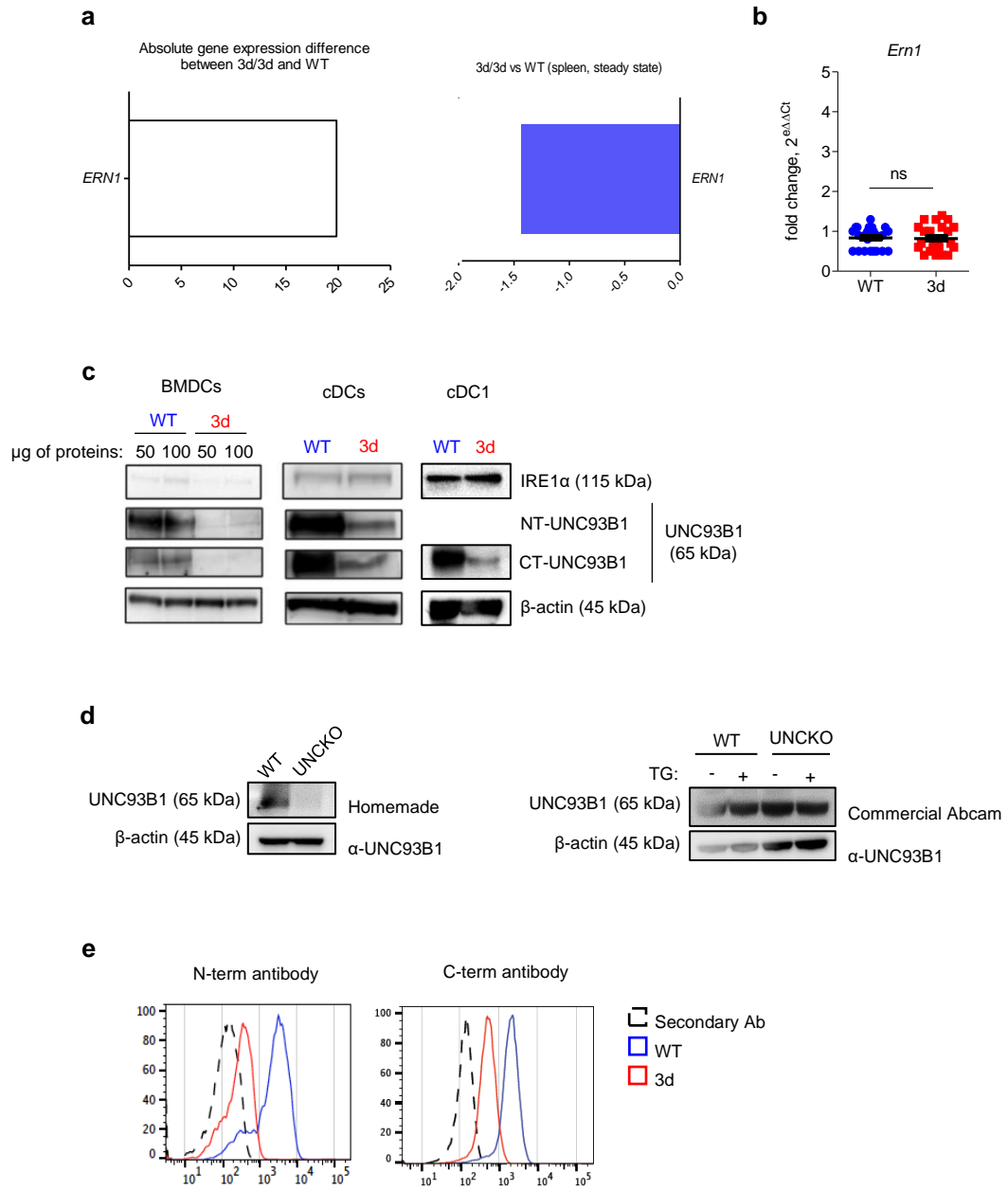
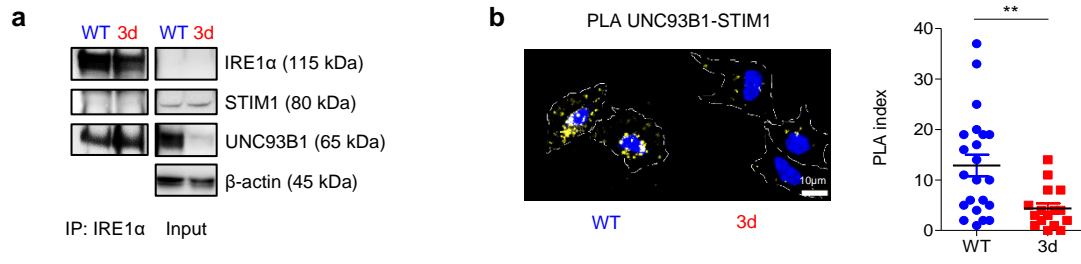


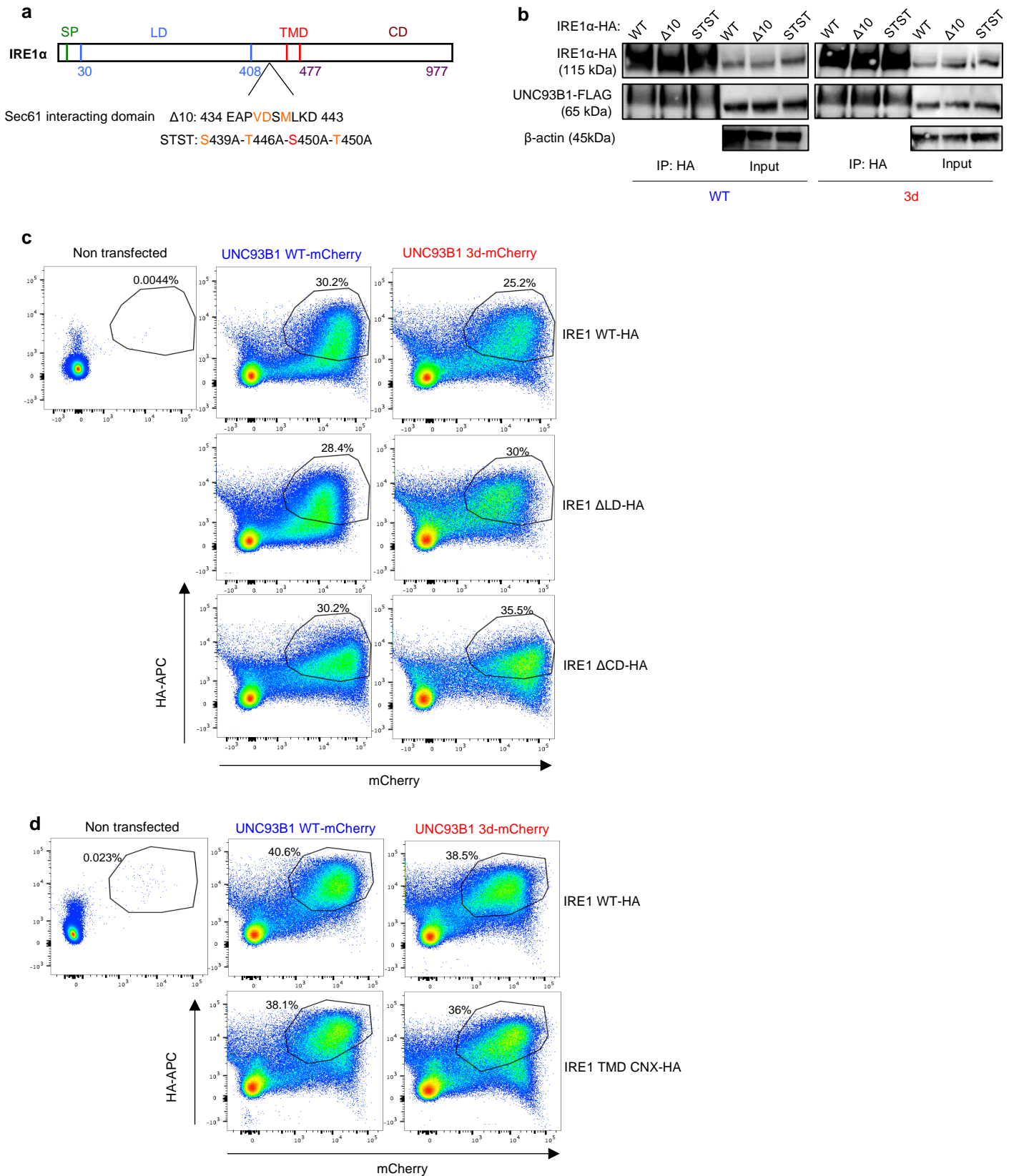
Figure 6



Supplementary Figure 1

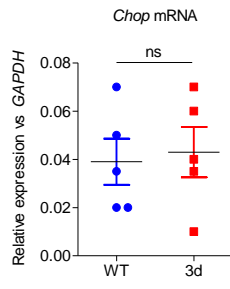


**Supplementary Figure 2**

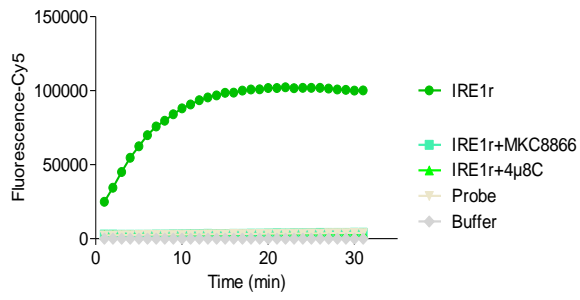


Supplementary Figure 3

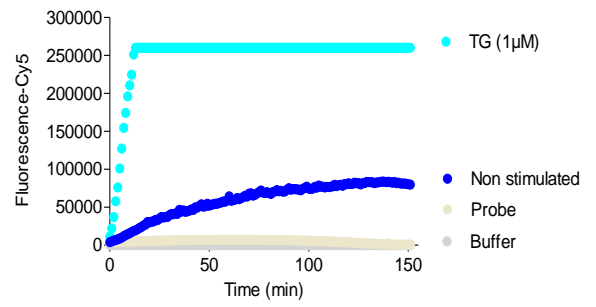
**a**



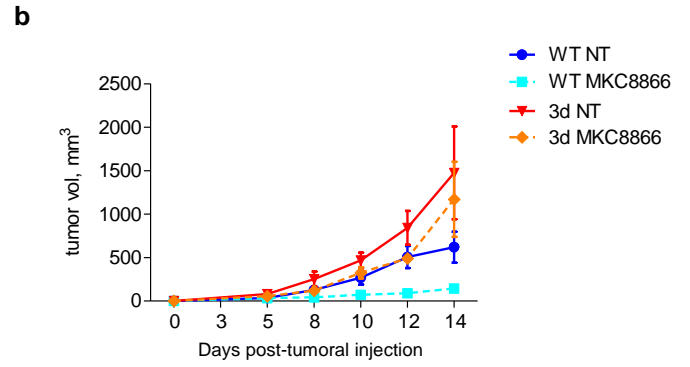
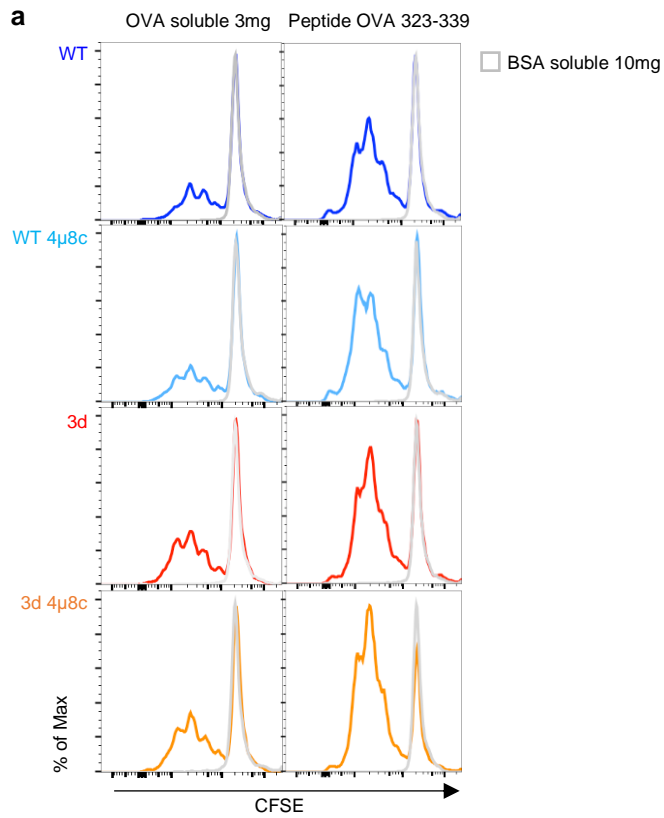
**b**



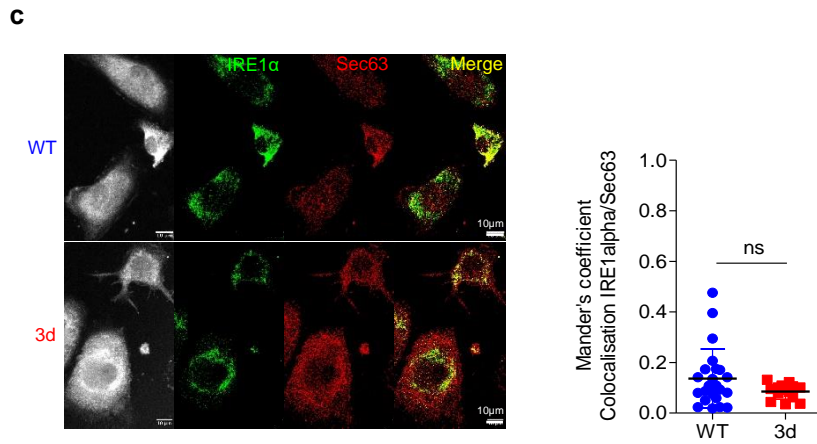
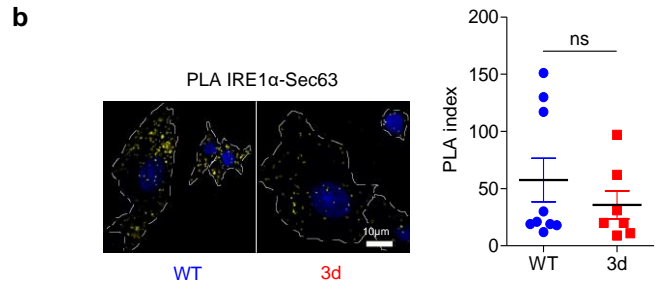
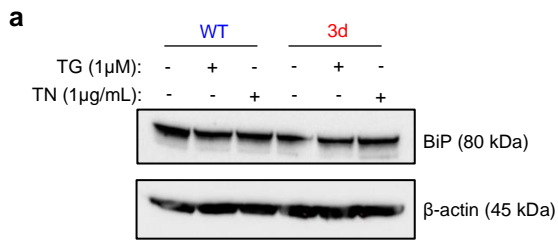
**c**



**Supplementary Figure 4**



Supplementary Figure 5



Supplementary Figure 6

Target	Dilution	Catalogue reference
<b>IRE1<math>\alpha</math></b>	WB: 1/100 IP: 1/50	Cell signaling technology, 3294S
<b>IRE1<math>\alpha</math></b>	PLA: 1/300 IF: 1/300	Santa Cruz Biotechnology, sc-390960
<b>UNC93B1 C-terminal and N-terminal</b>	WB: 1/1000 IP: 5 $\mu$ L PLA: 1/1000 FC: 1/300 IF: 1/10000	Homemade antibodies From Dr. Brinkmann (HZI, Braunschweig) Maschalidi et al., 2017. doi: 10.1038/s41467-017-01601-5.
<b><math>\beta</math>-Actin</b>	WB: 1/1000	Cell signaling technology, 3700S
<b>HA</b>	WB: 1/1000 FC: 1/200 IF: 1/300 PLA: 1/1000	Cell signaling technology, 3724S
<b>mCherry</b>	WB: 1/1000 FC: 1/200	Abcam, ab125096
<b>BiP</b>	WB: 1/1000 PLA: 1/500	Cell signaling technology, 3177S
<b>UNC93B1</b>	WB: 1/1000	Abcam, ab69497
<b>STIM1</b>	WB: 1/1000 PLA: 1/100	Abcam, ab108994
<b>FLAG</b>	WB: 1/1000 IF: 1/300 PLA: 1/1000	Cell signaling technology, 8146S
<b>KDEL</b>	IF: 1/300	Abcam, ab12223
<b>Sec63</b>	WB: 1/1000 PLA: 1/1000 IF: 1/500	From Dr. Hedge (MRC, Cambridge) Brambillasca et al., 2005. doi: 10.1038/sj.emboj.7600730.
<b>Sec61<math>\alpha</math>, <math>\beta</math></b>	IF: 1/500	From Dr. Hedge (MRC, Cambridge) Brambillasca et al., 2005. doi: 10.1038/sj.emboj.7600730.
<b>IgG Rabbit HRP</b>	WB: 1/5000	Cell signaling technology, 7074S
<b>IgG Mouse HRP</b>	WB: 1/5000	Cell signaling technology, 7076S

Supplementary table 1



Gene	Forward primer	Reverse primer	Concentration used ( $\mu$ M)	Annealing temperature ( $^{\circ}$ C)
<b>Ern1</b>	TGCTGAAACACCCCTTCTTC	GCCTCCTTTTCTATTCGGTCA	1	63
<b>Unc93b1</b>	CTACAGTGGCTTTGAGGTGCTC	GCTATGAGCAGGTATGCCAGTC	0.1	63
<b>Gapdh</b>	CCGTAGACAAAATGGTGAAGG	CGTGAGTGGAGTCATACTGGA	2	63
<b><math>\beta</math>-actin</b>	AAGCTGTGCTATGTTGCTCTAGACT	CACTTCATGATGGAATTGAATGTAG	0.5	61
<b>Tapbp</b>	ACCATTCCCAGGAACTCAA	GAGAAGAAGGCTGTTGTTCTGG	1	63
<b>BiP</b>	ATGAGGCTGTAGCCTATGGTG	GGGGACAAACATCAAGCAG	0.5	61
<b>Edem</b>	AAGCCCTCTGGAACCTGCG	AAGCCCTCTGGAACCTGCG	0.3	64
<b>Ergic3</b>	GTTCAAGAAACGACTAGACAAGGA	ACCTCGACTTTCCAAGCT	1	64
<b>Erp44</b>	GACACAGCCCCAGGAGAG	TCATCTCGATCCCTCAATAAAGTA	0.5	61
<b>Sec61<math>\alpha</math></b>	CTATTTCCAGGGCTTCCGAGT	AGGTGTTGTACTGGCCTCGGT	0.7	64
<b>Sec63</b>	TGGGCACTGTTCTTATTTCTTGC	TTAATTTCTGCCACTGTTGCTCC	0.7	64
<b>Bloc1s1</b>	AACACCAAGCCAAGCAGAACGA	TCACCTCATGGTCCAGCTTTCTC	0.5	63
<b>Chop</b>	CCCTGCCTTTACCTTGG	CCGCTCGTTCTCCTGCTC	0.5	63
<b>Xbp1</b>	ACACGCTTGGGAATGGACAC	CCATGGGAAGATGTTCTGGG	1	64
<b>Grp94</b>	GTTTCGTCAGAGCTGATGATGAA	GCGTTTAACCCATCCAACCTGAAT	0.5	63

**Supplementary table 2**

## **RESULTS \_ PART II: UNC93B1 regulates STING signalling in dendritic cells.**

Following the description of IRE1 $\alpha$  regulation by the ER chaperone UNC93B1 in DCs, we identified a new protein interacting with UNC93B1: STING.

STING is an ER resident protein essential for type I interferon response triggered by cytosolic, viral or self DNA. Upon its binding to cGAMP, the product produced by cGAS, STING translocates to the Golgi and activates TBK1, which in turns phosphorylates STING. Activated TBK1 recruits IRF3 to phosphorylated STING and drives type I INFs production. STIM1, TOLLIP and UNC93B1 have recently been identified to associate with STING (Srikanth et al., 2019; Pokatayev et al., 2020; He et al., 2021; Zhu et al., 2022). While TOLLIP stabilises STING, STIM1 and UNC93B1 were described to downregulate STING activation, and UNC93B1 was suggested to send STING to degradation. However, these experiments were performed in fibroblasts or HEK293T cell lines, and very few experiments were conducted in myeloid cells, where UNC93B1 is expressed and the interferon response is relevant.

Therefore, to address the role of UNC93B1 in STING signalling in DCs, we performed experiments in WT, UNC93B1 knockdown and UNC93B1 3d mutated dendritic cells.



## I. STING and WT or 3d UNC93B1 interact in DCs

First, to confirm that STING is a client of UNC93B1 in primary DCs, we assessed the formation of UNC93B1-STING complexes in BMDCs stimulated or not with 2'3'-cGAMP for 30 minutes. To do this, we immunoprecipitated STING and then immunoblotted for UNC93B1 and STING proteins. Figure 1 shows association between WT and 3d UNC93B1 and STING, with or without cGAMP stimulation.

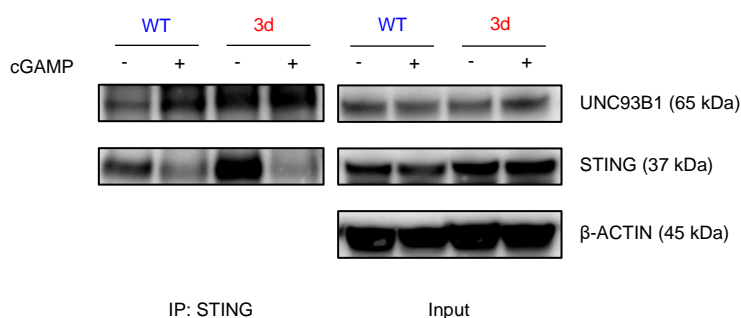


**Figure 1. STING and UNC93B1 associate in DCs.** STING was immunoprecipitated from WT and 3d DCs with a STING antibody, and the proteins UNC93B1 and STING were immunoblotted. Cells were treated with 10µg/mL of cGAMP for 30 minutes before immunoprecipitation (n=4).

## II. UNC93B1 positively regulates STING signalling

DCs expressing the 3d mutation or deficient for UNC93B1 are unable to respond efficiently to a large panel of viruses, as endosomal nucleic acid sensing TLRs are unstable and unable to activate their signalling cascade. Indeed, 3d mice are highly susceptible to several viral infections. Although TLR9 is often described as the main pathogenic DNA sensor in immune cells, cGAS is a major actor in cytosolic DNA molecules recognition. While we know that TLR9 signalling is abrogated in 3d cells, whether the cGAS-STING pathway is impacted or not had not been assessed.

To address this, we stimulated WT and 3d BMDCs with cGAMP for 6 hours and measured INF-β secretion by ELISA. Figure 2a shows a significant decrease in INF-β secretion by 3d DCs in comparison to WT cells. We then knocked-down the expression of UNC93B1 in BMDCs using a pool of siRNA and observed a reduction of UNC93B1

protein levels by 70% (Figure 2b). Similar to what was observed in 3d DCs, INF- $\beta$  levels were decreased in UNC93B1 knocked-down DCs compared to DCs transfected with control siRNA (Figure 2c). Altogether, these results indicate that UNC93B1 positively regulates STING-dependent type I INF secretion.

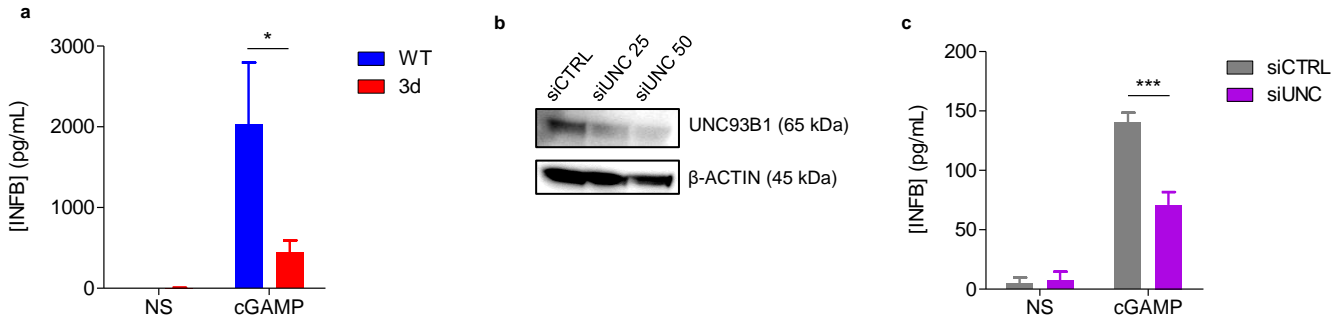


**Figure 2. UNC93B1 promotes STING-mediated INF- $\beta$  signalling in DCs.** **a.** WT and 3d BMDCs were stimulated for 6 hours with 50 $\mu$ g/mL of cGAMP. Secreted INF- $\beta$  levels were assessed by ELISA (n=4, mean  $\pm$  SEM, unpaired two-tailed t test, \*p<0.1). **b.** UNC93B1 was knocked down in BMDCs using 25 $\mu$ M or 50 $\mu$ M of siRNA and UNC93B1 expression was assessed by Western Blot. **c.** BMDCs transfected with control siRNA (siCTRL) or 50 $\mu$ M of UNC93B1 siRNA (siUNC) were stimulated for 6 hours with 50 $\mu$ g/mL of cGAMP. Secreted INF- $\beta$  levels were assessed by ELISA (n=4, mean  $\pm$  SEM, unpaired two-tailed t test, \*\*\*p<0.001). NS: Non stimulated.

### III. STING fails to translocate to the Golgi apparatus after activation in 3d DCs

A crucial step in STING signalling is its translocation to the Golgi apparatus following its activation. Since DCs expressing the 3d mutant show reduced STING-mediated INF signalling, we wondered if STING trafficking was also impaired in these cells. To assess this, we performed confocal microscopy. Upon immunofluorescence experiments, we observed a significant decrease of colocalization between STING and GM130 in 3d DCs when compared to WT cells (Figure 3). This result indicates that STING translocates to Golgi compartments upon cGAMP stimulation in WT DCs but not in 3d DCs, correlating with the decreased type I INF signalling in those cells.

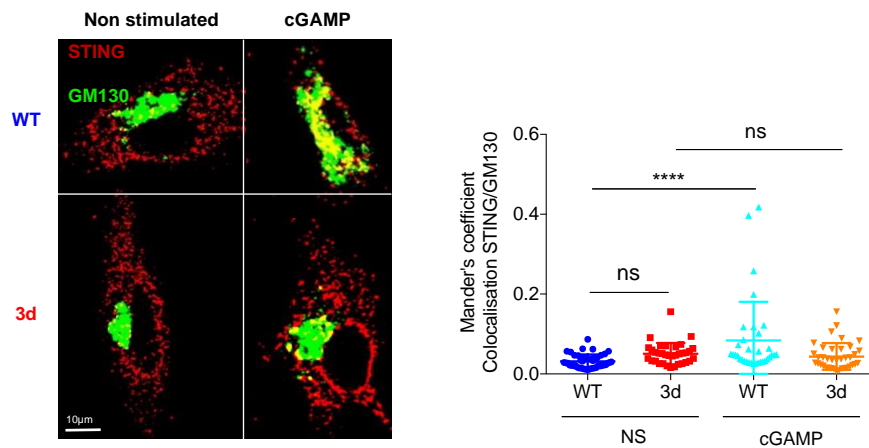


**Figure 3. UNC93B1 controls STING translocation to the Golgi upon cGAMP stimulation.** Colocalization between STING and GM130 (Golgi apparatus) was assessed by immunofluorescence. BMDCs were stimulated for 30 minutes with 10µg/mL of cGAMP (n=45 for WT, n=34 for 3d, n=33 for WT cGAMP, n=38 for 3d cGAMP, mean ± SEM, unpaired two-tailed t test, \*\*\*\*p<0.0001). NS: Non stimulated.

#### IV. STING activation cascade remains unchanged in WT or 3d DCs

Finally, to measure STING signalling cascade in 3d DCs, we performed immunoblot experiments for phosphorylated STING and its downstream adaptors TBK1 and IRF3. Activation of STING leads to its dimerization and phosphorylation by the cytosolic adaptor TBK1, which, in turn, autophosphorylates. Once activated, pTBK1 then phosphorylates IRF3, which, after binding to activated STING, can translocate to the nucleus and induce type I INFs genes transcription.

WT and 3d BMDCs were stimulated with cGAMP at different times. Cells were then lysed and phosphorylation of STING, TBK1 and IRF3 was detected by western blot. As expected, phosphorylation of STING, TBK1 and IRF3 was increased after cGAMP stimulation. However, no difference in STING, TBK1 and IRF3 phosphorylation was observed between WT and 3d BMDCs.

While STING-mediated type I INF response is impaired in UNC93B1 3d DCs, the first steps of STING signalling cascade, involving TBK1 and IRF3 phosphorylation, appear not to be altered in these cells.

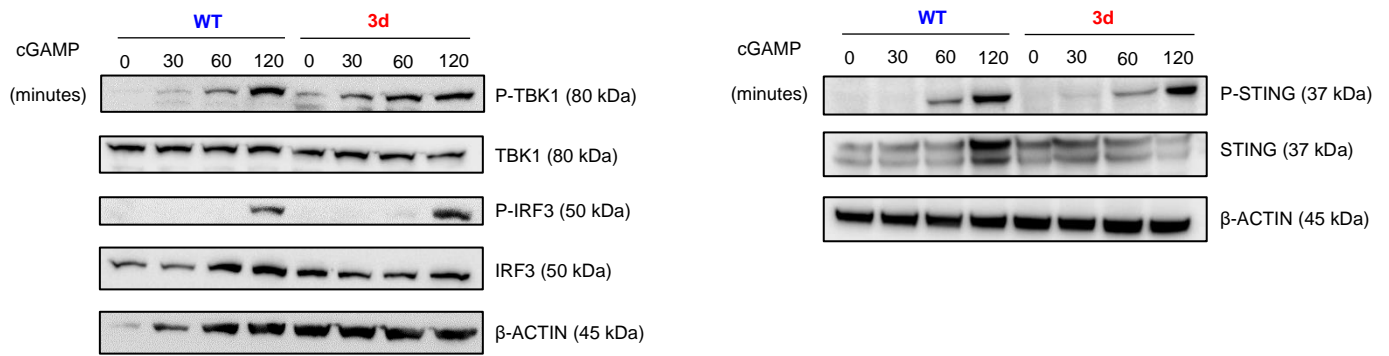


**Figure 4. STING and its downstream adaptors are phosphorylated in both WT and 3d DCs.** BMDCs were stimulated with 10µg/mL of cGAMP for 0, 30, 60 and 120 minutes. Protein levels were assessed by Western Blot (n=3).

## **MATERIALS AND METHODS \_ UNC93B1 regulates STING signalling in DCs**

### Bone marrow derived dendritic cells (BMDCs) differentiation

Bone marrow cells were harvested from leg bones of C57BL/6 WT and 3d mice. They were then filtered with a 40µm cell strainer and cultured in complete IMDM (Iscove's Modified Dulbecco's Medium, 10% FBS, 1% L-glutamine, 1% penicillin/streptomycin, 50µM β-mercaptoethanol). Cells from one leg were incubated in 20mL of medium supplemented with 20ng/mL of recombinant GM-CSF (Peprotech, 315-03) for 7 to 8 days. At the end of the culture, 80 to 90% of bone marrow cells are differentiated into dendritic cells.

### Immunoprecipitation and western blotting

Cells were stimulated or not with 10µg/mL of 2'3'-cGAMP (Invivogen, tlrl-nacga23) for 30 minutes before being lysed in NP-40 lysis buffer (150mM NaCl, 50mM Tris pH7.5, 5mM MgCl<sub>2</sub> and 0.5% NP-40) supplemented with protease inhibitors for 30 minutes on ice. To immunoprecipitate STING, magnetic protein G dynabeads were used (Thermo Fisher). The beads were first washed with PBS Tween 0.02% and incubated with STING antibody for an hour at 4°C. The magnetic beads were then washed again and incubated with 0.8 to 1mg of proteins from cell lysates overnight at 4°C. The next day, the beads were washed, and proteins were eluted with 4X LDS Sample Buffer at room temperature for 30 minutes. Washes were performed with PBS Tween 0.02%. The eluted proteins were then analysed by western blot.

For western blot, immunoprecipitated proteins or cell lysates were run on a 4-12% Bis-Tris Gel, using MOPS running buffer (Thermo Fisher). The proteins were then transferred on a PVDF membrane using the iBlot2 machine for a dry transfer method (Thermo Fisher, template P0). After blocking the membrane in TBS 0.1% Tween 5% Milk, primary antibodies (Supplementary table) were incubated overnight at 4°C. The next day, the membranes were washed, and secondary antibodies (Supplementary table) were incubated for at least an hour at room temperature. After washing, proteins were revealed by chemiluminescence using the PICO Plus ECL (Thermo Fisher).



## ELISA

BMDCs were plated in an adherent 96 well plate at the concentration of  $10^5$  cells per well. The next day, they were stimulated with  $50\mu\text{g/mL}$  of 2'3'-cGAMP for 6 hours and supernatants were collected. INF- $\beta$  levels were measured using the LumiKine Xpress mINF- $\beta$  2.0 ELISA kit (Invivogen) and following the protocol provided by the manufacturer.

## Immunofluorescence and colocalization analyses

BMDCs were left to adhere on fibronectin-treated coverslips overnight before stimulation with  $10\mu\text{g/mL}$  of 2'3'-cGAMP. The coverslips were then incubated in PHEM buffer (PHEM 2X: 120mM PIPES, 50mM Hepes, 20mM EGTA, 4mM MgAc, pH 6.9) diluted 1:1 in complete IMDM for 5 minutes at  $37^\circ\text{C}$  before being fixed with cold methanol for 3 minutes at room temperature. After fixation, the cells were washed with PBS and permeabilised with 17% TritonX-100, 0.05% BSA diluted in PBS for 30 minutes at room temperature. Primary antibodies (Supplementary table) diluted in permeabilization buffer were then incubated on the coverslips for an hour at room temperature. After washing, cells were incubated with secondary antibodies (Supplementary table) for 30 minutes at room temperature. Once stained, the cells went through a second step of fixation with 4% paraformaldehyde for 5 minutes at room temperature, and were then quenched with 50mM of  $\text{NH}_4\text{Cl}$  for 5 minutes as well. After washing, the coverslips were mounted on glass slides. Images were acquired on a Leica SP8 gSTED confocal microscope. Colocalization was assessed with Fiji, allowing us to measure the colocalization index for each cell using Mander's coefficient and JaCoP plugin. This process was automated thanks to a program written by Nicolas Goudin (INEM).

## siRNA transfection

Three days before they were fully differentiated, BMDCs were harvested and siRNAs ( $25\mu\text{M}$  or  $50\mu\text{M}$ ) targetting either control (control siRNA, OFF-target, Dharmacon) or UNC93B1 mRNA (UNC93B1 ON-target, Dharmacon) were transfected with the Amaxa Mouse Dendritic cell transfection kit (Lonza). Cells were then cultured in complete IMDM supplemented with  $20\text{ng/mL}$  of GM-CSF for 72 hours.

Target	Dilution	Catalogue reference
STING	WB: 1/1000 IF: 1/250 IP: 1/50	Cell signaling technology, 50494S
UNC93B1	WB: 1/1000	Homemade antibody From Dr. Brinkmann Maschalidi et al., 2017. doi: 10.1038/s41467-017-01601-5
$\beta$ -Actin	WB: 1/1000	Cell signaling technology, 3700S
P-TBK1	WB: 1/1000	Cell signaling technology, 5483S
TBK1	WB: 1/1000	Cell signaling technology, 38066S
P-IRF3	WB: 1/1000	Cell signaling technology, 29047S
IRF3	WB: 1/1000	Cell signaling technology, 4302S
P-STING	WB: 1/1000	Cell signaling technology, 72971S
IgG Rabbit HRP	WB: 1/5000	Cell signaling technology, 7074S
IgG Mouse HRP	WB: 1/5000	Cell signaling technology, 7076S
GM130	IF: 1/250	BD Biosciences, 610823
IgG Rabbit – Alexa Fluor 594	IF: 1/1000	Invitrogen, A121207
IgG Mouse – Alexa Fluor 488	IF: 1/1000	Invitrogen, A11001

Supplementary table. **List of antibodies used.** WB: Western Blot. IF: Immunofluorescence. IP: Immunoprecipitation.



## DISCUSSION AND CONCLUSION

UNC93B1 was originally described to bind endosomal TLRs, helping their folding and bringing them to their signalling compartments. In this PhD project, I was able to highlight new regulation pathways for IRE1 $\alpha$  and STING in dendritic cells, mediated by the ER chaperone UNC93B1.

### I. **UNC93B1 association with its interactants**

UNC93B1 binds the transmembrane domain of IRE1 $\alpha$  and, upon ER stress induced with thapsigargin, an increased interaction between the two proteins was observed. This result led us to the hypothesis that UNC93B1 promotes IRE1 $\alpha$  oligomerisation and activation through its association with the UPR factor. Furthermore, in mutated UNC93B1 3d DCs, IRE1 $\alpha$  is activated at steady state and shows increased interaction with UNC93B1 compared to WT DCs. It then appears that IRE1 $\alpha$  association with UNC93B1 is closely related to its activation in DCs. It is yet to be elucidated if the UNC93B1-IRE1 $\alpha$  interaction is required for IRE1 $\alpha$  oligomerisation and activation. To address this, it would be interesting to assess IRE1 $\alpha$  activity in UNC93B1 deficient DCs.

UNC93B1 being a 12-membrane spanning molecule, it is challenging to study sites of interaction within the protein as well as potential conformational changes. It is then complicated to assess UNC93B1 affinity for its known interactants: endosomal TLRs, STIM1, STING and IRE1 $\alpha$ . While UNC93B1 H412R (3d) mutation disrupts its association to intracellular TLRs and STIM1, steric changes in the protein explaining these effects remain hard to evaluate. Still, it is accepted that the 3d mutation in UNC93B1 leads to a change of conformation incompatible for the ER chaperone to associate with endosomal TLRs (Ishida et al., 2021b), and with STIM1 (Maschalidi et al., 2017). While this new UNC93B1 conformation loses its affinity for TLRs and STIM1, it gains affinity for IRE1 $\alpha$ . We then hypothesise that UNC93B1 change of conformation renders IRE1 $\alpha$  incompatible to associate with BiP, leading to IRE1 $\alpha$  chronic activation. Increased 3d UNC93B1 association with IRE1 $\alpha$  may indeed block the binding site of IRE1 $\alpha$  to BiP. Moreover, we showed that the expression of Sec63 and the proximity between IRE1 $\alpha$  and Sec63 is also decreased in 3d DCs. As previously explained,

Sec63 is involved in IRE1 $\alpha$  downregulation after its activation, by recruiting BiP back to IRE1 $\alpha$  luminal domain (Li et al., 2020). Thus, decreased interaction between Sec63 and IRE1 $\alpha$  in 3d DCs could be one of the causes for the inhibition of BiP binding to IRE1 $\alpha$  in these cells.

Studying IRE1 $\alpha$  affinity to UNC93B1 3d protein would need techniques such as cryo-electron microscopy to assess conformational changes and interaction sites. Such experiments were performed to study UNC93B1 association with endosomal TLRs 3 and 7. While TLRs bind UNC93B1 through their transmembrane domain, cryo-electron microscopy studies revealed that this association mainly takes place within UNC93B1 third transmembrane domain (TM3). They also determined that the sixth transmembrane domain (TM6) and several loops between transmembrane domains of UNC93B1 were involved in the interaction, though to a lesser extent than TM3 (Ishida et al., 2021b).

Interaction sites between UNC93B1 TM3 and TLR3 transmembrane domain were shown to be mediated mostly by hydrophobic residues. Hydrophobic and charged residues interactions are the most described between proteins. Although non-covalent, hydrophobic residues associations are robust and provide strong protein-to-protein bindings. The main hydrophobic interactions observed involve amino acids as tryptophan, leucine, isoleucine, phenylalanine, or proline. For endosomal TLRs and IRE1 $\alpha$ , UNC93B1 was reported to interact with their transmembrane domains, containing a majority of hydrophobic residues and therefore promoting protein-protein interactions.

As shown in Figure 1, TLR3 and TLR9 transmembrane domains are composed of hydrophobic residues as leucine, isoleucine or valine. TLR3 and TLR9 transmembrane domains contain 76% and 72% of hydrophobic residues respectively. For TLR3 interaction with UNC93B1, cryo-electron microscopy studies revealed precise hydrophobic interactions involving amino acids such as L713, H724 or I717 in TLR3 and F294, W137 or F140 in UNC93B1. IRE1 $\alpha$  transmembrane domain, shown to be the site of its association with UNC93B1, contains 77% of hydrophobic residues, mostly composed of leucine, isoleucine and phenylalanine. However, STIM1 was described to interact with UNC93B1 through its juxtamembrane luminal domain (Wang and Demarex, 2022), containing 40% of hydrophobic residues. We can then speculate

that UNC93B1 interaction with STIM1 is weaker compared to its association with IRE1 $\alpha$  or endosomal TLRs, although this matter has never been assessed.

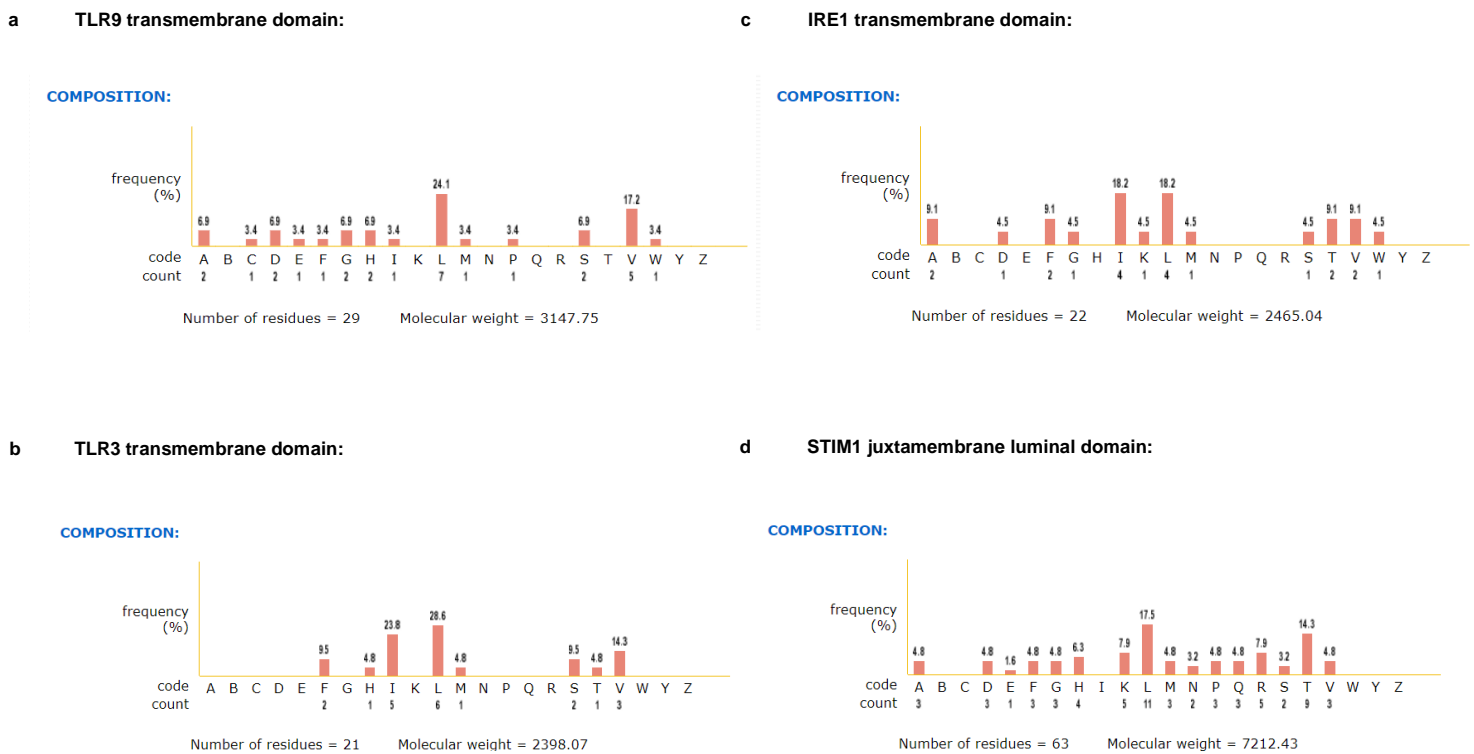


**Figure 1. Interacting domains composition of UNC93B1 partners.** Amino acid composition of TLR9 (a), TLR3 (b) and IRE1 $\alpha$  (c) transmembrane domains and of STIM1(d) juxtamembrane luminal domain assessed with the Protein Information Resource website.

UNC93B1 H412R or 3d mutation is localised in the ninth transmembrane domain (TM9). Cryo-electron microscopy studies reveal that UNC93B1 transmembrane domains are in tight conformation, a change in any of them then possibly altering the whole molecule. Accordingly, even if TM3 and TM9 are distant from one another, UNC93B1 H412R change of conformation would impact TM3 and its surroundings. In the case of UNC93B1 H412R mutation, the highly hydrophilic chain of arginine (R) is added in a hydrophobic environment. This addition is very likely to disrupt the overall conformation of the protein, potentially bringing transmembrane domains further away from one another. While UNC93B1 interaction with either endosomal TLRs and STIM1 is not stabilised anymore with the H412R mutation, the new conformation may allow more space for IRE1 $\alpha$  oligomers, increasing its affinity to the protein.

Another hypothesis for increased interaction between UNC93B1 3d and IRE1 $\alpha$  is the potential competition for IRE1 $\alpha$  binding between BiP and UNC93B1. Indeed, similar to what happens in 3d DCs, IRE1 $\alpha$  and UNC93B1 association is increased upon ER stress induction. We also know that both ER stress and the 3d mutation disrupt BiP association to IRE1 $\alpha$ , initiating its activation. In the case of the 3d mutation, BiP and IRE1 $\alpha$  association may be altered because of UNC93B1 change of conformation, potentially blocking the binding site of BiP on IRE1 $\alpha$ . We can then hypothesise that, in WT DCs, at steady state, IRE1 $\alpha$  has more affinity for BiP and their association is kept. In stressed or 3d DCs, however, BiP is brought apart from IRE1 $\alpha$  and the UPR factor can then interact more strongly with UNC93B1.

Concerning STING association to UNC93B1, the site of interaction between the two proteins has not been investigated to this day. However, it appears that their binding is stable enough not to be disrupted after UNC93B1 3d mutation and change of conformation.

Aside from UNC93B1 affinity for its interactants, its different pools and localisations in the ER can be discussed. In our data, we observed the presence of UNC93B1 when immunoprecipitating Sec63, highlighting a possible complex between IRE1 $\alpha$ , the Sec61 translocon and UNC93B1 (unpublished data). However, while UNC93B1 interacts with both IRE1 $\alpha$  and STIM1, these two proteins didn't immunoprecipitate together, indicating that the three ER proteins do not form a complex. We can then theorise that UNC93B1 comes in multiple complexes in the ER, interactions potentially taking place in different ER locations. For example, we can hypothesise that UNC93B1/STIM1 association takes place close to ER-plasma membrane contact sites as STIM1 activation leads to its interaction with the plasma membrane calcium channel ORAI1.

## **II. UNC93B1 and the UPR regulate STIM1 activity**

STIM1 activity maintains stable Ca<sup>2+</sup> flux in cells, especially in the ER and in endosomes, where it is crucial for MHC I antigen presentation in DCs. STIM1 is a calcium sensor that associates with the SOCE channel ORAI1 to allow Ca<sup>2+</sup> influx inside the ER and the creation of Ca<sup>2+</sup> hotspots in endosomes/phagosomes. UNC93B1 requirement for STIM1 activation has been previously published (Maschalidi et al.,

2017). Indeed, in UNC93B1  $-/-$  and UNC93B1 3d cells, where STIM1 and UNC93B1 association is abrogated, STIM1 activity is inhibited and  $Ca^{2+}$  influx in the ER or in endosomes is highly impaired. In the ER, UNC93B1 association with STIM1 is necessary for STIM1 to translocate to sites close to ER-plasma membrane contact sites, essential for its interaction with ORAI1 (Wang and Demaurex, 2022). The absence of STIM1 interaction with ORAI1 in 3d DCs eventually causes a defect in  $Ca^{2+}$  influx and a potential lack of  $Ca^{2+}$  in the ER which can impact ATP production in this organelle, required for chaperones activity such as BiP. This could explain the impaired inactivation of IRE1 $\alpha$  by BiP in 3d DCs. Thus, it would be interesting to study IRE1 $\alpha$  and BiP interaction in STIM1 deficient DCs, to assess whether the role of BiP to inactivate IRE1 $\alpha$  at steady state is STIM1-dependent.

It would also be interesting to address the role of UNC93B1 in PERK function. Indeed, as previously described (Introduction, chapter 7), PERK interacts with filamin A and regulates cell migration. Furthermore, this association is involved in ER remodelling, necessary for ER-plasma membrane contact sites to occur and STIM1 activation after ER calcium depletion (van Vliet and Agostinis, 2017). It would then be of interest to assess PERK association with filamin A in UNC93B1 mutated 3d DCs. If UNC93B1 mutation also disrupts PERK and filamin A association, this mechanism would explain the inhibition of STIM1 functions in 3d cells. UNC93B1-mediated STIM1 regulation could then happen at different steps, through their physical interaction and through the remodelling of the ER by filamin A.

### **III. IRE1 $\alpha$ activation in DCs and its impact on immune functions**

Chronic IRE1 $\alpha$  activation in UNC93B1 mutated 3d DCs induces both XBP1 and RIDD pathways. The XBP1 pathway involves IRE1 $\alpha$  splicing of *Xbp1* mRNA, giving rise to the transcription factor XBP1s, which activates the translation of ER chaperones, ESCRT members or apoptotic factors. Among these, some upregulated proteins are not specific targets of IRE1 $\alpha$  but are also triggered by PERK or ATF6 activation. CHOP, a pro-apoptotic transcription factor, is a key element of ER stress-mediated apoptosis and is induced through the three branches of the UPR. We reported its upregulation in 3d DCs at steady state, along with an abnormal dotted shape of the ER, previously observed in a context of stressed ER (Osorio et al., 2014). CHOP upregulation, splicing



of *Xbp1*, downregulation of several RIDD targets and a dotted ER indicate IRE1 $\alpha$  activation along with a chronic ER stress in 3d DCs. We can also wonder if the other two branches of the UPR, PERK and ATF6, are triggered in 3d DCs at steady state.

As previously mentioned, in splenic murine cDC1s, IRE1 $\alpha$  is activated at steady state (Osorio et al., 2014). It was described recently that PERK is also activated and phosphorylates eIF2 $\alpha$  in splenic cDC1s (Mendes et al., 2021). For both UPR pathways, this steady state activation in cDC1s doesn't lead to a decrease in protein load. Indeed, in this context, IRE1 $\alpha$  doesn't cleave its known RIDD targets, such as *Bloc1s1*, *Tapbp* or *Ergic3*, and phosphorylated eIF2 $\alpha$  doesn't inhibit protein translation. We can then speculate that activation of both UPR factors in cDC1s is mainly required to keep high levels of ER chaperones, ESCRT and ERAD members that are important for DCs phenotype and functions. Indeed, PERK activation was shown to be important for DC immune functions as type I INF production and migration with filamin-A and F-actin remodelling (van Vliet and Agostinis, 2017; Mendes et al., 2021). In addition, *Xbp1* splicing in DCs is important for their phenotype (Osorio et al., 2014) and for cytokine responses upon TLR stimulation (Janssens et al., 2014; Beisel et al., 2017).

As PERK activation has been previously linked to immune functions in DCs, it would be relevant to assess eIF2 $\alpha$  phosphorylation and expression of ATF4, a transcription factor increased following PERK activation, in 3d DCs. If, as IRE1 $\alpha$ , PERK is activated at steady state in 3d DCs, and induces phosphorylation of eIF2 $\alpha$ , it may also lead to inhibition of protein translation in this context. This function of p-eIF2 $\alpha$  might then play a role in the impaired immune functions of 3d DCs. In this case, we could hypothesise that chronic ER stress in 3d DCs, and not only IRE1 $\alpha$  activation, is deleterious for immune responses as antigen presentation.

The activation levels of the three UPR factors in 3d DCs can be measured by western blots or quantitative PCRs together with a recent technique called SNUPR, an unfolded stress response single nuclei analysis method. This cytometry technique would allow us to assess each UPR factor activation at steady state or after ER stress, by measuring the translocation of their transcription factors to the nucleus and the translational levels of their targets. We could then address the levels of activation of the three UPR branches, IRE1 $\alpha$ , PERK and ATF6 in 3d DCs.

### A. IRE1 $\alpha$ and antigen presentation

IRE1 $\alpha$  activation in DCs has been shown to be either beneficial or detrimental for MHC class I antigen presentation, depending on its level of activation. Indeed, *Xbp1* splicing, triggered after an infection, incubation with melanoma antigens, or at steady state in cDC1s, is required for efficient MHC I antigen presentation. These beneficial effects are probably due to XBP1s targets upregulation. Among them, we find ER chaperones, stabilising the different proteins of the PLC present in the ER, or ERAD members, involved in MHC I antigen cross-presentation cytosolic pathway. However, activation of the IRE1 $\alpha$ -dependent RIDD pathway has been described to be detrimental for MHC I antigen presentation. RIDD is mostly associated to long or strong ER stress and IRE1 $\alpha$  activation, and may be linked to a repressive effect on DCs immune responses. Indeed, the RIDD response may contribute to controlling and downregulating DC-mediated inflammation after long-term infections.

In 3d DCs, both XBP1 and RIDD pathways are chronically triggered, and cause impaired MHC I antigen cross-presentation. Throughout our investigation, we described RIDD targets, important for efficient MHC I antigen presentation, downregulated in 3d DCs at steady state. Among those, we find *Tapbp*, necessary for TAP-mediated peptide loading on MHC I, and *Erp44*, stabilising the peptide trimming enzymes ERAP in the ER. Downregulated in IRE1 $\alpha$   $-/-$  DCs, where the RIDD pathway is inhibited, ERp44 has not been defined as a definitive RIDD target. However, its degradation was reported to a higher level in *Xbp1*  $-/-$  DCs where RIDD is activated (Osorio et al., 2014). ERp44 is therefore probably cleaved by IRE1 $\alpha$ , though its downregulation is not specific to the UPR factor only.

A previous work in DCs has described MHC I as a RIDD target too, explaining the detrimental effects of RIDD activation on MHC I antigen presentation. However, in our experiments, the levels of MHC I between WT and 3d DCs were similar, with or without ER stress (Figure 2). Our data indicate that MHC I is not a RIDD target in our model, and is therefore not the cause of the antigen cross-presentation defect in 3d DCs.

We then managed to show that, inhibition of IRE1 $\alpha$  activity with the IRE1 $\alpha$  RNase inhibitor 4 $\mu$ 8c, restored antigen cross-presentation by 3d DCs. This result shows that activation of IRE1 $\alpha$ , and more likely of the RIDD pathway, in 3d DCs is indeed detrimental for antigen cross-presentation.

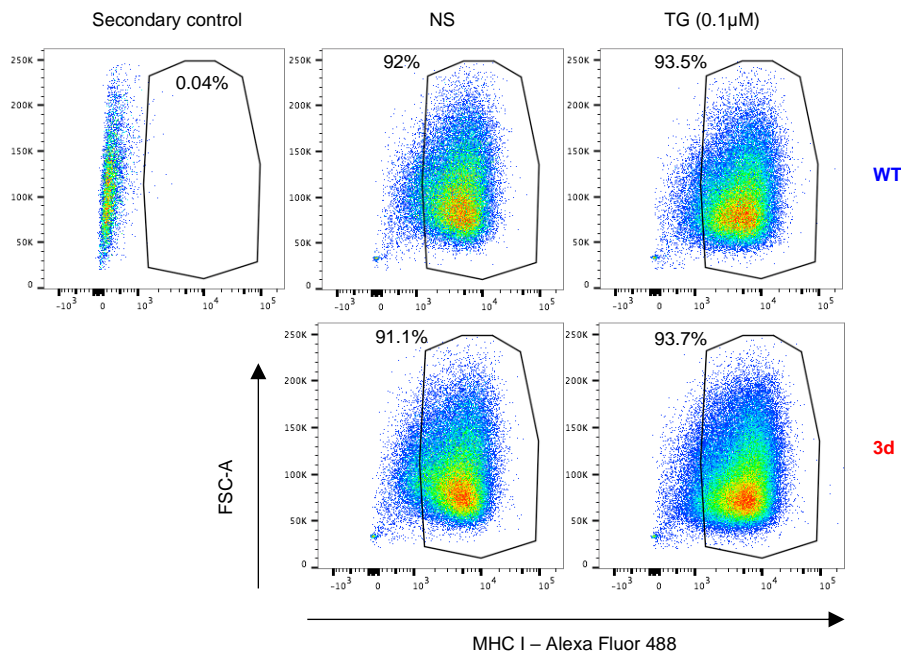


**Figure 2. MHC I levels are similar between WT and 3d DCs.** Intracellular MHC I levels were measured in BMDCs by flow cytometry using an anti-H2k<sup>b</sup> antibody (BioLegend, 116502) and a secondary antibody coupled to Alexa Fluor 488. Cells were stimulated for 24 hours with 0.1μM of thapsigargin.

### B. IRE1α and tumoral immune microenvironment

In concordance with the impaired antigen cross-presentation in 3d DCs, rapid tumour growth is observed in 3d mice injected with melanoma cells compared to WT mice. We then hypothesised that since IRE1α and RIDD activation was one of the causes for 3d DCs impaired cross-presentation, it would also be responsible for the abnormal tumoral growth in 3d mice. Our theory was confirmed as inhibition of IRE1α RNase activity with MKC8866 partially rescued tumoral growth in 3d mice. Furthermore, we could show that this was linked to antigen cross-presentation as injecting OT-I T cells, boosting antigen cross-presentation against B16-OVA melanoma, did decrease tumoral growth in WT mice but not in 3d mice. In 3d mice, injection of an IRE1α RNase inhibitor, along with OT-I T cells, was needed for tumoral growth decrease to occur.

However, throughout our experiments, we noticed that the sole inhibition of IRE1α RNase activity in WT mice bearing a tumour reduced tumoral growth. This data can be explained by transmissible ER stress (TERS) between cancer cells and their tumoral immune microenvironment. Indeed, tumour cells chronically face ER stress and their UPR pathways are constantly triggered. In the attempt of controlling tumoral growth,

cells in the immune microenvironment interact with tumour cells, inducing ER stress and the UPR pathways in these cells. This activation has been shown to be detrimental for efficient tumoral rejection by the immune microenvironment (Mahadevan et al., 2011, 2012). Therefore, in this context, inhibiting IRE1 $\alpha$  RNase activity in WT mice would reduce tumoral growth.

Nevertheless, a previous study has described activation of the IRE1 $\alpha$ /XBP1 pathway in DCs challenged with melanoma lysates, and showed a beneficial effect of *Xbp1* splicing in cross-presentation of tumour-associated antigens. IRE1 $\alpha$ -dependent RIDD activation must then become detrimental for antigen presentation and rejection of tumour under prolonged or chronic ER stress.

### C. IRE1 $\alpha$ and TLR signalling

*Xbp1* splicing by IRE1 $\alpha$  also has a synergetic effect with TLR signalling for myeloid cells to induce pro-inflammatory responses. Indeed, acute activation of IRE1 $\alpha$  highly increases the production of pro-inflammatory cytokines by macrophages and DCs following TLR stimulation (Smith et al., 2008; Martinon et al., 2010; Janssens et al., 2014). However, in 3d DCs, where IRE1 $\alpha$  is chronically activated, we didn't observe increased inflammatory response following surface TLR stimulation compared to WT cells. Perhaps, only strong and acute ER stress and IRE1 $\alpha$  activation leads to enhanced TLR responses.

3d DCs were originally characterised by the inhibition of endosomal TLR signalling. To address whether IRE1 $\alpha$  chronic activation in 3d DCs has a role in intracellular TLR signalling, we stimulated 3d DCs with endosomal TLR ligands after inhibiting IRE1 $\alpha$  RNase activity. We observed that IRE1 $\alpha$  inhibition did not rescue endosomal TLR signalling in 3d DCs (unpublished data), and concluded that their endosomal TLR defect was probably due to their inability to interact with UNC93B1.

#### **IV. UNC93B1 and STING**

Previous works have reported association between STING and UNC93B1 in fibroblasts or transfected HEK293T cell lines (He et al., 2021; Zhu et al., 2022). These studies have also highlighted the potential role of UNC93B1 as a negative regulator of STING, sending it to degradation to dampen its signalling. We then wondered about the regulation of STING by UNC93B1 in DCs, a relevant cell type for innate immune responses. Indeed, DCs possess all the machinery necessary for cGAS to detect danger-associated DNA molecules and STING to induce type I INFs and pro-inflammatory cytokines secretion.

First, our experiments showed that the interaction between UNC93B1 and STING was kept in both WT and 3d BMDCs. We also observed that knocking down UNC93B1 in DCs reduced STING-mediated INF- $\beta$  response. Altogether, this result indicates a different regulation of STING by UNC93B1 in DCs, as UNC93B1 is required for efficient type I INF signalling in these cells. Therefore, UNC93B1 appears not to send STING to degradation in DCs, but to rather help its activation.

We also reported that STING-mediated INF- $\beta$  secretion is decreased in 3d DCs, and showed that significantly less STING translocates to the Golgi apparatus after stimulation compared to WT cells. As it was previously suggested that UNC93B1 travels with STING after its activation, we can then hypothesise that 3d UNC93B1 and STING are retained in the ER, leading to a defect in STING translocation to the Golgi and the productive secretion of type I INFs. More than STING translocation to the Golgi, it would then be of interest to study UNC93B1 trafficking after 2'3'-cGAMP stimulation.

To further investigate STING signalling cascade in 3d DCs, we assessed phosphorylation of its downstream adaptors TBK1 and IRF3 after stimulation. No change in TBK1 and IRF3 phosphorylation was detected between WT and 3d DCs. Phosphorylation of IRF3 with no efficient type I INF response may be explained by either an impaired p-IRF3 translocation to the nucleus or a partial phosphorylation of the transcription factor. Indeed, IRF3 has to be phosphorylated on specific serine residues, namely S396 and S386, to induce INF genes. It would then be useful to look at p-IRF3 trafficking to the nucleus and its sites of phosphorylation in 3d DCs. Another

theory for decreased INF response could be a failed recruitment of IRF3 to STING after its phosphorylation which could be assessed by immunoprecipitation.

STING activation is controlled by multiple proteins in the ER. Indeed, STING associates with STIM1 in the ER to keep STING in an inactive state (Srikanth et al., 2019). Upon activation, STING dissociates from STIM1 and translocates to the Golgi apparatus.

In 3d DCs, STIM1 no longer interacts with UNC93B1 leading to impaired ER Ca<sup>2+</sup> flux. We can then hypothesise that STING activation or translocation to the Golgi is dependent on Ca<sup>2+</sup> flux in the ER. Impaired STIM1 activity would then lead to low type I INF responses following STING stimulation in 3d DCs. Another theory could be that since STIM1 doesn't interact with UNC93B1 in 3d DCs, it leaves more UNC93B1 molecules to associate to STING, potentially retaining it more in the ER. It would then be interesting to assess STING and UNC93B1 binding by proximity ligation assay, technique allowing us to quantify the interaction between two proteins.

TOLLIP, another STING interactant, is required for STING stability (Pokatayev et al., 2020). Indeed, in *Tollip* deficient cells, STING protein levels are significantly reduced, and its downstream type I INF response is strongly inhibited. Reduced STING expression is partially dependent on IRE1 $\alpha$ . The UPR factor is activated at steady state in *Tollip*  $-/-$  cells, causing splicing of *Xbp1* mRNA and upregulation of its targets. This permanent induction of the IRE1 $\alpha$ /XBP1s pathway leads to decreased STING protein levels; activated IRE1 $\alpha$  probably bringing STING to lysosomal degradation. Reduced STING protein levels were also observed in *Xbp1*  $-/-$  cells, where IRE1 $\alpha$  is activated. Therefore, in 3d DCs, where IRE1 $\alpha$  is chronically activated, STING lysosomal degradation may be increased and its downstream type I INF signalling impaired. It would then be of interest to assess the impact of IRE1 $\alpha$  inhibition on STING-mediated INF responses in 3d DCs. However, it has to be noted that no decrease of STING protein levels was observed in 3d cells. This could be because, in 3d DCs, IRE1 $\alpha$  is activated to a lower extent than in *Xbp1* or *Tollip* deficient cells, and it may not be enough to detect protein changes by western blot. There is also a possibility that STING lysosomal degradation is not the cause of reduced INF signalling in 3d DCs.

Finally, STING is involved in tumoral rejection and its activation was reported to slow down tumoral growth (Corrales et al., 2015). Thus, in 3d DCs, impaired STING signalling may be one of the causes for strong and rapid tumoral development.

## **V. Conclusion**

Throughout this thesis, we have looked at the regulation of two novel UNC93B1 clients in DCs: IRE1 $\alpha$  and STING.

First, we showed that the 3d UNC93B1 protein increases its association to IRE1 $\alpha$  and blocks BiP recruitment to IRE1 $\alpha$  leading to its activation at steady state. In 3d DCs and mice, IRE1 $\alpha$  chronic activation causes impaired antigen cross-presentation and rapid tumoral growth. These conclusions reinforce the hypothesis that the IRE1 $\alpha$ /RIDD pathway induced in DCs is detrimental for MHC I antigen presentation, and suggests UNC93B1 as a main regulator of IRE1 $\alpha$  in these cells. IRE1 $\alpha$  is linked to important immune responses in DCs, and identifying its interactants is then crucial to potentially regulate its activation in immunodeficiencies or autoimmune diseases.

STING has been both linked to interferonopathies and INF-mediated immunodeficiencies. Indeed, depending on the nature of the stimulation, STING can be a turning point in innate immune responses by myeloid cells. We showed that UNC93B1 promotes STING-mediated INF responses in DCs. Silencing UNC93B1 or the expression of the 3d mutation in DCs causes a loss of function in STING signalling, highlighting the role of UNC93B1 in this innate immune pathway. However, the molecular mechanisms by which UNC93B1 controls STING activation are not yet known.

## MATERIALS AND METHODS \_ DISCUSSION

### Flow cytometry

BMDCs were fixed and permeabilised using a FoxP3 permeabilization kit (Biolegend, 421403) following the manufacturer's instructions. Cells were then incubated with H-2k<sup>b</sup> antibody for 30 minutes at 4°C. They were washed and incubated with an anti-mouse secondary antibody coupled to Alexa Fluor 488 for 30 minutes at 4°C. After extensive washes, stained BMDCs acquired on a BD LSR Fortessa flow cytometer and analysed using the Flojow (Treestar) software.





## REFERENCES

- Ablasser, A., Goldeck, M., Cavlar, T., Deimling, T., Witte, G., Röhl, I., Hopfner, K.-P., Ludwig, J., Hornung, V., 2013. cGAS produces a 2'-5'-linked cyclic dinucleotide second messenger that activates STING. *Nature* 498, 380–384. <https://doi.org/10.1038/nature12306>
- Ackerman, A.L., Giodini, A., Cresswell, P., 2006. A Role for the Endoplasmic Reticulum Protein Retrotranslocation Machinery during Crosspresentation by Dendritic Cells. *Immunity* 25, 607–617. <https://doi.org/10.1016/j.immuni.2006.08.017>
- Alexopoulou, L., Holt, A.C., Medzhitov, R., Flavell, R.A., 2001. Recognition of double-stranded RNA and activation of NF- $\kappa$ B by Toll-like receptor 3. *Nature* 413, 732–738. <https://doi.org/10.1038/35099560>
- Anderson, D.A., Dutertre, C.-A., Ginhoux, F., Murphy, K.M., 2021. Genetic models of human and mouse dendritic cell development and function. *Nat. Rev. Immunol.* 21, 101–115. <https://doi.org/10.1038/s41577-020-00413-x>
- Anderson, K.V., Bokla, L., Nüsslein-Volhard, C., 1985. Establishment of dorsal-ventral polarity in the drosophila embryo: The induction of polarity by the Toll gene product. *Cell* 42, 791–798. [https://doi.org/10.1016/0092-8674\(85\)90275-2](https://doi.org/10.1016/0092-8674(85)90275-2)
- Andrade, W.A., Souza, M. do C., Ramos-Martinez, E., Nagpal, K., Dutra, M.S., Melo, M.B., Bartholomeu, D.C., Ghosh, S., Golenbock, D.T., Gazzinelli, R.T., 2013. Combined Action of Nucleic Acid-Sensing Toll-like Receptors and TLR11/TLR12 Heterodimers Imparts Resistance to *Toxoplasma gondii* in Mice. *Cell Host Microbe* 13, 42–53. <https://doi.org/10.1016/j.chom.2012.12.003>
- Auffray, C., Fogg, D., Garfa, M., Elain, G., Join-Lambert, O., Kayal, S., Sarnacki, S., Cumano, A., Lauvau, G., Geissmann, F., 2007. Monitoring of Blood Vessels and Tissues by a Population of Monocytes with Patrolling Behavior. *Science* 317, 666–670. <https://doi.org/10.1126/science.1142883>
- Bachem, A., Hartung, E., Güttler, S., Mora, A., Zhou, X., Hegemann, A., Plantinga, M., Mazzini, E., Stoitzner, P., Gurka, S., Henn, V., Mages, H.W., Kroczeck, R.A., 2012. Expression of XCR1 Characterizes the Batf3-Dependent Lineage of Dendritic Cells Capable of Antigen Cross-Presentation. *Front. Immunol.* 3. <https://doi.org/10.3389/fimmu.2012.00214>

Barbet, G., Nair-Gupta, P., Schotsaert, M., Yeung, S.T., Moretti, J., Seyffer, F., Metreveli, G., Gardner, T., Choi, A., Tortorella, D., Tampé, R., Khanna, K.M., García-Sastre, A., Blander, J.M., 2021. TAP dysfunction in dendritic cells enables noncanonical cross-presentation for T cell priming. *Nat. Immunol.* 22, 497–509. <https://doi.org/10.1038/s41590-021-00903-7>

Barton, G.M., Medzhitov, R., 2003. Toll-Like Receptor Signaling Pathways. *Science* 300, 1524–1525. <https://doi.org/10.1126/science.1085536>

Beisel, C., Ziegler, S., Martrus Zapater, G., Chapel, A., Griesbeck, M., Hildebrandt, H., Lohse, A.W., Altfeld, M., 2017. TLR7-mediated activation of XBP1 correlates with the IFN $\alpha$  production in humans. *Cytokine* 94, 55–58. <https://doi.org/10.1016/j.cyto.2017.04.006>

Benhamron, S., Hadar, R., Iwawaky, T., So, J.-S., Lee, A.-H., Tirosh, B., 2014. Regulated IRE1-dependent decay participates in curtailing immunoglobulin secretion from plasma cells: Molecular immunology. *Eur. J. Immunol.* 44, 867–876. <https://doi.org/10.1002/eji.201343953>

Bertolotti, A., Zhang, Y., Hendershot, L.M., Harding, H.P., Ron, D., 2000. Dynamic interaction of BiP and ER stress transducers in the unfolded-protein response. *Nat. Cell Biol.* 2, 326–332. <https://doi.org/10.1038/35014014>

Bettelli, E., Oukka, M., Kuchroo, V.K., 2007. TH-17 cells in the circle of immunity and autoimmunity. *Nat. Immunol.* 8, 345–350. <https://doi.org/10.1038/ni0407-345>

Beutler, B., 2004. Inferences, questions and possibilities in Toll-like receptor signalling. *Nature* 430, 257–263. <https://doi.org/10.1038/nature02761>

Biswas, C., Rao, S., Slade, K., Hyman, D., Dersh, D., Mantegazza, A.R., Zoltick, P.W., Marks, M.S., Argon, Y., Behrens, E.M., 2018. Tyrosine 870 of TLR9 is critical for receptor maturation rather than phosphorylation-dependent ligand-induced signaling. *PLOS ONE* 13, e0200913. <https://doi.org/10.1371/journal.pone.0200913>

Blasius, A.L., Beutler, B., 2010. Intracellular Toll-like Receptors. *Immunity* 32, 305–315. <https://doi.org/10.1016/j.immuni.2010.03.012>

Blees, A., Janulienė, D., Hofmann, T., Koller, N., Schmidt, C., Trowitzsch, S., Moeller, A., Tampé, R., 2017. Structure of the human MHC-I peptide-loading complex. *Nature* 551, 525–528. <https://doi.org/10.1038/nature24627>

Brinkmann, M.M., Spooner, E., Hoebe, K., Beutler, B., Ploegh, H.L., Kim, Y.-M., 2007. The interaction between the ER membrane protein UNC93B and TLR3, 7, and 9 is crucial for TLR signaling. *J. Cell Biol.* 177, 265–275. <https://doi.org/10.1083/jcb.200612056>

Brown, G.J., Cañete, P.F., Wang, H., Medhavy, A., Bones, J., Roco, J.A., He, Y., Qin, Y., Cappello, J., Ellyard, J.I., Bassett, K., Shen, Q., Burgio, G., Zhang, Y., Turnbull, C., Meng, X., Wu, P., Cho, E., Miosge, L.A., Andrews, T.D., Field, M.A., Tvorogov, D., Lopez, A.F., Babon, J.J., López, C.A., González-Murillo, Á., Garulo, D.C., Pascual, V., Levy, T., Mallack, E.J., Calame, D.G., Lotze, T., Lupski, J.R., Ding, H., Ullah, T.R., Walters, G.D., Koina, M.E., Cook, M.C., Shen, N., de Lucas Collantes, C., Corry, B., Gantier, M.P., Athanasopoulos, V., Vinuesa, C.G., 2022. TLR7 gain-of-function genetic variation causes human lupus. *Nature* 605, 349–356. <https://doi.org/10.1038/s41586-022-04642-z>

Calton, M., Zeng, H., Urano, F., Till, J.H., Hubbard, S.R., Harding, H.P., Clark, S.G., Ron, D., 2002. IRE1 couples endoplasmic reticulum load to secretory capacity by processing the XBP-1 mRNA. *Nature* 415, 92–96. <https://doi.org/10.1038/415092a>

Canton, J., Blees, H., Henry, C.M., Buck, M.D., Schulz, O., Rogers, N.C., Childs, E., Zelenay, S., Rhys, H., Domart, M.-C., Collinson, L., Alloatti, A., Ellison, C.J., Amigorena, S., Papayannopoulos, V., Thomas, D.C., Randow, F., Reis e Sousa, C., 2021. The receptor DNGR-1 signals for phagosomal rupture to promote cross-presentation of dead-cell-associated antigens. *Nat. Immunol.* 22, 140–153. <https://doi.org/10.1038/s41590-020-00824-x>

Carbone, F.R., Bevan, M.J., 1990. Class I-restricted processing and presentation of exogenous cell-associated antigen in vivo. *J. Exp. Med.* 171, 377–387. <https://doi.org/10.1084/jem.171.2.377>

Casrouge, A., Zhang, S.-Y., Eidenschenk, C., Jouanguy, E., Puel, A., Yang, K., Alcais, A., Picard, C., Mahfoufi, N., Nicolas, N., Lorenzo, L., Plancoulaine, S., Sénéchal, B., Geissmann, F., Tabeta, K., Hoebe, K., Du, X., Miller, R.L., Héron, B., Mignot, C., de Villemeur, T.B., Lebon, P., Dulac, O., Rozenberg, F., Beutler, B., Tardieu, M., Abel, L., Casanova, J.-L., 2006. Herpes Simplex Virus Encephalitis in Human UNC-93B Deficiency. *Science* 314, 308–312. <https://doi.org/10.1126/science.1128346>

Cebrian, I., Visentin, G., Blanchard, N., Jouve, M., Bobard, A., Moita, C., Enninga, J., Moita, L.F., Amigorena, S., Savina, A., 2011. Sec22b Regulates Phagosomal Maturation and Antigen Crosspresentation by Dendritic Cells. *Cell* 147, 1355–1368. <https://doi.org/10.1016/j.cell.2011.11.021>

Cella, M., Jarrossay, D., Facchetti, F., Alebardi, O., Nakajima, H., Lanzavecchia, A., Colonna, M., 1999. Plasmacytoid monocytes migrate to inflamed lymph nodes and produce large amounts of type I interferon. *Nat. Med.* 5, 919–923. <https://doi.org/10.1038/11360>

Chefalo, P.J., Grandea, A.G., Van Kaer, L., Harding, C.V., 2003. Tapasin<sup>-/-</sup> and TAP1<sup>-/-</sup> Macrophages Are Deficient in Vacuolar Alternate Class I MHC (MHC-I) Processing due to Decreased MHC-I Stability at Phagolysosomal pH. *J. Immunol.* 170, 5825–5833. <https://doi.org/10.4049/jimmunol.170.12.5825>

Chen, X., Cubillos-Ruiz, J.R., 2021. Endoplasmic reticulum stress signals in the tumour and its microenvironment. *Nat. Rev. Cancer* 21, 71–88. <https://doi.org/10.1038/s41568-020-00312-2>

Christensen, S.R., Shupe, J., Nickerson, K., Kashgarian, M., Flavell, R.A., Shlomchik, M.J., 2006. Toll-like Receptor 7 and TLR9 Dictate Autoantibody Specificity and Have Opposing Inflammatory and Regulatory Roles in a Murine Model of Lupus. *Immunity* 25, 417–428. <https://doi.org/10.1016/j.immuni.2006.07.013>

Coccia, E.M., Severa, M., Giacomini, E., Monneron, D., Remoli, M.E., Julkunen, I., Cella, M., Lande, R., Uzé, G., 2004. Viral infection and Toll-like receptor agonists induce a differential expression of type I and  $\lambda$  interferons in human plasmacytoid and monocyte-derived dendritic cells. *Eur. J. Immunol.* 34, 796–805. <https://doi.org/10.1002/eji.200324610>

Corrales, L., Glickman, L.H., McWhirter, S.M., Kanne, D.B., Sivick, K.E., Katibah, G.E., Woo, S.-R., Lemmens, E., Banda, T., Leong, J.J., Metchette, K., Dubensky, T.W., Gajewski, T.F., 2015. Direct Activation of STING in the Tumor Microenvironment Leads to Potent and Systemic Tumor Regression and Immunity. *Cell Rep.* 11, 1018–1030. <https://doi.org/10.1016/j.celrep.2015.04.031>

Cross, B.C.S., Bond, P.J., Sadowski, P.G., Jha, B.K., Zak, J., Goodman, J.M., Silverman, R.H., Neubert, T.A., Baxendale, I.R., Ron, D., Harding, H.P., 2012. The molecular basis for selective inhibition of unconventional mRNA splicing by an IRE1-binding small molecule. *Proc. Natl. Acad. Sci.* 109. <https://doi.org/10.1073/pnas.1115623109>

Crozat, K., Guiton, R., Contreras, V., Feuillet, V., Dutertre, C.-A., Ventre, E., Vu Manh, T.-P., Baranek, T., Storset, A.K., Marvel, J., Boudinot, P., Hosmalin, A., Schwartz-Cornil, I., Dalod, M., 2010. The XC chemokine receptor 1 is a conserved selective

marker of mammalian cells homologous to mouse CD8 $\alpha$ <sup>+</sup> dendritic cells. *J. Exp. Med.* 207, 1283–1292. <https://doi.org/10.1084/jem.20100223>

Cubillos-Ruiz, J.R., Silberman, P.C., Rutkowski, M.R., Chopra, S., Perales-Puchalt, A., Song, M., Zhang, S., Bettigole, S.E., Gupta, D., Holcomb, K., Ellenson, L.H., Caputo, T., Lee, A.-H., Conejo-Garcia, J.R., Glimcher, L.H., 2015. ER Stress Sensor XBP1 Controls Anti-tumor Immunity by Disrupting Dendritic Cell Homeostasis. *Cell* 161, 1527–1538. <https://doi.org/10.1016/j.cell.2015.05.025>

de Oliveira Mann, C.C., Orzalli, M.H., King, D.S., Kagan, J.C., Lee, A.S.Y., Kranzusch, P.J., 2019. Modular Architecture of the STING C-Terminal Tail Allows Interferon and NF- $\kappa$ B Signaling Adaptation. *Cell Rep.* 27, 1165-1175.e5. <https://doi.org/10.1016/j.celrep.2019.03.098>

Delamarre, L., Pack, M., Chang, H., Mellman, I., Trombetta, E.S., 2005. Differential Lysosomal Proteolysis in Antigen-Presenting Cells Determines Antigen Fate. *Science* 307, 1630–1634. <https://doi.org/10.1126/science.1108003>

Deng, Z., Chong, Z., Law, C.S., Mukai, K., Ho, F.O., Martinu, T., Backes, B.J., Eckalbar, W.L., Taguchi, T., Shum, A.K., 2020. A defect in COPI-mediated transport of STING causes immune dysregulation in COPA syndrome. *J. Exp. Med.* 217, e20201045. <https://doi.org/10.1084/jem.20201045>

Denzin, L.K., Cresswell, P., 1995. HLA-DM induces clip dissociation from MHC class II  $\alpha\beta$  dimers and facilitates peptide loading. *Cell* 82, 155–165. [https://doi.org/10.1016/0092-8674\(95\)90061-6](https://doi.org/10.1016/0092-8674(95)90061-6)

Diebold, S.S., Kaisho, T., Hemmi, H., Akira, S., Reis e Sousa, C., 2004. Innate Antiviral Responses by Means of TLR7-Mediated Recognition of Single-Stranded RNA. *Science* 303, 1529–1531. <https://doi.org/10.1126/science.1093616>

Ding, X., Yang, W., Shi, X., Du, P., Su, L., Qin, Z., Chen, J., Deng, H., 2011. TNF Receptor 1 Mediates Dendritic Cell Maturation and CD8 T Cell Response through Two Distinct Mechanisms. *J. Immunol.* 187, 1184–1191. <https://doi.org/10.4049/jimmunol.1002902>

Dingjan, I., Verboogen, D.R., Paardekooper, L.M., Revelo, N.H., Sittig, S.P., Visser, L.J., Mollard, G.F. von, Henriët, S.S., Figdor, C.G., ter Beest, M., van den Bogaart, G., 2016. Lipid peroxidation causes endosomal antigen release for cross-presentation. *Sci. Rep.* 6, 22064. <https://doi.org/10.1038/srep22064>

Dugast, M., Toussaint, H., Dousset, C., Benaroch, P., 2005. AP2 Clathrin Adaptor Complex, but Not AP1, Controls the Access of the Major Histocompatibility Complex (MHC) Class II to Endosomes. *J. Biol. Chem.* 280, 19656–19664. <https://doi.org/10.1074/jbc.M501357200>

Dzionic, A., Fuchs, A., Schmidt, P., Cremer, S., Zysk, M., Miltenyi, S., Buck, D.W., Schmitz, J., 2000. BDCA-2, BDCA-3, and BDCA-4: Three Markers for Distinct Subsets of Dendritic Cells in Human Peripheral Blood. *J. Immunol.* 165, 6037–6046. <https://doi.org/10.4049/jimmunol.165.11.6037>

Ewald, S.E., Engel, A., Lee, J., Wang, M., Bogoy, M., Barton, G.M., 2011. Nucleic acid recognition by Toll-like receptors is coupled to stepwise processing by cathepsins and asparagine endopeptidase. *J. Exp. Med.* 208, 643–651. <https://doi.org/10.1084/jem.20100682>

Ewald, S.E., Lee, B.L., Lau, L., Wickliffe, K.E., Shi, G.-P., Chapman, H.A., Barton, G.M., 2008. The ectodomain of Toll-like receptor 9 is cleaved to generate a functional receptor. *Nature* 456, 658–662. <https://doi.org/10.1038/nature07405>

Fairhurst, A., Hwang, S., Wang, A., Tian, X., Boudreaux, C., Zhou, X.J., Casco, J., Li, Q., Connolly, J.E., Wakeland, E.K., 2008. *Yaa* autoimmune phenotypes are conferred by overexpression of TLR7. *Eur. J. Immunol.* 38, 1971–1978. <https://doi.org/10.1002/eji.200838138>

Falschlehner, C., Ganten, T.M., Koschny, R., Schaefer, U., Walczak, H., 2009. TRAIL and Other TRAIL Receptor Agonists as Novel Cancer Therapeutics, in: Grewal, I.S. (Ed.), *Therapeutic Targets of the TNF Superfamily, Advances in Experimental Medicine and Biology*. Springer New York, New York, NY, pp. 195–206. [https://doi.org/10.1007/978-0-387-89520-8\\_14](https://doi.org/10.1007/978-0-387-89520-8_14)

Feske, S., Picard, C., Fischer, A., 2010. Immunodeficiency due to mutations in ORAI1 and STIM1. *Clin. Immunol.* 135, 169–182. <https://doi.org/10.1016/j.clim.2010.01.011>

Frakes, A.E., Dillin, A., 2017. The UPR ER: Sensor and Coordinator of Organismal Homeostasis. *Mol. Cell* 66, 761–771. <https://doi.org/10.1016/j.molcel.2017.05.031>

Fukui, R., Saitoh, S., Matsumoto, F., Kozuka-Hata, H., Oyama, M., Tabeta, K., Beutler, B., Miyake, K., 2009. Unc93B1 biases Toll-like receptor responses to nucleic acid in dendritic cells toward DNA- but against RNA-sensing. *J. Exp. Med.* 206, 1339–1350. <https://doi.org/10.1084/jem.20082316>

Fukui, R., Saitoh, S.-I., Kanno, A., Onji, Masahiro, Shibata, T., Ito, A., Onji, Morikazu, Matsumoto, M., Akira, S., Yoshida, N., Miyake, K., 2011. Unc93B1 Restricts Systemic Lethal Inflammation by Orchestrating Toll-like Receptor 7 and 9 Trafficking. *Immunity* 35, 69–81. <https://doi.org/10.1016/j.immuni.2011.05.010>

Garcia-Cattaneo, A., Gobert, F.-X., Müller, M., Toscano, F., Flores, M., Lescure, A., Del Nery, E., Benaroch, P., 2012. Cleavage of Toll-like receptor 3 by cathepsins B and H is essential for signaling. *Proc. Natl. Acad. Sci.* 109, 9053–9058. <https://doi.org/10.1073/pnas.1115091109>

Gardner, B.M., Walter, P., 2011. Unfolded Proteins Are Ire1-Activating Ligands That Directly Induce the Unfolded Protein Response. *Science* 333, 1891–1894. <https://doi.org/10.1126/science.1209126>

Gay, N.J., Keith, F.J., 1991. Drosophila Toll and IL-1 receptor. *Nature* 351, 355–356. <https://doi.org/10.1038/351355b0>

Geissmann, F., Jung, S., Littman, D.R., 2003. Blood Monocytes Consist of Two Principal Subsets with Distinct Migratory Properties. *Immunity* 19, 71–82. [https://doi.org/10.1016/S1074-7613\(03\)00174-2](https://doi.org/10.1016/S1074-7613(03)00174-2)

Geissmann, F., Manz, M.G., Jung, S., Sieweke, M.H., Merad, M., Ley, K., 2010. Development of Monocytes, Macrophages, and Dendritic Cells. *Science* 327, 656–661. <https://doi.org/10.1126/science.1178331>

Gentili, M., Liu, B., Papanastasiou, M., Dele-Oni, D., Schwartz, M.A., Carlson, R.J., Al'Khafaji, A.M., Krug, K., Brown, A., Doench, J.G., Carr, S.A., Hacohen, N., 2023. ESCRT-dependent STING degradation inhibits steady-state and cGAMP-induced signalling. *Nat. Commun.* 14, 611. <https://doi.org/10.1038/s41467-023-36132-9>

Gros, M., Segura, E., Rookhuizen, D.C., Baudon, B., Heurtebise-Chrétien, S., Burgdorf, N., Maurin, M., Kapp, E.A., Simpson, R.J., Kozik, P., Villadangos, J.A., Bertrand, M.J.M., Burbage, M., Amigorena, S., 2022. Endocytic membrane repair by ESCRT-III controls antigen export to the cytosol during antigen cross-presentation. *Cell Rep.* 40, 111205. <https://doi.org/10.1016/j.celrep.2022.111205>

Grotzke, J.E., Cresswell, P., 2015. Are ERAD components involved in cross-presentation? *Mol. Immunol.* 68, 112–115. <https://doi.org/10.1016/j.molimm.2015.05.002>



Grotzke, J.E., Kozik, P., Morel, J.-D., Impens, F., Pietrosevoli, N., Cresswell, P., Amigorena, S., Demangel, C., 2017. Sec61 blockade by mycolactone inhibits antigen cross-presentation independently of endosome-to-cytosol export. *Proc. Natl. Acad. Sci.* 114. <https://doi.org/10.1073/pnas.1705242114>

Guermónprez, P., Saveanu, L., Kleijmeer, M., Davoust, J., van Endert, P., Amigorena, S., 2003a. ER-phagosome fusion defines an MHC class I cross-presentation compartment in dendritic cells. *Nature* 425, 397–402. <https://doi.org/10.1038/nature01911>

Guermónprez, P., Saveanu, L., Kleijmeer, M., Davoust, J., van Endert, P., Amigorena, S., 2003b. ER-phagosome fusion defines an MHC class I cross-presentation compartment in dendritic cells. *Nature* 425, 397–402. <https://doi.org/10.1038/nature01911>

Gupta, S., Deepti, A., Deegan, S., Lisbona, F., Hetz, C., Samali, A., 2010. HSP72 Protects Cells from ER Stress-induced Apoptosis via Enhancement of IRE1 $\alpha$ -XBP1 Signaling through a Physical Interaction. *PLoS Biol.* 8, e1000410. <https://doi.org/10.1371/journal.pbio.1000410>

Guttman, O., Le Thomas, A., Marsters, S., Lawrence, D.A., Gutgesell, L., Zuazo-Gaztelu, I., Harnoss, J.M., Haag, S.M., Murthy, A., Strasser, G., Modrusan, Z., Wu, T., Mellman, I., Ashkenazi, A., 2022. Antigen-derived peptides engage the ER stress sensor IRE1 $\alpha$  to curb dendritic cell cross-presentation. *J. Cell Biol.* 221, e202111068. <https://doi.org/10.1083/jcb.202111068>

Harding, H.P., Novoa, I., Zhang, Y., Zeng, H., Wek, R., Schapira, M., Ron, D., 2000. Regulated Translation Initiation Controls Stress-Induced Gene Expression in Mammalian Cells. *Mol. Cell* 6, 1099–1108. [https://doi.org/10.1016/S1097-2765\(00\)00108-8](https://doi.org/10.1016/S1097-2765(00)00108-8)

Harding, H.P., Zhang, Y., Ron, D., 1999. Protein translation and folding are coupled by an endoplasmic-reticulum-resident kinase. *Nature* 397, 271–274. <https://doi.org/10.1038/16729>

Hattori, A., Goto, Y., Tsujimoto, M., 2012. Exon 10 Coding Sequence Is Important for Endoplasmic Reticulum Retention of Endoplasmic Reticulum Aminopeptidase 1. *Biol. Pharm. Bull.* 35, 601–605. <https://doi.org/10.1248/bpb.35.601>

Haze, K., Yoshida, H., Yanagi, H., Yura, T., Mori, K., 1999. Mammalian Transcription Factor ATF6 Is Synthesized as a Transmembrane Protein and Activated by Proteolysis in Response to Endoplasmic Reticulum Stress. *Mol. Biol. Cell* 10, 3787–3799. <https://doi.org/10.1091/mbc.10.11.3787>

He, Z., Ye, S., Xing, Y., Jiu, Y., Zhong, J., 2021. UNC93B1 curbs cytosolic DNA signaling by promoting STING degradation. *Eur. J. Immunol.* 51, 1672–1685. <https://doi.org/10.1002/eji.202048901>

Heil, F., Hemmi, H., Hochrein, H., Ampenberger, F., Kirschning, C., Akira, S., Lipford, G., Wagner, H., Bauer, S., 2004. Species-Specific Recognition of Single-Stranded RNA via Toll-like Receptor 7 and 8. *Science* 303, 1526–1529. <https://doi.org/10.1126/science.1093620>

Hemmi, H., Takeuchi, O., Kawai, T., Kaisho, T., Sato, S., Sanjo, H., Matsumoto, M., Hoshino, K., Wagner, H., Takeda, K., Akira, S., 2000. A Toll-like receptor recognizes bacterial DNA. *Nature* 408, 740–745. <https://doi.org/10.1038/35047123>

Henkart, P.A., Catalfamo, M., 2004. CD8+ Effector Cells, in: *Advances in Immunology*. Elsevier, pp. 233–252. [https://doi.org/10.1016/S0065-2776\(04\)83007-4](https://doi.org/10.1016/S0065-2776(04)83007-4)

Hetz, C., Bernasconi, P., Fisher, J., Lee, A.-H., Bassik, M.C., Antonsson, B., Brandt, G.S., Iwakoshi, N.N., Schinzler, A., Glimcher, L.H., Korsmeyer, S.J., 2006. Proapoptotic BAX and BAK Modulate the Unfolded Protein Response by a Direct Interaction with IRE1 $\alpha$ . *Science* 312, 572–576. <https://doi.org/10.1126/science.1123480>

Hetz, C., Chevet, E., Oakes, S.A., 2015. Erratum: Proteostasis control by the unfolded protein response. *Nat. Cell Biol.* 17, 1088–1088. <https://doi.org/10.1038/ncb3221>

Hildner, K., Edelson, B.T., Purtha, W.E., Diamond, M., Matsushita, H., Kohyama, M., Calderon, B., Schraml, B.U., Unanue, E.R., Diamond, M.S., Schreiber, R.D., Murphy, T.L., Murphy, K.M., 2008. *Batf3* Deficiency Reveals a Critical Role for CD8 $\alpha$ <sup>+</sup> Dendritic Cells in Cytotoxic T Cell Immunity. *Science* 322, 1097–1100. <https://doi.org/10.1126/science.1164206>

Hipp, M.M., Shepherd, D., Gileadi, U., Aichinger, M.C., Kessler, B.M., Edelmann, M.J., Essalmani, R., Seidah, N.G., Reis e Sousa, C., Cerundolo, V., 2013. Processing of Human Toll-like Receptor 7 by Furin-like Proprotein Convertases Is Required for Its Accumulation and Activity in Endosomes. *Immunity* 39, 711–721. <https://doi.org/10.1016/j.immuni.2013.09.004>

Hoeffel, G., Wang, Y., Greter, M., See, P., Teo, P., Malleret, B., Leboeuf, M., Low, D., Oller, G., Almeida, F., Choy, S.H.Y., Grisotto, M., Renia, L., Conway, S.J., Stanley, E.R., Chan, J.K.Y., Ng, L.G., Samokhvalov, I.M., Merad, M., Ginhoux, F., 2012. Adult Langerhans cells derive predominantly from embryonic fetal liver monocytes with a minor contribution of yolk sac-derived macrophages. *J. Exp. Med.* 209, 1167–1181. <https://doi.org/10.1084/jem.20120340>

Hollien, J., Lin, J.H., Li, H., Stevens, N., Walter, P., Weissman, J.S., 2009. Regulated Ire1-dependent decay of messenger RNAs in mammalian cells. *J. Cell Biol.* 186, 323–331. <https://doi.org/10.1083/jcb.200903014>

Hollien, J., Weissman, J.S., 2006. Decay of Endoplasmic Reticulum-Localized mRNAs During the Unfolded Protein Response. *Science* 313, 104–107. <https://doi.org/10.1126/science.1129631>

Hopfner, K.-P., Hornung, V., 2020. Molecular mechanisms and cellular functions of cGAS–STING signalling. *Nat. Rev. Mol. Cell Biol.* 21, 501–521. <https://doi.org/10.1038/s41580-020-0244-x>

Hsieh, C.-S., deRoos, P., Honey, K., Beers, C., Rudensky, A.Y., 2002. A Role for Cathepsin L and Cathepsin S in Peptide Generation for MHC Class II Presentation. *J. Immunol.* 168, 2618–2625. <https://doi.org/10.4049/jimmunol.168.6.2618>

Huh, J.-W., Shibata, T., Hwang, M., Kwon, E.-H., Jang, M.S., Fukui, R., Kanno, A., Jung, D.-J., Jang, M.H., Miyake, K., Kim, Y.-M., 2014. UNC93B1 is essential for the plasma membrane localization and signaling of Toll-like receptor 5. *Proc. Natl. Acad. Sci.* 111, 7072–7077. <https://doi.org/10.1073/pnas.1322838111>

Ise, W., Kurosaki, T., 2021. Plasma cell generation during T-cell-dependent immune responses. *Int. Immunol.* 33, 797–801. <https://doi.org/10.1093/intimm/dxab071>

Ishida, H., Asami, J., Zhang, Z., Nishizawa, T., Shigematsu, H., Ohto, U., Shimizu, T., 2021a. Cryo-EM structures of Toll-like receptors in complex with UNC93B1. *Nat. Struct. Mol. Biol.* 28, 173–180. <https://doi.org/10.1038/s41594-020-00542-w>

Ishida, H., Asami, J., Zhang, Z., Nishizawa, T., Shigematsu, H., Ohto, U., Shimizu, T., 2021b. Cryo-EM structures of Toll-like receptors in complex with UNC93B1. *Nat. Struct. Mol. Biol.* 28, 173–180. <https://doi.org/10.1038/s41594-020-00542-w>

Iwakoshi, N.N., Lee, A.-H., Vallabhajosyula, P., Otipoby, K.L., Rajewsky, K., Glimcher, L.H., 2003. Plasma cell differentiation and the unfolded protein response intersect at the transcription factor XBP-1. *Nat. Immunol.* 4, 321–329. <https://doi.org/10.1038/ni907>

Iwawaki, T., Hosoda, A., Okuda, T., Kamigori, Y., Nomura-Furuwatari, C., Kimata, Y., Tsuru, A., Kohno, K., 2001. Translational control by the ER transmembrane kinase/ribonuclease IRE1 under ER stress. *Nat. Cell Biol.* 3, 158–164. <https://doi.org/10.1038/35055065>

Janeway, C.A., Medzhitov, R., 2002. Innate Immune Recognition. *Annu. Rev. Immunol.* 20, 197–216. <https://doi.org/10.1146/annurev.immunol.20.083001.084359>

Janssens, S., Pulendran, B., Lambrecht, B.N., 2014. Emerging functions of the unfolded protein response in immunity. *Nat. Immunol.* 15, 910–919. <https://doi.org/10.1038/ni.2991>

Joffre, O.P., Segura, E., Savina, A., Amigorena, S., 2012. Cross-presentation by dendritic cells. *Nat. Rev. Immunol.* 12, 557–569. <https://doi.org/10.1038/nri3254>

Kagan, J.C., Su, T., Horng, T., Chow, A., Akira, S., Medzhitov, R., 2008. TRAM couples endocytosis of Toll-like receptor 4 to the induction of interferon- $\beta$ . *Nat. Immunol.* 9, 361–368. <https://doi.org/10.1038/ni1569>

Kalb, M.L., Glaser, A., Stary, G., Koszik, F., Stingl, G., 2012. TRAIL+ Human Plasmacytoid Dendritic Cells Kill Tumor Cells In Vitro: Mechanisms of Imiquimod- and IFN- $\alpha$ -Mediated Antitumor Reactivity. *J. Immunol.* 188, 1583–1591. <https://doi.org/10.4049/jimmunol.1102437>

Karagöz, G.E., Acosta-Alvear, D., Nguyen, H.T., Lee, C.P., Chu, F., Walter, P., 2017. An unfolded protein-induced conformational switch activates mammalian IRE1. *eLife* 6, e30700. <https://doi.org/10.7554/eLife.30700>

Kashuba, V.I., Protopopov, A.I., Kvasha, S.M., Gizatullin, R.Z., Wahlestedt, C., Kisselev, L.L., Klein, G., Zabarovsky, E.R., 2002. hUNC93B1: a novel human gene representing a new gene family and encoding an unc-93-like protein. *Gene* 283, 209–217. [https://doi.org/10.1016/S0378-1119\(01\)00856-3](https://doi.org/10.1016/S0378-1119(01)00856-3)

Kiener, S., Ribí, C., Keller, I., Chizzolini, C., Trendelenburg, M., Huynh-Do, U., von Kempis, J., on behalf of Swiss SLE Cohort Study (SSCS), Leeb, T., 2021. Variants

Affecting the C-Terminal Tail of UNC93B1 Are Not a Common Risk Factor for Systemic Lupus Erythematosus. *Genes* 12, 1268. <https://doi.org/10.3390/genes12081268>

Kim, Y.-M., Brinkmann, M.M., Paquet, M.-E., Ploegh, H.L., 2008. UNC93B1 delivers nucleotide-sensing toll-like receptors to endolysosomes. *Nature* 452, 234–238. <https://doi.org/10.1038/nature06726>

Kirkling, M.E., Cytlak, U., Lau, C.M., Lewis, K.L., Resteu, A., Khodadadi-Jamayran, A., Siebel, C.W., Salmon, H., Merad, M., Tsirigos, A., Collin, M., Bigley, V., Reizis, B., 2018. Notch Signaling Facilitates In Vitro Generation of Cross-Presenting Classical Dendritic Cells. *Cell Rep.* 23, 3658-3672.e6. <https://doi.org/10.1016/j.celrep.2018.05.068>

Koblansky, A.A., Jankovic, D., Oh, H., Hieny, S., Sungnak, W., Mathur, R., Hayden, M.S., Akira, S., Sher, A., Ghosh, S., 2013. Recognition of Profilin by Toll-like Receptor 12 Is Critical for Host Resistance to *Toxoplasma gondii*. *Immunity* 38, 119–130. <https://doi.org/10.1016/j.immuni.2012.09.016>

Koehn, J., Huesken, D., Jaritz, M., Rot, A., Zurini, M., Dwertmann, A., Beutler, B., Korthäuer, U., 2007. Assessing the function of human UNC-93B in Toll-like receptor signaling and major histocompatibility complex II response. *Hum. Immunol.* 68, 871–878. <https://doi.org/10.1016/j.humimm.2007.07.007>

Kovacsovics-Bankowski, M., Clark, K., Benacerraf, B., Rock, K.L., 1993. Efficient major histocompatibility complex class I presentation of exogenous antigen upon phagocytosis by macrophages. *Proc. Natl. Acad. Sci.* 90, 4942–4946. <https://doi.org/10.1073/pnas.90.11.4942>

Kovacsovics-Bankowski, M., Rock, K.L., 1995. A Phagosome-to-Cytosol Pathway for Exogenous Antigens Presented on MHC Class I Molecules. *Science* 267, 243–246. <https://doi.org/10.1126/science.7809629>

Krug, A., French, A.R., Barchet, W., Fischer, J.A.A., Dzionek, A., Pingel, J.T., Orihuela, M.M., Akira, S., Yokoyama, W.M., Colonna, M., 2004a. TLR9-Dependent Recognition of MCMV by IPC and DC Generates Coordinated Cytokine Responses that Activate Antiviral NK Cell Function. *Immunity* 21, 107–119. <https://doi.org/10.1016/j.immuni.2004.06.007>

Krug, A., Luker, G.D., Barchet, W., Leib, D.A., Akira, S., Colonna, M., 2004b. Herpes simplex virus type 1 activates murine natural interferon-producing cells through toll-like receptor 9. *Blood* 103, 1433–1437. <https://doi.org/10.1182/blood-2003-08-2674>

Lafaille, F.G., Pessach, I.M., Zhang, S.-Y., Ciancanelli, M.J., Herman, M., Abhyankar, A., Ying, S.-W., Keros, S., Goldstein, P.A., Mostoslavsky, G., Ordovas-Montanes, J., Jouanguy, E., Plancoulaine, S., Tu, E., Elkabetz, Y., Al-Muhsen, S., Tardieu, M., Schlaeger, T.M., Daley, G.Q., Abel, L., Casanova, J.-L., Studer, L., Notarangelo, L.D., 2012. Impaired intrinsic immunity to HSV-1 in human iPSC-derived TLR3-deficient CNS cells. *Nature* 491, 769–773. <https://doi.org/10.1038/nature11583>

Lauterbach, H., Bathke, B., Gilles, S., Traidl-Hoffmann, C., Lubber, C.A., Fejer, G., Freudenberg, M.A., Davey, G.M., Vremec, D., Kallies, A., Wu, L., Shortman, K., Chaplin, P., Suter, M., O’Keeffe, M., Hochrein, H., 2010. Mouse CD8 $\alpha$ <sup>+</sup> DCs and human BDCA3<sup>+</sup> DCs are major producers of IFN- $\lambda$  in response to poly IC. *J. Exp. Med.* 207, 2703–2717. <https://doi.org/10.1084/jem.20092720>

Le Reste, P.J., Pineau, R., Voutetakis, K., Samal, J., Jégou, G., Lhomond, S., Gorman, A.M., Samali, A., Patterson, J.B., Zeng, Q., Pandit, A., Aubry, M., Soriano, N., Etcheverry, A., Chatziioannou, A., Mosser, J., Avril, T., Chevet, E., 2020. Local intracerebral inhibition of IRE1 by MKC8866 sensitizes glioblastoma to irradiation/chemotherapy in vivo. *Cancer Lett.* 494, 73–83. <https://doi.org/10.1016/j.canlet.2020.08.028>

Lee, B.L., Moon, J.E., Shu, J.H., Yuan, L., Newman, Z.R., Schekman, R., Barton, G.M., 2013. UNC93B1 mediates differential trafficking of endosomal TLRs. *eLife* 2, e00291. <https://doi.org/10.7554/eLife.00291>

Lemaitre, B., Nicolas, E., Michaut, L., Reichhart, J.-M., Hoffmann, J.A., 1996. The Dorsoventral Regulatory Gene *Cassette* *spätzle*/Toll/cactus Controls the Potent Antifungal Response in *Drosophila* Adults. *Cell* 86, 973–983. [https://doi.org/10.1016/S0092-8674\(00\)80172-5](https://doi.org/10.1016/S0092-8674(00)80172-5)

Leuchowius, K., Weibrecht, I., Söderberg, O., 2011. In Situ Proximity Ligation Assay for Microscopy and Flow Cytometry. *Curr. Protoc. Cytom.* 56. <https://doi.org/10.1002/0471142956.cy0936s56>

Lhomond, S., Avril, T., Dejeans, N., Voutetakis, K., Doultinos, D., McMahon, M., Pineau, R., Obacz, J., Papadodima, O., Jouan, F., Bourien, H., Logotheti, M., Jégou, G., Pallares-Lupon, N., Schmit, K., Le Reste, P., Etcheverry, A., Mosser, J., Barroso, K., Vauléon, E., Maurel, M., Samali, A., Patterson, J.B., Pluquet, O., Hetz, C., Quillien,

V., Chatziioannou, A., Chevet, E., 2018. Dual IRE 1 RN ase functions dictate glioblastoma development. *EMBO Mol. Med.* 10. <https://doi.org/10.15252/emmm.201707929>

Li, X., Sun, S., Appathurai, S., Sundaram, A., Plumb, R., Mariappan, M., 2020. A Molecular Mechanism for Turning Off IRE1 $\alpha$  Signaling during Endoplasmic Reticulum Stress. *Cell Rep.* 33, 108563. <https://doi.org/10.1016/j.celrep.2020.108563>

Lin, S.-C., Lo, Y.-C., Wu, H., 2010. Helical assembly in the MyD88–IRAK4–IRAK2 complex in TLR/IL-1R signalling. *Nature* 465, 885–890. <https://doi.org/10.1038/nature09121>

Liu, S., Cai, X., Wu, J., Cong, Q., Chen, X., Li, T., Du, F., Ren, J., Wu, Y.-T., Grishin, N.V., Chen, Z.J., 2015. Phosphorylation of innate immune adaptor proteins MAVS, STING, and TRIF induces IRF3 activation. *Science* 347, aaa2630. <https://doi.org/10.1126/science.aaa2630>

Liu, Y., Jesus, A.A., Marrero, B., Yang, D., Ramsey, S.E., Montealegre Sanchez, G.A., Tenbrock, K., Wittkowski, H., Jones, O.Y., Kuehn, H.S., Lee, C.-C.R., DiMattia, M.A., Cowen, E.W., Gonzalez, B., Palmer, I., DiGiovanna, J.J., Biancotto, A., Kim, H., Tsai, W.L., Trier, A.M., Huang, Y., Stone, D.L., Hill, S., Kim, H.J., St. Hilaire, C., Gurprasad, S., Plass, N., Chapelle, D., Horkayne-Szakaly, I., Foell, D., Barysenka, A., Candotti, F., Holland, S.M., Hughes, J.D., Mehmet, H., Issekutz, A.C., Raffeld, M., McElwee, J., Fontana, J.R., Minniti, C.P., Moir, S., Kastner, D.L., Gadina, M., Steven, A.C., Wingfield, P.T., Brooks, S.R., Rosenzweig, S.D., Fleisher, T.A., Deng, Z., Boehm, M., Paller, A.S., Goldbach-Mansky, R., 2014. Activated STING in a Vascular and Pulmonary Syndrome. *N. Engl. J. Med.* 371, 507–518. <https://doi.org/10.1056/NEJMoa1312625>

Liu, Y.-P., Zeng, L., Tian, A., Bomkamp, A., Rivera, D., Gutman, D., Barber, G.N., Olson, J.K., Smith, J.A., 2012. Endoplasmic Reticulum Stress Regulates the Innate Immunity Critical Transcription Factor IRF3. *J. Immunol.* 189, 4630–4639. <https://doi.org/10.4049/jimmunol.1102737>

Lund, J., Sato, A., Akira, S., Medzhitov, R., Iwasaki, A., 2003. Toll-like Receptor 9–mediated Recognition of Herpes Simplex Virus-2 by Plasmacytoid Dendritic Cells. *J. Exp. Med.* 198, 513–520. <https://doi.org/10.1084/jem.20030162>

Machy, P., Serre, K., Leserman, L., 2000. Class I-restricted presentation of exogenous antigen acquired by Fc $\gamma$  receptor-mediated endocytosis is regulated in dendritic cells.

Eur. J. Immunol. 30, 848–857. [https://doi.org/10.1002/1521-4141\(200003\)30:3<848::AID-IMMU848>3.0.CO;2-Q](https://doi.org/10.1002/1521-4141(200003)30:3<848::AID-IMMU848>3.0.CO;2-Q)

Mahadevan, N.R., Anufreichik, V., Rodvold, J.J., Chiu, K.T., Sepulveda, H., Zanetti, M., 2012. Cell-Extrinsic Effects of Tumor ER Stress Imprint Myeloid Dendritic Cells and Impair CD8+ T Cell Priming. *PLoS ONE* 7, e51845. <https://doi.org/10.1371/journal.pone.0051845>

Mahadevan, N.R., Rodvold, J., Sepulveda, H., Rossi, S., Drew, A.F., Zanetti, M., 2011. Transmission of endoplasmic reticulum stress and pro-inflammation from tumor cells to myeloid cells. *Proc. Natl. Acad. Sci.* 108, 6561–6566. <https://doi.org/10.1073/pnas.1008942108>

Majer, O., Liu, B., Kreuk, L.S.M., Krogan, N., Barton, G.M., 2019a. UNC93B1 recruits syntenin-1 to dampen TLR7 signalling and prevent autoimmunity. *Nature* 575, 366–370. <https://doi.org/10.1038/s41586-019-1612-6>

Majer, O., Liu, B., Woo, B.J., Kreuk, L.S.M., Van Dis, E., Barton, G.M., 2019b. Release from UNC93B1 reinforces the compartmentalized activation of select TLRs. *Nature* 575, 371–374. <https://doi.org/10.1038/s41586-019-1611-7>

Manoury, B., Hewitt, E.W., Morrice, N., Dando, P.M., Barrett, A.J., Watts, C., 1998. An asparaginyl endopeptidase processes a microbial antigen for class II MHC presentation. *Nature* 396, 695–699. <https://doi.org/10.1038/25379>

Mantel, I., Sadiq, B.A., Blander, J.M., 2022. Spotlight on TAP and its vital role in antigen presentation and cross-presentation. *Mol. Immunol.* 142, 105–119. <https://doi.org/10.1016/j.molimm.2021.12.013>

Marcu, M.G., Doyle, M., Bertolotti, A., Ron, D., Hendershot, L., Neckers, L., 2002. Heat Shock Protein 90 Modulates the Unfolded Protein Response by Stabilizing IRE1 $\alpha$ . *Mol. Cell. Biol.* 22, 8506–8513. <https://doi.org/10.1128/MCB.22.24.8506-8513.2002>

Martinon, F., Chen, X., Lee, A.-H., Glimcher, L.H., 2010. TLR activation of the transcription factor XBP1 regulates innate immune responses in macrophages. *Nat. Immunol.* 11, 411–418. <https://doi.org/10.1038/ni.1857>

Martins, A.S., Alves, I., Helguero, L., Domingues, M.R., Neves, B.M., 2016. The Unfolded Protein Response in Homeostasis and Modulation of Mammalian Immune



Maschalidi, S., Nunes-Hasler, P., Nascimento, C.R., Sallent, I., Lannoy, V., Garfa-Traore, M., Cagnard, N., Sepulveda, F.E., Vargas, P., Lennon-Duménil, A.-M., van Endert, P., Capiod, T., Demaurex, N., Darrasse-Jèze, G., Manoury, B., 2017. UNC93B1 interacts with the calcium sensor STIM1 for efficient antigen cross-presentation in dendritic cells. *Nat. Commun.* 8, 1640. <https://doi.org/10.1038/s41467-017-01601-5>

Medel, B., Costoya, C., Fernandez, D., Pereda, C., Lladser, A., Sauma, D., Pacheco, R., Iwawaki, T., Salazar-Onfray, F., Osorio, F., 2019. IRE1 $\alpha$  Activation in Bone Marrow-Derived Dendritic Cells Modulates Innate Recognition of Melanoma Cells and Favors CD8<sup>+</sup> T Cell Priming. *Front. Immunol.* 9, 3050. <https://doi.org/10.3389/fimmu.2018.03050>

Medvedev, A.E., Piao, W., Shoenfelt, J., Rhee, S.H., Chen, H., Basu, S., Wahl, L.M., Fenton, M.J., Vogel, S.N., 2007. Role of TLR4 Tyrosine Phosphorylation in Signal Transduction and Endotoxin Tolerance. *J. Biol. Chem.* 282, 16042–16053. <https://doi.org/10.1074/jbc.M606781200>

Medzhitov, R., Janeway, C.A., 1997. Innate immunity: impact on the adaptive immune response. *Curr. Opin. Immunol.* 9, 4–9. [https://doi.org/10.1016/S0952-7915\(97\)80152-5](https://doi.org/10.1016/S0952-7915(97)80152-5)

Medzhitov, R., Preston-Hurlburt, P., Janeway, C.A., 1997. A human homologue of the *Drosophila* Toll protein signals activation of adaptive immunity. *Nature* 388, 394–397. <https://doi.org/10.1038/41131>

Meissner, T.B., Li, A., Biswas, A., Lee, K.-H., Liu, Y.-J., Bayir, E., Iliopoulos, D., van den Elsen, P.J., Kobayashi, K.S., 2010. NLR family member NLRC5 is a transcriptional regulator of MHC class I genes. *Proc. Natl. Acad. Sci.* 107, 13794–13799. <https://doi.org/10.1073/pnas.1008684107>

Ménager, J., Ebstein, F., Oger, R., Hulin, P., Nedellec, S., Duverger, E., Lehmann, A., Kloetzel, P.-M., Jotereau, F., Guilloux, Y., 2014. Cross-Presentation of Synthetic Long Peptides by Human Dendritic Cells: A Process Dependent on ERAD Component p97/VCP but Not sec61 and/or Derlin-1. *PLoS ONE* 9, e89897. <https://doi.org/10.1371/journal.pone.0089897>

Mendes, A., Gigan, J.P., Rodriguez Rodrigues, C., Choteau, S.A., Sanseau, D., Barros, D., Almeida, C., Camosseto, V., Chasson, L., Paton, A.W., Paton, J.C., Argüello, R.J., Lennon-Duménil, A.-M., Gatti, E., Pierre, P., 2021. Proteostasis in dendritic cells is controlled by the PERK signaling axis independently of ATF4. *Life Sci. Alliance* 4, e202000865. <https://doi.org/10.26508/lsa.202000865>

Menges, M., Rößner, S., Voigtländer, C., Schindler, H., Kukutsch, N.A., Bogdan, C., Erb, K., Schuler, G., Lutz, M.B., 2002. Repetitive Injections of Dendritic Cells Matured with Tumor Necrosis Factor  $\alpha$  Induce Antigen-specific Protection of Mice from Autoimmunity. *J. Exp. Med.* 195, 15–22. <https://doi.org/10.1084/jem.20011341>

Misawa, T., Takahama, M., Kozaki, T., Lee, H., Zou, J., Saitoh, T., Akira, S., 2013. Microtubule-driven spatial arrangement of mitochondria promotes activation of the NLRP3 inflammasome. *Nat. Immunol.* 14, 454–460. <https://doi.org/10.1038/ni.2550>

Moresco, E.M.Y., LaVine, D., Beutler, B., 2011. Toll-like receptors. *Curr. Biol.* 21, R488–R493. <https://doi.org/10.1016/j.cub.2011.05.039>

Nakagawa, T., Roth, W., Wong, P., Nelson, A., Farr, A., Deussing, J., Villadangos, J.A., Ploegh, H., Peters, C., Rudensky, A.Y., 1998. Cathepsin L: Critical Role in li Degradation and CD4 T Cell Selection in the Thymus. *Science* 280, 450–453. <https://doi.org/10.1126/science.280.5362.450>

Neefjes, J., Jongstra, M.L.M., Paul, P., Bakke, O., 2011. Towards a systems understanding of MHC class I and MHC class II antigen presentation. *Nat. Rev. Immunol.* 11, 823–836. <https://doi.org/10.1038/nri3084>

Norian, L.A., Rodriguez, P.C., O'Mara, L.A., Zabaleta, J., Ochoa, A.C., Cella, M., Allen, P.M., 2009. Tumor-Infiltrating Regulatory Dendritic Cells Inhibit CD8+ T Cell Function via L-Arginine Metabolism. *Cancer Res.* 69, 3086–3094. <https://doi.org/10.1158/0008-5472.CAN-08-2826>

Nunes, P., Cornut, D., Bochet, V., Hasler, U., Oh-Hora, M., Waldburger, J.-M., Demarex, N., 2012. STIM1 Juxtaposes ER to Phagosomes, Generating Ca<sup>2+</sup> Hotspots that Boost Phagocytosis. *Curr. Biol.* 22, 1990–1997. <https://doi.org/10.1016/j.cub.2012.08.049>

Nunes-Hasler, P., Maschalidi, S., Lippens, C., Castelbou, C., Bouvet, S., Guido, D., Bermont, F., Bassoy, E.Y., Page, N., Merkle, D., Hugues, S., Martinvalet, D., Manoury, B., Demarex, N., 2017. STIM1 promotes migration, phagosomal maturation and

antigen cross-presentation in dendritic cells. *Nat. Commun.* 8, 1852. <https://doi.org/10.1038/s41467-017-01600-6>

Oikawa, D., Kimata, Y., Kohno, K., Iwawaki, T., 2009. Activation of mammalian IRE1 $\alpha$  upon ER stress depends on dissociation of BiP rather than on direct interaction with unfolded proteins. *Exp. Cell Res.* 315, 2496–2504. <https://doi.org/10.1016/j.yexcr.2009.06.009>

Onoé, K., Yanagawa, Y., Minami, K., Iijima, N., Iwabuchi, K., 2007. Th1 or Th2 balance regulated by interaction between dendritic cells and NKT cells. *Immunol. Res.* 38, 319–332. <https://doi.org/10.1007/s12026-007-0011-5>

Osorio, F., Tavernier, S.J., Hoffmann, E., Saeys, Y., Martens, L., Vettters, J., Delrue, I., De Rycke, R., Parthoens, E., Pouliot, P., Iwawaki, T., Janssens, S., Lambrecht, B.N., 2014. The unfolded-protein-response sensor IRE-1 $\alpha$  regulates the function of CD8 $\alpha$ + dendritic cells. *Nat. Immunol.* 15, 248–257. <https://doi.org/10.1038/ni.2808>

Ostrand-Rosenberg, S., Sinha, P., 2009. Myeloid-Derived Suppressor Cells: Linking Inflammation and Cancer. *J. Immunol.* 182, 4499–4506. <https://doi.org/10.4049/jimmunol.0802740>

Papp, K.A., Blauvelt, A., Bukhalo, M., Gooderham, M., Krueger, J.G., Lacour, J.-P., Menter, A., Philipp, S., Sofen, H., Tying, S., Berner, B.R., Visvanathan, S., Pamulapati, C., Bennett, N., Flack, M., Scholl, P., Padula, S.J., 2017. Risankizumab versus Ustekinumab for Moderate-to-Severe Plaque Psoriasis. *N. Engl. J. Med.* 376, 1551–1560. <https://doi.org/10.1056/NEJMoa1607017>

Park, B., Brinkmann, M.M., Spooner, E., Lee, C.C., Kim, Y.-M., Ploegh, H.L., 2008. Proteolytic cleavage in an endolysosomal compartment is required for activation of Toll-like receptor 9. *Nat. Immunol.* 9, 1407–1414. <https://doi.org/10.1038/ni.1669>

Park, S.-M., Kang, T.-I., So, J.-S., 2021. Roles of XBP1s in Transcriptional Regulation of Target Genes. *Biomedicines* 9, 791. <https://doi.org/10.3390/biomedicines9070791>

Pelka, K., Bertheloot, D., Reimer, E., Phulphagar, K., Schmidt, S.V., Christ, A., Stahl, R., Watson, N., Miyake, K., Hacohen, N., Haas, A., Brinkmann, M.M., Marshak-Rothstein, A., Meissner, F., Latz, E., 2018. The Chaperone UNC93B1 Regulates Toll-like Receptor Stability Independently of Endosomal TLR Transport. *Immunity* 48, 911–922.e7. <https://doi.org/10.1016/j.immuni.2018.04.011>

Pfeifer, J.D., Wick, M.J., Roberts, R.L., Findlay, K., Normark, S.J., Harding, C.V., 1993. Phagocytic processing of bacterial antigens for class I MHC presentation to T cells. *Nature* 361, 359–362. <https://doi.org/10.1038/361359a0>

Pifer, R., Benson, A., Sturge, C.R., Yarovinsky, F., 2011. UNC93B1 Is Essential for TLR11 Activation and IL-12-dependent Host Resistance to *Toxoplasma gondii*. *J. Biol. Chem.* 286, 3307–3314. <https://doi.org/10.1074/jbc.M110.171025>

Pincus, D., Chevalier, M.W., Aragón, T., van Anken, E., Vidal, S.E., El-Samad, H., Walter, P., 2010. BiP Binding to the ER-Stress Sensor Ire1 Tunes the Homeostatic Behavior of the Unfolded Protein Response. *PLoS Biol.* 8, e1000415. <https://doi.org/10.1371/journal.pbio.1000415>

Plumb, R., Zhang, Z.-R., Appathurai, S., Mariappan, M., 2015. A functional link between the co-translational protein translocation pathway and the UPR. *eLife* 4, e07426. <https://doi.org/10.7554/eLife.07426>

Pokatayev, V., Yang, K., Tu, X., Dobbs, N., Wu, J., Kalb, R.G., Yan, N., 2020. Homeostatic regulation of STING protein at the resting state by stabilizer TOLLIP. *Nat. Immunol.* 21, 158–167. <https://doi.org/10.1038/s41590-019-0569-9>

Poltorak, A., He, X., Smirnova, I., Liu, M.-Y., Huffel, C.V., Du, X., Birdwell, D., Alejos, E., Silva, M., Galanos, C., Freudenberg, M., Ricciardi-Castagnoli, P., Layton, B., Beutler, B., 1998. Defective LPS Signaling in C3H/HeJ and C57BL/10ScCr Mice: Mutations in *Tlr4* Gene. *Science* 282, 2085–2088. <https://doi.org/10.1126/science.282.5396.2085>

Poncet, A.F., Bosteels, V., Hoffmann, E., Chehade, S., Rennen, S., Huot, L., Peucelle, V., Maréchal, S., Khalife, J., Blanchard, N., Janssens, S., Marion, S., 2021. The UPR sensor IRE1 $\alpha$  promotes dendritic cell responses to control *Toxoplasma gondii* infection. *EMBO Rep.* 22. <https://doi.org/10.15252/embr.201949617>

Rapoport, T.A., 2007. Protein translocation across the eukaryotic endoplasmic reticulum and bacterial plasma membranes. *Nature* 450, 663–669. <https://doi.org/10.1038/nature06384>

Raposo, G., van Santen, H.M., Leijendekker, R., Geuze, H.J., Ploegh, H.L., 1995. Misfolded major histocompatibility complex class I molecules accumulate in an expanded ER-Golgi intermediate compartment. *J. Cell Biol.* 131, 1403–1419. <https://doi.org/10.1083/jcb.131.6.1403>

Reith, W., LeibundGut-Landmann, S., Waldburger, J.-M., 2005. Regulation of MHC class II gene expression by the class II transactivator. *Nat. Rev. Immunol.* 5, 793–806. <https://doi.org/10.1038/nri1708>

Riese, R.J., Wolf, P.R., Brömme, D., Natkin, L.R., Villadangos, J.A., Ploegh, H.L., Chapman, H.A., 1996. Essential Role for Cathepsin S in MHC Class II–Associated Invariant Chain Processing and Peptide Loading. *Immunity* 4, 357–366. [https://doi.org/10.1016/S1074-7613\(00\)80249-6](https://doi.org/10.1016/S1074-7613(00)80249-6)

Robbins, G.R., Truax, A.D., Davis, B.K., Zhang, L., Brickey, W.J., Ting, J.P.-Y., 2012. Regulation of Class I Major Histocompatibility Complex (MHC) by Nucleotide-binding Domain, Leucine-rich Repeat-containing (NLR) Proteins. *J. Biol. Chem.* 287, 24294–24303. <https://doi.org/10.1074/jbc.M112.364604>

Robbins, S.H., Walzer, T., Dembélé, D., Thibault, C., Defays, A., Bessou, G., Xu, H., Vivier, E., Sellars, M., Pierre, P., Sharp, F.R., Chan, S., Kastner, P., Dalod, M., 2008. Novel insights into the relationships between dendritic cell subsets in human and mouse revealed by genome-wide expression profiling. *Genome Biol.* 9, R17. <https://doi.org/10.1186/gb-2008-9-1-r17>

Roche, P.A., Furuta, K., 2015. The ins and outs of MHC class II-mediated antigen processing and presentation. *Nat. Rev. Immunol.* 15, 203–216. <https://doi.org/10.1038/nri3818>

Romagnani, S., 1995. Biology of human TH1 and TH2 cells. *J. Clin. Immunol.* 15, 121–129. <https://doi.org/10.1007/BF01543103>

Romani, N., Koide, S., Crowley, M., Witmer-Pack, M., Livingstone, A.M., Fathman, C.G., Inaba, K., Steinman, R.M., 1989. Presentation of exogenous protein antigens by dendritic cells to T cell clones. Intact protein is presented best by immature, epidermal Langerhans cells. *J. Exp. Med.* 169, 1169–1178. <https://doi.org/10.1084/jem.169.3.1169>

Sallusto, F., Cella, M., Danieli, C., Lanzavecchia, A., 1995. Dendritic cells use macropinocytosis and the mannose receptor to concentrate macromolecules in the major histocompatibility complex class II compartment: downregulation by cytokines and bacterial products. *J. Exp. Med.* 182, 389–400. <https://doi.org/10.1084/jem.182.2.389>

Sallusto, F., Lanzavecchia, A., 1994. Efficient presentation of soluble antigen by cultured human dendritic cells is maintained by granulocyte/macrophage colony-stimulating factor plus interleukin 4 and downregulated by tumor necrosis factor alpha. *J. Exp. Med.* 179, 1109–1118. <https://doi.org/10.1084/jem.179.4.1109>

Sallusto, F., Palermo, B., Lenig, D., Miettinen, M., Matikainen, S., Julkunen, I., Forster, R., Burgstahler, R., Lipp, M., Lanzavecchia, A., 1999. Distinct patterns and kinetics of chemokine production regulate dendritic cell function. *Eur. J. Immunol.* 29, 1617–1625. [https://doi.org/10.1002/\(SICI\)1521-4141\(199905\)29:05<1617::AID-IMMU1617>3.0.CO;2-3](https://doi.org/10.1002/(SICI)1521-4141(199905)29:05<1617::AID-IMMU1617>3.0.CO;2-3)

Samakai, E., Hooper, R., Soboloff, J., 2013. The critical role of STIM1-dependent Ca<sup>2+</sup> signalling during T-cell development and activation. *Int. J. Biochem. Cell Biol.* 45, 2491–2495. <https://doi.org/10.1016/j.biocel.2013.07.014>

Sanarico, N., Ciaramella, A., Sacchi, A., Bernasconi, D., Bossù, P., Mariani, F., Colizzi, V., Vendetti, S., 2006. Human monocyte-derived dendritic cells differentiated in the presence of IL-2 produce proinflammatory cytokines and prime Th1 immune response. *J. Leukoc. Biol.* 80, 555–562. <https://doi.org/10.1189/jlb.1105690>

Sancho-Shimizu, V., Pérez de Diego, R., Lorenzo, L., Halwani, R., Alangari, A., Israelsson, E., Fabrega, S., Cardon, A., Maluenda, J., Tatematsu, M., Mahvelati, F., Herman, M., Ciancanelli, M., Guo, Y., AlSum, Z., Alkhamis, N., Al-Makadma, A.S., Ghadiri, A., Boucherit, S., Plancoulaine, S., Picard, C., Rozenberg, F., Tardieu, M., Lebon, P., Jouanguy, E., Rezaei, N., Seya, T., Matsumoto, M., Chaussabel, D., Puel, A., Zhang, S.-Y., Abel, L., Al-Muhsen, S., Casanova, J.-L., 2011. Herpes simplex encephalitis in children with autosomal recessive and dominant TRIF deficiency. *J. Clin. Invest.* 121, 4889–4902. <https://doi.org/10.1172/JCI59259>

Santini, S.M., Lapenta, C., Logozzi, M., Parlato, S., Spada, M., Di Pucchio, T., Belardelli, F., 2000. Type I Interferon as a Powerful Adjuvant for Monocyte-Derived Dendritic Cell Development and Activity in Vitro and in Hu-Pbl-Scid Mice. *J. Exp. Med.* 191, 1777–1788. <https://doi.org/10.1084/jem.191.10.1777>

Sasai, M., Linehan, M.M., Iwasaki, A., 2010a. Bifurcation of Toll-Like Receptor 9 Signaling by Adaptor Protein 3. *Science* 329, 1530–1534. <https://doi.org/10.1126/science.1187029>

Saveanu, L., Carroll, O., Weimershaus, M., Guermonprez, P., Firat, E., Lindo, V., Greer, F., Davoust, J., Kratzer, R., Keller, S.R., Niedermann, G., van Endert, P., 2009.

IRAP Identifies an Endosomal Compartment Required for MHC Class I Cross-Presentation. *Science* 325, 213–217. <https://doi.org/10.1126/science.1172845>

Segura, E., 2016. Review of Mouse and Human Dendritic Cell Subsets, in: Segura, E., Onai, N. (Eds.), *Dendritic Cell Protocols, Methods in Molecular Biology*. Springer New York, New York, NY, pp. 3–15. [https://doi.org/10.1007/978-1-4939-3606-9\\_1](https://doi.org/10.1007/978-1-4939-3606-9_1)

Segura, E., Albiston, A.L., Wicks, I.P., Chai, S.Y., Villadangos, J.A., 2009. Different cross-presentation pathways in steady-state and inflammatory dendritic cells. *Proc. Natl. Acad. Sci.* 106, 20377–20381. <https://doi.org/10.1073/pnas.0910295106>

Sepulveda, D., Rojas-Rivera, D., Rodríguez, D.A., Groenendyk, J., Köhler, A., Lebeaupin, C., Ito, S., Urra, H., Carreras-Sureda, A., Hazari, Y., Vasseur-Cognet, M., Ali, M.M.U., Chevet, E., Campos, G., Godoy, P., Vaisar, T., Bailly-Maitre, B., Nagata, K., Michalak, M., Sierralta, J., Hetz, C., 2018a. Interactome Screening Identifies the ER Luminal Chaperone Hsp47 as a Regulator of the Unfolded Protein Response Transducer IRE1 $\alpha$ . *Mol. Cell* 69, 238-252.e7. <https://doi.org/10.1016/j.molcel.2017.12.028>

Sepulveda, D., Rojas-Rivera, D., Rodríguez, D.A., Groenendyk, J., Köhler, A., Lebeaupin, C., Ito, S., Urra, H., Carreras-Sureda, A., Hazari, Y., Vasseur-Cognet, M., Ali, M.M.U., Chevet, E., Campos, G., Godoy, P., Vaisar, T., Bailly-Maitre, B., Nagata, K., Michalak, M., Sierralta, J., Hetz, C., 2018b. Interactome Screening Identifies the ER Luminal Chaperone Hsp47 as a Regulator of the Unfolded Protein Response Transducer IRE1 $\alpha$ . *Mol. Cell* 69, 238-252.e7. <https://doi.org/10.1016/j.molcel.2017.12.028>

Sepulveda, F.E., Maschalidi, S., Colisson, R., Heslop, L., Ghirelli, C., Sakka, E., Lennon-Duménil, A.-M., Amigorena, S., Cabanie, L., Manoury, B., 2009a. Critical Role for Asparagine Endopeptidase in Endocytic Toll-like Receptor Signaling in Dendritic Cells. *Immunity* 31, 737–748. <https://doi.org/10.1016/j.immuni.2009.09.013>

Sepulveda, F.E., Maschalidi, S., Colisson, R., Heslop, L., Ghirelli, C., Sakka, E., Lennon-Duménil, A.-M., Amigorena, S., Cabanie, L., Manoury, B., 2009b. Critical Role for Asparagine Endopeptidase in Endocytic Toll-like Receptor Signaling in Dendritic Cells. *Immunity* 31, 737–748. <https://doi.org/10.1016/j.immuni.2009.09.013>

Shang, G., Zhu, D., Li, N., Zhang, J., Zhu, C., Lu, D., Liu, C., Yu, Q., Zhao, Y., Xu, S., Gu, L., 2012. Crystal structures of STING protein reveal basis for recognition of cyclic di-GMP. *Nat. Struct. Mol. Biol.* 19, 725–727. <https://doi.org/10.1038/nsmb.2332>

Shapiro-Shelef, M., Lin, K.-I., McHeyzer-Williams, L.J., Liao, J., McHeyzer-Williams, M.G., Calame, K., 2003. Blimp-1 Is Required for the Formation of Immunoglobulin Secreting Plasma Cells and Pre-Plasma Memory B Cells. *Immunity* 19, 607–620. [https://doi.org/10.1016/S1074-7613\(03\)00267-X](https://doi.org/10.1016/S1074-7613(03)00267-X)

Shen, L., Sigal, L.J., Boes, M., Rock, K.L., 2004. Important Role of Cathepsin S in Generating Peptides for TAP-Independent MHC Class I Crosspresentation In Vivo. *Immunity* 21, 155–165. <https://doi.org/10.1016/j.immuni.2004.07.004>

Shen, Z., Reznikoff, G., Dranoff, G., Rock, K.L., 1997. Cloned dendritic cells can present exogenous antigens on both MHC class I and class II molecules. *J. Immunol. Baltim. Md 1950* 158, 2723–2730.

Shi, Z., Cai, Z., Sanchez, A., Zhang, T., Wen, S., Wang, J., Yang, J., Fu, S., Zhang, D., 2011. A Novel Toll-like Receptor That Recognizes Vesicular Stomatitis Virus. *J. Biol. Chem.* 286, 4517–4524. <https://doi.org/10.1074/jbc.M110.159590>

Siegal, F.P., Kadowaki, N., Shodell, M., Fitzgerald-Bocarsly, P.A., Shah, K., Ho, S., Antonenko, S., Liu, Y.-J., 1999. The Nature of the Principal Type 1 Interferon-Producing Cells in Human Blood. *Science* 284, 1835–1837. <https://doi.org/10.1126/science.284.5421.1835>

Smith, J.A., Turner, M.J., DeLay, M.L., Klenk, E.I., Sowders, D.P., Colbert, R.A., 2008. Endoplasmic reticulum stress and the unfolded protein response are linked to synergistic IFN- $\beta$  induction via X-box binding protein 1. *Eur. J. Immunol.* 38, 1194–1203. <https://doi.org/10.1002/eji.200737882>

Song, H.-S., Park, S., Huh, J.-W., Lee, Y.-R., Jung, D.-J., Yang, C., Kim, S.H., Kim, H.M., Kim, Y.-M., 2022. N-glycosylation of UNC93B1 at a Specific Asparagine Residue Is Required for TLR9 Signaling. *Front. Immunol.* 13, 875083. <https://doi.org/10.3389/fimmu.2022.875083>

Srikanth, S., Woo, J.S., Wu, B., El-Sherbiny, Y.M., Leung, J., Chupradit, K., Rice, L., Seo, G.J., Calmettes, G., Ramakrishna, C., Cantin, E., An, D.S., Sun, R., Wu, T.-T., Jung, J.U., Savic, S., Gwack, Y., 2019. The Ca<sup>2+</sup> sensor STIM1 regulates the type I interferon response by retaining the signaling adaptor STING at the endoplasmic reticulum. *Nat. Immunol.* 20, 152–162. <https://doi.org/10.1038/s41590-018-0287-8>



Steimle, V., Siegrist, C.-A., Mottet, A., Lisowska-Grospierre, B., Mach, B., 1994. Regulation of MHC Class II Expression by Interferon- $\gamma$  Mediated by the Transactivator Gene CIITA. *Science* 265, 106–109. <https://doi.org/10.1126/science.8016643>

Steinman, R.M., Cohn, Z.A., 1974. IDENTIFICATION OF A NOVEL CELL TYPE IN PERIPHERAL LYMPHOID ORGANS OF MICE. *J. Exp. Med.* 139, 380–397. <https://doi.org/10.1084/jem.139.2.380>

Steinman, R.M., Cohn, Z.A., 1973. IDENTIFICATION OF A NOVEL CELL TYPE IN PERIPHERAL LYMPHOID ORGANS OF MICE. *J. Exp. Med.* 137, 1142–1162. <https://doi.org/10.1084/jem.137.5.1142>

Sun, L., Wu, J., Du, F., Chen, X., Chen, Z.J., 2013. Cyclic GMP-AMP Synthase Is a Cytosolic DNA Sensor That Activates the Type I Interferon Pathway. *Science* 339, 786–791. <https://doi.org/10.1126/science.1232458>

Sundaram, A., Plumb, R., Appathurai, S., Mariappan, M., 2017. The Sec61 translocon limits IRE1 $\alpha$  signaling during the unfolded protein response. *eLife* 6, e27187. <https://doi.org/10.7554/eLife.27187>

Tabeta, K., Hoebe, K., Janssen, E.M., Du, X., Georgel, P., Crozat, K., Mudd, S., Mann, N., Sovath, S., Goode, J., Shamel, L., Herskovits, A.A., Portnoy, D.A., Cooke, M., Tarantino, L.M., Wiltshire, T., Steinberg, B.E., Grinstein, S., Beutler, B., 2006. The Unc93b1 mutation 3d disrupts exogenous antigen presentation and signaling via Toll-like receptors 3, 7 and 9. *Nat. Immunol.* 7, 156–164. <https://doi.org/10.1038/ni1297>

Takahashi, K., Honeyman, M.C., Harrison, L.C., 1997. Dendritic Cells Generated from Human Blood in Granulocyte Macrophage-Colony Stimulating Factor and Interleukin-7. *Hum. Immunol.* 55, 103–116. [https://doi.org/10.1016/S0198-8859\(97\)00094-3](https://doi.org/10.1016/S0198-8859(97)00094-3)

Takahashi, K., Shibata, T., Akashi-Takamura, S., Kiyokawa, T., Wakabayashi, Y., Tanimura, N., Kobayashi, T., Matsumoto, F., Fukui, R., Kouro, T., Nagai, Y., Takatsu, K., Saitoh, S., Miyake, K., 2007. A protein associated with Toll-like receptor (TLR) 4 (PRAT4A) is required for TLR-dependent immune responses. *J. Exp. Med.* 204, 2963–2976. <https://doi.org/10.1084/jem.20071132>

Takeuchi, O., Akira, S., 2010. Pattern Recognition Receptors and Inflammation. *Cell* 140, 805–820. <https://doi.org/10.1016/j.cell.2010.01.022>

Tatematsu, M., Funami, K., Ishii, N., Seya, T., Obuse, C., Matsumoto, M., 2015. LRRC59 Regulates Trafficking of Nucleic Acid–Sensing TLRs from the Endoplasmic Reticulum via Association with UNC93B1. *J. Immunol.* 195, 4933–4942. <https://doi.org/10.4049/jimmunol.1501305>

Tavernier, Q., Bennana, E., Poindessous, V., Schaeffer, C., Rampoldi, L., Pietrancosta, N., Pallet, N., 2018. Regulation of IRE1 RNase activity by the Ribonuclease inhibitor 1 (RNH1). *Cell Cycle* 17, 1901–1916. <https://doi.org/10.1080/15384101.2018.1506655>

Tavernier, S.J., Osorio, F., Vandersarren, L., Vettters, J., Vanlangenakker, N., Van Isterdael, G., Vergote, K., De Rycke, R., Parthoens, E., van de Laar, L., Iwawaki, T., Del Valle, J.R., Hu, C.-C.A., Lambrecht, B.N., Janssens, S., 2017. Regulated IRE1-dependent mRNA decay sets the threshold for dendritic cell survival. *Nat. Cell Biol.* 19, 698–710. <https://doi.org/10.1038/ncb3518>

Tirasophon, W., Welihinda, A.A., Kaufman, R.J., 1998. A stress response pathway from the endoplasmic reticulum to the nucleus requires a novel bifunctional protein kinase/endoribonuclease (Ire1p) in mammalian cells. *Genes Dev.* 12, 1812–1824. <https://doi.org/10.1101/gad.12.12.1812>

Townsend, A., Öhlén, C., Bastin, J., Ljunggren, H.-G., Foster, L., Kärre, K., 1989. Association of class I major histocompatibility heavy and light chains induced by viral peptides. *Nature* 340, 443–448. <https://doi.org/10.1038/340443a0>

Urrea, H., Henriquez, D.R., Cánovas, J., Villarroel-Campos, D., Carreras-Sureda, A., Pulgar, E., Molina, E., Hazari, Y.M., Limia, C.M., Alvarez-Rojas, S., Figueroa, R., Vidal, R.L., Rodriguez, D.A., Rivera, C.A., Court, F.A., Couve, A., Qi, L., Chevet, E., Akai, R., Iwawaki, T., Concha, M.L., Glavic, Á., Gonzalez-Billault, C., Hetz, C., 2018. IRE1 $\alpha$  governs cytoskeleton remodelling and cell migration through a direct interaction with filamin A. *Nat. Cell Biol.* 20, 942–953. <https://doi.org/10.1038/s41556-018-0141-0>

van Vliet, A.R., Agostinis, P., 2017. PERK and filamin A in actin cytoskeleton remodeling at ER-plasma membrane contact sites. *Mol. Cell. Oncol.* 4, e1340105. <https://doi.org/10.1080/23723556.2017.1340105>

Voorhees, R.M., Hegde, R.S., 2016. Structure of the Sec61 channel opened by a signal sequence. *Science* 351, 88–91. <https://doi.org/10.1126/science.aad4992>

Wang, Q., Franks, H.A., Lax, S.J., El Refaee, M., Malecka, A., Shah, S., Spendlove, I., Gough, M.J., Seedhouse, C., Madhusudan, S., Patel, P.M., Jackson, A.M., 2013. The Ataxia Telangiectasia Mutated Kinase Pathway Regulates IL-23 Expression by Human Dendritic Cells. *J. Immunol.* 190, 3246–3255. <https://doi.org/10.4049/jimmunol.1201484>

Wang, W.-A., Demaurex, N., 2022. The mammalian trafficking chaperone protein UNC93B1 maintains the ER calcium sensor STIM1 in a dimeric state primed for translocation to the ER cortex. *J. Biol. Chem.* 298, 101607. <https://doi.org/10.1016/j.jbc.2022.101607>

Weimershaus, M., Maschalidi, S., Sepulveda, F., Manoury, B., van Endert, P., Saveanu, L., 2012. Conventional Dendritic Cells Require IRAP-Rab14 Endosomes for Efficient Cross-Presentation. *J. Immunol.* 188, 1840–1846. <https://doi.org/10.4049/jimmunol.1101504>

Wen, H., Miao, E.A., Ting, J.P.-Y., 2013. Mechanisms of NOD-like Receptor-Associated Inflammasome Activation. *Immunity* 39, 432–441. <https://doi.org/10.1016/j.immuni.2013.08.037>

Wiest, D.L., Burkhardt, J.K., Hester, S., Hortsch, M., Meyer, D.I., Argon, Y., 1990. Membrane biogenesis during B cell differentiation: most endoplasmic reticulum proteins are expressed coordinately. *J. Cell Biol.* 110, 1501–1511. <https://doi.org/10.1083/jcb.110.5.1501>

Woehlbier, U., Hetz, C., 2011. Modulating stress responses by the UPRosome: A matter of life and death. *Trends Biochem. Sci.* 36, 329–337. <https://doi.org/10.1016/j.tibs.2011.03.001>

Wong, G.H., Tartaglia, L.A., Lee, M.S., Goeddel, D.V., 1992. Antiviral activity of tumor necrosis factor is signaled through the 55-kDa type I TNF receptor [corrected]. *J. Immunol. Baltim. Md 1950* 149, 3350–3353.

Wu, S., Hong, F., Gewirth, D., Guo, B., Liu, B., Li, Z., 2012. The Molecular Chaperone gp96/GRP94 Interacts with Toll-like Receptors and Integrins via Its C-terminal Hydrophobic Domain. *J. Biol. Chem.* 287, 6735–6742. <https://doi.org/10.1074/jbc.M111.309526>

Yamamoto, M., Sato, S., Mori, K., Hoshino, K., Takeuchi, O., Takeda, K., Akira, S., 2002. Cutting Edge: A Novel Toll/IL-1 Receptor Domain-Containing Adapter That

Preferentially Activates the IFN- $\beta$  Promoter in the Toll-Like Receptor Signaling. *J. Immunol.* 169, 6668–6672. <https://doi.org/10.4049/jimmunol.169.12.6668>

Yarovinsky, F., Zhang, D., Andersen, J.F., Bannenberg, G.L., Serhan, C.N., Hayden, M.S., Hieny, S., Sutterwala, F.S., Flavell, R.A., Ghosh, S., Sher, A., 2005. TLR11 Activation of Dendritic Cells by a Protozoan Profilin-Like Protein. *Science* 308, 1626–1629. <https://doi.org/10.1126/science.1109893>

Yoshida, H., Haze, K., Yanagi, H., Yura, T., Mori, K., 1998. Identification of the cis-Acting Endoplasmic Reticulum Stress Response Element Responsible for Transcriptional Induction of Mammalian Glucose-regulated Proteins. *J. Biol. Chem.* 273, 33741–33749. <https://doi.org/10.1074/jbc.273.50.33741>

Yoshida, H., Matsui, T., Yamamoto, A., Okada, T., Mori, K., 2001. XBP1 mRNA Is Induced by ATF6 and Spliced by IRE1 in Response to ER Stress to Produce a Highly Active Transcription Factor. *Cell* 107, 881–891. [https://doi.org/10.1016/S0092-8674\(01\)00611-0](https://doi.org/10.1016/S0092-8674(01)00611-0)

Zehner, M., Chasan, A.I., Schuette, V., Embgenbroich, M., Quast, T., Kolanus, W., Burgdorf, S., 2011. Mannose receptor polyubiquitination regulates endosomal recruitment of p97 and cytosolic antigen translocation for cross-presentation. *Proc. Natl. Acad. Sci.* 108, 9933–9938. <https://doi.org/10.1073/pnas.1102397108>

Zehner, M., Marschall, A.L., Bos, E., Schloetel, J.-G., Kreer, C., Fehrenschild, D., Limmer, A., Ossendorp, F., Lang, T., Koster, A.J., Dübel, S., Burgdorf, S., 2015. The Translocon Protein Sec61 Mediates Antigen Transport from Endosomes in the Cytosol for Cross-Presentation to CD8+ T Cells. *Immunity* 42, 850–863. <https://doi.org/10.1016/j.immuni.2015.04.008>

Zeng, L., Liu, Y.-P., Sha, H., Chen, H., Qi, L., Smith, J.A., 2010. XBP-1 Couples Endoplasmic Reticulum Stress to Augmented IFN- $\beta$  Induction via a *cis*-Acting Enhancer in Macrophages. *J. Immunol.* 185, 2324–2330. <https://doi.org/10.4049/jimmunol.0903052>

Zhang, C., Shang, G., Gui, X., Zhang, X., Bai, X., Chen, Z.J., 2019. Structural basis of STING binding with and phosphorylation by TBK1. *Nature* 567, 394–398. <https://doi.org/10.1038/s41586-019-1000-2>

Zhang, K., Wong, H.N., Song, B., Miller, C.N., Scheuner, D., Kaufman, R.J., 2005. The unfolded protein response sensor IRE1 $\alpha$  is required at 2 distinct steps in B cell lymphopoiesis. *J. Clin. Invest.* 115, 268–281. <https://doi.org/10.1172/JCI200521848>

Zhang, S.L., Yu, Y., Roos, J., Kozak, J.A., Deerinck, T.J., Ellisman, M.H., Stauderman, K.A., Cahalan, M.D., 2005. STIM1 is a Ca<sup>2+</sup> sensor that activates CRAC channels and migrates from the Ca<sup>2+</sup> store to the plasma membrane. *Nature* 437, 902–905. <https://doi.org/10.1038/nature04147>

Zhao, B., Shu, C., Gao, X., Sankaran, B., Du, F., Shelton, C.L., Herr, A.B., Ji, J.-Y., Li, P., 2016. Structural basis for concerted recruitment and activation of IRF-3 by innate immune adaptor proteins. *Proc. Natl. Acad. Sci.* 113. <https://doi.org/10.1073/pnas.1603269113>

Zhu, H., Zhang, R., Yi, L., Tang, Y., Zheng, C., 2022. UNC93B1 attenuates the cGAS–STING signaling pathway by targeting STING for autophagy–lysosome degradation. *J. Med. Virol.* 94, 4490–4501. <https://doi.org/10.1002/jmv.27860>

Zinkernagel, R.M., Doherty, P.C., 1979. MHC-Restricted Cytotoxic T Cells: Studies on the Biological Role of Polymorphic Major Transplantation Antigens Determining T-Cell Restriction-Specificity, Function, and Responsiveness, in: *Advances in Immunology*. Elsevier, pp. 51–177. [https://doi.org/10.1016/S0065-2776\(08\)60262-X](https://doi.org/10.1016/S0065-2776(08)60262-X)

## TABLE DES FIGURES

### Introduction

Figure 1. Dendritic cell subsets characteristics in human and mouse.....	19
Figure 2. A toll-like receptor dimer structure. ....	22
Figure 3. Surface and endosomal TLRs signalling induce the production of pro-inflammatory cytokines and type I interferons. ....	25
Figure 4. STING signalling pathway.....	28
Figure 5. Major histocompatibility complex molecules class I and II structures.	31
Figure 6. MHC class I antigen presentation pathways. ....	38
Figure 7. MHC class II exogenous antigen presentation pathway. ....	40
Figure 8. UNC93B1 interaction with intracellular TLRs regulates their trafficking from ER to endosomes. ....	47
Figure 9. UNC93B1 H412R (3d) mutation.....	48
Figure 10. Activation of the three arms of the unfolded protein response (UPR), PERK, IRE1 and ATF6, following ER stress. ....	54
Figure 11. Synergism between TLR signalling and IRE1 $\alpha$ activation for pro-inflammatory cytokine and type I interferons production. ....	56
Figure 12. Model: Regulation of IRE1 $\alpha$ activation by the Sec61 translocon and BiP, and targets up and downregulated following IRE1 $\alpha$ RNase activity. ....	64

### Results Part I: UNC93B1 regulates the unfolded protein response sensor IRE1 $\alpha$ in dendritic cells.

Figure 1. IRE1 $\alpha$ associates with UNC93B1 in DCs and the interaction is enhanced in 3d cells. ....	96
Figure 2. The transmembrane region of IRE1 $\alpha$ is required for its association with UNC93B1. ....	97
Figure 3. UNC93B1 controls IRE1 $\alpha$ activity in DCs. ....	98
Figure 4. IRE1 $\alpha$ inhibition partially restores MHC I antigen cross-presentation and limits tumor growth in 3d DCs and mice.....	99
Figure 5. IRE1 $\alpha$ /BiP interaction is disrupted in 3d DCs.....	100
Figure 6. UNC93B1 regulation of IRE1 $\alpha$ activity and its impact on antigen cross-presentation. ....	101

Supplementary figure 1. IRE1 $\alpha$ and UNC93B1 expression in different DC subtypes, using conformational UNC93B1 antibodies. ....	102
Supplementary figure 2. STIM1 associates with WT UNC93B1 but not with IRE1 $\alpha$ . ....	103
Supplementary figure 3. IRE1 $\alpha$ -HA mutants are transfected equally in HeLa cells. ....	104
Supplementary figure 4. IRE1 $\alpha$ activity is upregulated in 3d cDC1s and can be measured with a fluorescence assay.....	105
Supplementary figure 5. IRE1 $\alpha$ inhibition doesn't affect MHC II antigen presentation by DCs, and decreases tumoral growth in both WT and 3d mice.	106
Supplementary figure 6. IRE1 $\alpha$ association to BiP and Sec63 is reduced in 3d DCs. ....	107

**Results Part II: UNC93B1 regulates STING signalling in DCs.**

Figure 1. STING and UNC93B1 associate in DCs. ....	112
Figure 2. UNC93B1 promotes STING-mediated INF- $\beta$ signalling in DCs. ....	113
Figure 3. UNC93B1 controls STING translocation to the Golgi upon cGAMP stimulation. ....	114
Figure 4. STING and its downstream adaptors are phosphorylated in both WT and 3d DCs.....	115

**Discussion**

Figure 1. Interacting domains composition of UNC93B1 partners.....	122
Figure 2. MHC I levels are similar between WT and 3d DCs. ....	127

**LISTE DES TABLES**

**Part I: UNC93B1 regulates the unfolded protein response sensor IRE1 $\alpha$  in dendritic cells.**

Supplementary table 1. List of antibodies used. ....	108
Supplementary table 2. List of primers used for PCR. ....	109

**Part II: UNC93B1 regulates STING signalling in DCs.**

Supplementary table. List of antibodies used. ....	118
--	-----

## ANNEXES

### Résumé substantiel

Tohme et al., 2020. **TLR7 trafficking and signaling in B cells is regulated by the MHCII-associated invariant chain**, *Journal of Cell Science*, 133, jcs236711.

Manoury et al., 2022. **The role of endoplasmic reticulum stress in the MHC class I antigen presentation pathway of dendritic cells**, *Molecular Immunology*, 144 (2022) 44–48.

Maisonneuve and Manoury. **In vitro and in vivo assays to evaluate dendritic cell phagocytic capacity**. In press, *Methods Molecular Biology*, Vol. 2618, Vanja Sisirak (Eds): Dendritic Cells, 978-1-0716-2937-6, 502291\_1\_En, (Chapter 20).

De Lavergne et al. **The role of the antigen processing machinery in the regulation and trafficking of intracellular TLR molecules**. In revision, *Current Opinion in Immunology*.





## RESUME SUBSTANTIEL

**Introduction.** Les cellules dendritiques (CDs) sont des effecteurs clés de l'immunité innée et adaptative. Elles font en effet partie des premières cellules à rencontrer et à agir contre un antigène du non-soi, pouvant provenir d'un agent pathogène. De plus, elles sont aussi capables de présenter l'antigène rencontré aux lymphocytes T, cellules de l'immunité adaptative. Les CDs sont donc primordiales dans l'élimination des divers dangers que peut rencontrer l'organisme.

Présents principalement dans les cellules de l'immunité innée et les cellules présentatrices d'antigène (CPA), les récepteurs Toll-like (TLRs) permettent la reconnaissance d'un large panel de motifs microbiens. Ils initient alors la production et sécrétion de cytokines pro-inflammatoires et l'expression de molécules de co-stimulation dans les CPA. Ces réponses sont clés dans l'activation des cellules immunitaires environnantes et des lymphocytes T et B. Les TLRs peuvent être présents à la surface des cellules, comme le TLR4, ou bien dans les endosomes, comme les TLRs 3, 7 et 9. Les TLRs endosomaux sont spécialisés dans la reconnaissance des acides nucléiques, et leur signalisation est alors cruciale dans les réponses antivirales. Ils sont assemblés dans le réticulum endoplasmique (RE) avant de migrer vers les endosomes, où ils rencontrent leur ligand. La stabilisation des TLRs endosomaux dans le RE ainsi que leur trafic vers les endosomes sont dépendants d'une chaperone du RE, UNC93B1 (Unc-93 homolog B1).

UNC93B1 est une protéine transmembranaire du RE qui interagit avec les TLRs endosomaux (Brinkmann et al., 2007). L'association de ces TLRs avec UNC93B1 est nécessaire pour leur stabilisation dans le RE (Pelka et al., 2018), leur translocation aux endosomes (Lee et al., 2013), et leur subséquente signalisation. N'étant pas seulement une protéine chaperone des TLRs intracellulaires, UNC93B1 est aussi impliquée dans l'activité d'autres protéines transmembranaires du RE. En effet, STIM1 (Stromal interaction molecule 1), un senseur calcique jouant un rôle primordial dans le flux du calcium dans le cytosol et le RE, s'associe avec UNC93B1 (Maschalidi et al., 2017). Une déplétion en calcium dans le RE entraîne l'activation de STIM1, son oligomérisation, et l'apposition du RE et de STIM1 à la membrane plasmique. STIM1 va alors interagir avec le canal calcique ORAI1 et engendrer l'entrée de calcium dans la cellule. L'association entre STIM1 et UNC93B1 est nécessaire à l'activation de STIM1 dans le RE.

Une mutation d'UNC93B1, H412R ou 3d, est à l'origine d'un défaut de signalisation des TLRs endosomaux (Tabeta et al., 2006) et d'une inhibition de l'activation de STIM1 dans les CDs (Maschalidi et al., 2017). En effet, le mutant 3d/3d d'UNC93B1 ne s'associe pas aux TLRs intracellulaires ou à STIM1, engendrant leur incapacité à s'activer. De plus, les CDs 3d/3d sont caractérisées par un défaut de présentation croisée antigénique, présentation des antigènes exogènes sur le complexe majeur d'histocompatibilité (CMH) de classe I. Ce défaut est en partie dû à l'incapacité de STIM1 à s'activer, engendrant un défaut de calcium dans les endosomes et phagosomes, nécessaire à la dégradation efficace des antigènes en peptides (Maschalidi et al., 2017 ; Nunes-Hasler et al., 2017). Cependant, d'autres mécanismes non décrits dans la littérature sont certainement impliqués dans ce processus.

Au cours de ma thèse, notre but fût d'identifier de nouveaux clients d'UNC93B1 dans les CDs et d'étudier leur régulation dans les cellules 3d/3d. Pour cela, nous avons analysé des microarrays comparant l'expression de gènes entre les rates murines sauvages (WT) et 3d/3d. Parmi les gènes dont l'expression était plus faible dans les rates 3d/3d, nous avons observé STIM1, identifié comme un client d'UNC93B1, et IRE1 $\alpha$  (Inositol-requiring enzyme 1).

IRE1 $\alpha$  est un senseur du stress du RE, activé à la suite d'une accumulation de protéines mal conformées dans le RE. IRE1 $\alpha$  a alors pour but de ré-établir l'homéostasie du RE en augmentant l'expression de chaperones et en réduisant le taux de protéines dans l'organelle. Sous sa forme inactive, IRE1 $\alpha$  est lié à la protéine chaperone BiP dans le RE. Lors d'un stress du RE, BiP se dissocie d'IRE1 $\alpha$  et lie les protéines mal conformées, engendrant l'activation des domaines kinase et RNase d'IRE1 $\alpha$ . Une fois activé, IRE1 $\alpha$  épisse de façon non conventionnelle l'ARN messenger (ARNm) d'XBP1 (X-box binding protein 1), donnant lieu à la production du facteur de transcription XBP1s, pour XBP1 spliced. XBP1s va alors activer la transcription de protéines chaperones du RE ou encore de membres d'ESCRT (Endosomal sorting complex required for transport), impliqués dans le trafic des protéines mal conformées vers la dégradation. De plus, IRE1 $\alpha$  clive également des ARNm spécifiques, permettant une réduction du taux de protéines entrant le RE, via la voie RIDD (Regulated IRE1-dependent decay).

Dans les CDs, IRE1 $\alpha$  joue aussi un rôle dans la présentation croisée antigénique. En effet, les CDs déficientes pour XBP1 ont un défaut de présentation croisée

antigénique. Dans ces cellules, IRE1 $\alpha$  est fortement activé à l'état basal et clive les ARNm spécifiques de la voie RIDD. Parmi ces ARNm, des facteurs importants à la présentation antigénique tels que *Tapbp* ou *Ergic3* sont trouvés (Osorio et al., 2014). *Tapbp* code pour la tapasine, protéine clé dans l'acheminement des peptides vers le RE ou les endosomes et dans leur liaison au CMH de classe I. *Ergic3* est impliqué dans le trafic du complexe CMH I-peptide vers le compartiment intermédiaire entre le RE et le Golgi (ERGIC) et vers la membrane plasmique. Le clivage de ces ARNm dans les CD $\alpha$  déficientes en XBP1 entraîne probablement le défaut de présentation croisée antigénique observé. L'activation de la voie RIDD dans les CD $\alpha$  semble alors avoir un effet délétère sur leur fonction de cellules présentatrices d'antigènes.

STING (Stimulator of interferon genes) est un autre client d'UNC93B1, identifié dans les cellules HeLa et dans les fibroblastes (He et al., 2021 ; Zhu et al., 2022). STING est impliqué dans la réponse aux molécules d'ADN qui se retrouvent dans le cytosol à la suite d'une infection ou d'un stress cellulaire. Ces molécules d'ADN sont reconnues par cGAS (Cyclic GMP-AMP synthase), qui va engendrer la production de cGAMP (Cyclic GMP-AMP) et l'activation de STING. STING va alors recruter TBK1 et IRF3, donnant lieu à la production de cytokines pro-inflammatoires et d'interférons de type I. STING interagit avec UNC93B1 dans le RE, et il fût théorisé qu'UNC93B1 promeut la dégradation de STING et l'arrêt de sa signalisation (He et al., 2021). En revanche, les expériences ont été conduites dans des cellules HeLa et des fibroblastes, dont le mécanisme de production de cytokines et d'interférons est différent des cellules myéloïdes, et des CD $\alpha$ .

Au cours de ma thèse, notre but a été d'identifier si IRE1 $\alpha$  et STING sont des clients d'UNC93B1 dans les CD $\alpha$  et d'étudier leur régulation dans les cellules 3d/3d.

**Méthodes.** Pour mener nos expériences, nous avons différencié des cellules de moelle osseuse murines WT et 3d/3d en CD $\alpha$  *in vitro*. Pour cela, les cellules souches de moelle osseuse ont été mises en culture dans du milieu complété avec du GM-CSF pendant 7 à 10 jours. Nous avons également purifié des CD $\alpha$  murines primaires de rate de souris WT et 3d/3d. Après avoir injecté des cellules de mélanome B16 sécrétant la cytokine Flt3-ligand dans les souris, nous avons purifié la population amplifiée de CD $\alpha$  conventionnelles de type I dans la rate par cytométrie en flux. Nous avons ensuite étudié l'interaction d'UNC93B1 avec IRE1 $\alpha$  et STING par immunoprécipitation et PLA (Proximity Ligation Assay), et avons déterminé l'activation

de ces protéines dans les CD3d/3d par western blot ou RT-qPCR. Nous avons également étudié l'une des fonctions principales des CD3d, la présentation croisée antigénique. Pour cela, la prolifération de lymphocytes T après leur coculture avec des CD3d WT et 3d/3d présentant un antigène a été évaluée. Des expériences de pousse tumorale ont aussi été effectuées dans les souris WT et 3d/3d.

**Résultats.** Nous avons tout d'abord décrit l'association entre IRE1 $\alpha$  et UNC93B1 dans les CD3d WT et 3d/3d, interaction qui est augmentée dans les cellules 3d/3d. De plus, lorsque les CD3d sont soumises à un stress du RE, l'association entre IRE1 $\alpha$  et UNC93B1 est également amplifiée. Par transfection de mutants d'IRE1 $\alpha$  dans les cellules HeLa, nous avons observé qu'IRE1 $\alpha$  interagit avec UNC93B1 via son domaine transmembranaire. Ensuite, alors que l'interaction entre IRE1 $\alpha$  et UNC93B1 est augmentée dans les CD3d/3d, nous avons voulu savoir si cela avait un impact sur l'activation d'IRE1 $\alpha$ . En effet, dans les cellules portant la mutation 3d/3d d'UNC93B1, IRE1 $\alpha$  est actif à l'état basal, épisse *Xbp1* et clive des ARNm spécifiques via la voie RIDD tels que *Tapbp* ou *ERp44*. Le clivage de ces ARNm par IRE1 $\alpha$  entraîne un défaut de présentation croisée antigénique dans les CD3d/3d, qui sont capables de présenter l'antigène efficacement après inhibition de l'activité RNase d'IRE1 $\alpha$ . De plus, dans les souris 3d/3d, dans lesquelles la pousse tumorale est significativement plus accrue que dans les souris WT, l'inhibition de l'activité RNase d'IRE1 $\alpha$  réduit la croissance tumorale. Enfin, nous nous sommes intéressés au mécanisme d'activation d'IRE1 $\alpha$  dans les CD3d/3d. La protéine chaperone BiP, gardant IRE1 $\alpha$  sous forme inactive, ne se lie pas au senseur du stress du RE dans les CD3d/3d à l'état basal, entraînant son activation.

Nous avons ensuite identifié un nouveau client d'UNC93B1 dans les CD3d, STING. UNC93B1 et STING interagissent dans le RE dans les CD3d WT et 3d/3d. En revanche, dans les cellules 3d/3d, la réponse interféron liée à l'activation de STING est significativement plus faible que dans les cellules WT. Cette faible signalisation de STING est aussi retrouvée dans les CD3d déficientes pour UNC93B1. Cela indique qu'UNC93B1 promeut l'activation de STING dans les CD3d. De plus, dans les CD3d/3d, la translocation de STING au Golgi après sa stimulation, nécessaire à la production d'interféron de type I, est réduite. En revanche, les phosphorylations de STING, de la molécule adaptatrice TBK1 et du facteur de transcription IRF3, induites après stimulation de STING, restent inchangées entre les CD3d WT et 3d/3d.

**Discussion/Conclusion.** Dans les CDs, nous avons pu identifier deux nouveaux clients d'UNC93B1, IRE1 $\alpha$  et STING. D'après nos observations, différents pools d'UNC93B1 existent dans le RE. En effet, bien qu'UNC93B1 interagisse avec IRE1 $\alpha$  et STIM1 respectivement, ces deux protéines ne s'associent pas, nous indiquant une formation de divers complexes par UNC93B1. Ces différents complexes pourraient alors avoir des rôles bien distincts, et différentes localisations dans le RE. UNC93B1 étant une protéine comportant 12 domaines transmembranaires, il est cependant compliqué d'étudier les dynamiques et les sites d'interaction d'UNC93B1 avec ses différents partenaires, ainsi que ses changements de conformation. Il fut cependant montré que la mutation 3d/3d d'UNC93B1 entraîne un changement de conformation de la protéine, empêchant son interaction avec les TLRs endosomaux et STIM1, mais conservant celle avec IRE1 $\alpha$  et STING. IRE1 $\alpha$  s'associe plus avec UNC93B1 3d/3d dans les CDs, entraînant probablement son activation par le détachement de BiP. UNC93B1 semble alors promouvoir l'activation d'IRE1 $\alpha$ , et nous pouvons nous demander si UNC93B1 est de plus nécessaire à son activité.

L'activation d'IRE1 $\alpha$  dans les CDs, et notamment de la voie RIDD, apparaît être délétère pour la présentation croisée antigénique. En effet, d'autres travaux ont précédemment montré un défaut de présentation antigénique dû au clivage d'ARNm spécifiques par IRE1 $\alpha$  (Osorio et al., 2014 ; Guttman et al., 2022). Dans les CDs 3d/3d, cette activité d'IRE1 $\alpha$  à l'état basal ainsi que l'incapacité de STIM1 à s'activer et à créer des hotspots de calcium dans les endosomes/phagosomes, entraînent un défaut de présentation croisée antigénique.

Les CDs 3d/3d rencontrent également un défaut dans la signalisation de la voie STING. Bien que nous sachions que la translocation de STING vers le Golgi est réduite dans les CDs 3d/3d, le mécanisme de cette baisse de signalisation est encore à élucider. Parmi les hypothèses pouvant être émises, STING pourrait être envoyé à la dégradation avant de pouvoir établir une réponse interféron efficace dans ces cellules, ou la forme 3d/3d d'UNC93B1 pourrait retenir STING dans le RE et empêcher sa signalisation.

Mots clés : Cellule dendritique, Récepteurs Toll-like, UNC93B1, IRE1 $\alpha$ , STING.



## CORRECTION

# Correction: TLR7 trafficking and signaling in B cells is regulated by the MHCII-associated invariant chain

Mira Tohme, Lucie Maisonneuve, Karim Achour, Michaël Dussiot, Sophia Maschalidi and Bénédicte Manoury

There was an error in *J. Cell. Sci.* (2020) 133, jcs236711 (doi:10.1242/jcs.236711).

The authors wish to correct an error in the 'Cells and stimulations' section of the Materials and Methods of this article, where the text incorrectly described the kit used to purify splenic B cells as a CD19-negative selection kit, instead of a CD19-positive selection kit.

The correct text is as follows:

'Splenic IgM<sup>+</sup>/IgD<sup>+</sup> mature B cells were isolated using a CD19-positive selection kit [Miltenyi Biotec (130-121-301), 90–95% purity as determined by fluorescence-activated cell sorting (FACS)] and immature IgM<sup>+</sup>/IgD<sup>-</sup> B cells were isolated and collected by flow cytometry.'

The authors apologise to readers for this error, which does not impact the results or the conclusions of the article. Both the online full text and PDF versions of the article have been corrected.



# TLR7 trafficking and signaling in B cells is regulated by the MHCII-associated invariant chain

Mira Tohme<sup>1</sup>, Lucie Maisonneuve<sup>2,3</sup>, Karim Achour<sup>4</sup>, Michaël Dussiot<sup>5</sup>, Sophia Maschalidi<sup>6</sup> and Bénédicte Manoury<sup>2,3,\*</sup>

## ABSTRACT

Toll-like receptor 7 (TLR7) is an endosomal receptor that recognizes single-stranded RNA from viruses. Its trafficking and activation is regulated by the endoplasmic reticulum (ER) chaperone UNC93B1 and lysosomal proteases. UNC93B1 also modulates major histocompatibility complex class II (MHCII) antigen presentation, and deficiency in MHCII protein diminishes TLR9 signaling. These results indicate a link between proteins that regulate both innate and adaptive responses. Here, we report that TLR7 resides in lysosomes and interacts with the MHCII-chaperone molecule, the invariant chain (Ii) or CD74, in B cells. In the absence of CD74, TLR7 displays both ER and lysosomal localization, leading to an increase in pro-inflammatory cytokine production. Furthermore, stimulation with TLR7 but not TLR9, is inefficient in boosting antigen presentation in Ii-deficient cells. In contrast, in B cells lacking TLR7 or mutated for UNC93B1, which are able to trigger TLR7 activation, antigen presentation is enhanced. This suggests that TLR7 signaling in B cells is controlled by the Ii chain.

**KEY WORDS:** Toll-like receptor 7, Invariant chain, B cells, UNC93B1

## INTRODUCTION


Toll-like receptors (TLRs) recognize specific motifs from microbial molecules and initiate immune responses. TLRs belong to the family of single membrane-spanning receptors and are expressed in immune cells including B cells. Intracellular TLRs sense nucleic acids. Indeed, RNA or DNA from pathogen is recognized by TLR3, TLR7, TLR8 and TLR9 specifically. TLR7 senses imidazoquinoline derivatives such as imiquimod and single-stranded RNA from a wide variety of viruses such as influenza and HIV (Hemmi et al., 2002; Lund et al., 2004). Activation of intracellular TLRs by their ligands induces the recruitment of adaptor molecules, MyD88 for TLR7, TLR8 and TLR9, and TRIF (also known as TICAM1) for TLR3. Once recruited to their specific TLRs, adaptor proteins can activate two signaling pathways: the translocation of NF- $\kappa$ B or interferon response factor (IRF) into the nucleus for transcription of pro-inflammatory or interferon genes,

respectively. The localization, traffic and folding of intracellular TLRs are regulated by the endoplasmic reticulum (ER)-resident protein UNC93B1 (Tabeta et al., 2006; Brinkmann et al., 2007; Pelka et al., 2018; Majer et al., 2019). UNC93B1 binds directly to the transmembrane region of TLR3, TLR7, TLR8 and TLR9 in the ER and transports them to endocytic compartments upon stimulation (Kim et al., 2008). In dendritic cells (DCs) purified from mice expressing a point mutation in UNC93B1 (3d), intracellular TLRs are retained in the ER, preventing DCs from secreting cytokines upon engagement of TLR3, TLR7 and TLR9 (Tabeta et al., 2006). However, in B cells, even though UNC93B1 is still required for intracellular TLR signaling, TLR9 seems, at the steady state, to reside in lysosomal compartments (Avalos et al., 2013). In addition, mice or humans deficient for UNC93B1 are susceptible to multiple infections (Tabeta et al., 2006; Casrouge et al., 2006; Melo et al., 2010; Caetano et al., 2011). Intracellular TLRs require proteolytic cleavage in acidic endosomes for their activity (Park et al., 2008; Matsumoto et al., 2008; Ewald et al., 2008; Sepulveda et al., 2009). Indeed, cells from different origins and deficient for asparagine endopeptidase (AEP) show significant decrease in cytokine production following TLR7 stimulation with imiquimod or infection with influenza virus (Maschalidi et al., 2012). Also, inhibition of furin-like proprotein convertases severely diminishes TLR7 signaling (Hipp et al., 2013).

B cells are dedicated cells in adaptive immunity as they present exogenous antigen on major histocompatibility complex class II (MHCII) molecules to CD4<sup>+</sup> T cells. MHCII  $\alpha$  and  $\beta$  chains assemble and form heterodimers in the ER, where they associate with a chaperone molecule, the invariant chain (Ii) or CD74 (Roche et al., 1991). A prerequisite for peptide loading onto MHCII molecules is the proteolytic destruction of Ii. The N-terminal cytoplasmic domain of Ii targets the MHCII–Ii complexes to the endocytic pathway (Zhong et al., 1997). Ii is sequentially cleaved, leaving a C-terminal portion: the class II invariant chain peptide or CLIP, which protects the class II peptide binding groove from binding peptides outside the endocytic compartments. In lysosomal vesicles, the chaperone molecule DM interacts with the complex MHCII–CLIP and facilitates the exchange of CLIP for peptides generated in the endocytic pathway (Denzin and Cresswell, 1995). Thus, Ii chains plays a critical role in MHCII antigen presentation to CD4<sup>+</sup> T cells by stabilising MHCII in the ER and directing MHCII to endocytic compartments. Ii also interacts with MHCI and promotes antigen cross-presentation by DCs (Basha et al., 2012). In addition to their classical functions in antigen presentation, a recent study has shown that MHCII molecules are important components in the TLR response (Liu et al., 2011). MHCII deficiency in DCs and macrophages lowers the secretion of pro-inflammatory cytokines and type I interferon following TLR3, TLR4 or TLR9 stimulation. MHCII forms a complex with the activated Bruton's tyrosine kinase (Btk) induced by TLR stimulation, allowing a

<sup>1</sup>Nkarta Therapeutics, South San Francisco, CA 94080, USA. <sup>2</sup>Institut Necker Enfant Malade, INSERM U1151-CNRS UMR 8253, 75015 Paris, France. <sup>3</sup>Université Paris, Faculté de médecine, 75015 Paris, France. <sup>4</sup>Institut de recherche Servier, 3 rue de la république, 92150 Suresnes, France. <sup>5</sup>Institut Imagine, INSERM U1163, CNRS ERL 8254, Université Paris Descartes, Sorbonne Paris-Cité, Laboratoire d'Excellence GR-Ex, 75015 Paris, France. <sup>6</sup>VIB-UGent Center for Inflammation Research, UGent-VIB Research Building F5VM, Technologiepark 71, 9052 Ghent, Belgium.

\*Author for correspondence (benedicte.manoury@inserm.fr)

 B.M., 0000-0001-7784-3389

sustained interaction with MyD88 and activation of the NF- $\kappa$ B and IRF pathways.

Because Ii chain is a key chaperone in MHCII trafficking and folding, we investigated the role of CD74 in regulating TLR7 and TLR9 responses. Here, we show that CD74 interacts with TLR7 expressed in lysosomes and modulates specifically TLR7 but not TLR9 response in B cells. In B cells lacking CD74, stimulation of TLR7 initiates cytokine production and inhibits antigen presentation, whereas in B cells lacking TLR7 or mutated for UNC93B1, antigen presentation is increased. These results suggest that Ii chain in B cells dampens TLR7 innate immune responses to promote adaptive immunity.

## RESULTS

### Absence of Ii expression promotes TLR7 signaling in B cells

To assess whether Ii plays a role in TLR signaling, we stimulated membrane and intracellular TLRs from wild type (wt) (Ii<sup>+/+</sup>) and Ii-deficient (Ii<sup>-/-</sup>) bone marrow-derived dendritic cells (BMDCs), macrophages (BMDMs) and B cells with TLR-specific ligands. Ii-deficient B cells produced significantly more interleukin 6 (IL-6) and tumor necrosis alpha (TNF- $\alpha$ ) than wt B cells in response to two TLR7 ligands: imiquimod and gardiquimod (Fig. 1A; Fig. S1A). In contrast, Ii<sup>-/-</sup> B cells responded normally to TLR9 and TLR4 stimulation and produced similar amounts of IL-6 and TNF- $\alpha$  to those produced by Ii<sup>+/+</sup> B cells (Fig. 1A; Fig. S1A). No difference in TLR7 mRNA or protein expression was detected between Ii<sup>+/+</sup> and Ii<sup>-/-</sup> B cells (Fig. S1B,C). In addition, CD69, an activation marker expressed by B cells, was upregulated in Ii-deficient B cells upon TLR7, but not TLR9, stimulation (Fig. 1B) in comparison to wt cells. Surprisingly, no difference in cytokines secretion was observed when wt BMDCs or BMDCs lacking Ii chain were stimulated with TLR4, TLR7 or TLR9 ligands (Fig. S1D). Similar results were obtained with BMDMs (Fig. S1E). TLR7 stimulation induces the recruitment of the adaptor protein MyD88 followed by the translocation of the transcription factor NF- $\kappa$ B into the nucleus leading to the production of pro-inflammatory cytokines. Thus, increased TLR7 signaling correlates with stronger activation of the transcription factor NF- $\kappa$ B. To investigate whether or not the increase in TLR7 signaling in Ii<sup>-/-</sup> B cells resulted in enhanced proximity/interaction between the adaptor protein MyD88 and NF- $\kappa$ B, we used an *in situ* proximity-ligation assay (PLA) method that gives a signal if two different molecules are localized within 40 nm of each other. This method has been widely used to monitor spatial proximity of two proteins at the subcellular level and potentially would allow us to detect and visualize MyD88 conjugated to NF- $\kappa$ B (Yamazaki et al., 2009; Leuchowius et al., 2011; Misawa et al., 2013; Babdor et al., 2017). First, to validate this method, we monitored interaction signals between Ii and MHCII detected as red dots by confocal microscopy. As expected, we found spatial proximity of Ii with MHCII (Fig. S2A), which was significantly reduced in the absence of Ii. We then investigated interaction and proximity signals between MyD88 and NF- $\kappa$ B. In Ii<sup>+/+</sup> B cells, interaction signals between endogenous MyD88 and NF- $\kappa$ B were detected when cells were stimulated with imiquimod (Fig. 1C) and were significantly increased in Ii<sup>-/-</sup> B cells. Furthermore, no signal was observed in unstimulated cells (Fig. 1C). As expected, similar interaction signals between MyD88 and NF- $\kappa$ B were observed in TLR7-stimulated Ii<sup>+/+</sup> and Ii<sup>-/-</sup> BMDCs (Fig. S2B).

It was reported by the group of Cao that MHCII molecules promote full activation of TLR3, TLR4 and TLR9 in macrophages and DCs by interacting with CD40 and Btk to prolong Btk phosphorylation needed for TLR activation (Liu et al., 2011). Thus,

we investigated whether MHCII was also required for TLR7 function in B cells. We then stimulated wt (MHCII<sup>+/+</sup>) and MHCII-deficient (MHCII<sup>-/-</sup>) B cells with different TLR agonists. We observed no substantial difference in cytokine production between MHCII<sup>+/+</sup> and MHCII<sup>-/-</sup> B cells when TLR4, TLR7 or TLR9 were activated (Fig. S2C). Accordingly, expression of Btk or CD40 was the same in Ii<sup>+/+</sup> and Ii<sup>-/-</sup> resting and TLR7-stimulated B cells (Fig. S2D).

Recognition of the B-cell receptor (BCR) by antigen triggers BCR signaling and endocytosis. CpG-DNA- and BCR-induced TLR9 and antigen signaling have been shown to synergize in NF- $\kappa$ B induction and p38 phosphorylation (Chaturvedi et al., 2008). Thus, we treated wt and Ii-deficient B cells with imiquimod to stimulate TLR7 or with Fab-anti-mouse IgM together with imiquimod to engage both BCR and TLR7 and monitored cytokine production. As expected, dual stimulation through BCR and TLR7 increased IL-6 and TNF $\alpha$  production in wt B cells in comparison to TLR7 activation alone. This response was further amplified in Ii-deficient B cells but not in MHCII<sup>-/-</sup> B cells (Fig. 1D). Ii deficiency was shown to alter B cell maturation. Therefore, to exclude the hypothesis that the increased in TLR7 response detected in B cells lacking Ii was a result of a lack of B cell maturation, immature B cells were purified from bone marrow and TLRs were stimulated. Overall, wt immature B cells were unresponsive to TLR activation. However, similarly to mature B cells, Ii<sup>-/-</sup> immature B cells produced more IL-6 and TNF- $\alpha$  in response to TLR7 but not to TLR9 and TLR4 stimulation (Fig. S3).

### Ii chain interacts with TLR7 upon stimulation

The results described above indicate that Ii might be part of the TLR7 signaling pathway. To address this, complementary DNA (cDNA) coding for hemagglutinin (HA)-tagged full-length TLR7 and wt Ii were co-transfected in fibroblast. Forty-eight hours later, TLR7-Ii complexes were immunoprecipitated with an HA-conjugated antibody and blotted for Ii expression. As shown in Fig. 2A, Ii interacts with TLR7 upon imiquimod stimulation. However, to look at possible Ii-TLR7-MyD88 proximity/interactions in B cells, we used the DuoLink *in situ* PLA method described above because specific antibodies for detecting endogenous TLR7 working in immunofluorescence or immunoprecipitation were unavailable. We transfected a cDNA coding for HA-tagged full-length TLR7 in B cells and monitored the interaction of the transfected TLR7 protein with endogenous Ii. In a wt mouse B cell line (IIA1.6), interaction signals between endogenous Ii chain and transfected TLR7 were detected only when cells were stimulated with imiquimod (Fig. 2B). To investigate whether this interaction was specific for Ii chain, we used short hairpin RNA (shRNA) lentiviral particles targeting the Ii chain to silence Ii chain expression. Ii chain knockdown was confirmed using the individual shRNA 89 construct targeting a specific region of Ii and visualized by western blotting (Fig. 2C). The lower expression of Ii chain resulted in a significant decrease in the interaction signal between TLR7 and Ii previously observed upon TLR7 stimulation (Fig. 2B,C). Interestingly, the peak of interaction between Ii chain and TLR7 was observed after 30 min of imiquimod incubation (Fig. 2B, right panel). Upon imiquimod sensing, TLR7 associates with MyD88 to allow signal transduction (Ewald et al., 2008; Maschalidi et al., 2012). Therefore, we performed similar experiments as described above to visualize the proximity signal between Ii chain and MyD88. Upon TLR7 engagement, positive PLA signals corresponding to proximity between Ii and MyD88 were present in the cells (Fig. 2D, left). Again the maximum signal was visualized after

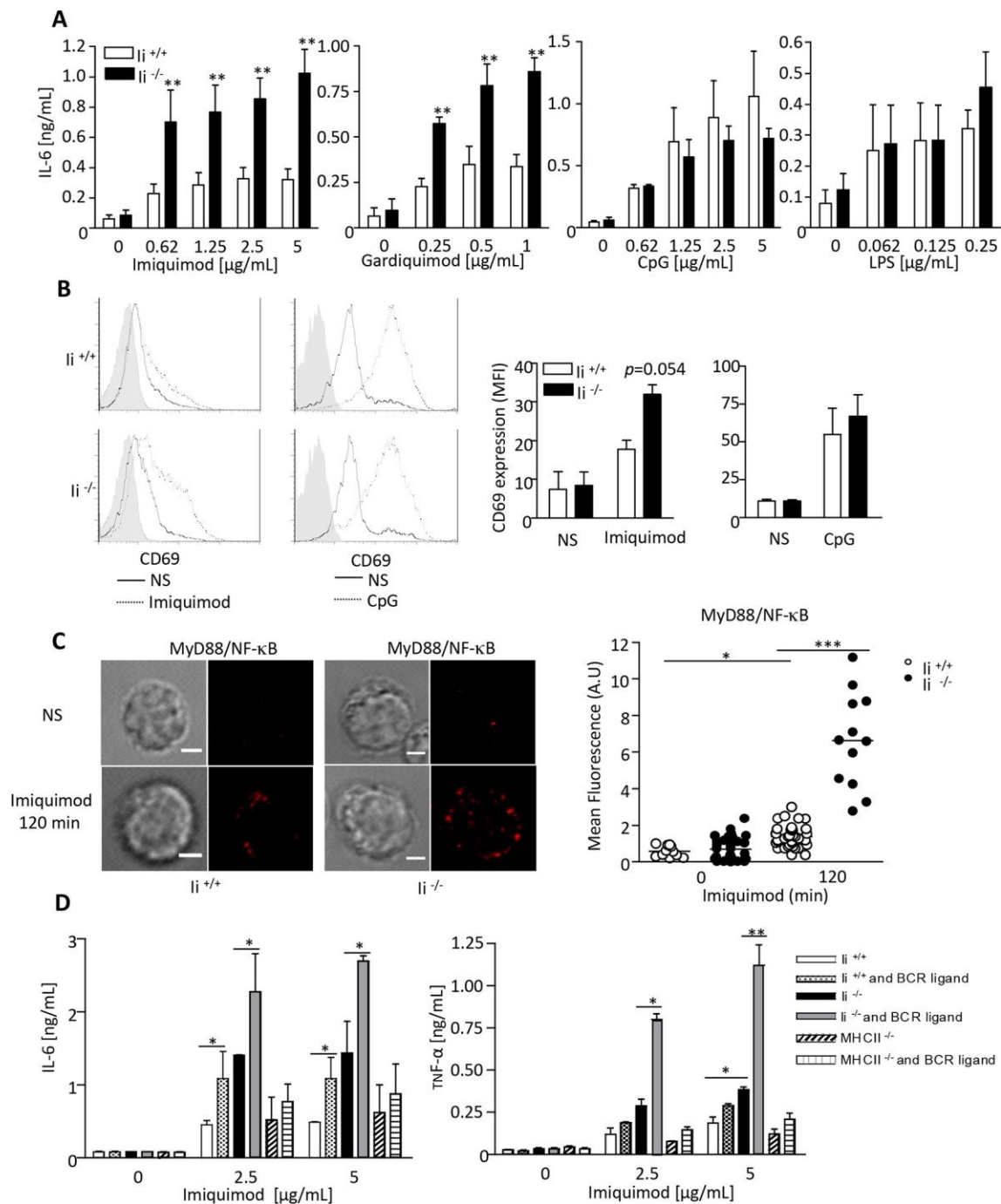


**Fig. 1.** TLR7-specific stimulation increases IL-6 production, CD69 expression and Myd88-NF-κB interaction in Ii-deficient B cells. (A) Ii<sup>+/+</sup> or Ii<sup>-/-</sup> mature splenic B cells were stimulated with different TLR ligands for 12 h and secretion of IL-6 was measured by ELISA ( $n=8$ , graphs show mean $\pm$ s.e.m., \*\* $P<0.01$ ). (B) Mouse splenic B cells were treated without (black lines) or with (dashed lines) 5  $\mu$ g/ml imiquimod or 10  $\mu$ g/ml CpGB for 16 h and stained for CD69 expression using fluorescent antibodies. Gray histograms represent staining of B cells with the antibody isotype control. Quantification of three experiments using Prism is shown on the right. (C) Detection of Myd88 and NF-κB interaction using the proximity ligation assay (PLA) *in situ* in Ii<sup>+/+</sup> and Ii<sup>-/-</sup> mature splenic B cells unstimulated (NS) or stimulated with imiquimod for 120 min. PLA signals are shown in red. One representative experiment out of three is shown. Quantification of mean fluorescence using ImageJ software is shown on the right ( $n=12-30$  cells, \* $P<0.05$ , \*\*\* $P<0.001$ ). (D) IL-6 and TNF- $\alpha$  production in supernatants from Ii<sup>+/+</sup>, Ii<sup>-/-</sup>, MHCII<sup>+/+</sup> or MHCII<sup>-/-</sup> mature B cells stimulated with imiquimod alone or together with BCR ligand ( $n=3$ , graphs show mean $\pm$ s.e.m., \* $P<0.05$ ). Scale bars: 5  $\mu$ m.

30 min of TLR7 engagement (Fig. 2D, right). To confirm that this interaction involved TLR7, Ii-MyD88 association in primary mouse B cells was monitored in the absence of TLR7. Indeed, no association between Ii chain and the adaptor protein MyD88 was observed in TLR7<sup>-/-</sup> B cells in comparison to TLR7<sup>+/+</sup> cells

(Fig. 2E). In contrast, we did not observe any interaction between TLR9 and Ii chain in B cells when TLR9 was stimulated (Fig. 2F). In conclusion, Ii chain specifically associates with TLR7 and its adaptor molecule MyD88 but not with TLR9 in B cells.

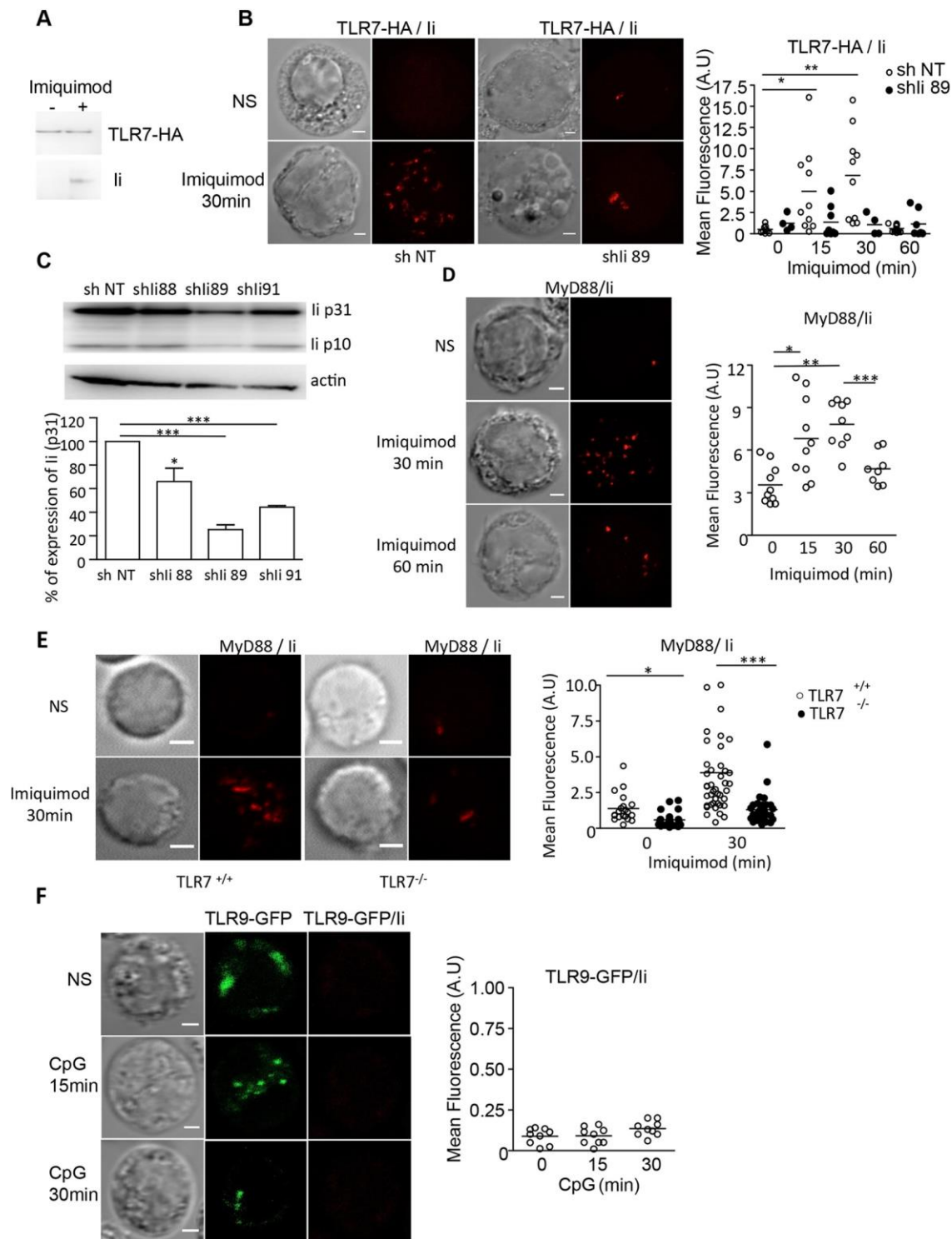


Fig. 2. Ii interacts with or is in proximity to TLR7 and the adaptor molecule MyD88. (A) Fibroblasts were stimulated with imiquimod (5  $\mu$ g/ml) for 30 min. TLR7 was immunoprecipitated from lysates and TLR7 and Ii expression was analyzed by western blot. One representative experiment out of three is shown. (B) Detection of Ii and TLR7 interaction using PLA *in situ* with anti-HA and anti-Ii specific mAbs in IIA1.6 B cell line infected with lentiviruses carrying a shRNA sequence for Ii or a shRNA sequence control (ShNT). Cells were stimulated or not (NS) with imiquimod for different times. PLA positive signals are shown in red. One representative experiment out of three is shown. Quantification of mean fluorescence using ImageJ software ( $n=10$  cells,  $*P<0.05$ ,  $**P<0.01$ ). (C) Anti-Ii and  $\beta$ -actin immunoblot of the B cell line IIA1.6 line infected with lentiviruses carrying different shRNA sequences for Ii or shRNA sequence control (ShNT). Quantification of three experiments using ImageJ software is shown below ( $n=3$ ,  $*P<0.05$ ,  $**P<0.001$ ). (D) Detection of MyD88 and Ii interaction using PLA *in situ* with anti-MyD88 and anti-Ii specific mAbs in IIA1.6 B cell line (D) or in TLR7<sup>+/+</sup> or TLR7<sup>-/-</sup> primary B cells (E) following imiquimod stimulation for different times. One representative experiment out of three is shown. Quantification of mean fluorescence using ImageJ is shown on the right of each panel ( $n=10$  cells for C and  $n=30$  cells for D,  $*P<0.05$ ,  $**P<0.01$ ,  $***P<0.001$ ). (F) Detection of Ii and TLR9 interaction using PLA *in situ* with anti GFP and anti-Ii specific mAbs in resting and CpG-stimulated primary B cells for different times, left panel. Quantification of mean fluorescence using ImageJ is shown on the right ( $n=10$  cells). Lines in scatter plots indicate mean values. Scale bars: 5  $\mu$ m.

### Ii chain regulates TLR7 trafficking in B cells

To determine where TLR7 is localized in Ii<sup>+/+</sup> B cells and whether or not Ii chain influences TLR7 trafficking, we first assessed by confocal microscopy the subcellular distribution of HA-tagged TLR7 construct in resting and activating Ii<sup>+/+</sup> and Ii<sup>-/-</sup> B cells. Transfection efficiency of the HA-tagged TLR7 construct was the same in Ii<sup>+/+</sup> and Ii<sup>-/-</sup> B cells (~30%; Fig. S4). Ii acts as a chaperone for MHCII folding, transport and antigen presentation, and thus, in the absence of Ii, MHCII might accumulate in ER-related structures (Viville et al., 1993). Thus, to investigate the integrity of lysosomes in Ii-deficient B cells, we incubate B cells with the Lysotracker dye, which stains lysosomes. Similar lysosomal fluorescence was detected in both Ii<sup>+/+</sup> and Ii<sup>-/-</sup> B cells expressing either TLR7 or TLR9 (Fig. 3A,B). Using confocal microscopy in TLR7-HA-expressing B cells, TLR7 staining was observed in small intracellular vesicles that contained the accessory protein H2-DM, Ii chain and MHCII molecules (Fig. 4A; Fig. S5A) both at steady state and upon TLR7 stimulation. These intracellular vesicles correspond to lysosomes as they stain positive for the lysosomal marker LAMP-1 (Fig. S6A). Additional experiments indicated that TLR7 did not reside in the ER, the ER-Golgi intermediate compartment or in early endosomes, as shown by the absence of TLR7 localization in calreticulin-, TAP1-, ERGIC53 (also known as LMAN1)- or VAMP3-positive compartments (Fig. S6B,C). In contrast, in resting or activated Ii<sup>-/-</sup> B cells, TLR7 was localized in ER vesicles that stained positive for calreticulin and less in the ER-Golgi intermediate compartment positive for ERGIC53 or in small intracellular vesicles containing VAMP3, H2-DM, Ii chain and

MHCII molecules (Fig. 4A; Figs S5A and S6B,C). Quantification showed that the difference in TLR7-HA localization between Ii<sup>-/-</sup> and Ii<sup>+/+</sup> B cells is highly significant (Fig. 4A, bottom panel). Next, we monitored endogenous TLR7 localization using imaging flow cytometry. In resting or activated Ii<sup>-/-</sup> B cells, TLR7 levels were higher in ER vesicles that stained positive for calnexin in comparison to Ii<sup>+/+</sup> B cells (Fig. 4B; Fig. S5B). However, TLR7 was also detected in LAMP-1-positive lysosomal organelles, although significantly less than in Ii<sup>+/+</sup> B cells (Fig. 4B). In addition, cross-linking the BCR with anti-IgM along with imiquimod treatment did not change the localization of TLR7 (Fig. 5A) in Ii-deficient B cells. Like TLR7, at steady state and upon CpG stimulation with or without BCR cross-linking, TLR9 also resides in lysosomal compartments and not in the ER, as it colocalizes with MHCII and H2-DM but not with calreticulin marker (Fig. 5B; Fig. S7A,B).

Altogether, these results demonstrate that TLR7 and TLR9, unlike in DCs, reside in lysosomal compartments in B cells at steady state after intracellular TLR stimulation, and that Ii regulates TLR7 trafficking in B cells.

TLR7 subcellular localization is independent of UNC93B1  
UNC93B1 is a chaperone molecule for endosomal TLRs (Tabeta et al., 2006; Pelka et al., 2018). It associates with intracellular TLRs resident in the ER and mediates their translocation to endosomal or lysosomal compartments (Kim et al., 2008; Majer et al., 2019). Surprisingly, we observed that TLR9, unlike TLR7, partially colocalized with UNC93B1 when cells were activated or not with CpG or imiquimod (Fig. 6A). UNC93B1 and Ii staining seems to

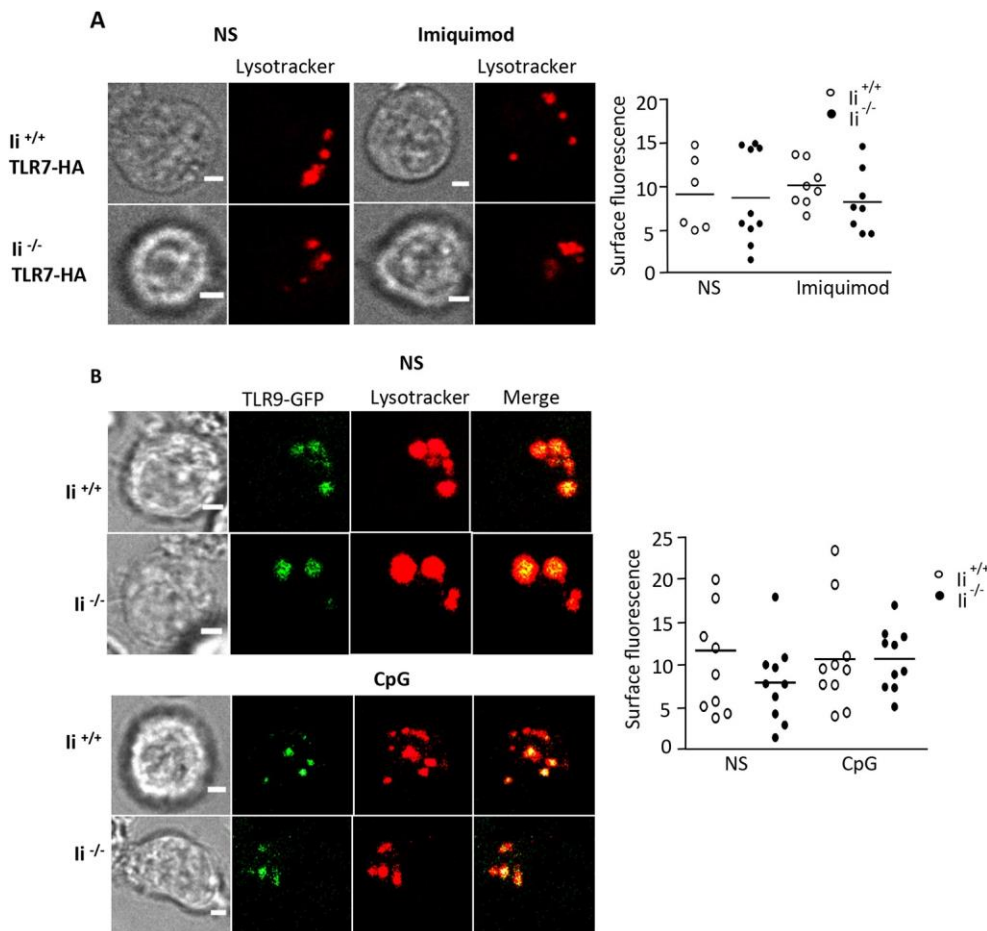


Fig. 3. Lysosome integrity is intact in Ii-deficient B cells. Immunofluorescence microscopy of resting or TLR-stimulated Ii<sup>+/+</sup> and Ii<sup>-/-</sup> splenic B cells transfected with full-length (FL)-TLR7-tagged HA (A) or with FL-TLR9-tagged GFP (B) and immunostained for TLR9 (green) and lysosomes (red) using Lysotracker dye. Images shown are taken 30 min after incubation with the Lysotracker. One experiment representative of three is shown. Graphs on the right in A and B show quantification of fluorescence intensity using ImageJ software ( $n=6-10$  cells). Lines in scatter plots indicate mean values. Scale bars: 5  $\mu$ m.

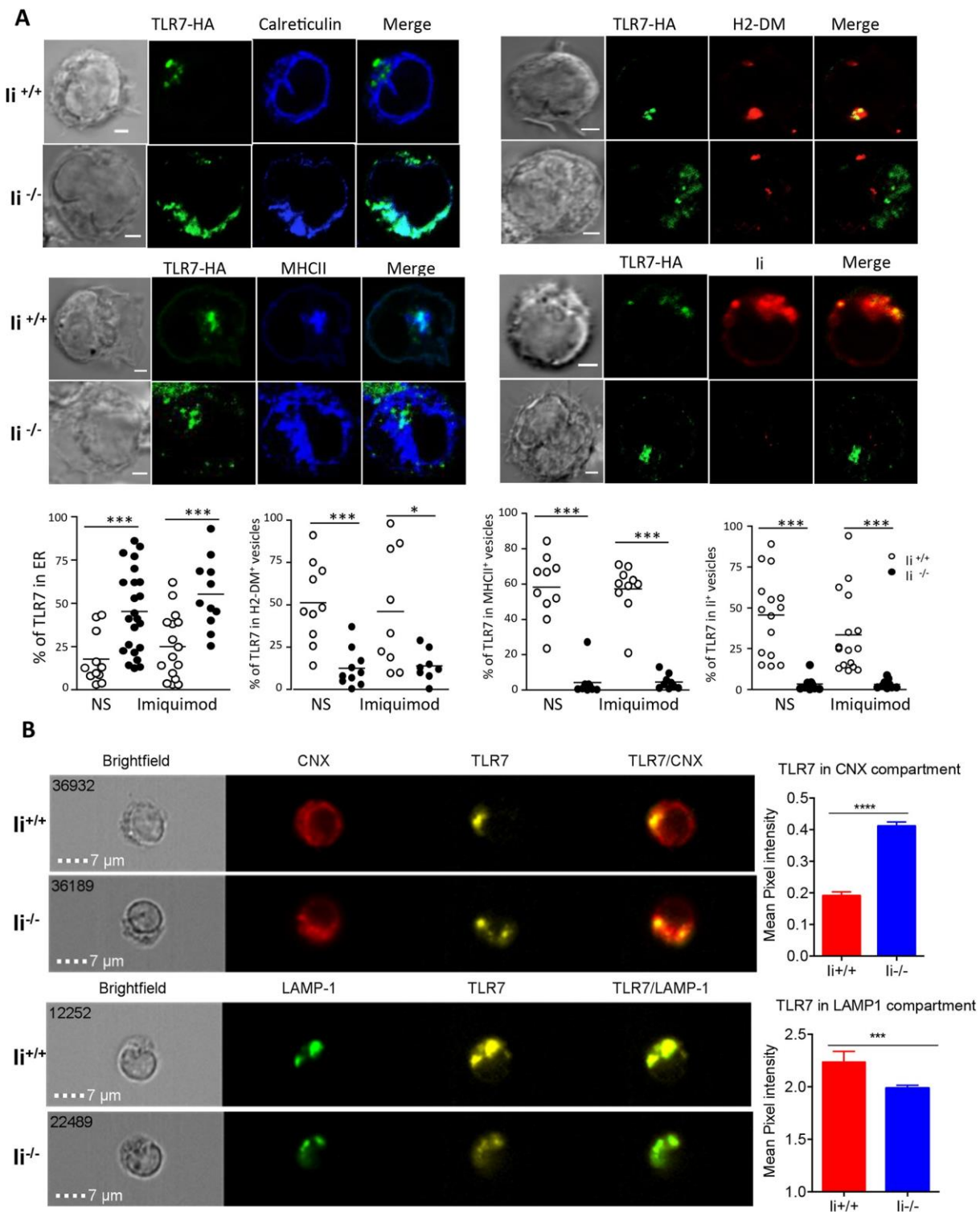


Fig. 4. Ii regulates TLR7 trafficking in B cells. (A) Immunofluorescence microscopy of resting Ii<sup>+/+</sup> or Ii<sup>-/-</sup> splenic B cells transfected with FL-TLR7-tagged HA and immunostained for TLR7 (green), calreticulin (blue), H2-DM (red), MHCII (blue) and Ii (red). One experiment representative of three is shown. Quantification of colocalization using ImageJ is shown in graphs below ( $n=10$  cells,  $*P<0.05$ ,  $***P<0.001$ ). (B) Representative images of calnexin (CNX), LAMP-1 and TLR7 intracellular staining in resting B cells from Ii<sup>+/+</sup> or Ii<sup>-/-</sup> acquired by imaging flow cytometry. First column shows cells in brightfield, second column ER or lysosomal markers (CNX or LAMP-1), third column TLR7, fourth column merged. Graphs show quantification of colocalization (mean pixel intensity $\pm$ s.e.m.; CNX-TLR7: Ii<sup>+/+</sup>,  $0.1905\pm 0.012$ ,  $n=5045$  and Ii<sup>-/-</sup>,  $0.4110\pm 0.0013$ ,  $n=6478$ ; LAMP-1-TLR7: Ii<sup>+/+</sup>,  $2.236\pm 0.1017$ ,  $n=1328$  and Ii<sup>-/-</sup>,  $1.987\pm 0.0278$ ,  $n=6213$ ;  $***P<0.001$ ,  $****P<0.0001$ ). One experiment of three is shown. Lines in scatter plots indicate mean values. Scale bars: 5  $\mu$ m.

overlap, indicating that UNC93B1 might also be localized in lysosomal vesicles in B cells (Fig. 6B). This result is strengthened by experiments using imaging flow cytometry, which showed

weak colocalization of TLR7 and UNC93B1 in Ii<sup>-/-</sup> B cells, suggesting again, ER localization for TLR7 in B cells deficient in Ii (Fig. 6C).

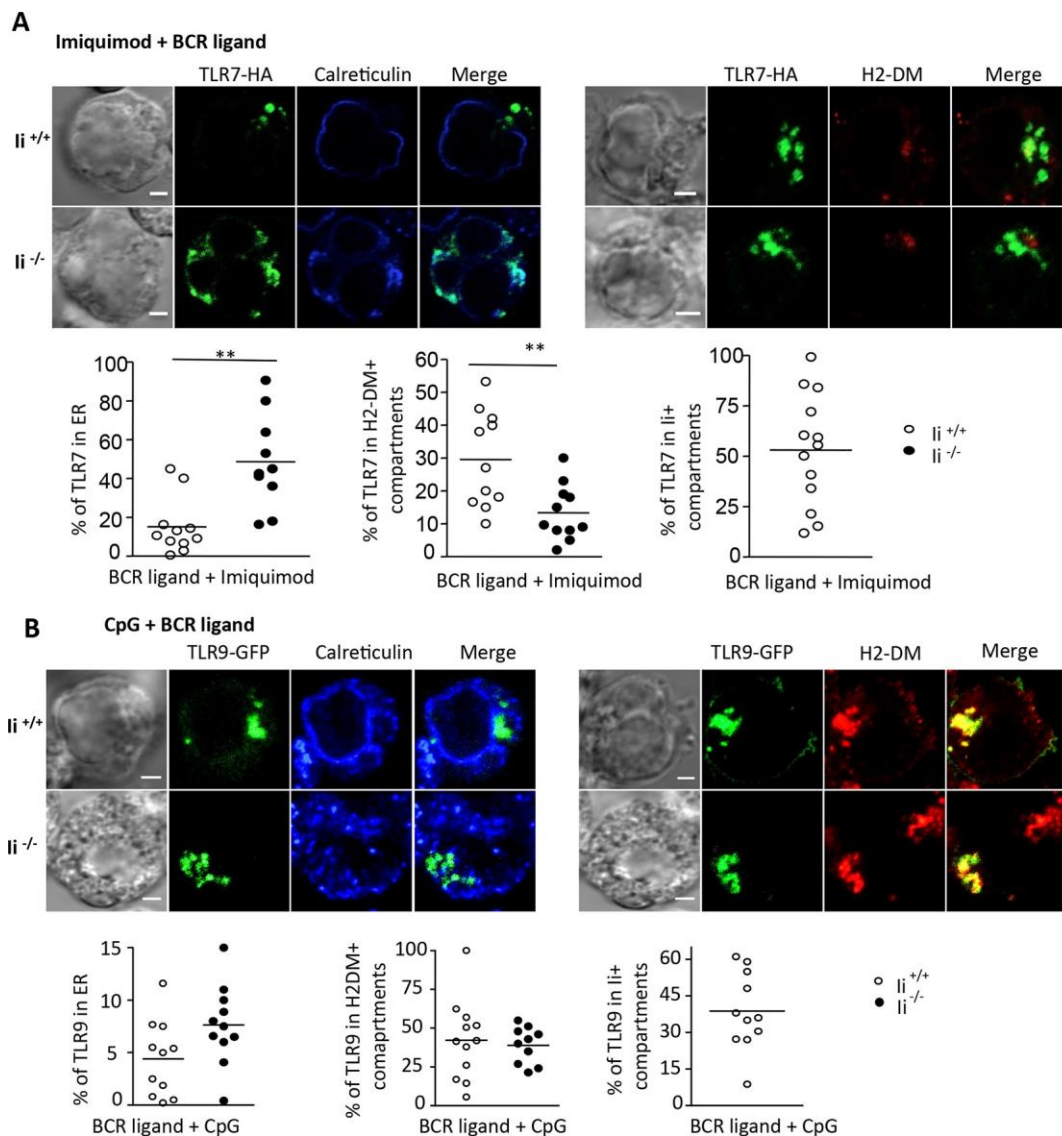


Fig. 5. BCR cross-linking does not affect TLR7 or TLR9 localization in B cells. Immunofluorescence microscopy of TLR7 or TLR9- and BCR-stimulated *li*<sup>+/+</sup>, *li*<sup>-/-</sup> splenic B cells transfected with FL-TLR7-tagged HA (A) or FL-TLR9-tagged GFP (B) and immunostained for TLR7 or TLR9 (green), calreticulin (blue) and H2-DM (red). One experiment representative of three is shown. Quantification of colocalization using ImageJ ( $n=10-13$  cells,  $**P<0.01$ ) is shown in lower panels of A and B. Lines in scatter plots indicate mean values. Scale bars: 5  $\mu$ m.

The innate, but not the adaptive, function of TLR7 is exacerbated in the absence of Ii

In the absence of Ii, MHCII antigen presentation is abolished (Teyton and Peterson, 1992). So, to test the possibility that the lack of Ii regulates the balance between innate and adaptive TLR7-dependent response in B cells, as described above, in promoting cytokine production upon TLR7 sensing, we chose to assess MHC class I antigen cross-presentation. Indeed, B lymphocytes are able to cross-present exogenous antigens when they are internalized via their BCR, and MHC I cross-presentation was shown to be further enhanced when the antigen is coupled to TLR9 ligand (Heit et al., 2004; Ke and Kapp, 1996; Jiang et al., 2011). First, we assessed whether MHC I antigen cross-presentation was increased in the presence of TLR ligands. *Ii*<sup>+/+</sup>, *Ii*<sup>-/-</sup> and TLR7<sup>-/-</sup> B cells were stimulated with soluble ovalbumin with or without imiquimod, CpG or lipopolysaccharide (LPS) for 12 h. Then, B cells were washed and incubated with carboxyfluorescein succinimidyl ester (CFSE)-labeled T cells specific for ovalbumin (OT-I cells). Three days later,

T-cell proliferation was analyzed. In wt, *Ii*- and TLR7-deficient B cells, ovalbumin antigenic presentation led to a weak proliferation of T cells (Fig. 7A, gray histograms). However, T-cell stimulation was increased in wt B cells incubated with both ovalbumin and LPS or CpG or imiquimod (Fig. 7A, black lines). As expected, similar proliferation of OTI T cells was observed in TLR7<sup>-/-</sup> B cells activated with ovalbumin in the presence or absence of imiquimod, demonstrating that TLR7 stimulation specifically increases MHC I antigen cross-presentation in wt cells (Fig. 7A, bottom row). Surprisingly, the boost in T-cell proliferation observed when wt cells were stimulated with imiquimod was abolished in *Ii*<sup>-/-</sup> B cells and to a similar extent as in TLR7-deficient cells (Fig. 7A, black lines, middle row, quantification in Fig. 7B). In contrast, no difference was detected between CpG- or LPS-stimulated *Ii*<sup>+/+</sup> and *Ii*<sup>-/-</sup> cells. In addition, two concentrations of OVA-control peptide triggered similar proliferation in all cell types tested (Fig. 7C). These results suggest that TLR stimulation increases MHC I antigen cross-presentation in B cells, and that Ii chain promotes TLR7-dependent

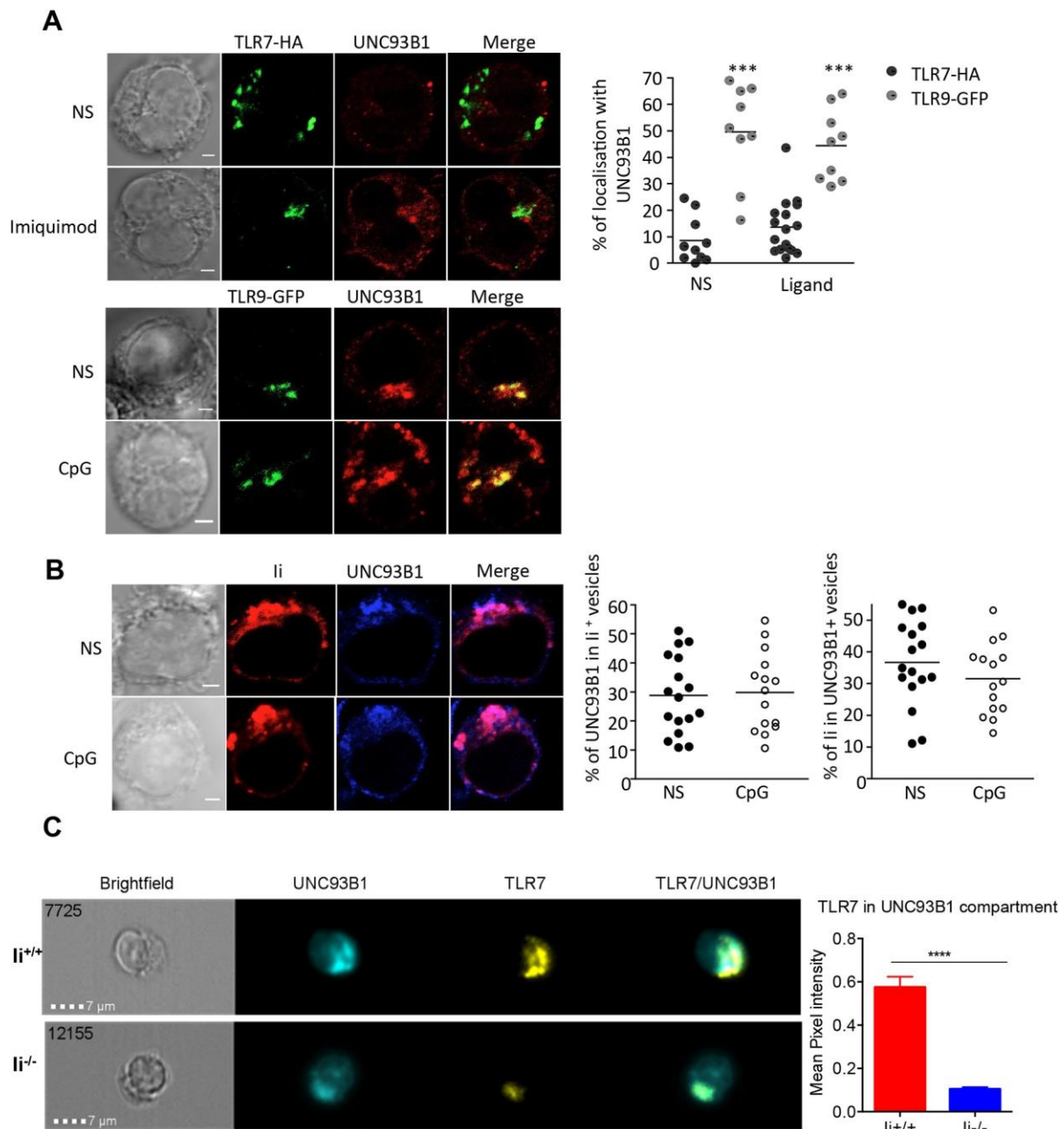


Fig. 6. TLR9, but not TLR7, colocalizes with UNC93B1. (A) Immunofluorescence microscopy of resting (NS) or TLR-stimulated splenic B cells transfected with FL-TLR7-tagged HA (top) or FL-TLR9-tagged GFP (bottom) and immunostained for TLR7 or TLR9 (green) and UNC93B1 (red). One experiment representative of three is shown. Quantification of colocalization using ImageJ is shown to the right ( $n=10$  cells,  $***P<0.001$ ). (B) Immunofluorescence microscopy of resting (NS) or TLR9-stimulated splenic B cells immunostained for Ii (red) and UNC93B1 (blue). One experiment representative of three is shown. Quantification of colocalization using ImageJ is on the right ( $n=15-17$  cells). (C) Representative images of UNC93B1 and TLR7 intracellular staining in resting B cells from Ii<sup>+/+</sup> or Ii<sup>-/-</sup> acquired by imaging flow cytometry. Graphs show quantification of colocalization of UNC93B1 and TLR7 (mean pixel intensity  $\pm$  s.e.m. Ii<sup>+/+</sup>,  $0.5752 \pm 0.048$ ,  $n=1294$  and Ii<sup>-/-</sup>,  $0.1043 \pm 0.0092$ ,  $n=4411$ ;  $****P<0.0001$ ). Lines in scatter plots indicate mean values. Scale bars: 5  $\mu$ m.

adaptive but not innate function in B cells. Many laboratories have described the important role of UNC93B1 in TLR trafficking, signaling, and MHC I and MHC II antigen-presentation pathways (Tabeta et al., 2006; Maschalidi et al., 2017). We then wondered whether UNC93B1 might play a similar role to Ii chain in regulating the innate and adaptive function in B cells. To address the contribution of UNC93B1 in the adaptive response in B cells, wt and UNC93B1 mutated (3d) B cells, which harbor a mutation in the transmembrane domain of UNC93B1 and inhibit intracellular TLRs signaling, were incubated with beads coated with myelin

oligodendrocyte (MOG) antigen alone or coupled with BCR ligand (anti-IgM) for 6 h. Then, B cells were washed and incubated with a CD4<sup>+</sup> T cell hybridoma specific for MOG, and MOG antigenic presentation was evaluated by the secretion of IL-2. In UNC93B1-defective B cells, TLR signaling was abolished (Fig. 7D, left); however, significant increase in IL-2 production was detected compared to control cells even in the absence of BCR stimulation (Fig. 7D, middle). MOG peptide presentation was identical between wt and 3d cells (Fig. 7D, right). Furthermore, no difference in MHC II expression was detected between wt and



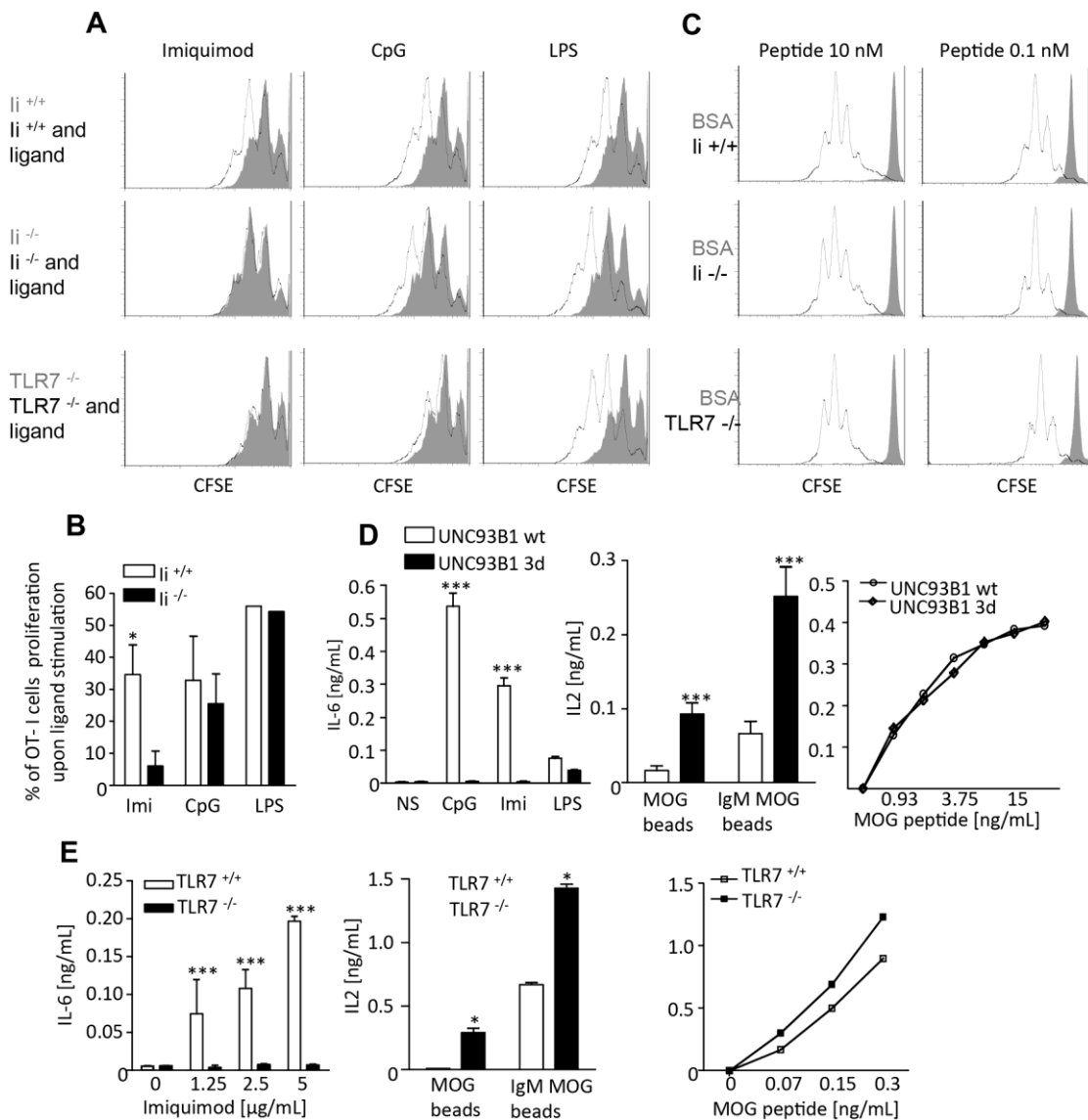


Fig. 7. Regulation of antigen presentation by Ii, UNC93B1 and TLR7. (A) Proliferation of OT-I T cells cultured with li<sup>+/+</sup>, li<sup>-/-</sup> or TLR7<sup>-/-</sup> B cells incubated with soluble ovalbumin (gray histograms) with or without imiquimod, CpGB or LPS (dark lines). (B) Quantification of four independent experiments (mean±s.e.m., \**P*<0.05). (C) SIINFEKL was used as an OVA-peptide control ('Peptide') in unstimulated cells. (D) WT (white bars) and UNC93B1 mutated (black bars) B cells were stimulated with TLR ligands and IL-6 secretion was measured in the supernatants (*n*=3, graphs show mean±s.e.m., \*\*\**P*<0.001). WT and UNC93B1 mutated (D) or TLR7<sup>+/+</sup> and TLR7<sup>-/-</sup> (E) B cells were incubated with MOG-coated beads or MOG- and IgM-coated beads for 6 h, washed and co-cultured with a CD4<sup>+</sup> T cell hybridoma specific for MOG. IL-2 secretion in the supernatant was monitored by ELISA. MOG peptide was used as control (*n*=3, graphs show mean±s.e.m., \**P*<0.05, \*\*\**P*<0.001). (D,E) WT or TLR7<sup>+/+</sup> (white bars) and UNC93B1 mutated or TLR7<sup>-/-</sup> (black bars) B cells were stimulated with TLR ligands and IL-6 secretion was measured in the supernatants (*n*=3, graphs show mean±s.e.m., \*\*\**P*<0.001).

UNC93B1-defective B cells (Fig. 8A). In addition, MHCII colocalized with LAMP-1 in lysosomal compartments in wt cells, and to the same extent as in UNC93B1 mutated B cells, as shown by immunofluorescence studies (Fig. 8B). To further investigate the role of TLR7 in innate versus adaptive immunity in B cells, we stimulated TLR7-deficient B cells with TLR7 ligand and measured cytokine production and MHCII MOG antigen presentation. As expected, TLR7<sup>-/-</sup> B cells failed to secrete IL-6 upon imiquimod addition (Fig. 7E, left). However, MHC class II presentation was enhanced in B cells lacking TLR7 in both MOG- and MOG coupled to BCR-treated cells (Fig. 7E, middle). Again, MHCII expression and localization were similar in wt and TLR7-deficient B cells (Fig. 8C,D). However, we noticed that TLR7<sup>-/-</sup> B cells express slightly more Ii at the cell surface and in

LAMP-1 positive lysosomes in comparison to TLR7<sup>+/+</sup> B cells (Fig. 8E,F). Altogether, these results show that, in B cells, TLR stimulation increases MHCII antigen cross-presentation; Ii chain promotes TLR7-dependent adaptive but not innate function; and UNC93B1 has the opposite role to Ii in favoring innate, but not adaptive, response.

## DISCUSSION

The mechanisms by which intracellular TLRs are regulated remain poorly understood. Growing evidence has described the importance of a number of proteins such as the chaperone molecule UNC93B1, the MHCII complex, the clathrin adaptors (AP) and insulin responsive aminopeptidase (IRAP) in intracellular TLR trafficking, folding and signaling (Tabeta et al., 2006; Brinkmann

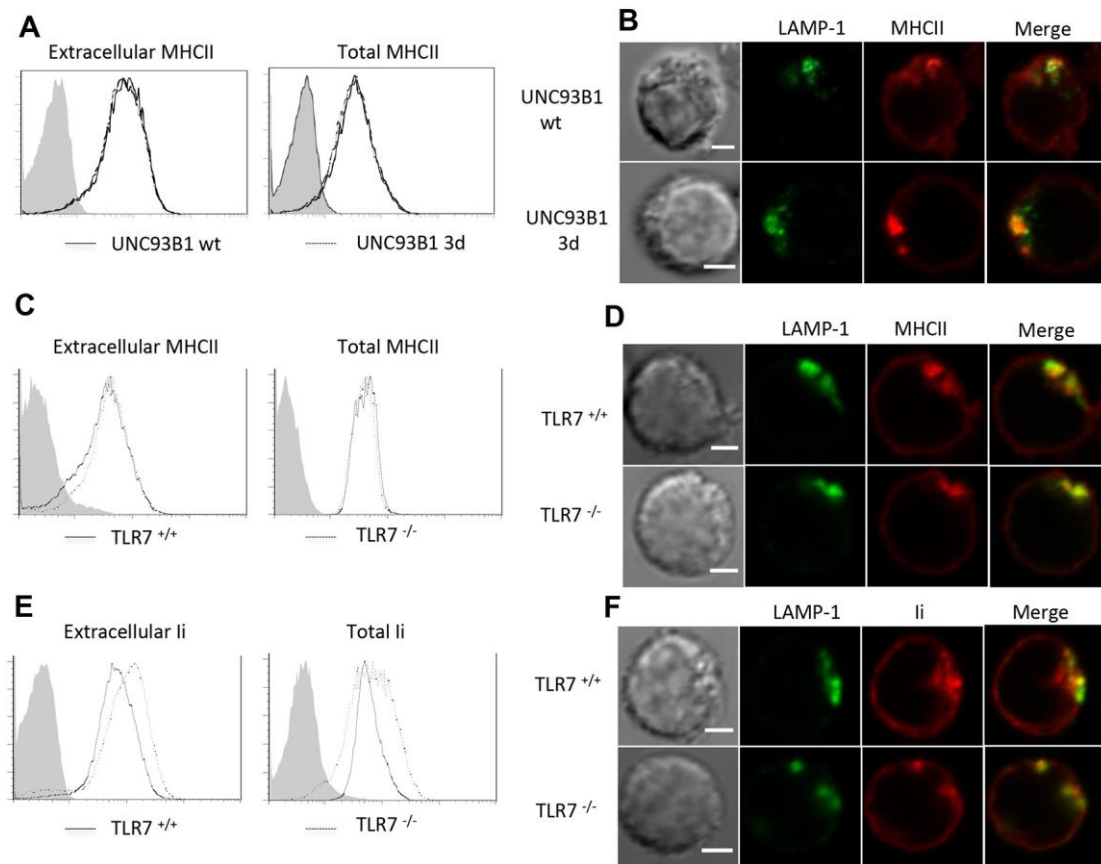


Fig. 8. MHCII and Ii chain expression and localization in TLR7- and UNC93B1-defective B cells. TLR7<sup>+/+</sup> (black lines), TLR7<sup>-/-</sup> (dashed lines) or WT (black lines), UNC93B1 mutated (dashed lines) splenic B cells were stained for MHCII (A,C) or Ii chain (E) using fluorescent antibodies. Gray histograms represent staining of B cells with the antibody isotype control. Immunofluorescence microscopy of WT, UNC93B1 mutated (B), TLR7<sup>+/+</sup>, TLR7<sup>-/-</sup> (D,F) B cells immunostained for LAMP-1 (green), MHCII (red) and Ii (red). One experiment representative of three is shown. Scale bars: 5 μm.

et al., 2007; Kim et al., 2008; Sasai et al., 2010; Liu et al., 2011; Lee et al., 2011; Babbor et al., 2017).

In resting cells, TLR9 resides in the ER and, after stimulation, it is addressed to endosomal compartments (Latz et al., 2004; Leifer et al., 2004) positive for VAMP3 (Sasai et al., 2013) and IRAP (Babbor et al., 2017). There, TLR9 is cleaved and triggers the recruitment of the adaptor molecule MyD88, NF-κB activation and subsequent production of pro-inflammatory cytokines. Then, processed TLR9 is translocated to lysosomal compartments containing LAMP-1, in an AP3-dependent manner. In lysosomes, TLR9 activates IRF and the secretion of type I interferon. In UNC93B1- or AP3-deficient cells, TLR9 remains in the ER or in VAMP3-positive endosomes, whereas in DCs lacking IRAP, TLR9 is localized in LAMP-1 lysosome, leading to enhanced cytokine secretion. In addition, AP2 facilitates TLR9 transport to the cell surface and subsequent internalization in the endosomes. It has been suggested that TLR7 instead requires AP4 to travel directly from the trans-Golgi network to the endosomes, bypassing cell surface localization (Lee et al., 2013). Thus, these results indicate that identifying the specific intracellular organelles in which TLR9 resides is crucial for the outcome of the innate immune response. However, very few studies have investigated TLR7 trafficking and signaling in antigen-presenting cells, especially in B cells, probably because of the lack of antibodies specific for endogenous TLR7.

The results presented here provide evidence for a novel pathway, by which Ii chain in B cells regulates TLR7 responses by influencing the subcellular localization of TLR7. Here, we show

that, in B cells, unstimulated or stimulated with TLR7 agonist, TLR7 resides in lysosomal compartments positive for MHCII, Ii chain, H-2DM and LAMP-1. In addition, the localization of TLR7 is unaltered in wt BCR cross-linked B cells. However, in Ii-deficient B cells, TLR7 relocalized partially in the ER. This suggests that expression of TLR7 in the ER might be required for the enhanced secretion of pro-inflammatory cytokines but not for the increase in MHCII antigen cross-presentation.

Two groups have recently described TLR9 trafficking and localization in B cells but nothing on TLR7 was reported. TLR7 and TLR9 trafficking require UNC93B1, a molecular chaperone, which controls their folding and transport from the ER to endolysosomes in macrophages and DCs (Kim et al., 2008; Pelka et al., 2018). Indeed, a single mutation within the UNC93B1 transmembrane domain is sufficient to abolish intracellular TLR signaling (Tabeta et al., 2006). The group of Pierce investigated endogenous TLR9 trafficking in primary B cells (Chaturvedi et al., 2008), while the group of Brinkmann generated a transgenic mouse expressing a TLR9-GFP fusion protein (Avalos et al., 2013). Pierce and colleagues reported that TLR9 resides in endosomal compartments positive for EEA1 and transferrin receptor in resting primary B cells. However, upon BCR cross-linking with labeled anti-IgM alone or together with CpG-DNA, TLR9 relocalized in LAMP-1 positive lysosomes, which contain internalized IgM (Chaturvedi et al., 2008). In contrast, the group of Brinkmann described TLR9-GFP localization in lysosomal compartments visualized by LysoTracker in resting B cells (Avalos

et al., 2013). In addition, they showed an alteration of TLR9 endosomal localization in UNC93B1-defective B cells, in which TLR9 was found in the ER and not in the lysosomes. The fact that these two groups used different tools to visualize TLR9 trafficking might account for the discrepancy observed.

Ii or CD74 is a critical chaperone for MHCII molecules (Cresswell, 1996). Ii was also shown to regulate MHCI trafficking from the ER to the endolysosomes (Basha et al., 2012). In addition, CD74 has been already characterized as an accessory signaling molecule by inducing activation of NF- $\kappa$ B p65/RelA homodimer and its co-activator TAF<sub>II</sub> 105 and the signaling cascade involving the Syk tyrosine kinase and the PI3K/Akt pathway resulting in B-cell proliferation, survival and development (Starlets et al., 2006). Interestingly, the lack of MHCII molecules resulted in reduced TLR3, TLR4 and TLR9 signaling in macrophages and DCs (Liu et al., 2011). Following TLR3, TLR4 and TLR9 stimulation, MHCII facilitates Btk phosphorylation and interaction with CD40 in the endosomes, thus promoting pro-inflammatory cytokine production. Surprisingly, our results showed no difference in TLR4-, TLR7- and TLR9-induced pro-inflammatory cytokine secretion in both wt and MHCII-deficient B cells. However, Ii seems to selectively regulate TLR7 responses in primary B cells. In fact, we show that, in the absence of Ii, TLR7 is found in the ER together with TAP1, calreticulin and calnexin, whereas in wt cells TLR7 preferentially localizes in Ii-, H2-DM-, MHCII- and LAMP-1-positive compartments. In addition to this specific TLR7 ER localization in Ii-deficient cells, B cells lacking Ii secrete significantly more cytokines when stimulated with TLR7. In contrast, TLR9 response remains intact in Ii-deficient B cells.

Why the lack of Ii triggers significant increase in cytokine production following TLR7 stimulation is still not elucidated. Interestingly, a connection between TLR7 stimulation and the molecular chaperone calreticulin has been described by the group of Jeffries (Byrne et al., 2013). Upon TLR7 stimulation, Btk kinase is phosphorylated and associates with calreticulin. Interaction between Btk and calreticulin induces calreticulin activation and transport to the cell surface, where it colocalizes with CD91. Btk-CD91 contact will allow the cells to uptake apoptotic debris. In addition, Btk is also shown to be involved in promoting optimal TLR9-driven cytokine production in macrophages and B cells (Hasan et al., 2008; Vijayan et al., 2011). In our study, we show colocalization of TLR7 with calreticulin and calnexin in B cells lacking Ii. Thus, perhaps TLR7 stimulation in Ii-deficient B cells induces Btk phosphorylation and association with calreticulin, promoting cytokine production. In addition, Ii chain and MyD88 might compete for the binding of TLR7. Thus, in the absence of Ii chain, more MyD88 molecules might associate with TLR7, resulting in an increase in cytokine production following TLR7 stimulation. We are currently performing experiments to address this hypothesis.

By performing Duolink experiments, we show that Ii forms a complex together with MyD88, suggesting a probable role for Ii, not only in facilitating transport of TLR7 from the ER to lysosomes, but also by contributing to the signaling complex containing TLR7. In addition, Ii contains targeting motifs, two di-leucine-based signals in its cytoplasmic tail, shown to be involved in MHCII-Ii complex trafficking to early endosomes either directly or via the plasma membrane (Pond et al., 1995). Ii interacts *in vitro* with the clathrin adaptors AP1 and AP2, and these interactions are dependent on the two di-leucine-based sorting motif in its tail (Hofmann et al., 1999). Also, TLR7 transport to lysosomes might require AP4. Whether or not the same di-leucine-based motifs in Ii also interact with TLR7

with the help of AP1, AP2 or AP4 and mediate TLR7 traffic in primary B cells remains to be investigated.

Cleavage of TLR7 is critical for its activation. Previous studies have described the role of different cysteine proteases in processing TLR7 in DCs and macrophages (Ewald et al., 2011; Maschalidi et al., 2012). However, in this study, we were not able to identify the proteases cleaving TLR7 in B cells. Indeed, AEP-, cathepsin B-, cathepsin L-, cathepsin S-deficient B cells show similar cytokine production upon imiquimod stimulation (Fig. S8). Furthermore, expression of cathepsins did not differ between Ii<sup>-/-</sup> and Ii<sup>+/+</sup> B cells, indicating that TLR7 processing might not be required in B cells, or that a yet unidentified protease might be involved. Indeed, work from the group of Cerundolo describes a role for furin-like proprotein convertases in TLR7 activation in human B cells (Hipp et al., 2013). However, we did not observe any difference in cytokine production between wt B cells and B cells incubated with a specific furin inhibitor following TLR7 stimulation (data not shown).

Interestingly, Ii deficiency favors TLR7-dependent innate and not adaptive response. Indeed TLR7 does not promote MHCI antigen cross-presentation in the absence of Ii in B cells. Furthermore, in B cells lacking TLR7, Ii expression and MHCII antigen presentation are increased. Altogether, these results demonstrate a mutual regulation between TLR7 and Ii and highlight a new role for Ii in maintaining a balance between innate and adaptive responses in B cells. In addition, these results uncover a new role for Ii in modulating MHCI and MHCII, and also TLR7, transport from the ER to the lysosomes.

In conclusion, these findings suggest that targeting Ii in pathological situations in which the TLR7 pathway is dysregulated, such as diabetes and lupus, could perhaps benefit the host.

## MATERIALS AND METHODS

### Mice

Female or male (8- to 12-week-old) Ii<sup>-/-</sup>, MHCII<sup>-/-</sup>, AEP<sup>-/-</sup>, cathepsin B<sup>-/-</sup>, cathepsin S<sup>-/-</sup> and cathepsin L<sup>-/-</sup> mice were backcrossed ten times on the C57Bl6 background, and bred in a pathogen-free environment at Institut Necker-Enfants Malades (INEM) and Institut Curie animal facilities. All animal care and experimental procedures were performed in accordance with the guidelines and regulations of the French Veterinary Department and approved by ethical committee (A-75-2003).

### Cells and stimulations

A single-cell suspension was generated by mechanical disruption of spleens from 8- to 12-week-old mice. Splenic IgM<sup>+</sup>/IgD<sup>+</sup> mature B cells were isolated using a CD19-positive selection kit [Miltenyi Biotec (130-121-301), 90–95% purity as determined by fluorescence-activated cell sorting (FACS)] and immature IgM<sup>+</sup>/IgD<sup>-</sup> B cells were isolated and collected by flow cytometry. The mouse lymphoma cell line IIA1.6 (Lankar et al., 2002) and the MOG T-cell hybridoma (kindly provided by S. Anderton, University of Edinburgh, Edinburgh, UK) were cultured in complete RPMI medium and were authenticated and tested for contamination. BMDCs and BDDMs were generated as previously described (Sepulveda et al., 2009). Cell differentiation was controlled by FACS (anti-CD11c, HL3 and anti-CD11b, M1/70, BD Biosciences). Plated cells in 96-well plates were treated overnight with the TLR ligands (LPS from Sigma-Aldrich; imiquimod, gardiquimod and resiquimod from Invivogen; CpGB, 5'-TGACTGTGAACGTTTCGAGATGA-3', from Trilink Biotechnologies) and goat affinity purified F(ab')<sub>2</sub> anti-IgM (10  $\mu$ g/ml) as a BCR ligand from MP Biomedicals. Cytokines were measured in supernatants using commercial ELISA kits (TNF- $\alpha$ , IL-6, eBioscience).

### Preparation of antigen-coated beads

To prepare antigen-coated beads, 4 $\times$ 10<sup>7</sup> 3  $\mu$ m latex NH2 beads (Polyscience) were activated with 8% glutaraldehyde for 2 h at room

temperature (RT). Beads were washed with PBS and incubated overnight (O/N) with different ligands: 100 µg/ml of F(ab')<sub>2</sub> goat anti-mouse-IgM and 100 µg/ml of MOG or MOG protein alone.

#### FACS staining

Cells were permeabilized with BD Cytofix/Cytoperm and then incubated with anti-TLR7 (ab24184, Abcam, 1:100), anti-Btk (ab25971, Abcam, 1:100), anti-CD69 (552879 clone H1, 2F3, BD Biosciences, 1:100), anti-CD40 (558695, clone 3/23, BD Biosciences, 1:100), anti-MHCII (Manoury et al., 2003, Y3P antibody, 1:250) and anti-Ii (555317, clone In-1, BD Biosciences, 1:200) in PBS 1% bovine serum albumin (BSA). Cells were then analyzed by flow cytometry (FACS Calibur) using FlowJo software.

#### Primary B cell transfection and immunofluorescence

Splenic purified B cells were stimulated with 35 µg/ml LPS in complete RPMI medium (10% FBS, 2 mM glutamine, 50 µg/ml penicillin/streptomycin, 50 µM β-mercaptoethanol, 25 mM HEPES, 1× non-essential amino acids, 1 mM sodium pyruvate) overnight at a concentration of 2×10<sup>6</sup> cells/ml. Then, 5×10<sup>6</sup> B cells were transfected with 2.5 µg cDNA coding for mouse full-length TLR7-HA tagged or for mouse full-length TLR9-GFP using a mouse B cell Amaxa kit (Lonza, Germany). Twenty-four hours later, cells were harvested and stimulated with TLR7, TLR9 ligands and/or BCR ligand for different times. For immunofluorescence studies, transfected B cells were grown on IBIDI channels (Biovalley) for 2 h, then stimulated and fixed with 4% paraformaldehyde for 10 min at RT and quenched in 100 mM glycine for 5 min. Fixed cells were permeabilized for 20 min and incubated at RT with anti-HA (3F10 clone, Sigma-Aldrich, 1:100), anti-GFP (1814460, Roche, 1:100), anti-H2DM (gift from D. Lankar, Institut Curie, Paris, France), anti-calreticulin (ab2907, Abcam, 1:200), anti-ERGIC-53 (ab129179, Abcam, 1:100), anti-Ii (555317, clone In-1, BD Biosciences, 1:100), anti-UNC93B1 (sc-135545, Santa Cruz Biotechnology, 1:100), anti-TAP1 (sc-11465, Santa Cruz Biotechnology, 1:100), anti-MHCII (Manoury et al., 2003, Y3P clone, 1:200), anti-VAMP3 (104203, SynapticSystems, 1:100) and anti-CD107α LAMP1 (553792, clone 1D4B, BD Biosciences, 1:200) antibodies in PBS, 0.2% BSA, 0.05% saponin for 1 h. Secondary antibodies (anti-mouse, anti-rat and anti-rabbit; 1:250) are from Jackson ImmunoResearch. Immunofluorescence images were acquired on a Zeiss confocal microscope (laser scanning confocal microscope LSM700; 63×/1.4 NA oil DicM27 plan apochromat objective) with the acquisition software Zen 2009, and were analysed and quantified with ImageJ software.

#### Lysotracker staining

Splenic B cells (2×10<sup>5</sup>) were grown on IBIDI channels (Biovalley) for 2 h in complete RPMI medium and were incubated with 75 nM Lysotracker Red (Molecular Probes, Invitrogen) for 30 min at 37°C. Time-lapse images were obtained every 10 min for 2 h with a Zeiss LSM confocal microscope.

#### In situ proximity ligation assay (PLA)

A Duolink *in situ* PLA kit was used according to the manufacturer's instructions (Olink, Biosciences) for *in situ* PLAs. Briefly, B cells were grown on coverslips and then fixed in 4% paraformaldehyde for 10 min before permeabilization in PBS, 0.05% saponin-0.2% BSA for 10 min. Cells were then blocked in 3% BSA/PBS and incubated with primary antibodies (anti-MyD88, D80F5, Cell Signaling Technology; anti-NF-κB, sc-372, Santa Cruz Biotechnology; anti-HA, CF29F4, Sigma-Aldrich; anti-Ii, 555317, clone In-1, BD Biosciences, and anti-GFP, ab290, Abcam; all at 1:100 dilution). After washing the cells, PLA probes were added, followed by hybridization, ligation and amplification for 90 min at 37°C. TLR7-Ii, MyD88-Ii, TLR9-Ii, Myd88-NF-κB and MHCII-Ii interactions (red) were visualized after incubation with the detection solution. Slides were analyzed by confocal microscopy. Quantification of mean fluorescence was performed using ImageJ software.

#### Real-time polymerase chain reaction

Total RNA was extracted from 5×10<sup>6</sup> splenic mature B cells using an RNeasy Mini Kit according to manufacturer's instructions (Qiagen). Corresponding cDNA was synthesized using a reverse transcriptase kit

from Promega. Real-time polymerase chain reaction (RT-PCR) was then performed using an ABI 7900 RT-PCR detection system (Applied Biosystems, Foster City, CA) in 10 µl reactions containing 1 µl of diluted cDNA, 300 nM of forward and reverse primers and SYBR Green PCR Master Mix (Thermo Fisher Scientific). Each sample was run in duplicate for *Tlr7* gene and the relative quantity (RQ) of mRNA was calculated based on the housekeeping gene *Hprt*. The sequences of the primers used are the following: Fw: 5'-CAGGCCAGATTGTGGAT-3'; Rv: 5'-TTGCGCTCATCTTAGGCTTT-3' for mouse *Hprt* and Fw: 5'-CCACAGGCTCACCCATACTTC-3'; Rv: 5'-GGGATGTCCTAGGTGGTGACA-3' for murine *Tlr7*.

#### Antigen presentation assays

*In vitro* cross-presentation assays were performed as previously described (Maschalidi et al., 2017). Briefly, Ii<sup>+/+</sup>, Ii<sup>-/-</sup> and TLR7<sup>-/-</sup> splenic B cells were incubated with 10 mg of soluble OVA or BSA and stimulated or not with 10 µg/ml imiquimod, 10 µg/ml CpGB or 1 µg/ml LPS. Then, CFSE-labeled OT-I T cells were added to the culture and the proliferation of T cells was monitored 3 days later. MOG antigen was coupled to glutaraldehyde-activated NH2 beads together with or without F(ab')<sub>2</sub> anti-mouse-IgM in equal concentrations. Spleen mature B (2×10<sup>5</sup> cells/well) cells from wt, UNC93B1 mutated and TLR7<sup>-/-</sup> mice were incubated with MOG-coated beads in the presence or absence of F(ab')<sub>2</sub> anti-mouse-IgM or with MOG peptide for 6 h at 37°C in 96-well plates. B cells were then washed and incubated with 10<sup>5</sup> MOG T-cell hybridoma for 24 h. IL-2 was measured in the supernatants using an ELISA kit from BD Biosciences.

#### Lentivirus infection

For shRNA experiments, purified pLKO.1 lentiviral plasmids carrying shRNA sequences for Ii (NM\_010545, Sigma-Aldrich) or control shRNA (SHC002, Sigma-Aldrich) were used to generate lentiviral particles. Briefly, HEK 293T packaging cells were co-transfected with the transfer (pLKO/shRNA), packaging (pPAX2) and envelope (pMD2G) plasmids, using GeneJuice Transfection Reagent (Novagen) as recommended by the manufacturer. Virus supernatant was titered and added to the cell culture containing the IIA1.6 B cell line at day 2 and at a multiplicity of 0.03 pg p24/cell. The medium was changed at day 3 and infected cells were selected with 4.5 µg/ml of puromycin added in the medium from day 4 to day 6. Several washes were done during the selection process to eliminate dead cells. Infected B cells were used for Duolink experiments and western blot analysis.

#### Constructs

Murine *Tlr7* and *Tlr9* constructs were generated as previously described (Serpulveda et al., 2009; Maschalidi et al., 2012). Briefly, *Tlr7* and *Tlr9* cDNAs containing the FL sequence followed by a HA tag or GFP tag were cloned into pcDNA3.1 by PCR of the pUNO mTLR7-HA or pUNO mTLR9-HA plasmid (Invivogen).

#### Imaging flow cytometry analysis (Imagestream)

Purified spleen B cells (3×10<sup>6</sup>) were first incubated in complete medium for 30 min at 37°C with or without TLR7 ligand (guardiquimod 1 µg/ml). Cells were then placed on ice and washed with FACS buffer (PBS, 5 mM EDTA, 3% fetal calf serum) before fixation and permeabilization using a BD Cytofix/Cytoperm kit (BD Biosciences) for 2 h. Fixed and permeabilized cells were incubated at room temperature for 30 min with anti-LAMP-1 (553792, clone 1D4B, Pharmingen, 1:200), anti-calnexin (kindly provided by E. Chevet, University of Rennes, Rennes, France, 1:200), anti-UNC93B1 and anti-TLR7 PE (565557, clone A94B10, BD Biosciences, 1:100). Secondary antibodies anti-rat Alexa Fluor 488 (712-605-143, Jackson ImmunoResearch, 1:200) and anti-rabbit Alexa Fluor 647 (711-545-152, Jackson ImmunoResearch, 1:100) antibodies were then added for 30 min at 4°C in the dark. After washing, cells were stained with 4',6-diamidino-2-phenylindole (DAPI) and image acquisition was performed. Samples were run on an Imagestream ISX mkII (Amnis Corp, Luminex, Seattle, WA) and 60× magnification was used for all acquisitions. Data were acquired using the INSPIRE software (Amnis Corp) and analyzed using IDEAS™ software (version 6.2 Amnis Corp). On average, 30,000–50,000 events were

collected in all experiments. Single-stain controls were run for each fluorochrome used and spectral compensation was performed. Cells were gated for single cells using the area and aspect ratio of the brightfield image, gated for focused cells using the gradient RMS feature, and viable cells were selected on the basis of positive expression of DAPI. LAMP-1, CNX and UNC93B1 masks were created to study the localization and expression of TLR7. TLR7 quantification was expressed as mean pixel intensity value, which is the intensity normalized to the surface area of the mask for each compartment. Normalization between  $Ii^{+/+}$ ,  $Ii^{-/-}$  was done by dividing this value by the mean pixel intensity of TLR7 of the mask of the whole cell.

## Statistics

Statistical significance was determined by unpaired Student's *t*-test or two-way ANOVA. \* $P < 0.05$ , \*\* $P < 0.01$  and \*\*\* $P < 0.001$ .

## Acknowledgements

We are grateful to S. Akira (Osaka, Japan) and N. Doyen (Institut Pasteur, France) for providing the TLR7<sup>-/-</sup> mice, and to the animal facility of the Institut Curie for hosting  $Ii^{-/-}$  mice. The UNC93B1 mutated mice (3d) were kindly provided by Dr B. Ryffel (CDTA, Orléans). We also thank N. Goudin, R. Desvieux and M. Garfa-Traore (Plateforme d'Imagerie Dynamique, Institut Necker, France) for their help with the confocal microscope and F. X. Mauvais (INEM, France) for advice on imaging flow cytometry. Cell sorting of immature B cells was performed with the help of S. Korniotis (UMR 8147, France).

## Competing interests

The authors declare no competing or financial interests.

## Author contributions

Conceptualization: M.T., M.D., S.M., B.M.; Methodology: M.T., L.M., K.A., M.D., S.M., B.M.; Validation: M.T., B.M.; Investigation: M.T.; Resources: B.M.; Writing - original draft: B.M.; Supervision: B.M.; Funding acquisition: B.M.

## Funding

This study was supported by a grant from Agence Nationale de la Recherche [MIDI 008 01 to B.M.] and PhD fellowships from Association de Recherche contre le Cancer, Institut Curie and Ministère de la Recherche et de la Technologie to S.M., M.T. and L.M., respectively.

## Supplementary information

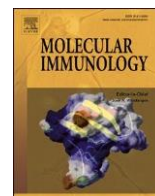
Supplementary information available online at <http://jcs.biologists.org/lookup/doi/10.1242/jcs.236711.supplemental>

## References

- Avalos, A. M., Kirak, O., Oelkers, J. M., Pils, M. C., Kim, Y.-M., Ottinger, M., Jaenisch, R., Ploegh, H. L. and Brinkmann, M. M. (2013). Cell-specific TLR9 trafficking in primary APCs of transgenic TLR9-GFP mice. *J. Immunol.* 190, 695-702. doi:10.4049/jimmunol.1202342
- Babdor, J., Descamps, D., Adiko, A. C., Tohmé, M., Maschalidi, S., Evnouchidou, I., Vasconcellos, L. R., De Luca, M., Mauvais, F.-X., Garfa-Traore, M. et al. (2017). IRAP<sup>+</sup> endosomes restrict TLR9 activation and signaling. *Nat. Immunol.* 18, 509-518. doi:10.1038/ni.3711
- Basha, G., Omilusik, K., Chavez-Steenbock, A., Reinicke, A. T., Lack, N., Choi, K. B. and Jefferies, W. A. (2012). A CD74-dependent MHC class I endolysosomal cross-presentation pathway. *Nat. Immunol.* 13, 237-245. doi:10.1038/ni.2225
- Brinkmann, M. M., Spooner, E., Hoebe, K., Beutler, B., Ploegh, H. L. and Kim, Y.-M. (2007). The interaction between the ER membrane protein UNC93B and TLR3, 7, and 9 is crucial for TLR signaling. *J. Cell. Biol.* 177, 265-275. doi:10.1083/jcb.200612056
- Byrne, J. C., NíGabhann, J., Stacey, K. B., Coffey, B. M., McCarthy, E., Thomas, W. and Jefferies, C. A. (2013). Bruton's tyrosine kinase is required for apoptotic cell uptake via regulating the phosphorylation and localization of calreticulin. *J. Immunol.* 190, 5207-5215. doi:10.4049/jimmunol.1300057
- Caetano, B. C., Carmo, B. B., Melo, M. B., Cerny, A., Dos Santos, S. L., Bartholomeu, D. C., Golenbock, D. T. and Gazzinelli, R. T. (2011). Requirement of UNC93B1 reveals a critical role for TLR7 in host resistance to primary infection with *Trypanosoma cruzi*. *J. Immunol.* 187, 1903-1911. doi:10.4049/jimmunol.1003911
- Casrouge, A., Zhang, S.-Y., Eidenschenk, C., Jouanguy, E., Puel, A., Yang, K., Alcais, A., Picard, C., Mahfoufi, N., Nicolas, N. et al. (2006). Herpes simplex virus encephalitis in human UNC-93B deficiency. *Science* 314, 308-312. doi:10.1126/science.1128346
- Chaturvedi, A., Dorward, D. and Pierce, S. K. (2008). The B cell receptor governs the subcellular location of Toll-like receptor 9 leading to hyperresponses to DNA-containing antigens. *Immunity* 28, 799-809. doi:10.1016/j.immuni.2008.03.019
- Cresswell, P. (1996). Invariant chain structure and MHCII function. *Cell* 4, 505-507. doi:10.1016/s0092-8674(00)81025-9
- Denzin, L. K. and Cresswell, P. (1995). HLA-DM induces CLIP dissociation from MHC class II  $\alpha$ B dimers and facilitates peptide loading. *Cell* 82, 155-165. doi:10.1016/0092-8674(95)90061-6
- Ewald, S. E., Engel, A., Lee, J., Wang, M., Bogoy, M. and Barton, G. M. (2011). Nucleic acid recognition by Toll-like receptors is coupled to stepwise processing by cathepsins and asparagine endopeptidase. *J. Exp. Med.* 4, 643-651. doi:10.1084/jem.20100682
- Ewald, S. E., Lee, B. L., Lau, L., Wickliffe, K. E., Shi, G.-P., Chapman, H. A. and Barton, G. M. (2008). The ectodomain of Toll-like receptor 9 is cleaved to generate a functional receptor. *Nature* 456, 658-662. doi:10.1038/nature07405
- Hasan, M., Lopez-Herrera, G., Blomberg, K. E. M., Lindvall, J. M., Berglöf, A., Smith, C. I. E. and Vargas, L. (2008). Defective Toll-like receptor 9-mediated cytokine production in B cells from Bruton's tyrosine kinase-deficient mice. *Immunology* 123, 239-249. doi:10.1111/j.1365-2567.2007.02693.x
- Heit, A., Huster, K. M., Schmitz, F., Schiemann, M., Busch, D. H. and Wagner, H. (2004). CpG-DNA aided cross-priming by cross-presenting B cells. *J. Immunol.* 172, 1501-1507. doi:10.4049/jimmunol.172.3.1501
- Hemmi, H., Kaisho, T., Sato, S., Sanjo, H., Hoshino, K., Horiuchi, T., Tomizawa, H., Takeda, K. and Akira, S. (2002). Small anti-viral compounds activate immune cells via the TLR7/MyD88-dependent signaling pathway. *Nat. Immunol.* 3, 196-200. doi:10.1038/ni758
- Hipp, M. M., Shepherd, D., Gileadi, U., Aichinger, M. C., Kessler, B. M., Edelmann, M. J., Essalmani, R., Seidah, N. G., Reis e Sousa, C. and Cerundolo, V. (2013). Processing of human toll-like receptor 7 by Furin-like proprotein convertases is required for its accumulation and activity in endosomes. *Immunity* 39, 711-721. doi:10.1016/j.immuni.2013.09.004
- Hofmann, M. W., Höning, S., Rodionov, D., Dobberstein, B., von Figura, K. and Bakke, O. (1999). The leucine-based sorting motifs in the cytoplasmic domain of the invariant chain are recognized by the clathrin adaptors AP1 and AP2 and their medium chains. *J. Biol. Chem.* 274, 36153-36158. doi:10.1074/jbc.274.51.36153
- Jiang, W., Lederman, M. M., Harding, C. V. and Sieg, S. F. (2011). Presentation of soluble antigens to CD8<sup>+</sup> T cells by CpG oligodeoxynucleotide-primed human naive B cells. *J. Immunol.* 186, 2080-2086. doi:10.4049/jimmunol.1001869
- Ke, Y. and Kapp, J. A. (1996). Exogenous antigens gain access to the major histocompatibility complex class I processing pathway in B cells by receptor-mediated uptake. *J. Exp. Med.* 184, 1179-1184. doi:10.1084/jem.184.3.1179
- Kim, Y.-M., Brinkmann, M. M., Paquet, M.-E. and Ploegh, H. L. (2008). UNC93B1 delivers nucleotide-sensing toll-like receptors to endolysosomes. *Nature* 452, 234-238. doi:10.1038/nature06726
- Lankar, D., Vincent-Schneider, H., Briken, V., Yokozeki, T., Raposo, G. and Bonnerot, C. (2002). Dynamics of major histocompatibility complex class II compartments during B cell receptor-mediated cell activation. *J. Exp. Med.* 195, 461-472. doi:10.1084/jem.20011543
- Latz, E., Schoenemeyer, A., Visintin, A., Fitzgerald, K. A., Monks, B. G., Knetter, C. F., Lien, E., Nilsen, N. J., Espevik, T. and Golenbock, D. T. (2004). TLR9 signals after translocating from the ER to CpG DNA in the lysosome. *Nat. Immunol.* 5, 190-198. doi:10.1038/ni1028
- Lee, B. L., Moon, J. E., Shu, J. H., Yuan, L., Newman, Z. R., Schekman, R. and Barton, G. M. (2013). UNC93B1 mediates differential trafficking of endosomal TLRs. *eLife* 2, e00291. doi:10.7554/eLife.00291
- Leifer, C. A., Kennedy, M. N., Mazzoni, A., Lee, C. W., Kruhlak, M. J. and Segal, D. M. (2004). TLR9 is localized in the endoplasmic reticulum prior to stimulation. *J. Immunol.* 173, 1179-1183. doi:10.4049/jimmunol.173.2.1179
- Leuchowius, K.-J., Weibrecht, I. and Söderberg, O. (2011). In situ proximity ligation assay for microscopy and flow cytometry. *Curr. Protoc. Cytom.* 56, 9.36.1-9.36.15. doi:10.1002/0471142956.cy0936s56
- Liu, X., Zhan, Z., Li, D., Xu, L., Ma, F., Zhang, P., Yao, H. and Cao, X. (2011). Intracellular MHC class II molecules promote TLR-triggered innate immune responses by maintaining activation of the kinase Btk. *Nat. Immunol.* 12, 416-424. doi:10.1038/ni.2015
- Lund, J. M., Alexopoulou, L., Sato, A., Karow, M., Adams, N. C., Gale, N. W., Iwasaki, A. and Flavell, R. A. (2004). Recognition of single-stranded RNA viruses by Toll-like receptor 7. *Proc. Natl. Acad. Sci. USA* 101, 5598-5603. doi:10.1073/pnas.0400937101
- Majer, O., Liu, B., Woo, B. J., Kreuk, L. S. M., Van Dis, E. and Barton, G. M. (2019). Release from UNC93B1 reinforces the compartmentalized activation of select TLRs. *Nature* 575, 371-374. doi:10.1038/s41586-019-1611-7
- Manoury, B., Mazzeo, D., Li, D. N., Billson, J., Loak, K., Benaroch, P. and Watts, C. (2003). Asparagine endopeptidase can initiate the removal of the MHC class II invariant chain chaperone. *Immunity* 4, 489-498. doi:10.1016/S1074-7613(03)00085-2
- Maschalidi, S., Hässler, S., Blanc, F., Sepulveda, F. E., Tohme, M., Chignard, M., van Ender, P., Si-Tahar, M., Descamps, D. and Manoury, B. (2012). Asparagine endopeptidase controls anti-influenza virus immune responses

- through TLR7 activation. *PLoS. Pathog.* 8, e1002841. doi:10.1371/journal.ppat.1002841
- Maschalidi, S., Nunes-Hasler, P., Nascimento, C. R., Sallent, I., Lannoy, V., Garfa-Traore, M., Cagnard, N., Sepulveda, F. E., Vargas, P., Lennon-Duménil, A.-M. et al. (2017). UNC93B1 interacts with the calcium sensor STIM1 for efficient antigen cross-presentation in dendritic cells. *Nat. Commun.* 8, 1640. doi:10.1038/s41467-017-01601-5
- Matsumoto, F., Saitoh, S.-I., Fukui, R., Kobayashi, T., Tanimura, N., Konno, K., Kusumoto, Y., Akashi-Takamura, S. and Miyake, K. (2008). Cathepsins are required for Toll-like receptor 9 responses. *Biochem. Biophys. Res. Commun.* 367, 693-699. doi:10.1016/j.bbrc.2007.12.130
- Melo, M. B., Kasperkowitz, P., Cerny, A., Könen-Waisman, S., Kurt-Jones, E. A., Lien, E., Beutler, B., Howard, J. C., Golenbock, D. T. and Gazzinelli, R. T. (2010). UNC93B1 mediates host resistance to infection with *Toxoplasma gondii*. *PLoS. Pathog.* 6, e1001071. doi:10.1371/journal.ppat.1001071
- Misawa, T., Takahama, M., Kozaki, T., Lee, H., Zou, J., Saitoh, T. and Akira, S. (2013). Microtubule-driven spatial arrangement of mitochondria promotes activation of the NLRP3 inflammasome. *Nat. Immunol.* 14, 454-460. doi:10.1038/ni.2550
- Park, B., Brinkmann, M. M., Spooner, E., Lee, C. C., Kim, Y.-M. and Ploegh, H. L. (2008). Proteolytic cleavage in an endolysosomal compartment is required for activation of Toll-like receptor 9. *Nat. Immunol.* 9, 1407-1414. doi:10.1038/ni.1669
- Pelka, K., Bertheloot, D., Reimer, E., Phulphagar, K., Schmidt, S. V., Christ, A., Stahl, R., Watson, N., Miyake, K., Hacohen, N. et al. (2018). The chaperone UNC93B1 regulates toll-like receptor stability independently of endosomal TLR transport. *Immunity* 48, 911-922.e7. doi:10.1016/j.immuni.2018.04.011
- Pond, L., Kuhn, L. A., Teyton, L., Schutze, M.-P., Tainer, J. A., Jackson, M. R. and Peterson, P. A. (1995). A role for acidic residues in di-leucine motif-based targeting to the endocytic pathway. *J. Biol. Chem.* 270, 19989-19997. doi:10.1074/jbc.270.34.19989
- Roche, P. A., Marks, M. S. and Cresswell, P. J. (1991). Formation of a nine-subunit complex by HLA class II glycoproteins and the invariant chain. *Nature* 354, 392-394. doi:10.1038/354392a0
- Sasai, M., Linehan, M. M. and Iwasaki, A. (2010). Bifurcation of Toll-like receptor 9 signaling by adaptor protein 3. *Science* 329, 1530-1534. doi:10.1126/science.1187029
- Sepulveda, F. E., Maschalidi, S., Colisson, R., Heslop, L., Ghirelli, C., Sakka, E., Lennon-Duménil, A.-M., Amigorena, S., Cabanie, L. and Manoury, B. (2009). Critical role for asparagine endopeptidase in endocytic Toll-like receptor signaling in dendritic cells. *Immunity* 31, 737-748. doi:10.1016/j.immuni.2009.09.013
- Starlets, D., Gore, Y., Binsky, I., Haran, M., Harpaz, N., Shvidel, L., Becker-Herman, S., Berrebi, A. and Shachar, I. (2006). Cell-surface CD74 initiates a signaling cascade leading to cell proliferation and survival. *Blood* 107, 4807-4816. doi:10.1182/blood-2005-11-4334
- Tabeta, K., Hoebe, K., Janssen, E. M., Du, X., Georgel, P., Crozat, K., Mudd, S., Mann, N., Sovath, S., Goode, J. et al. (2006). The Unc93b1 mutation 3d disrupts exogenous antigen presentation and signaling via Toll-like receptors 3, 7 and 9. *Nat. Immunol.* 7, 156-164. doi:10.1038/ni1297
- Teyton, L. and Peterson, P. A. (1992). Invariant chain—a regulator of antigen presentation. *Trends Cell. Biol.* 2, 52-56. doi:10.1016/0962-8924(92)90163-H
- Vijayan, V., Baumgart-Vogt, E., Naidu, S., Qian, G. and Immenschuh, S. (2011). Bruton's tyrosine kinase is required for TLR-dependent heme oxygenase-1 gene activation via Nrf2 in macrophages. *J. Immunol.* 187, 817-827. doi:10.4049/jimmunol.1003631
- Viville, S., Neefjes, J., Lotteau, V., Dierich, A., Lemeur, M., Ploegh, H., Benoist, C. and Mathis, D. (1993). Mice lacking the MHC class II-associated invariant chain. *Cell* 72, 635-648. doi:10.1016/0092-8674(93)90081-Z
- Yamazaki, T., Yoshimatsu, Y., Morishita, Y., Miyazono, K. and Watabe, T. (2009). COUP-TFII regulates the functions of Prox1 in lymphatic endothelial cells through direct interaction. *Genes Cells* 14, 425-434. doi:10.1111/j.1365-2443.2008.01279.x
- Zhong, G., Romagnoli, P. and Germain, R. N. (1997). Related leucine-based cytoplasmic targeting signals in invariant chain and major histocompatibility complex class II molecules control endocytic presentation of distinct determinants in a single protein. *J. Exp. Med.* 185, 429-438. doi:10.1084/jem.185.3.429





# The role of endoplasmic reticulum stress in the MHC class I antigen presentation pathway of dendritic cells

Bénédicte Manoury<sup>\*</sup>, Lucie Maisonneuve, Katrina Podsypanina<sup>\*</sup>

Institut Necker Enfants Malades, INSERM U1151- CNRS UMR 8253, Faculté de médecine Necker, Université de Paris, 156–160 rue de Vaugirard, 75015 Paris, France

## ARTICLE INFO

### Keywords:

Endoplasmic reticulum stress  
IRE1 $\alpha$   
Dendritic cells  
MHCI antigen presentation

## ABSTRACT

Dendritic cells (DCs) have the unique capacity to link innate to adaptive immunity. While most cells that express major histocompatibility (MHC) molecules are able to present antigens to activated T cells, DCs possess the means for presenting antigens to naïve T cells, and, as such, are able to instruct T cells to initiate immune response. There are two cascades of events necessary for DCs to start their instructive function. First, DCs enzymatically process proteins to make T cells recognize an antigen as unique peptide-MHC complexes. Second, DCs provide secretory cytokines and co-stimulatory functions for T cells to respond to this antigen. Thus, the compartments for protein degradation and for protein synthesis are central to DC function. The endoplasmic reticulum (ER), a vast network of membranes and vesicles, connects these compartments and helps modulate DC-specific performance, such as antigen capture and presentation. However, while the health of ER appears relevant for DC function, the intersection between ER stress and antigen presentation remains to be explored.

## 1. Brief introduction to dendritic cells maturation and function

Hematopoietic stem cells (HSC) in the bone marrow produce multipotents progenitors, which can give rise, to common dendritic cell progenitors (CDP) and pre-conventional CDP, precursors of conventional dendritic cells (cDC). Pre-cDC leaves the bone marrow to travel to the blood where they reach the lymphoid organs and the peripheral tissues to differentiate into cDCs. cDCs are defined by the expression of CD45, CD135, CD11c and Major histocompatibility complex class II (MHCII) and can be subdivided into two subsets: cDC1 and cDC2.

cDC1 and cDC2 in the lymph nodes (LN) can be resident or migratory arriving from the tissues by the afferent lymph. A few genes can distinguish cDCs from monocytes, pDCs, or other immune cell populations such as the zinc finger transcription factor *Zbtb46*, the *fms*-related receptor tyrosine kinase 3 (FLT3) and CCR7 and as such can be used to identify and manipulate cDCs in the experimental setting (Meredith et al., 2012). In addition, murine cDC1s express the CD8 $\alpha\alpha$  homodimer in lymphoid organs (lymph nodes, spleen, thymus) and the E-cadherin-binding integrin  $\alpha E$  or CD103 at the periphery and in tissues (Shortman, 2020). Thus, migratory CD103<sup>+</sup> cDC1s arrive to lymph nodes (LN) from peripheral tissues. The two cDC1 populations share

similar gene expression profiles, and in mice, expression of CD8 $\alpha\alpha$  and CD103 is used to discriminate between these two cDC1 subsets (Böttcher and Reis e Sousa, 2018). Furthermore, both cDC1 populations express the chemokine receptor XCR1 and the C-type lectin receptor DNGR-1 or CLEC9A (Ahrens et al., 2012). cDC2s do not express cDC1 markers and can be identified by their high expression of CD4, CD11b and SIRP $\alpha$ . More recently, specific transcription factors important for cDC development and differentiation uniquely expressed in cDC1 or cDC2 have been identified. Deletion of *Batf3*, *Irf8*, *Nfil3* and *Id2* results in loss of cDC1 at the steady state (Murphy et al., 2016; Hildner et al., 2008) and *Irf4* and *Irf2* in the absence or dysfunction of cDC2. In humans, DCs, which, are found in the blood, lymphoid organs and tissues, can also be subdivided into cDC1 and cDC2 based on the specific expression of XCR1, DGMR-1, BATF3 and IRF8 for cDC1 (Crozat et al., 2010; Collin and Ginhoux, 2019; Poulin et al., 2012) and SIRP $\alpha$  for cDC2. The development and proliferation of human and mouse DCs at the steady state is dependent on the *fms*-related tyrosine kinase 3 ligand (Flt3L) and GM-CSF, and may be used to generate DC-like cells from bone marrow (BMDCs) in vitro (Steinman, 2012).

DCs express a wide variety of innate immune receptors and as such are key sensor of pathogens (Janeway, 1989). For example, TLR3, an

Abbreviations: MHC, Major histocompatibility complex; DC, Dendritic cells; ER, Endoplasmic reticulum; IRE1 $\alpha$ , Insositol-requiring enzyme 1 $\alpha$ .

<sup>\*</sup> Corresponding authors.

E-mail addresses: [benedicte.manoury@inserm.fr](mailto:benedicte.manoury@inserm.fr) (B. Manoury), [lucie.maisonneuve@inserm.fr](mailto:lucie.maisonneuve@inserm.fr) (L. Maisonneuve), [katrina.podsypanina@inserm.fr](mailto:katrina.podsypanina@inserm.fr) (K. Podsypanina).

<https://doi.org/10.1016/j.molimm.2022.02.007>

Received 22 July 2021; Received in revised form 21 December 2021; Accepted 7 February 2022

Available online 17 February 2022

0161-5890/© 2022 Published by Elsevier Ltd.



endosomal TLR which recognizes double stranded RNA from virus infected cells, is highly expressed in cDC1 and when activated initiates cross priming of CD8<sup>+</sup> T cells against virus infected cells (Schulz et al., 2005). In contrast, TLR7, an endosomal TLR that senses single stranded RNA is only expressed in cDC2 (Edwards et al., 2003).

Upon recognition of specific microbial patterns, DCs will undergo a maturation process by up regulating their co-stimulatory molecules (CD80, CD86 and CD40) and the chemokine receptor CCR7 allowing them to migrate from the periphery to lymphoid tissues where they will present antigens to T cells. DC maturation unleashes acidification of the endosomal content, leading to the breakdown of protein antigens and the MHC class II-associated invariant chain and formation of MHCII-peptide complexes (Pierre et al., 1997). In addition, in DCs, exogenous proteins can be internalized, processed and loaded onto MHC class I (MHCI), a phenomenon known as cross-presentation (Blum et al., 2013). Antigenic processing and loading during MHCI antigen cross presentation can occur exclusively within the endosomal-phagosomal compartment (vacuolar pathway) or require a cytosolic step relying on antigenic degradation by the proteasome where antigens have to be transferred from phagosomes to cytosol (cytosolic pathway). In the cytosolic pathway, exogenous antigens are internalized in endosomal/phagosomal organelles, transported into the cytosol for partial degradation by the proteasome and readdressed either to the endosomal/phagosomal compartments or to the ER for loading onto MHCI molecules. MHCI antigen cross-presentation is especially efficient for antigens endocytosed by the cDC1 subset, while cDC2 are more efficient in presenting antigens to MHCII-restricted T cells, irrespective of the route of antigen capture (Kamphorst et al., 2010). Specialization of cDC1 for MHCI antigen cross presentation relies on (1) neutral endosomal-phagosomal PH to avoid excessive antigenic degradation and (2) expression of specific receptors for uptake of cell-associated antigens and transporters able to transfer phagosomal antigens to cytosol (Savina et al., 2006; Weimershaus et al., 2012, 2018; Zelenay et al., 2012; Zehner et al., 2015).

Because cDC1s efficiently cross-present exogenous cell-associated and soluble antigens on MHCI, they are the major presenters of antigens derived from pathogens (Shortman and Heath, 2010). Indeed, mature lymphoid-resident CD8 $\alpha$ <sup>+</sup> DCs are the main producers of IL-12 and stimulate inflammatory responses following bacterial infection (Shortman and Heath, 2010).

The outcome of the DC-T cell interaction is determined by the activation status of DCs. In the absence of maturation signals, antigen presentation by DCs leads to tolerance, most prominently through expansion of antigen-specific regulatory T (Treg) cells (Darrasse-Jèze et al., 2009). Antigen presentation by the mature DCs to CD8<sup>+</sup> T lymphocytes leads to activation of T cells and cytotoxicity (Chen and Mellman, 2013).

## 2. ER stress and its resolution

ER stress is a response to physiological signals, such as an increase in protein folding and assembly requirements, for example activation of hormone synthesis, antibody production and cytokine secretion. Such “physiological” ER stress also follows an increase in lipid and sterol biosynthesis, as may be required for endosome production and phagolysosome fusion. ER is also an important Ca<sup>2+</sup> reservoir and perturbation in Ca<sup>2+</sup> transport both follow ER stress and can induce ER stress (Krebs et al., 2015).

Resolution of the physiological ER stress proceeds through the “three actors” of the unfolded protein response (UPR): Inositol-requiring enzyme 1 $\alpha$  (IRE1 $\alpha$ ), activating transcription factor 6 (ATF6) and PKR-like ER kinase (PERK). Upon accumulation of misfolded proteins in the ER, BIP or binding immunoglobulin protein dissociates from these 3 sensors triggering their activation as well as the initiation of the UPR (Urano et al., 2000). All three pathways lead to transcriptional activation of genes coding for components of protein folding and membrane

assembly. IRE1 $\alpha$  does this by directly processing the mRNA of a master transcription factor, XBP1 for X Box Binding Protein 1, thanks to its ribonuclease activity (Bashir et al., 2021). Activated IRE1 $\alpha$  also degrades other mRNAs and microRNAs (called IRE1 $\alpha$ -dependent decay (RID), Bashir et al., 2021), and is associated with global shortening of transcripts (switch from distal to proximal polyadenylation site 3'UTR). This helps to reduce the load of misfolded transmembrane and secretory proteins, and participate in a process collectively referred to as ER-associated degradation (ERAD) (Tsai et al., 2002).

All UPR factors can be seen as a part of an UPosome, a dynamic multiprotein complex, interacting with proteins involved in the cell cycle, transport, differentiation, response to viral infection and immune response (Urta et al., 2020). Often studied as linear processes, recent evidence suggests that the crosstalk between branches amplifies ER stress relief (Vidal et al., 2021). There is also evidence for UPR crosstalk with DNA damage response (DDR) (Dufey et al., 2020).

In pathological situations ER stress becomes unresolvable and will result in cell death by apoptosis (Lin et al., 2007; Sano and Reed, 2013). Because dying DCs can then be engulfed by other DCs, the antigens of DC that failed to resolve ER stress, both cellular and exogenous, are presented either via MHCII to helper T cells, or cross-presented to cytotoxic T cells via MHCI, and lead to tolerance.

## 3. Antigen uptake and ER stress in immature DCs

The primary activity of immature DCs is antigen uptake. The scanning of the contents of the microenvironment involves continuous phagocytosis, macropinocytosis, and endocytosis. Internalized antigens are eventually directed to late endosomal compartment, where they await processing and loading onto MHCII molecules. However, downstream processing requires a maturation stimulus, that will trigger endosomal acidification and initiate the breakdown of protein antigens and the MHCII-associated invariant chain (Pierre et al., 1997). Thus, in immature DC, the MHCII molecules are largely sequestered within the endocytic system, and in the absence of an inflammatory signal there is no presentation to the naïve T cell compartment (van Niel et al., 2006).

The endogenous (cytosolic) proteins are processed primarily by the action of the proteasome. Proteasome-generated peptides are then transported into the ER by a specific molecular pump Transported for Antigen Processing, TAP, for subsequent assembly with MHCI molecules (Momburg et al., 1994). Thus, if the immature DCs experience ER stress, then the products of ERAD are more likely to be presented through MHCI. Such an outcome is expected because, while the substrates of ERAD are unfolded proteins in the ER, they are not degraded in the ER lumen, but rather retro-transported out of the ER lumen into the cytosol and degraded by the ubiquitin-proteasome system (Imai et al., 2020). Ultimately, such MHCI presentation of the ERAD products by immature DC will lead to tolerance. Thus, as long as ERAD products include only cellular proteins, ER stress in immature DCs is not expected to drive pathological immune response.

### 3.1. DC maturation and ER-stress-induced UPR response intersect at the innate immune sensing

Dendritic cell maturation, or activation, is induced when the phagocytosed or endocytosed cargo triggers innate immune signaling. The innate immune pathway is activated by a set of invariable molecules expressed in pathogens, such as lipopolysaccharide of the bacterial wall, RNA/DNA hybrid, or unmethylated DNA oligonucleotide. These molecules, called danger signals, ligate cellular Toll-like receptors (TLRs, Kawai and Akira, 2010). Ligation of the TLRs initiates a signaling cascade that culminates in activation and translocation to the nucleus of the master transcription factors NF- $\kappa$ B and IRF (interferon regulating factor). It might also leads, depending on the time and type of stimulation, to acceleration of phagosome maturation (Blander and Medzhitov, 2004; Alloatti et al., 2015) and to down-regulation of antigen

uptake. The NF- $\kappa$ B most likely acts as a pioneer factor to initiate the

epigenetic reprogramming toward activated DC phenotype (Blander and Medzhitov, 2004). Phenotypic markers of DC maturation typically include increased expression of CD40/80/86, as well as CD273 (PD-L2) and CD274 (PD-L1) (Blander and Medzhitov, 2004). ER stress in danger signal-exposed mature DCs may potentially lead to a situation where self-peptides together with non-self-peptides (depending on the context) are presented to T cells and trigger autoimmune inflammation.

Both macrophages and BMDCs exposed to bacterial lipopolysaccharide (LPS) (TLR4 agonist) or fungal zymosan (Dectin-1 and TLR2 agonist) exhibit IRE1 $\alpha$ -dependent Xbp1 splicing (Martinon et al., 2010; Chopra et al., 2019). However, this XBP1 activation is not accompanied by an upregulation of canonical XBP1 target genes, RIDD, or activation of other UPR branches. In turn, Xbp1 is necessary to maintain a normal morphology of the ER in CD8 $\alpha^+$  conventional dendritic cells, whereas RIDD has a critical function in regulating the expression of integrins and components of the MHC I antigen-presentation machinery in these cells. RIDD is necessary in CD8 $\alpha^+$  dendritic cells for cross-presentation of cell-derived antigens via MHC I to CD8 $^+$  T cells (Osorio et al., 2014).

The bulk production of MHC molecules themselves that takes place in the ER of DCs, may present challenges to the ER folding machinery. Moreover, the stability of the complexes MHC-antigenic peptides may depend on the nature of the peptide, and thus some peptide-MHC complexes may produce ER stress. This feature may underlie the requirement for constitutive XBP1 mRNA splicing for DC viability (Iwakoshi et al., 2007), and the constitutive IRE1 $\alpha$  activation in cDC1 (Osorio et al., 2014) suggests that partial UPR activation has anticipatory rather than an adaptive role, at least at the steady state. This view is further supported by the observation that RIDD activation helps DC survival, although only in tissue-specific context (Tavernier et al., 2017). In agreement with this, systematic bioinformatics analysis shows that IRE1 $\alpha$  interacts with partners involved in immune responses including antigen processing and presentation via MHC class I, cytokine production and secretion, and phagocytosis (Urrea et al., 2020).

Live parasites trigger innate immunity and as such may participate in the ER stress induced immune response. DCs infected by live but not heat killed *Toxoplasma gondii* induce the IRE1 $\alpha$  /XBP1s pathway. Stimulation of XBP1 leads to production of IL-6 and IL-12 while IRE1 $\alpha$  dependent but XBP1-independent activation elicits MHC I antigen presentation. Most importantly, altogether it produces an efficient T cell response for controlling parasite dissemination in *Toxoplasma gondii* infected mice (Poncet et al., 2021).

### 3.2. DC maturation and ER-stress-induced UPR response are sensitive to metabolic changes

Functionally, a critical initial step in maturation of DCs is the massive increase in production and secretion of inflammatory cytokines (Steinman, 2012). Production of some cytokines can increase more than 100-fold, indicating that the maturation can drastically change translational demands of DCs. In addition, activated DC initiates synthesis of new fatty acids for ER and Golgi expansion essential for production and secretion of cytokines. This synthesis critically depends on a burst of glycolytic flux within minutes of exposure to TLR agonists (Krawczyk et al., 2010). Importantly, metabolic perturbations translate into changes in DC activation pathway through activation of ER stress.

Blocking glycolysis with 2-deoxyglucose, which inhibits hexokinase activity, impairs both phenotypic and functional consequences of LPS-mediated DC activation in a transcription-independent fashion. Instead, the increase in the synthesis, transport and secretion of MHC and accessory molecules is dependent on the expansion of the ER and Golgi by lipogenesis and synthesis of additional membranes, which can be attenuated by the inhibition of fatty acid synthesis (Everts et al., 2014). Suppression of glycolysis also induces a distinct transcriptomic signature in DCs, with IL-23 as a hallmark, associated with some chronic inflammatory conditions, such as psoriasis, presumably due to

perturbations in tricarboxylic acid cycle metabolism following

fatty-acid-mediated suppression of TLR-induced hexokinase activity. Moreover, these metabolic changes enhance mitochondrial reactive oxygen species (mtROS) production that in turn activates UPR. Indeed, reducing mtROS production, or DC-specific deficiency in XBP1 attenuates IL-23 expression and skin inflammation in an IL-23-dependent model of psoriasis (Mogilenko et al., 2019).

In naïve DCs, metabolic by-products of lipid peroxidation, such as the unsaturated aldehyde 4-hydroxy-trans-2-nonenal (4-HNE), also fuel into DC maturation via the UPR pathway. 4-HNE causes ER stress by forming stable adducts with ER-resident chaperones. In response, IRE1 $\alpha$  activates XBP1, and XBP1-mediated production of triglyceride biosynthetic genes. In tumor-associated DCs, constitutive activation of XBP1 is a consequence of IRE1 $\alpha$  activation following ER stress linked to accumulation of oxidized lipids. Constitutive activation of XBP1s in this context diminishes DC immunogenicity, while XBP1-deficiency or IRE1 $\alpha$  RNase inhibitor 4 $\mu$ 8c reduces lipid biogenesis in DCs, and renders them more immunogenic. Mechanistically, 4-NHE-associated triglyceride accumulation in BMDC decreases surface expression of MHC I-peptide complexes and thus reduced CD8 $^+$  T cell proliferation, at least in the context of cancer. Accordingly, DC-specific XBP1 deletion or XBP1 silencing in DCs can restore their T cell stimulatory activity (Cubillos-Ruiz et al., 2015).

Although these studies suggest that IRE1 $\alpha$ -XBP1 pathway leads to suppressed immune response, at least in the context of tumor development, there is some circumstantial evidence suggesting that UPR can positively regulate DC-mediated presentation. For one, an XBP1 target gene is Sec61, an ER protein that is recruited into endosomes upon TLR activation and is thought to be required to translocate antigens for cross-presentation (Zehner et al., 2015). In fibroblasts, GADD34, another important component of the UPR, synergizes with TLR signaling for optimal type I IFN and IL-6 production (Clavarino et al., 2012), and type I IFNs is critical for the innate immune recognition by CD8 $^+$  DCs (Fuertes et al., 2011).

### 3.3. UPR shapes cytokine profiles of activated immune cells

IRE1 $\alpha$  loss in myeloid cells does not affect BMDC generation or survival in response to GM-CSF, but profoundly changes transcriptional output following LPS or zymosan exposure, and many of the differentially expressed genes are shared by the two stimuli. IRE1 $\alpha$  deficiency influenced transcriptional processes upon stimulation with agonists engaging plasma membrane-bound but not endosomal TLRs. Stimulated IRE1 $\alpha$ -deficient BMDCs express less IL-6 and its associated target genes. Posttranslational protein modification, cellular maintenance and survival, biosynthesis and metabolism of eicosanoids are also affected by IRE1 $\alpha$  deficiency (Chopra et al., 2019).

Endoplasmic reticulum stress-induced transcription factor, CHOP, is crucial for dendritic cell IL-23 expression (Goodall et al., 2010). Activation of the PERK/CHOP branch contributes to secretion of IL-6 in myeloid derived suppressor cells (MDSC) resulting in immunosuppressive effect in the context of tumor development (Thevenot et al., 2014).

### 3.4. Cross-presentation may change ER lipid bilayer composition

Lipid disequilibrium interferes with secretory capacity. When exposed to supernatants from ER-stressed tumor cells, cultured macrophages and Bone Marrow Derived Macrophages display transmissible ER stress, where hallmarks of activation, such as up regulation of IL-6, IL-23p19, and TNF- $\alpha$  transcripts, as well as an increase in CD86 surface expression are accompanied by up-regulation of Grp78, Gadd34, Chop, and Xbp-1 splicing (Mahadevan et al., 2011). BMDC are also subject to transmissible ER stress, resulting in impaired antigen cross-presentation to CD8 $^+$  T cells (Mahadevan et al., 2012). Tumor-associated DCs, (CD8 $^+$  cell population, which differs from the cross-presenting CD103 $^+$  cDC1s), compared with closely related CD11c $^+$ MHC-II $^+$ CD11b $^+$  splenic DCs,

show higher expression of total and spliced Xbp1 mRNA, accompanied by up regulation of canonical XBP1 target genes ERdj4 and Sec61a1, as well as general ER stress response markers Hspa5 (BiP) and Ddit3 (CHOP) (which are recruited to the promoters of Il-6, Il-23, and TNF- $\alpha$  following TLR activation in macrophages or monocyte-derived dendritic cells) (Martinon et al., 2010; Goodall et al., 2010), and up regulation of XBP1-controlled triglyceride biosynthetic genes, such as Agpat6, Fasn, Scd2, and Lpar1 (Cubillos-Ruiz et al., 2015).

The amplification of proinflammatory cytokine production that accompanies melanoma-induced IRE1 $\alpha$  activation suggests that DC response is exacerbated by high-fatty-acid tumor content. Interestingly, exposure of BMDCs to melanoma lysates is associated with activation of IRE1 $\alpha$  endonuclease. This activation is necessary for efficient cross-presentation of melanoma-associated antigens and enhances CD8<sup>+</sup> T cell specific responses against tumor antigens (Medel et al., 2019). Expression of CD11c-driven activated XBP1 (XBP1s) in BMDCs potentiate vaccine-induced immunity to tumor antigens and increased IL-6, IL-12, TNF- $\alpha$  production and CD86 expression (Tian et al., 2012). (Incidentally, immunogenic cancer cell death also occurs in ER stress-dependent manner, in large part through exposing intracellular danger signals, such as surface-exposed ER chaperones (Krysko et al., 2012)). In thymoma cells, ER stress affects processing of MHC I-associated peptides, cytosolic more than ER-based (Granados et al., 2009).

#### 4. Conclusion

DCs are professional antigen presenting cells uniquely capable of initiating immune response. Their ability to present antigens to non-activated effector T cells relies on decoding signals from their environment through the specific activation of pattern recognition receptors to generate an appropriate immune response. The different stages of the DC life cycle, including migration, maturation, antigen uptake, processing, and presentation, pose unique demands on the cellular organelles, including ER. Because of swift changes in protein, lipid, and calcium homeostasis associated with DCs maturation, these cells are prone to express some hallmarks of ER stress, most prominently the activation of IRE1 $\alpha$ , a branch of the UPR. The evidence of partial UPR activation by some DC subsets, and sensitivity to ER dysfunction suggest that anticipating ER stress is a central requirement for timely and robust antigen presentation by DCs.

#### Declaration of Competing Interests

The authors declare that they have no known competing financial interests or personal relationships that could have appeared to influence the work reported in this paper.

#### Acknowledgments

This work was supported by INSERM.

#### References

Ahrens, S., Zelenay, S., Sancho, D., Hanč, P., Kjør, S., Feest, C., Fletcher, G., Durkin, C., Postigo, A., Skehel, M., Batista, F., Thompson, B., Way, M., Reis e Sousa, C., Schulz, O., 2012. F-actin is an evolutionary conserved damage-associated molecular pattern recognized by DGMR-1, a receptor for dead cells. *Immunity* 36 (4), 635–645. <https://doi.org/10.1016/j.immuni.2012.03.008>.

Alloati, A., Kotsias, F., Pauwels, A.M., Carpiere, J.M., Jouve, M., Timmerman, E., Pace, L., Vargas, P., Maurin, M., Gehrmann, U., Joannas, L., Vivar, O.I., Lennon-Dumenil, A. M., Savina, A., Gevaert, K., Beyaert, R., Hoffmann, E., Amigorena, S., 2015. Toll-like receptor 4 engagement on dendritic cells restrains phago-lysosome fusion and promotes cross presentation of antigens. *Immunity* 43 (6), 1087–1100. <https://doi.org/10.1016/j.immuni.2015.11.006>.

Bashir, S., Bandy, M., Qadri, O., Bashir, A., Hilal, N., Nida-I-Fatima, Rader, S., Fazili, K. M., 2021. The molecular mechanism and functional diversity of UPR signaling sensor IRE1. *Life Sci. Jan 15* (265), 118740 doi: 10.1016/j.lfs.2020.118740.

Blander, J.M., Medzhitov, R., 2004. Regulation of phagosome maturation by signals from toll-like receptors. *Science* 304 (5673), 1014–1018. <https://doi.org/10.1126/science.109615>.

Blum, J.S., Wears, P.A., Cresswell, P., 2013. Pathway of antigen processing. *Ann. Rev. Immunol.* 31, 443–473. <https://doi.org/10.1146/annurev-immunol-032712-095910>.

Böttcher, P., Reis e Sousa, C., 2018. The role of type 1 conventional dendritic cells in cancer immunity. *Trends Cancer* 4 (11), 784–792. <https://doi.org/10.1016/j.trecan.2018.09.001>.

Chen, D.S., Mellman, I., 2013. Oncology meets immunology: the cancer-immunity cycle. *Immunity* 39 (1), 1–10. <https://doi.org/10.1016/j.immuni.2013.07.012>.

Chopra, S., Giovanelli, P., Alvarado-Vazquez, P.A., Alonso, S., Song, M., Sandoval, T.A., Chae, C.S., Tan, C., Fonseca, M.M., Gutierrez, S., Jimenez, L., Subbaramaiah, K., Iwakaki, T., Kingsley, P.J., Marnett, L.J., Kossenkov, A.V., Crespo, M.S., Dannenberg, A.J., Glimcher, L.H., Romero-Sandoval, E.A., Cubillos-Ruiz, J.R., 2019. IRE1 $\alpha$ -XBP1 signaling in leukocytes controls prostaglandin biosynthesis and pain. *Science* 365 (6450), eaau6499. <https://doi.org/10.1126/science.aau6499>.

Clavirino, G., Cláudio, N., Couderc, T., Dalet, A., Judith, D., Camosseto, V., Schmidt, E. K., Wenger, T., Lecuit, M., Gatti, E., Pierre, P., 2012. Induction of GADD34 is necessary for dsRNA-dependent interferon- $\beta$  production and participates in the control of Chikungunya virus infection. *PLoS Path.* 8 (5), e1002708 <https://doi.org/10.1371/journal.ppat.1002708>.

Collin, M., Ginhoux, F., 2019. Human dendritic cells. *Semin. Cell Dev. Biol.* 86, 1–2. <https://doi.org/10.1016/j.semdb.2018.04.015>.

Crozat, K., Guiton, R., Contreras, V., Feuillet, V., Dutertre, C.A., Ventre, E., Vu Manh, T. P., Baranek, T., Storset, A.K., Marvel, J., Boudinot, P., Hosmalin, A., Schwartz-Cornil, I., Dalod, M., 2010. The XC chemokine receptor 1 is a conserved selective marker of mammalian cells homologous to mouse CD8 $\alpha$  dendritic cells. *J. Exp. Med.* 207 (6), 1283–1292. <https://doi.org/10.1084/jem.20100223>.

Cubillos-Ruiz, J.R., Silberman, P.C., Rutkowski, M.R., Chopra, S., Perales-Puchalt, A., Song, M., Zhang, S., Bettigole, S.E., Gupta, D., Holcomb, K., Ellenson, L.H., Caputo, T., Lee, A.H., Conejo-Garcia, J.R., Glimcher, L.H., 2015. ER stress sensor XBP1 controls anti-tumor immunity by disrupting dendritic cell homeostasis. *Cell* 161 (7), 1527–1538. <https://doi.org/10.1016/j.cell.2015.05.025>.

Darrasse-Jèze, G., Deroubaix, S., Mouquet, H., Victora, G.D., Eisenreich, T., Yao, K.H., Masilamani, R.F., Dustin, M.L., Rudensky, A., Liu, K., Nussenzweig, M.C., 2009. Feedback control of regulatory T cell homeostasis by dendritic cells in vivo. *J. Exp. Med.* 206 (9), 1853–1862. <https://doi.org/10.1084/jem.20090746>.

Dufey, E., Bravo-San Pedro, J.M., Eggers, C., González-Quiroz, M., Urrea, H., Sagredo, A. I., Sepulveda, D., Pihán, P., Carreras-Sureda, A., Hazari, Y., Sagredo, E.A., Gutierrez, D., Valls, C., Papaioannou, A., Acosta-Alvarez, D., Campos, G., Domingos, P.M., Pedoux, R., Chevot, E., Alvarez, A., Godoy, P., Walter, P., Glavic, A., Kroemer, G., Hetz, C., 2020. Genotoxic stress triggers the activation of IRE1 $\alpha$ -dependent RNA decay to modulate the DNA damage response. *Nat. Commun.* 11 (1), 2401. <https://doi.org/10.1038/s41467-020-15694-y>.

Edwards, A.D., Diebold, S.S., Slack, E.M., Tomizawa, H., Hemmi, H., Kaisho, T., Akira, S., Reis e Sousa, C., 2003. Toll-like receptor expression in murine DC subsets: lack of TLR7 expression by CD8 $\alpha$  DCs correlates with unresponsiveness to imidazoquinolines. *Eur. J. Immunol.* 33 (4), 827–833. <https://doi.org/10.1002/eji.200323797>.

Everts, B., Amiel, E., Huang, S.C., Smith, A.M., Chang, C.H., Lam, W.Y., Redmann, V., Freitas, T.C., Blagih, J., van der Windt, G.J., Artymov, M.N., Jones, R.G., Pearce, E. L., Pearce, E.J., 2014. TLR-driven early glycolytic reprogramming via the kinases TBK1-IRK1 supports the anabolic demands of dendritic cell activation. *Nat. Immunol.* 15 (4), 323–332. <https://doi.org/10.1038/ni.2833>.

Fuertes, M.B., Kacha, A.K., Kline, J., Woo, S.R., Kranz, D.M., Murphy, K.M., Gajewski, T., 2011. Host type I IFN signals are required for antitumor CD8<sup>+</sup> T cell responses through CD8 $\alpha$  dendritic cells. *J. Exp. Med.* 208 (10), 2005–2016. <https://doi.org/10.1084/jem.20101159>.

Goodall, J.C., Wu, C., Zhang, Y., McNeill, L., Ellis, L., Saudek, V., Gaston, J.S., 2010. Endoplasmic reticulum stress-induced transcription factor, CHOP, is crucial for dendritic cell IL-23 expression. *Proc. Natl. Acad. Sci. USA* 107 (41), 17698–17703. <https://doi.org/10.1073/pnas.1011736107>.

Granados, D.P., Tanguay, P.L., Hardy, M.P., Caron, E., de Verteuil, D., Meloche, S., Perreault, C., 2009. ER stress affects processing of MHC class I-associated peptides. *BMC Immunol.* 10, 10. <https://doi.org/10.1186/1471-2172-10-10>.

Hildner, K., Edelson, B.T., Purtha, W.E., Diamond, M., Matsushita, H., Kohyama, M., Calderon, B., Schraml, B.U., Unanue, E.R., Diamond, M.S., Schreiber, R.D., Murphy, T.L., Murphy, K.M., 2008. Baft3 deficiency reveals a critical role for CD8 $\alpha$  dendritic cells in cytotoxic T cell immunity. *Science* 322 (5904), 1097–1100. <https://doi.org/10.1126/science>.

Imai, J., Ohashi, S., Sakai, T., 2020. Endoplasmic reticulum-associated degradation-dependent processing in cross-presentation and its potential for dendritic cell vaccinations: a review. *Pharmaceutics* 12 (2), 153. <https://doi.org/10.3390/pharmaceutics12020153>.

Iwakoshi, N.N., Pypaert, M., Glimcher, L.H., 2007. The transcription factor XBP-1 is essential for the development and survival of dendritic cells. *J. Exp. Med.* 204 (10), 2267–2275. <https://doi.org/10.1084/jem.20070525>.

Janevay, C.A., 1989. Approaching the asymptote? Evolution and revolution in immunology. *Cold Spring Harb. Symp. Quant. Biol.* 54 (Pt 1), 1–13. <https://doi.org/10.1101/sqb.1989.054.01.003>.

Kamphorst, A.O., Guermonez, P., Dudziak, D., Nussenzweig, M.C., 2010. Route of antigen uptake differentially impacts presentation by dendritic cells and activated monocytes. *J. Immunol.* 185 (6), 3426–3435. <https://doi.org/10.4049/jimmunol.1001205>.

Kawai, T., Akira, S., 2010. The role of pattern-recognition receptors in innate immunity: update on Toll-like receptors. *Nat. Immunol.* 11 (5), 373–384. <https://doi.org/10.1038/ni.1863>.

- Krawczyk, C.M., Holowka, T., Sun, J., Blagih, J., Amiel, E., DeBerardinis, R.J., Cross, J. R., Jung, E., Thompson, C.B., Jones, R.G., Pearce, E.J., 2010. Toll-like receptor-induced changes in glycolytic metabolism regulate dendritic cell activation. *Blood* 115 (23), 4742–4749. <https://doi.org/10.1182/blood-2009-10-249540>.
- Krebs, J., Agellon, L.B., Michalak, M., 2015. Ca(2+) homeostasis and endoplasmic reticulum (ER) stress: an integrated view of calcium signaling. *Biochem. Biophys. Res. Commun.* 460 (1), 114–121. <https://doi.org/10.1016/j.bbrc.2015.02.004>.
- Krysko, D.V., Garg, A.D., Kaczmarek, A., Krysko, O., Agostinis, P., Vandenabeele, P., 2012. Immunogenic cell death and DAMPs in cancer therapy. *Nat. Rev. Cancer* 12 (12), 860–875. <https://doi.org/10.1038/nrc3380>.
- Lin, J.H., Li, H., Yasumura, D., Cohen, H.R., Zhang, C., Panning, B., Shokat, K.M., Lavail, M.M., Walter, P., 2007. IRE1 signaling affects cell fate during the unfolded protein response. *Science* 318 (5852), 944–949. <https://doi.org/10.1126/science.1146361>.
- Mahadevan, N.R., Rodvold, J., Sepulveda, H., Rossi, S., Drew, A.F., Zanetti, M., 2011. Transmission of endoplasmic reticulum stress and pro-inflammation from tumor cells to myeloid cells. *Proc. Natl. Acad. Sci. USA* 108 (16), 6561–6566. <https://doi.org/10.1073/pnas.1008942108>.
- Mahadevan, N.R., Anufreichik, V., Rodvold, J.J., Chiu, K.T., Sepulveda, H., Zanetti, M., 2012. Cell-extrinsic effects of tumor ER stress impart myeloid dendritic cells and impair CD8+ T cell priming. *PLOS One* 7 (12), e51845. <https://doi.org/10.1371/journal.pone.0051845>.
- Martinson, F., Chen, X., Lee, A.H., Glimcher, L.H., 2010. TLR activation of the transcription factor XBP1 regulates innate immune responses in macrophages. *Nat. Immunol.* 11 (5), 411–418. <https://doi.org/10.1038/ni.1857>.
- Medel, B., Costoya, C., Fernandez, D., Pereda, C., Lladser, A., Sauma, D., Pacheco, R., Iwakaki, T., Salazar-Onfray, F., Osorio, F., 2019. IRE1 $\alpha$  activation in bone marrow-derived dendritic cells modulates innate recognition of melanoma cells and favors CD8+ T cell priming. *Front. Immunol.* 9, 3050. <https://doi.org/10.3389/fimmu.2018.03050>.
- Mereditth, M.M., Liu, K., Darrasse-Jeze, G., Kamphorst, A.O., Schreiber, H.A., Guermontprez, P., Idoyaga, J., Cheong, C., Yao, K.H., Nee, R.E., Nussenzweig, M.C., 2012. Expression of the zinc finger transcription factor ZDC (Zbtb46, Btbd4) defines the classical dendritic cell lineage. *J. Exp. Med.* 209 (6), 1153–1165. <https://doi.org/10.1084/jem.20112675>.
- Mogilenko, D.A., Haas, J.T., L'homme, L., Fleury, S., Quemener, S., Levavasseur, M., Becquart, C., Wartelle, J., Bogomolova, A., Pineau, L., Molendi-Coste, O., Lancel, S., Dehondt, H., Gheeraert, C., Melchior, A., Dewas, C., Nikitin, A., Pic, S., Rabhi, N., Annicotte, J.S., Oyadomari, S., Velasco-Hernandez, T., Cammenga, J., Foretz, M., Viollet, B., Vukovic, M., Villacreses, A., Kranc, K., Carmeliet, P., Marot, G., Boulter, A., Tavernier, S., Berod, L., Longhi, M.P., Paget, C., Janssens, S., Staumont-Sallé, D., Aksoy, E., Staels, B., Dombrowicz, D., 2019. Metabolic and innate immune cues merge into a specific inflammatory response via the UPR. *Cell* 177 (5), 1201–1216. <https://doi.org/10.1016/j.cell.2019.03.018>.
- Momburg, F., Neefjes, J.J., Hämmerling, G.J., 1994. Peptide selection by MHC-encoded TAP transporters. *Curr. Opin. Immunol.* 6 (1), 32–37. [https://doi.org/10.1016/0952-7915\(94\)90030-2](https://doi.org/10.1016/0952-7915(94)90030-2).
- Murphy, T.L., Grajales-Reyes, G.E., Wu, X., Tussiwand, R., Briseño, C.G., Iwata, A., Kretzer, N.M., Durai, V., Murphy, K.M., 2016. Transcriptional control of dendritic cell development. *Annu. Rev. Immunol.* 34, 93–119. <https://doi.org/10.1146/annurev-immunol-032713-120204>.
- Osorio, F., Tavernier, S.J., Hoffmann, E., Saeys, Y., Martens, L., Vettters, J., Delrue, I., De Rycke, R., Parthoens, E., Pouliot, P., Iwakaki, T., Janssens, S., Lambrecht, B.N., 2014. The unfolded-protein-response sensor IRE-1 $\alpha$  regulates the function of CD8 $\alpha$ + dendritic cells. *Nat. Immunol.* 15 (3), 248–257. <https://doi.org/10.1038/ni.2808>.
- Pierre, P., Turley, S.J., Gatti, E., Hull, M., Meltzer, J., Mirza, A., Inaba, K., Steinman, R. M., Mellman, I., 1997. Developmental regulation of MHC class II transport in mouse dendritic cells. *Nature* 388 (6644), 787–792. <https://doi.org/10.1038/42039>.
- Poncet, A.F., Bosteels, V., Hoffmann, E., Chehade, S., Rennen, S., Huot, L., Peucelle, V., Maréchal, S., Khalife, J., Blanchard, N., Janssens, S., Marion, S., 2021. The UPR sensor IRE1 $\alpha$  promotes dendritic cells responses to control toxoplasma gondii infection. *EMBO Rep.* 22 (3), e49617. <https://doi.org/10.15252/embr.201949617>.
- Poulin, L.F., Reyat, Y., Uronen-Hansson, H., Schraml, B.U., Sancho, D., Murphy, K.M., Håkansson, U.K., Moita, L.F., Agace, W.W., Bonnet, D., Reis e Sousa, C., 2012. DGNR-1 is a specific and universal marker of mouse and human Batf3-dependent dendritic cells in lymphoid and nonlymphoid tissues. *Blood* 119 (25), 6052–6062. <https://doi.org/10.1182/blood-2012-01-406967>.
- Sano, R., Reed, J.C., 2013. ER stress-induced cell death mechanisms. *Biochim. Biophys. Acta* 1833 (12), 3460–3470. <https://doi.org/10.1016/j.bbamcr.2013.06.028>.
- Savina, A., Jancic, C., Hugues, S., Guermontprez, P., Vargas, P., Moura, I.C., Lennon-Duménil, A.M., Seabra, M.C., Raposo, G., Amigorena, S., 2006. NOX2 controls phagosomal pH to regulate antigen processing during crosspresentation by dendritic cells. *Cell* 126 (1), 205–218. <https://doi.org/10.1016/j.cell.2006.05.035>.
- Schulz, O., Diebold, S.S., Chen, M., Näsrlund, T.I., Nolte, M.A., Alexopoulou, L., Azuma, Y. T., Flavell, R.A., Liljeström, P., Reis e Sousa, C., 2005. Toll-like receptor 3 promotes cross priming to virus-infected cells. *Nature* 433 (7028), 887–892. <https://doi.org/10.1038/nature03326>.
- Shortman, K., 2020. Dendritic cell development: a personal historical perspective. *Mol. Immunol.* 119, 64–68. <https://doi.org/10.1016/j.molimm.2019.12.016>.
- Shortman, K., Heath, W.R., 2010. The CD8+ dendritic cell subset. *Immunol. Rev.* 234 (1), 18–31. <https://doi.org/10.1111/j.0105-2896.2009.00870.x>.
- Steinman, R., 2012. Decision about dendritic cells: past, present, and future. *Annu. Rev. Immunol.* 30, 1–22. <https://doi.org/10.1146/annurev-immunol-100311-102839>.
- Tavernier, S.J., Osorio, F., Vandersarren, L., Vettters, J., Vanlangenakker, N., Van Isterdael, G., Vergote, K., De Rycke, R., Parthoens, E., van de Laar, L., Iwakaki, T., Del Valle, J.R., Hu, C.C., Lambrecht, B.N., Janssens, 2017. Regulated IRE1-dependent mRNA decay sets the threshold for dendritic cell survival. *Nat. Cell. Biol.* 19 (6), 698–710. doi: 10.1038/ncb3518.
- Thevenot, P.T., Sierra, R.A., Raber, P.L., Al-Khami, A.A., Trillo-Tinoco, J., Zareii, P., Ochoa, A.C., Cui, Y., Del Valle, L., Rodriguez, P.C., 2014. The stress-response sensor chop regulates the function and accumulation of myeloid-derived suppressor cells in tumors. *Immunity* 41 (3), 389–401. <https://doi.org/10.1016/j.immuni.2014.08.015>.
- Tian, S., Liu, Z., Donahue, C., Falo jr, D.F., You, Z., 2012. Genetic targeting of the active transcription factor XBP1s to dendritic cells potentiates vaccine-induced prophylactic and therapeutic antitumor immunity. *Mol. Ther.* 20 (2), 432–442.
- Tsai, B., Ye, Y., Rapoport, T.A., 2002. Retro-translocation of proteins from the endoplasmic reticulum into the cytosol. *Nat. Rev. Mol. Cell. Biol.* 3 (4), 246–255. <https://doi.org/10.1038/nrm780>.
- Urano, F., Bertolotti, A., Ron, D., 2000. IRE1 and efferent signaling from the endoplasmic reticulum. *J. Cell. Sci.* 113 (Pt 21), 3697–3702 (Nov).
- Urra, H., Pihán, P., Hetz, C., 2020. The UPRosome – decoding novel biological outputs of IRE1 $\alpha$  function. *J. Cell. Sci.* 133 (15), jcs218107. <https://doi.org/10.1242/jcs.218107>.
- van Niel, G., Wubolts, R., Ten Broeke, T., Buschow, S.I., Ossendorp, F.A., Melief, C.J., Raposo, G., van Balkom, B.W., Stoorvogel, W., 2006. Dendritic cells regulate exposure of MHC class II at their plasma membrane by oligoubiquitination. *Immunity* 25 (6), 885–894. <https://doi.org/10.1016/j.immuni.2006.11.001>.
- Vidal, R.L., Sepulveda, D., Troncoso-Escudero, P., Garcia-Huerta, P., Gonzalez, C., Plate, L., Jerez, C., Canovas, J., Rivera, C.A., Castillo, V., Cisternas, M., Leal, S., Martinez, A., Grandjean, J., Sonia, D., Lashuel, H.A., Martin, A.J.M., Latapiat, V., Matus, S., Sardi, S.P., Wiseman, R.L., Hetz, C., 2021. Enforced dimerization between XBP1s and ATF6f enhances the protective effects of the UPR in models of neurodegeneration. *Mol. Ther.* 29 (5), 1862–1882. <https://doi.org/10.1016/j.ymthe.2021.01.033>.
- Weimershaus, M., Maschalidi, S., Sepulveda, F., Manoury, B., van Endert, P., Saveanu, L., 2012. Conventional dendritic cells require IRAP-Rab14 for efficient antigen cross presentation. *J. Immunol.* 188 (4), 1840–1846. <https://doi.org/10.4049/jimmunol.1101504>.
- Weimershaus, M., Mauvais, F.X., Saveanu, L., Adiko, C., Babdor, J., Abramova, A., Montealegre, S., Lawand, M., Evnouchidou, I., Huber, K.J., Chadt, A., Zwick, M., Vargas, P., Dussiot, M., Lennon-Dumenil, A.M., Brocker, T., Al-Hasani, H., van Endert, P., 2018. Innate immune signals induce anterograde endosomal transport promoting MHC class I antigen cross presentation. *Cell Rep.* 24 (13), 3568–3581. <https://doi.org/10.1016/j.celrep.2018.08.041>.
- Zehner, M., Marschall, A.L., Bos, E., Schloetel, J.G., Kreer, C., Fehrenschild, D., Limmer, A., Ossendorp, F., Lang, T., Koster, A.J., Dübel, S., Burgdorf, S., 2015. The translocon protein Sec61 mediates antigen transport from endosomes in the cytosol for cross-presentation to CD8(+) T cells. *Immunity* 42 (5), 850–863. <https://doi.org/10.1016/j.immuni.2015.04.008>.
- Zelenay, S., Keller, A.M., Whitney, P.G., Schraml, B.U., Deddouche, S., Rogers, N.C., Schulz, O., Sancho, D., Reis e Sousa, C., 2012. The dendritic cell receptor DGNR-1 controls endocytic handling of necrotic cell antigens to favor cross-priming of CTL in virus-infected mice. *J. Clin. Investig.* 122 (5), 1615–1627. <https://doi.org/10.1172/JCI60644>.



# In vitro and in vivo assays to evaluate Dendritic Cell phagocytic capacity

Lucie Maisonneuve<sup>1</sup> and Bénédicte Manoury<sup>1</sup>

1. Institut Necker Enfants Malades, INSERM U1151-CNRS UMR 8253, Université de Paris, Faculté de Médecine Necker

## Abstract

Phagocytosis is a process by which specific immune cells such as macrophages or dendritic cells engulf large particles. It is an important innate immune defence mechanism for removing a wide variety of pathogens and apoptotic cells. Following phagocytosis, nascent phagosomes are formed which, when fused to lysosome to become phago-lysosome containing acidic proteases, will allow the degradation of ingested material. The protocol described here in vitro and in vivo assays to measure phagocytosis in murine dendritic cells using amine beads coupled with streptavidin Alexa 488. This protocol can also be applied to monitor phagocytosis in human dendritic cells.

**Key words** Phagocytosis, Dendritic cells, Amine beads, Streptavidin A488, Flow cytometry.

## 1 Introduction

Phagocytic cells such as neutrophils, macrophages and dendritic cells (DCs) play an important role in innate immunity, internalizing foreign particles or microbes that could be harmful for our organism (1). In DCs, phagocytosis play a major role in antigen cross presentation, consisting of presentation of exogenous antigens on major histocompatibility complex (MHC) class I molecules. This process is essential for the priming of cytotoxic CD8<sup>+</sup> T cells against viruses and tumour antigens (2-3). Internalization of antigens or infected cells in DCs trigger phagosome formation which when fused to lysosome allows the proteolysis of ingested material. In DCs, nascent phagosome contain low level of acidic proteases preserving the excessive proteolysis of antigens and thus favouring MHC class I antigen cross presentation (4-6). Several bacterial factors, such as clostridium botulinum, Helicobacter Pylori, Mycobacterium tuberculosis, are known to inhibit phagocytosis or to delay phago-lysosome fusion protecting them from degradation and recognition by the immune system (7-8). Measuring phagocytic capacity of DCs has consequently becomes valuable in several pathogenic infection, as well as to understand how each type of DC take up and present antigens especially for type 1 conventional DC (cDC1) which are highly efficient in cross presenting antigens. Several methods have been written in past publications on phagocytosis assays, describing the use of beads (latex beads, lipid-coated beads, amine-coated beads, etc.) as particles engulfed by the cells. Often coupled to fluorescent dyes or probes, cells phagocytic capacity can be measured using flow cytometry or cytometry imaging.

This chapter will describe a phagocytosis assay using amine beads of different size coupled to streptavidin and the fluorophore Alexa Fluor 488 in DCs generating in vitro or freshly purified ex vivo. In this assay, amine beads of different diameter are used for assessing phagocytosis in vitro either in Bone-Marrow-Derived-DC (BM-DC) (9) or in cDC1 obtained with OP9-FLt3L cell culture (10) or ex vivo in cDC1 purified from spleens after intra venous (i.v) beads injection. Following beads uptake, phagocytosis is visualized by flow cytometry in cD11C positive DCs.

## 2 Materials

### 2.1 *In vitro* generation of Bone Marrow Derived Dendritic cells (BMDCs):

1. C57BL/6 mice.
2. Dissection tools.
3. BMDC medium: Iscove's modified Dubelcco's medium, 10% foetal calf serum heat inactivated, 1% L-glutamine, 1% penicillin/streptavidin, 50 $\mu$ M  $\beta$ -mercaptoethanol, 20ng/mL granulocyte macrophage colony stimulating factor (GM-CSF).
4. Low adherant petri dishes for tissue culture 145x20mm (Greiner bio-one, 639102).
5. PBS EDTA 5mM.
6. 40 $\mu$ m cell strainers.
7. 1.5 mL Eppendorf tubes.
8. 15 mL and 50 mL Falcon tubes.

### 2.2 *In vitro* generation of conventional Dendritic Cells type 1 (cDC1)

1. Tissue culture media (TCM): Roswell Park Memorial Institute (RPMI) 1640, 10% foetal calf serum heat denatured, 1% L-glutamine, 1% Penicillin/streptomycin, 50 $\mu$ M  $\beta$ -mercaptoethanol.
2. OP9 medium: Minimum Essential Medium Eagle alpha (MEM $\alpha$ ), 20% foetal calf serum heat inactivated, 1% L-glutamine, 0.5% Penicillin/streptomycin.
3. FMS-like tyrosine kinase 3 ligand (Flt3-L).
4. 6-well plate or 24-well plate for adherent cells.
5. 6-well plate or 24-well plate for suspension cells.
6. Trypsin-EDTA 0.05%, phenol red.
7. Red blood cell (RBC) lysis buffer.
8. FACS buffer: PBS, 3% heat-inactivated FCS, 1 mM EDTA.
9. Fluorochrome conjugated antibodies: anti-CD45-PECy7, anti cDC11c-BV711, anti-MHCII-PE, anti-XCR1-APC, anti-CD24-BV605 and anti-CD11b-APC eFluor780 (see Table 1).
10. Cell sorter equipped with lasers and emission filters suitable for the analysis of cells stained with antibodies coupled to specific fluorochromes.

**Table 1** List of antibodies used for the identification of cDC1 *in vitro* and *ex vivo*.

Antibodies	Fluorochrome	Dilutions	Clone	Provider and reference
CD45	PECy7	1/200	30-F11	BioLegend – 103114
CD11c	BV711	1/150	HL3	BD Biosciences – 563048
CD24	BV605	1/100	M1/69	BD Biosciences – 563060
MHCII I-A/I-E	PE	1/200	M5/114.15.2	BioLegend – 107608
XCR1	APC	1/150	ZET	BioLegend – 148206
CD3 $\epsilon$	PE	1/100	145-2C11	BioLegend – 100308
CD8 $\alpha$	BV605	1/150	53-6.7	BD Biosciences – 563152
CD11b	APC eFluor780	1/120	M1/70	Invitrogen – 47-0112-82
CD19	BV510	1/100	1D3	BD Biosciences – 562956

### **2.3 Ex vivo purification of conventional Dendritic Cells type 1 (cDC1)**

1. TCM: RPMI 1640, 10% foetal calf serum heat denatured, 1% L-glutamine, 1% Penicillin/streptomycin, 50 $\mu$ M  $\beta$ -mercaptoethanol.
2. 1 mL syringe with a 25-G needle.
3. 5 mL syringe with an 18-G needle.
4. Collagenase D.
5. DNase I.
6. Red blood cell (RBC) lysis buffer.
7. FACS buffer: PBS, 3% heat-inactivated FCS, 1 mM EDTA.
8. Fluorochrome-conjugated antibodies: anti-CD3 $\epsilon$ -PE, anti-CD19-BV510, anti CD11c-BV711, anti-CD11b-APC eFluor780 and anti-CD8 $\alpha$ -BV605 (see Table 1).
9. Cell sorter equipped with lasers and emission filters suitable for the analysis of cells stained with antibodies coupled to specific fluorochromes.

### **2.3 Phagocytosis assay**

1. NH<sub>2</sub> beads (Polybead<sup>®</sup> Amino Microspheres 2 and 3  $\mu$ m, Polysciences).
2. Sulfo-NHS-LC Biotin.
3. PBS glycine 1M.
4. Streptavidin coupled with Alexa Fluor 488.
5. Trypan blue.
6. 1M citrate buffer, pH4.
7. IMDM
8. Flow cytometer equipped with lasers and emission filters suitable for the analysis of cells stained with antibodies coupled to specific fluorochromes.

## **3 Methods**

### **3.1 Generating BM-DCs and cDC1**

#### **3.1.1 Day 0: Collection of Bone Marrow from the femur and tibia**

1. Euthanize C57BL/6 mice according to institutional guidelines.
2. In sterile conditions, harvest femurs and tibias.
3. Cut a sterile 200 $\mu$ L tip into a sterile 1.5mL Eppendorf tube.
4. Clean the bones with alcohol, separate the femur from the tibia, and cut each bone at one extremity.
5. Place the cut bones into the tip, the cutting side facing the bottom of the Eppendorf tube. One whole leg can fit into one tip.
6. Centrifuge for 2 min, 1800 g at 4°C, and check the presence of a red pellet after the centrifugation.

#### **3.1.2 Generation of BMDCs**

1. Resuspend the pellet in 1 mL of BM-DC medium.
2. Place the cell suspension in a 15 mL Falcon tube and complete to 5 mL with BM-DC medium.
3. Filter the cell suspension through a 40 $\mu$ m cell strainer into a 50 mL Falcon tube.
4. Add BM-DC medium up to 20 mL to the filtered cell suspension and plate the cells in a petri dish (one leg in a 145x20 mm petri dish).
5. After 4 days of culture, split the generated BM-DCs as follows.



6. Collect the supernatant into 50 mL falcon tubes and centrifuge at 400g for 10 min at room temperature (RT).
7. Add 10 mL of PBS-EDTA, 5mM into each petri dishes.
8. Incubate at 37°C for 10 minutes.
9. Detach the cells by flushing up and down using a 5 mL pipet. Make sure to go through the whole surface, to get as many cells as possible.
10. Pool cells (supernatant + pellet) and centrifuge the cells at 400g for 10 min at RT. Resuspend the pellet in medium and count the cells.
11. Plate the cells in petri dishes at  $10^7$  cells per 20 mL per petri dish.
12. The cells are differentiated between days 7 and 8. Follow the protocol described above (6,7,8,9,10) to harvest BM-DCs, pool adherent and suspension cells, and count (see **Note 1**).

### 3.1.3 Generation of cDC1

#### Preparation of the OP9-DL1 feeder cell line

1. *Day 0*: Seed OP9-DL1 cells in T75 flask at  $5 \times 10^6$  in 15 mL OP9 culture medium pre-warmed to 37°C (see Note 2) as follows.
2. When cells reach 90% confluence, discard culture medium and wash the cells with PBS pre-warmed to 37°C.
3. Treat the OP9-DL1 cells with 5 mL of 0.05% trypsin pre-warmed to 37°C, and place them in the incubator at 37°C until the cells detach from the flask (~ 5 min).
4. Harvest the OP9-DL1 cells in OP9 culture medium (10 mL) and transfer the cell suspension in a 15 mL Falcon tube.
5. Centrifuge cells at 400 g for 5 min at RT and resuspend the cell pellet in a desired volume of OP9 culture medium.
6. Count the cells and plate them either at  $2 \times 10^5$  / 4 mL per well in a 6-well plate or  $5 \times 10^4$  / 2 mL per well in a 24-well plate (adherent).

#### Differentiation of BM Cells into cDC1

1. Day 0: On the same day, seed the bone marrow cells in plates with Flt3-L as follows.
2. Resuspend the BM pellet obtained in 3.1.1 in 1mL of RBC lysis buffer and incubate at RT for 1-2 min.
3. Add 10 mL of TCM, filter the cells through a 40  $\mu$ m cell strainer, and centrifuge at 400 g for 10 min at RT.
4. Resuspend the cell pellet in a desired volume of TCM and count the cells.
5. Plate the cells either at  $8 \times 10^6$  / 8 mL in a 6-well plate or at  $2 \times 10^6$  / 2 mL in a 24-well plate (suspension).
6. Add 250 ng/mL Flt3-L in each cultured well and place in the incubator at 37°C for 3 days.
7. At day 3: seed the bone marrow cells on top of the OP9-DL1 as follows.
8. Discard the medium from the OP9-DL1 cells and add new OP9 culture medium supplemented with 250ng/mL Flt3-L (1mL for 24-well plate or 4mL for 6-well plate).
9. Resuspend the bone marrow cells in the well using a 1000 $\mu$ L pipet (see Note 3).
10. Seed 1mL (for 24-well plate) or 4mL (for 6-well plate) on top of OP9-DL1 cells and place in the incubator at 37°C for 5 days.
11. At day 8: change the medium of OP9/bone marrow cell culture as follows.
12. Take out 1mL (24-well plate) or 4mL (6-well plate) of medium from the OP9/bone marrow cells culture and spin down the cells that are in suspension, 400 g for 10 min at RT.

13. Resuspend the cells in 1mL (24-well plate) or 4mL (6-well plate) of OP9-DL1 medium + TCM (1:1), adding 250ng/mL Flt3-L, and add 1mL (24-well plate) or 4mL (6-well plate) back into the well (see Note 4) and place in the incubator for 2 to 4 extra days.
14. Between day 10 and 12, bone marrow cells are fully differentiated mostly into cDC1 and to a lesser extent into cDC2 (see Note 5).
15. Harvest the cells using cold PBS, they should detach easily.
16. Wash the cells in FACS buffer twice by centrifugation at 400 g for 5 min at 4°C.
17. Stain the cells with the following antibodies: anti-CD45-PECy7, anti-MHCII-PE, anti-CD11c-BV711, anti-XCR1-APC and anti-CD24-BV605 (see Table 1) for 30 min on ice.
18. Wash the cells in FACS buffer by centrifugation at 400 g for 5 min at 4°C.
19. Sort cDC1s using flow cytometry following this gating strategy: CD45<sup>+</sup> → CD11c<sup>+</sup>MHCII<sup>high</sup> → CD24<sup>+</sup>XCR1<sup>+</sup> (see Note 6).
20. Centrifuge the purified cDC1 population at 400 g for 5 min at 4°C and resuspend the cells in a desired volume of buffer.

### 3.2 Ex vivo cDC1 purified from the spleen

1. Euthanize C57BL/6 mice according to institutional guidelines.
2. Collect the spleens 30 min or 2h after intravenous injection of beads (See subheading 3.4.2).
3. Inject the spleens with 500 µl of TCM medium containing 1mg/ml of collagenase D and 20 µg/ml of DNase I, using a 1 mL syringe capped with a 25-G needle. Incubate at 37°C for 15 min.
4. Cut the spleen into small pieces with a scissor and incubate again 15 min at 37°C.
5. Aspirate and flush the spleens with a 5 ml syringe capped with an 18-G needle and filter the cell suspension using a 40 µM cell strainer.
6. Centrifuge for 10 minutes at 400 g at RT.
7. Resuspend the pellet in 1 mL of RBC lysis buffer, incubate at RT for 1-2 min, and add 10 mL of TCM to stop the lysis.
8. Filter the cells through a 40µm cell strainer and centrifuge at 400 g for 10 min at RT.
9. Wash the cell in FACS buffer twice by centrifugation at 400 g for 5 min at 4°C.
10. Stain the cells with the following antibodies: anti-CD3ε-PE, anti-CD19-BV510, anti-CD11c-BV711, anti-CD8α-BV605 and anti-CD11b-APC eFluor780 (see Table 1) for 30 min on ice.
11. Wash the cells again in FACS buffer by centrifugation at 400 g for 5 min at 4°C.
12. Immediately run the flow cytometry experiment using the following gating strategy to gate on cDC1 population: CD3ε<sup>-</sup> CD19<sup>-</sup> → CD11c<sup>+</sup> → CD11b<sup>-</sup> and CD8α<sup>+</sup>. Phagocytosis is measured in the yellow channel (Alexa 488) (see Fig.2).

### 3.3 Preparation of NH2-beads

1. Take 500 µl beads (1.7 x 10<sup>6</sup> beads/µl).
2. Wash twice with PBS and then add 2mg/ml sulfo-NHS-LC biotin to activate the NH2 beads.
3. Incubate the beads for 1h, slowly rotating (15 rpm) at RT.
4. Centrifuge for 10 min at RT at 11200 g and discard the supernatant.
5. Wash beads with 500 µl PBS, 1M glycine.
6. Centrifuge the beads for 4 minutes at 11200 g and discard supernatant.
7. Wash the beads twice with PBS and resuspend in 500 µl PBS.
8. Take 300 µl of beads and add 1:50 streptavidin Alexa 488.
9. Incubate the beads for 30 minutes, slowly rotating (15 rpm) at 4°C.

10. Repeat step 6 and resuspend the beads in 500  $\mu$ l PBS.

### 3.4 Phagocytosis assay

#### 3.4.1 In vitro phagocytosis assay

1. Use  $5 \times 10^6$  BMDCs or cDC1 per condition.
2. The ratios of cells:beads will be 1:1, 1:5, 1:10.
3. Take the appropriate amount of beads and resuspend the beads in 300  $\mu$ l of IMDM for each condition (for example if the ratio cells: beads is 1:1, you will resuspend 3  $\mu$ l of beads in 300  $\mu$ l of IMDM).
4. Mix BM-DCs or cDC1 with 300  $\mu$ l of IMDM (see Note 7).
5. Incubate in the incubator at 37°C for 30 minutes.
6. Stop the reaction with 5 mL cold PBS.
7. Take 1 mL out of the 5 mL, centrifuge the cells for 5 min at 400 g, and resuspend the pellet in 350  $\mu$ l of 0.2mg/mL trypan blue, 1M citrate, pH 4 (see Note 8).
8. Repeat step 7 but resuspend the pellet in 20 mM Na citrate, pH 4.
9. Immediately run the flow cytometry experiment as described in subheadings 3.1 and 3.2. Phagocytosis is measured in the yellow channel (Alexa 488) (see Fig 1).

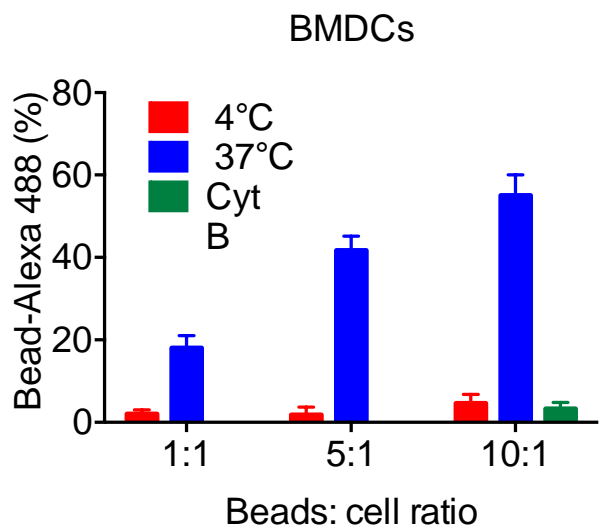


**Fig 1.** Measurement of BM-DC phagocytosis in vitro. BMDCs were differentiated from bone marrow for 7 days in the presence of GM-CSF. BMDCs were then incubated with beads labelled with Alexa 488 at different ratios in the absence or presence of 10  $\mu$ M of cytochalasin B (CytB). Cells were collected, stained with anti mouse CD11c antibody coupled to BV711, and the percent of beads uptake among CD11c<sup>+</sup> BMDCs was assessed in the yellow channel (Alexa 488) using the flow cytometer BD LSR Fortessa SORP.

#### 3.4.2 Ex vivo phagocytosis assay

1. Inject 100  $\mu$ l of NH<sub>2</sub> beads coupled to streptavidin Alexa 488, intravenously using a 500  $\mu$ l syringe capped with a 28-G needle.
2. After 30 min to 2h, collect the spleens and proceed as described in subheading 3.2 (see Fig. 2).

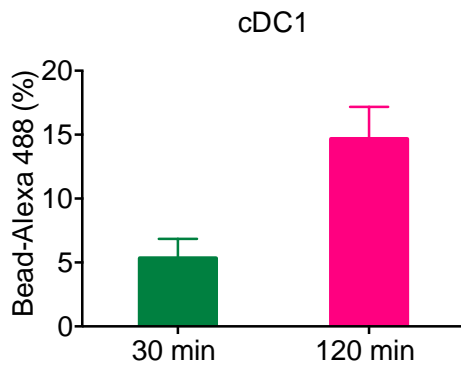


**Fig 2.** Measurement of phagocytosis in cDC1 ex vivo. Following iv injection of beads labelled with Alexa 488 beads, total spleen were stained with anti-mouse CD3 $\epsilon$  antibody coupled to PE, anti-mouse CD19 antibody coupled to BV510, anti-mouse CD11c antibody coupled to BV711, anti-mouse CD8 $\alpha$  antibody coupled to BV605 and anti-mouse CD11b antibody coupled to APC eFluor780. The percent of beads among cDC1 (CD11c<sup>+</sup>CD8 $\alpha$ <sup>+</sup>CD11b<sup>-</sup>) were measured in the yellow channel (Alexa 488) using the flow cytometer BD LSR Fortessa SORP.

#### 4 Notes

1. At day 7-8, BM-DCs are fully differentiated and the expression of CD11c is between 80 and 90%.
2. OP9-DL1 cells must be previously cultured in T75 or T175 flasks and at least split once prior their use for the differentiation of BM cells into cDC1 to generate enough OP9-DL1 cells.
3. At this stage of BM, cell culture cells are not adherent and should detach easily.
4. Seed twice more OP9-DL1 wells than bone marrow wells. Indeed, you only seed half a well on bone marrow cells into one well of OP9-DL1 cells.
5. Some cells differentiate into cDC2 after being cultured on OP9-DL1 cells. You can sort cDC2 cells based on the expression of CD11b (CD45<sup>+</sup>  $\rightarrow$  CD11c<sup>+</sup>MHCII<sup>+</sup>  $\rightarrow$  CD11b<sup>+</sup>).
6. Usually, the number of cDC1 generated using the OP9-DL1/Flt3L culture is  $3 \times 10^6$  from one 6-well plate culture.
7. As a negative control for phagocytosis, you can treat DCs with 10 $\mu$ M cytochalasin B before incubating them with the beads. Cytochalasin B is an actin polymerization inhibitor and will thus block endocytosis.
8. Trypan is used to quench beads that have not been internalized and bound to the cell surface. Therefore, this step allows you to only detect the fluorescence of the beads that have been internalized and not the beads sticking to the cell surface.

## Acknowledgments

This work is supported by INSERM, INCaPLBIO and Fondation Vaincre Alzheimer.

## References

1. S Gordon (2016). Phagocytosis: an immunobiologic process. *Immunity* 44(3) : 463-475.
2. Joffre OP, Segura E, Savina A, Amigorena S (2012). Cross presentation by dendritic cells. *Nat Rev Immunol* 12 : 557-559.
3. ST Ferris, V Durai, R Wu, DJ Theisen, JP Ward, MD Bern, JT Davidson 4th, P Bagadia, T Liu, CG Briseño, L Li, WE Gillanders, GF Wu, VM Yokoyama, TL Murphy, RD Schreiber, KM Murphy (2020). cDC1 prime and are licensed by CD4(+) T cells to induce anti tumour immunity. *Nature* 584:624-629
4. A Savina, A Peres, I Cebrian, N Carmo, C Moita, N Hacohen, LF Moita, S Amigorena (2009). The small GTPase Rac2 controls phagosomal alkalisation and antigen cross presentation selectively in CD8+ dendritic cells. *Immunity* 30: 544-555.
5. L Delamarre L, M Pack, H Chang, I Mellman, ES Trombetta (2005). Differential lysosomal proteolysis in antigen-presenting cells determines antigen fate. *Science* 307 :1630-1634.
6. AM Lennon-Dumenil, AH Bakker, R Maehr, E Fiebiger, HS Overkleeft, M Roseblatt, HL Ploegh, C Lagaudrière-Gesbert (2002). Analysis of protease activity in live antigen-presenting cells shows regulation of the phagosomal proteolytic contents during dendritic cell activation. *J Exp Med* 196:529-540.
7. JD Ernst (2000). Bacterial inhibition of phagocytosis. *Cell Microbiol* 2:379-86.
8. K Rohde, RM Yates, GE Purdy, DG Russell (2007). Mycobacterium tuberculosis and the environment within the phagosome. *Immunol Rev* 219:37-54.
9. YR Na YR, D Jung, GJ Gu, SH Seok (2016). GM-CSF grown bone marrow derived cells are composed of phenotypically different dendritic cells and macrophages. *Mol Cells* 39:734-741.
10. ME Kirkling, U Cytlak, CM Lau, KL Lewis, A Resteu, A Khodadadi-Jamayran, CW Siebel, H Salmon, M Merad, A Tsigos, M Collin, V Bigley, B Reizis (2018). Notch signaling facilitates in vitro generation of cross-presenting classical dendritic cells. *Cell Rep* 23:3658-3672.

**The role of the antigen processing machinery in the regulation and trafficking of intracellular TLR molecules**

Moïse de Lavergne<sup>1</sup>, Lucie Maisonneuve<sup>1</sup>, Katrina Podsypanina<sup>1</sup> and Bénédicte Manoury<sup>1\*</sup>

Institut Necker Enfants Malades, INSERM U1151-CNRS UMR 8253, Université Paris Cité, Faculté de Médecine Necker, France

\* corresponding author

Intracellular Toll-like receptors (TLRs) are key components of the innate immune system. Their expression in antigen presenting cells (APCs), and in particular dendritic cells (DCs), make them critical in the induction of the adaptive immune response. Here, we will discuss the tight relationship they have with the antigen processing machinery in APCs for their trafficking and activation.

## **Introduction**

Pattern Recognition Receptors (PRRs) recognize Pathogen Associated Molecular Pattern, conserved structure expressed by microbial pathogens. PRRs can be broadly categorized into secreted, transmembrane, and cytosolic classes. The transmembrane PRRs include the Toll-like receptor (TLR) family, which are either expressed on the plasma membrane or in endosomal/lysosomal organelles. Intracellular TLRs (TLR3, TLR7, TLR9) mainly detect microbial nucleic acids and also sense endogenous ligands or DAMPs for Damage Associated Molecular Patterns, such as self-DNA released, for example, during self-tissue damage, or cancer cell death. Intracellular TLRs are highly expressed in antigen presenting cells (APCs) such as dendritic cells (DCs) and macrophages that constitutively express major histocompatibility complex class II (MHCII) molecules. In DCs, antigen presentation coupled to TLRs activation induces their maturation through the expression of co-stimulatory molecules, chemokine receptors and cytokine production. Maturation makes DCs immunogenic, whereas the absence of TLR signal leads to tolerance. Several lines of evidence link intracellular TLR signalling and antigen presentation process. First, in bacteria- infected macrophages, TLRs signalling regulate several steps of antigen presentation, such as antigen uptake and phagosomal maturation [1,2]. Next, TLR activation stimulates tubulation of endo-lysosomes in DCs containing MHCII-peptide complexes facilitating their delivery to the plasma membrane [3,4]. Finally, seminal work from Medzhitov laboratory shows that TLR activation in DCs targets antigens in phagosomal compartment, a site for processing of the MHCII chaperone, the invariant chain (Ii) [5]. MHCII molecules require Ii for their folding and trafficking. Similarly, intracellular TLRs associate with the chaperone molecule UNC93B1 which, helps their traffic to endosomal compartments for cleavage by proteases and activation [6–9].

Thus, several features of intracellular TLRs, such as folding, trafficking, and processing in APCs, are shared with MHCII molecules.

Here we will discuss how intracellular TLRs utilize the antigen processing machinery, mainly in DCs, for their optimal trafficking and activation, resulting in enhanced antigen presentation. We will start with the identification of proteases required for their cleavage and activation. Then, we will highlight the role of the chaperone molecule, UNC93B1, in their folding and endosomal trafficking. Finally, we will discuss the nature of the endo-lysosomal compartments they reached for optimum specific cytokine response.

## **Proteases**

Initial experiments suggesting a role for endo-lysosomal proteases in intracellular TLR signalling is that drugs that block lysosomal acidification inhibit TLR7 and TLR9 activation [10]. The generation of antigenic peptides, and their loading on MHCII molecules that involves removal of the chaperone molecule Ii, also depends on endo-lysosomal proteases in APCs. Indeed, a role for the cysteine protease family, specifically cathepsins L and S, is

confirmed in li chain processing and generation of peptides during antigen processing [11–17]. Other studies show that the lysosomal Asparagine endopeptidase (AEP) could also initiate li processing, and make the initial cleavage sites of tetanus toxin antigen (TTCF), or destroy the immunodominant peptide of myelin basic protein (MBP) 85-99 in human cells [18–20]. Mice deficient for AEP also show mild defect in TTCF processing [21].

TLR9 and TLR7 cleavage was first reported by the group of G Barton in a macrophage cell line expressing TLR9/TLR7-HA, and in primary macrophages and DCs transduced with retroviruses encoding TLR9-HA [8]. The identification of proteases cleaving TLR7 and TLR9 was then addressed in DCs deficient for members of the cysteine protease family such as cathepsins L and S, and indicated their contribution in TLR7 and TLR9 activation [7]. Compromised TLR7 and TLR9 cleavage and signalling is also described in AEP-deficient DCs, and in human plasmacytoid DCs (pDCs) treated with a specific AEP inhibitor [9,22]. In addition, AEP-deficient mice show altered response to TLR7 and TLR9 signals following pathogen infection and, are not able to elicit T cells proliferation upon TLR7 and TLR9 stimulation *in vivo* [9,22].

In MHC class I (MHCI) antigen presentation, trimming of pre-processed antigenic substrates into peptides of suitable size ready for loading on MHCI molecules is performed by a different set of proteases than cathepsins, such as ERAAP (ER aminopeptidase associated with antigen processing), or IRAP for insulin responding aminopeptidase [23]. IRAP deficient DCs show reduced MHCI antigen cross presentation of endocytosed and phagocytosed antigens and thus confirm a role for IRAP in antigen cross presentation [24]. IRAP interacts with MHCI molecules and they both co-localize in DCs in a specific subset of endosomes, the slow recycling storage endosome (SRSE). These structures express Rab14 and syntaxin 6 and contain antigen internalized by endocytosis [25]. The IRAP<sup>+</sup> endosomes partially overlap with VAMP3 organelles, where TLR9 travels before reaching LAMP1<sup>+</sup> lysosomes [26,27]. Indeed, traffic of TLR9 to IRAP<sup>+</sup> endosomes is mandatory for proper TLR9 signalling, as the absence of IRAP led to an increase in CpG and TLR9 trafficking directly into LAMP1<sup>+</sup> lysosomal organelles as well, as accelerated TLR9 cleavage and activation. This accelerated TLR9 trafficking is independent of IRAP enzymatic activity, but requires an association between IRAP and FHOD4, a member of the formin family of actin-nucleating proteins involved in the attachment of vesicles to the actin skeleton [27].

Lysosomal activity in DCs is regulated by the NADPH oxidase, the V-ATPase, and the transcription factor EB (TFEB), which controls the activation of genes, involved in lysosome biogenesis and function, in particular phagosomal acidification. Indeed, level of TFEB expression sets the threshold for MHCI antigen cross presentation [28]. High expression of TFEB favours MHCII antigen presentation by promoting phagosomal acidification and proteases expression, whereas low expression of TFEB leads to an increase in MHCI antigen cross presentation, as a consequence of slower degradation of antigenic substrates. In Raw264.7 macrophages, TLR9 stimulation induces TFEB activation helping its translocation to the nucleus, while inhibition of TLR9 cleavage results in TFEB inactivation [29]. A mechanism for TFEB activation in TLR4 stimulated DCs is proposed via the release of Ca<sup>2+</sup> in lysosomes by TRPLM1 channel [30]. Whether the intracellular TLRs use the same mechanism to activate TFEB is not yet known.

Similarly, intracellular TLR stimulation leads to DCs maturation and increased lysosomal acidification, which is accompanied by enhanced V-ATPase activity [31]. In that context, intracellular TLR activation is anticipated to support MHCII antigen presentation. But an alternative prediction is that intracellular TLR localised in perinuclear lysosomes slow down



phago-lysosomal fusion, and preserve the arrival of antigenic substrates in acidic compartment, and thus promote MHCII antigen cross presentation, as it was shown for TLR4 [32].

### **Chaperone molecules**

Ii is a type II transmembrane protein that associates with the MHCII molecules in the ER [33]. Studies using cells expressing MHCII and different isoforms of Ii or mice lacking Ii indicate that Ii is required for the folding and assembly of MHCII. Intact MHCII-Ii complexes are then targeted to the endo-lysosomal pathway where Ii is sequentially cleaved into CLIP, or Invariant Chain Peptide, to protect the MHCII groove from the loading of peptides outside the endo-lysosomal compartments [34].

UNC93B1 is a conserved 12-membrane spanning molecule residing in the ER, essential for functional intracellular TLR cleavage in endosomes. UNC93B1 is highly expressed in myeloid cells, whereas non immune cells, such as epithelial or fibroblasts have low levels of UNC93B1 [8,35]. The role of UNC93B1 in the TLR pathway was discovered using a forward genetic screen in mice [6]. This led to the identification of a *3d* mutant mouse, which expressed a single non-conservative amino acid substitution (H in position 412 to R) and was unable to respond to intracellular TLRs whereas the response to membrane TLRs was intact. As a consequence, expression of the *3d* mutant in mice and human cells leads to a higher susceptibility to various pathogen infection [6,36]. UNC93B1 binds the juxtamembrane region of intracellular TLRs and the N-terminal region of UNC93B1 is required for TLR7 and TLR9 ER egress [37–39]. UNC93B1 also controls intracellular TLRs trafficking and their packaging into COPII-coated vesicles in ER membranes [40]. In fact, UNC93B1 might act as a cargo receptor for trafficking to the Golgi, like Sec24, which is the principal cargo binding for the COPII coat. The group of Latz demonstrated that UNC93B1 is needed for intracellular TLRs folding [41]. Thus, the absence of UNC93B1 or the UNC93B1 H412R mutation compromise TLRs expression. In addition, UNC93B1 regulates differently TLR9 and TLR7 upon ligand stimulation. In the endosomes, activation of TLR9 requires its dissociation from UNC93B1, whereas TLR7 remains bound to UNC93B1 for its activation [42,43].

Altogether, these results assert the role of UNC93B1 in stabilizing and preventing the degradation of endosomal TLRs, and suggest an UNC93B1-TLR9 or TLR7 chaperone-client relationship similar to that of Ii-MHCII.

UNC93B1 is also central to antigen presentation. The same mutation that alters intracellular TLRs delivery to endosomes also partially inhibits MHCII antigen presentation and strongly blocks MHCII antigen cross presentation independent of TLR signalling [6,44]. This function requires an interaction between UNC93B1 and an ER calcium sensor, the stromal interaction protein molecule STIM1 [44,45]. In UNC93B1 H412R DCs, key features of DCs antigen cross presentation such as endosomal/phagosomal pH; lysosomal proteolytic activity and antigen export to the cytosol are linked to the loss of STIM1-UNC93B1 interaction and failure to activate membrane Ca<sup>2+</sup> channels. Loss of STIM1-UNC93B1 interaction in *3d* mutant mice impairs antigen degradation that leads to altered antigen cross-presentation [44,45].

### **Subcellular compartments involved in peptide loading, TLR trafficking and cytokine response**

At the steady state, intracellular TLR reside in the ER and translocate in early endosomal compartments upon stimulation with their ligands. Adaptor proteins (APs) family consist of 5 members (AP-1 to AP-5). APs are composed of several subunits, expressed in different intracellular compartments, which select cargo into vesicles for their delivery to the endo-lysosomal pathway. In vitro, cell surface AP-2 was shown to bind the di-leucine motif in the cytosolic tail of Ii and in cells silenced for AP-2, Ii mislocalization led to reduced formation of MHCII-peptide complexes at the cell surface [46]. In a similar fashion, UNC93B1-C terminal domain interacts with AP-2, and absence of AP-2 results in accumulation of TLR9 in the Golgi [39]. Thus, both the MHCII-Ii and the UNC93B1-TLR9 complexes require AP-2 for their traffic and delivery from the plasma membrane to endosomal compartments. In contrast depletion of AP-4 had no effect in MHCII-Ii complexes trafficking but is necessary for TLR7 delivery to endosomes via direct ER-TGN (trans Golgi network) direct route.

Iwasaki and colleagues demonstrated that TLR9, shortly after stimulation, goes in VAMP3 endosomes, where it binds AP-3 and then translocate in LAMP1<sup>+</sup> lysosome, promoting production of type I interferon (IFN) through IRF7 activation [47]. Altogether, these results suggest that the first steps of UNC93B1-TLR9 trafficking from the ER to the plasma membrane and then to early endosomes might be similar between UNC93B1-TLR9 and MHCII-Ii. Later steps diverge as UNC93B1-TLR9 proteins are targeted to lysosome-related organelles (LRO) or lysosomes via AP-3, while MHCII-Ii complexes go to MVB/MiIC compartments independently of AP-3. Additional host factors required for lysosome biogenesis including BLOC1 (biogenesis of lysosome related organelles complex 1), which is controlled by TFEB and BLOC2 are crucial for TLR9 signalling in pDCs, as BLOC-1 and BLOC-2 deficient mice produced less type I IFN after TLR9 stimulation in comparison to control mice [48]. BLOC-1 complex binds AP-3, is involved in the biogenesis of LRO and share some subunits with the BLOC-1 related complex (BORC). BORC associates peripherally with lysosomal membranes, to recruit the small GTPase Arl8b, which, when activated promotes kinesin-1-dependent movement of lysosomes. Arl8b deficient cells show a defect in MHCII-peptide complex formation and its delivery to the plasma membrane [49]. TLR7 activation induces Arl8b-TLR7 association, which promotes microtubule polymerization, enabling TLR7 trafficking in Arl8b<sup>+</sup> compartment for type I INF response [50]. Thus, similarly to AP-3 which expression is needed to transfer TLR9 from endosomes to lysosome for type I INF response, Arl8b is required for TLR7 to translocate to lysosomes, also for type I INF response.

### **Concluding remarks**

Antigen presentation and TLRs activation in APCs are essential processes for triggering CD4<sup>+</sup> and CD8<sup>+</sup> T cells responses to exogenous antigens. Accumulating evidence has described the role of the antigen processing machinery for intracellular TLRs activation. The findings suggest that intracellular TLRs use proteases, chaperones molecules, adaptor protein complexes and endo-lysosomal compartments for their trafficking and cleavage, as do the MHCII molecules (**Figure 1**). However, because of the complexity of the processing machinery and its unique features for each APCs, many questions still remain unanswered.

### **Conflict of interest statement**

Nothing to declare

### **Author's contribution**

BM wrote the manuscript and LM, MDL and KP made comments on the manuscript.

### Funding

This work was supported by INSERM (ANR2 2010 MIDI 008 01 to BM), CNRS and Université Paris Cité.

### Figure 1

TLR7 and TLR9 pathway in dendritic cells

TLR7 and TLR9 bind UNC93B1 in the ER. Upon TLR9 stimulation, TLR9-UNC93B1 complexes traffic to the plasma membrane and are internalized via AP-2 in early endosomes expressing VAMP3 and IRAP proteins. Within VAMP3<sup>+</sup> IRAP<sup>+</sup> endosomes, TLR9 dissociates from UNC93B1 and is cleaved by AEP and other proteases. This allows the recruitment of the adaptor molecule MyD88 and induces NF- $\kappa$ B signalling. Cleaved TLR9 then move to LAMP1<sup>+</sup> lysosome with the help of AP-3 to trigger type I INF signalling. In contrast, TLR7-UNC93B1 complexes bind AP-4 or/and Arl8b (depending on the cell type) and are transferred directly from the ER to LAMP1<sup>+</sup> lysosome following TLR7 stimulation. In lysosome, TLR7 remained associated with UNC93B1 for the induction of type I INF.

### References and recommended reading

- of interest
- of outstanding interest

1. West MA, Wallin RPA, Matthews SP, Svensson HG, Zaru R, Ljunggren HG, *et al.*: **Enhanced Dendritic Cell Antigen Capture via Toll-Like Receptor-Induced Actin Remodeling.** *Science* 2004, 305:1153–1157.
2. Blander JM, Medzhitov R: **Regulation of Phagosome Maturation by Signals from Toll-Like Receptors.** *Science* 2004, 304:1014–1018.  
\*\* Studies to demonstrate that TLR expressed in bacteria regulates antigen internalization and phagosome maturation.
3. Boes M, Cerny J, Massol R, Op den Brouw M, Kirchhausen T, Chen J, *et al.*: **T-cell engagement of dendritic cells rapidly rearranges MHC class II transport.** *Nature* 2002, 418:983–988.  
\*\* Using MHCII tagged with GFP, the authors show that TLR activation in dendritic cells leads to the redistribution of MHCII-GFP from lysosomes to the plasma membrane.
4. Kleijmeer M, Ramm G, Schuurhuis D, Griffith J, Rescigno M, Ricciardi-Castagnoli P, *et al.*: **Reorganization of multivesicular bodies regulates MHC class II antigen presentation by dendritic cells.** *J Cell Biol* 2001, 155:53–64.
5. Blander JM, Medzhitov R: **Toll-dependent selection of microbial antigens for presentation by dendritic cells.** *Nature* 2006, 440:808–812.  
\*\* First report on the generation of MHCII-peptides in phagosomes controlled by TLR.

6. Tabeta K, Hoebe K, Janssen EM, Du X, Georgel P, Crozat K, *et al.*: **The Unc93b1 mutation 3d disrupts exogenous antigen presentation and signaling via Toll-like receptors 3, 7 and 9.** *Nat Immunol* 2006, 7:156–164.  
 \*\* In this paper, the authors identify the 3d mutant by chemical mutagenesis and demonstrate the essential role of UNC93B1 in intracellular TLRs signalling. The 3d mutation prevents intracellular signalling, decreases MHCII antigen presentation and causes susceptibility to several pathogen infection.
  
7. Park B, Brinkmann MM, Spooner E, Lee CC, Kim YM, Ploegh HL: **Proteolytic cleavage in an endolysosomal compartment is required for activation of Toll-like receptor 9.** *Nat Immunol* 2008, 9:1407–1414.  
 \*\* First report of cleaved TLR9 binding CpG and having a role in signalling.
  
8. Ewald SE, Lee BL, Lau L, Wickliffe KE, Shi GP, Chapman HA, *et al.*: **The ectodomain of Toll-like receptor 9 is cleaved to generate a functional receptor.** *Nature* 2008, 456:658–662.  
 \*\* First study to describe TLR7 and TLR9 cleavages and to demonstrate that the processed receptors recruit MyD88 and are functional.
  
9. Sepulveda FE, Maschalidi S, Colisson R, Heslop L, Ghirelli C, Sakka E, *et al.*: **Critical Role for Asparagine Endopeptidase in Endocytic Toll-like Receptor Signaling in Dendritic Cells.** *Immunity* 2009, 31:737–748.  
 \*\* A significant paper showing that the lysosomal protease, AEP, processes TLR9 to generate a functional receptor for dendritic cells maturation and MHCII antigen presentation.
  
10. Yi AK, Tuetken R, Redford T, Waldschmidt M, Kirsch J, Krieg AM: **CpG motifs in bacterial DNA activate leukocytes through the pH-dependent generation of reactive oxygen species.** *J Immunol Baltim Md* 1950 1998, 160:4755–4761.
  
11. Riese RJ, Wolf PR, Brömme D, Natkin LR, Villadangos JA, Ploegh HL, *et al.*: **Essential Role for Cathepsin S in MHC Class II–Associated Invariant Chain Processing and Peptide Loading.** *Immunity* 1996, 4:357–366.
  
12. Nakagawa T, Roth W, Wong P, Nelson A, Farr A, Deussing J, *et al.*: **Cathepsin L: Critical Role in li Degradation and CD4 T Cell Selection in the Thymus.** *Science* 1998, 280:450–453.
  
13. Shi GP, Villadangos JA, Dranoff G, Small C, Gu L, Haley KJ, *et al.*: **Cathepsin S Required for Normal MHC Class II Peptide Loading and Germinal Center Development.** *Immunity* 1999, 10:197–206.
  
14. Hsieh CS, deRoos P, Honey K, Beers C, Rudensky AY: **A Role for Cathepsin L and Cathepsin S in Peptide Generation for MHC Class II Presentation.** *J Immunol* 2002, 168:2618–2625.

15. Plüger EBE, Boes M, Alfonso C, Schröter CJ, Kalbacher H, Ploegh HL, *et al.*: **Specific role for cathepsin S in the generation of antigenic peptides in vivo.** *Eur J Immunol* 2002, 32:467–476.
16. Shen L, Sigal LJ, Boes M, Rock KL: **Important Role of Cathepsin S in Generating Peptides for TAP-Independent MHC Class I Crosspresentation In Vivo.** *Immunity* 2004, 21:155–165.
17. Villadangos JA, Bryant RAR, Deussing J, Driessen C, Lennon-Dumenil AM, Riese RJ, *et al.*: **Proteases involved in MHC class II antigen presentation.** *Immunol Rev* 1999, 172:109–120.
18. Manoury B, Hewitt EW, Morrice N, Dando PM, Barrett AJ, Watts C: **An asparaginyl endopeptidase processes a microbial antigen for class II MHC presentation.** *Nature* 1998, 396:695–699.
19. Manoury B, Mazzeo D, Fugger L, Viner N, Ponsford M, Streeter H, *et al.*: **Destructive processing by asparagine endopeptidase limits presentation of a dominant T cell epitope in MBP.** *Nat Immunol* 2002, 3:169–174.
20. Manoury B, Mazzeo D, Li DN, Billson J, Loak K, Benaroch P, *et al.*: **Asparagine Endopeptidase Can Initiate the Removal of the MHC Class II Invariant Chain Chaperone.** *Immunity* 2003, 18:489–498.
21. Matthews SP, Werber I, Deussing J, Peters C, Reinheckel T, Watts C: **Distinct Protease Requirements for Antigen Presentation In Vitro and In Vivo.** *J Immunol* 2010, 184:2423–2431.
22. Maschalidi S, Hässler S, Blanc F, Sepulveda FE, Tohme M, Chignard M, *et al.*: **Asparagine Endopeptidase Controls Anti-Influenza Virus Immune Responses through TLR7 Activation.** *PLoS Pathog* 2012, 8:e1002841.
- \* Identification of TLR7 cleavage site targeted by AEP and the role of TLR7 processing in influenza infection.
23. Saveanu L, Carroll O, Weimershaus M, Guermonprez P, Firat E, Lindo V, *et al.*: **IRAP Identifies an Endosomal Compartment Required for MHC Class I Cross-Presentation.** *Science* 2009, 325:213–217.
24. Weimershaus M, Maschalidi S, Sepulveda F, Manoury B, van Endert P, Saveanu L: **Conventional Dendritic Cells Require IRAP-Rab14 Endosomes for Efficient Cross-Presentation.** *J Immunol* 2012, 188:1840–1846.
25. Weimershaus M, Mauvais FX, Saveanu L, Adiko C, Babdor J, Abramova A, *et al.*: **Innate Immune Signals Induce Anterograde Endosome Transport Promoting MHC Class I Cross-Presentation.** *Cell Rep* 2018, 24:3568–3581.
26. Iwasaki A, Medzhitov R: **Regulation of Adaptive Immunity by the Innate Immune System.** *Science* 2010, 327:291–295.

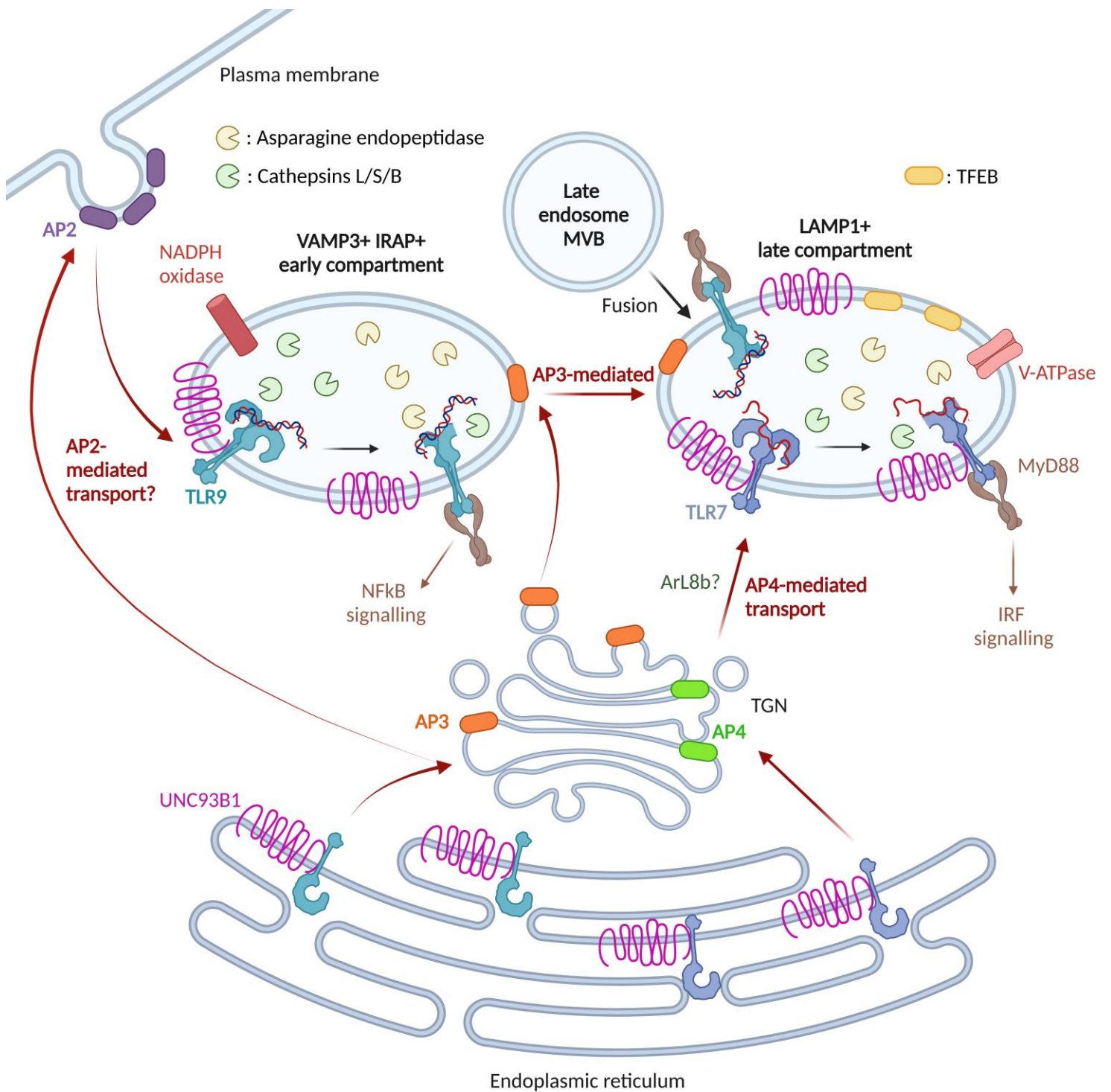
27. Babdor J, Descamps D, Adiko AC, Tohmé M, Maschalidi S, Evnouchidou I, *et al.*: **IRAP+ endosomes restrict TLR9 activation and signaling.** *Nat Immunol* 2017, 18:509–518.  
 \*\* Authors show the different steps of TLR9 trafficking in the endosomal pathway of dendritic cells.
28. Samie M, Cresswell P: **The transcription factor TFEB acts as a molecular switch that regulates exogenous antigen-presentation pathways.** *Nat Immunol* 2015, 16:729–736.  
 \*\* Important finding that demonstrate the regulation of TFEB in different subset of dendritic cells and its impact on exogenous antigen presentation.
29. Wei W, Ren J, Yin W, Ding H, Lu Q, Tan L, *et al.*: **Inhibition of Ctsk modulates periodontitis with arthritis via downregulation of TLR9 and autophagy.** *Cell Prolif* 2020, 53.
30. Bretou M, Sáez PJ, Sanséau D, Maurin M, Lankar D, Chabaud M, *et al.*: **Lysosomesignaling controls the migration of dendritic cells.** *Sci Immunol* 2017, 2:eaak9573.
31. Trombetta ES, Ebersold M, Garrett W, Pypaert M, Mellman I: **Activation of Lysosomal Function During Dendritic Cell Maturation.** *Science* 2003, 299:1400–1403.
32. Alloatti A, Kotsias F, Pauwels AM, Carpiér JM, Jouve M, Timmerman E, *et al.*: **Toll-like Receptor 4 Engagement on Dendritic Cells Restrains Phago-Lysosome Fusion and Promotes Cross-Presentation of Antigens.** *Immunity* 2015, 43:1087–1100.  
 \* Kinetic studies to demonstrate that TLR4 induces lysosomal clustering and inhibits phago-lysosomal fusion to preserve MHCI antigen cross presentation.
33. Kvist S, Wiman K, Claesson L, Peterson PA, Dobberstein B: **Membrane insertion and oligomeric assembly of HLA-DR histocompatibility antigens.** *Cell* 1982, 29:61–69.
34. Lotteau V, Teyton L, Peleraux A, Nilsson T, Karlsson L, Schmid SL, *et al.*: **Intracellular transport of class II MHC molecules directed by invariant chain.** *Nature* 1990, 348:600–605.
35. Avalos AM, Kirak O, Oelkers JM, Pils MC, Kim YM, Ottinger M, *et al.*: **Cell-Specific TLR9 Trafficking in Primary APCs of Transgenic TLR9-GFP Mice.** *J Immunol* 2013, 190:695–702.
36. Casrouge A, Zhang SY, Eidenschenk C, Jouanguy E, Puel A, Yang K, *et al.*: **Herpes Simplex Virus Encephalitis in Human UNC-93B Deficiency.** *Science* 2006, 314:308–312.
37. Kim YM, Brinkmann MM, Paquet ME, Ploegh HL: **UNC93B1 delivers nucleotide-sensing toll-like receptors to endolysosomes.** *Nature* 2008, 452:234–238.
38. Brinkmann MM, Spooner E, Hoebe K, Beutler B, Ploegh HL, Kim YM: **The interaction between the ER membrane protein UNC93B and TLR3, 7, and 9 is crucial for TLR signaling.** *J Cell Biol* 2007, 177:265–275.  
 \*\* First report describing the association between UNC93B1 and intracellular TLRs.

39. Fukui R, Saitoh S, Ichiroh, Matsumoto F, Kozuka-Hata H, Oyama M, Tabeta K, *et al.*: **UNC93B1 biases Toll-like receptor responses to nucleic acid in dendritic cells toward DNA- but against RNA-sensing.** *J Exp Med* 2009, 206:1339–1350.
40. Lee BL, Moon JE, Shu JH, Yuan L, Newman ZR, Schekman R, *et al.*: **UNC93B1 mediates differential trafficking of endosomal TLRs.** *eLife* 2013, 2:e00291.
41. Pelka K, Bertheloot D, Reimer E, Phulphagar K, Schmidt SV, Christ A, *et al.*: **The Chaperone UNC93B1 Regulates Toll-like Receptor Stability Independently of Endosomal TLR Transport.** *Immunity* 2018, 48:911-922.
- \*\* First report on the significance of UNC93B1 in intracellular TLRs folding.
42. Majer O, Liu B, Woo BJ, Kreuk LSM, Van Dis E, Barton GM: **Release from UNC93B1 reinforces the compartmentalized activation of select TLRs.** *Nature* 2019, 575:371–374.
- \* Mechanism of UNC93B1-TLR9 interaction that suggest differential regulation of TLR9 and TLR7 by UNC93B1.
43. Majer O, Liu B, Kreuk LSM, Krogan N, Barton GM: **UNC93B1 recruits syntenin-1 to dampen TLR7 signalling and prevent autoimmunity.** *Nature* 2019, 575:366–370.
- \* Authors show that post-translational modification in UNC93B1 regulates TLR7 sorting in MVB for degradation.
44. Maschalidi S, Nunes-Hasler P, Nascimento CR, Sallent I, Lannoy V, Garfa-Traore M, *et al.*: **UNC93B1 interacts with the calcium sensor STIM1 for efficient antigen cross-presentation in dendritic cells.** *Nat Commun* 2017, 8:1640.
- \* Important paper showing the cooperation between UNC93B1 and STIM1 for efficient MHC I antigen cross presentation.
45. Nunes-Hasler P, Maschalidi S, Lippens C, Castelbou C, Bouvet S, Guido D, *et al.*: **STIM1 promotes migration, phagosomal maturation and antigen cross-presentation in dendritic cells.** *Nat Commun* 2017, 8:1852.
46. McCormick PJ, Martina JA, Bonifacino JS: **Involvement of clathrin and AP-2 in the trafficking of MHC class II molecules to antigen-processing compartments.** *Proc Natl Acad Sci* 2005, 102:7910–7915.
47. Sasai M, Linehan MM, Iwasaki A: **Bifurcation of Toll-Like Receptor 9 Signaling by Adaptor Protein 3.** *Science* 2010, 329:1530–1534.
- \*\* Identification of the adaptor protein AP-3 responsible for TLR9 trafficking from endosomes to lysosomes for type I interferon response.
48. Blasius AL, Arnold CN, Georgel P, Rutschmann S, Xia Y, Lin P, *et al.*: **Slc15a4, AP-3, and Hermansky-Pudlak syndrome proteins are required for Toll-like receptor signaling in plasmacytoid dendritic cells.** *Proc Natl Acad Sci* 2010, 107:19973–19978.
49. Michelet X, Garg S, Wolf BJ, Tuli A, Ricciardi-Castagnoli P, Brenner MB: **MHC Class II Presentation Is Controlled by the Lysosomal Small GTPase, Arl8b.** *J Immunol* 2015, 194:2079–2088.

50. Saitoh SI, Abe F, Kanno A, Tanimura N, Mori Saitoh Y, Fukui R, *et al.*: **TLR7 mediated viral recognition results in focal type I interferon secretion by dendritic cells.** *Nat Commun* 2017, 8:1592.



Figure 1.



Les cellules dendritiques (CDs) sont des effecteurs clés reliant l'immunité innée et adaptative. Elles reconnaissent directement les agents pathogènes infectants par le biais de récepteurs de l'immunité innée (Pattern recognition receptors ou PRR), comme les récepteurs Toll-like (TLR), et initient des réponses immunitaires efficaces contre eux. Elles produisent en effet un large panel de cytokines et chimiokines pro-inflammatoires et augmentent l'expression de leurs molécules de co-stimulation suite à une infection. Les cellules dendritiques sont des cellules présentatrices d'antigènes (CPA) cruciales, capables de présenter des peptides pathogéniques ou associés à une tumeur via les molécules du CMH pour activer les lymphocytes T et initier une réponse adaptative.

Fortement exprimée dans les CDs, UNC93B1, une molécule hautement conservée, composée de 12 passages transmembranaires et résidant dans le réticulum endoplasmique (RE), a été identifiée comme un régulateur clé dans le repliement et le trafic vers les endosomes des TLRs intracellulaires qui détectent les acides nucléiques des microbes. En effet, une mutation du gène *Unc93b1* (mutation 3d) entraîne une inhibition de l'interaction entre UNC93B1 et les TLRs intracellulaires et bloque leur signalisation. Chez la souris, la mutation 3d d'UNC93B1 entraîne également un défaut de présentation croisée antigénique et une subséquente croissance tumorale accrue et rapide, probablement en raison d'un défaut de présentation croisée des antigènes associés aux tumeurs par les CDs. N'interagissant pas seulement avec les TLRs, UNC93B1 a pour rôle de médier l'activation d'autres protéines dans le RE, comme STIM1 et STING.

Dans le RE, IRE1 $\alpha$  est l'un des 3 acteurs majeurs de l'UPR, une réponse adaptative déclenchée lors de la perturbation de l'homéostasie des protéines du RE et dont la fonction est de restaurer les fonctions altérées de l'organelle. Si l'homéostasie du RE ne peut pas être restaurée, l'UPR induit alors des signaux pro-apoptotiques. La régulation de l'activation d'IRE1 $\alpha$  reste peu claire, en particulier dans les CDs où il joue un rôle majeur dans la survie des CDs et la présentation croisée antigénique du CMH de classe I. Nous apportons la preuve qu'UNC93B1 lie le domaine transmembranaire d'IRE1 $\alpha$  et régule sa fonction. Nous avons montré que dans les CDs portant la mutation 3d, IRE1 $\alpha$  n'est plus associé à BiP, ce qui entraîne son activation. De plus, l'inhibition de l'activité d'IRE1 $\alpha$  dans les CDs 3d restaure la présentation croisée antigénique *in vitro* et limite la croissance tumorale *in vivo*. Dans l'ensemble, nos données mettent en évidence le rôle essentiel d'UNC93B1 dans la régulation de la présentation antigénique du CMH de classe I dans les CDs en contrôlant l'activité d'IRE1 $\alpha$ .

En plus d'IRE $\alpha$ , nous avons également examiné la régulation de STING par UNC93B1, car il a été démontré que les deux protéines interagissent, UNC93B1 favorisant potentiellement la régulation négative de STING. Nous avons constaté que, dans les CDs, UNC93B1 contrôle STING différemment et semble essentiel pour sa signalisation. De plus, dans les CDs 3d, l'interaction entre UNC93B1 et STING est conservée mais la mutation induit une diminution significative du trafic et de la signalisation STING. Ces données préliminaires indiquent, qu'en plus de favoriser l'activation d'IRE1 $\alpha$ , UNC93B1 semble jouer un rôle important dans la voie interféron médiée par STING.

Dendritic cells (DCs) are key immune cells linking innate and adaptive immunity. They express a wide range of pattern recognition receptors (PRRs), such as Toll-like receptors (TLRs), which recognize specific molecular patterns expressed by pathogens. Following pathogen infection, DCs produce a large panel of pro-inflammatory cytokines and chemokines and increase the expression of their co-stimulatory molecules to present pathogenic-associated peptides on MHC molecules to prime T cells and initiate adaptive immunity.

Strongly expressed in DCs, UNC93B1, a highly conserved 12-membrane spanning molecule residing in the endoplasmic reticulum (ER), has been identified as a key regulator in the folding and trafficking to endosomes of intracellular TLRs that detect microbial nucleic acids. A single mutation in the *Unc93b1* gene (3d mutation) results in the absence of UNC93B1 interaction with intracellular TLRs and inhibition of their signalling, indicating that the association of UNC93B1 to intracellular TLRs is mandatory for their function. UNC93B1 also associates with the ER calcium sensor, STIM1 and this interaction is mandatory for MHC class I antigen cross presentation in DCs. UNC93B1 is also shown to control the production of type I interferon (IFN $\alpha$ ) mediated by STING, an innate immune receptor involved in antiviral response.

In the ER, IRE1 $\alpha$  is one of the 3 sensor proteins of the Unfolded Protein Response (UPR) which is an adaptive response triggered upon disruption of ER protein homeostasis and whose function is to restore the altered functions of the ER. If ER homeostasis cannot be restored, the UPR then induces pro-apoptotic signals. Regulation of IRE1 $\alpha$  activation is not well understood, particularly in DCs where it plays a major role in survival and MHC class I antigen cross presentation. We provide evidence that UNC93B1 binds the transmembrane domain of IRE1 $\alpha$  and regulates its function. We find that in DCs bearing the 3d mutation, IRE1 $\alpha$  is no longer associated to BiP which leads to increased IRE1 $\alpha$  activity. Furthermore, inhibition of IRE1 $\alpha$  activity in 3d DCs restores MHC class I antigen cross presentation in vitro and limits tumour growth in vivo. Our data highlight the essential role of UNC93B1 in regulating MHC class I antigen presentation in DCs by controlling IRE1 $\alpha$  activity.

We also find that UNC93B1 associates with STING and positively regulates IFN $\alpha$ -STING dependent signalling. In DCs silenced for UNC93B1 or expressing the 3d mutant, trafficking of STING from ER to Golgi is delayed which leads to reduced IFN $\alpha$  secretion.

Altogether, our data suggest an important role for UNC93B1 in regulating IRE1 $\alpha$  and STING activities in DCs.